FACULTÉ DES ÉTUDES SUPÉRIEURES ET POSTOCTORALES

uOttawa

L'Université canadienne
Canada's university

FACULTY OF GRADUATE AND POSDOCTORAL STUDIES

Mary Ann Petrunewich
AUTEUR DE LA THÈSE / AUTHOR OF THESIS

M.Sc. (Cellular and Molecular Medicine)
GRADE / DEGREE

Department of Cellular and Molecular Medicine
FACULTÉ, ÉCOLE, DÉPARTEMENT / FACULTY, SCHOOL, DEPARTMENT

The Effect of Pharmacology Perturbations of Maturation Promoting Factor (MPF) and Mitogen Activated Protein Kinase (MAPK) in Mouse Eggs

TITRE DE LA THÈSE / TITLE OF THESIS

M. Baltz
DIRECTEUR (DIRECTRICE) DE LA THÈSE / THESIS SUPERVISOR

CO-DIRECTEUR (CO-DIRECTRICE) DE LA THÈSE / THESIS CO-SUPERVISOR

EXAMINATEURS (EXAMINATRICES) DE LA THÈSE / THESIS EXAMINERS

M. Mbikay

K. Turksen

Gary W. Slater
LE DOYEN DE LA FACULTÉ DES ÉTUDES SUPÉRIEURES ET POSTDOCTORALES /
DEAN OF THE FACULTY OF GRADUATE AND POSTDOCORAL STUDIES

THE EFFECT OF PHARMACOLOGICAL PERTURBATIONS OF MATURATION PROMOTING FACTOR (MPF) AND MITOGEN ACTIVATED PROTEIN KINASE (MAPK) IN MOUSE EGGS

Mary Ann Petrunewich

This thesis is submitted as a partial fulfillment of the

M.Sc program in Cellular and Molecular Medicine

Submitted on January 2005

Your file Votre référence
ISBN: 0-494-14937-X
Our file Notre référence
ISBN: 0-494-14937-X

AUTHORIZATION

Some of the data presented within this thesis has been published. The appropriate permissions have been obtained for the use of figure and tables.

Phillips KP, Petrunewich MA, Collins JL, Booth RA, Liu XJ, Baltz JM. 2002a. Inhibition of MEK or cdc2 kinase parthenogenetically activates mouse eggs and yields the same phenotypes as Mos(-/-) parthenogenotes. Dev Biol. 2002 Jul 1;247(1):210-23.

According to the publisher website, as an author, I retain the right the right to include the article in full or in part in a thesis or dissertation (provided that this is not to be published commercially). These rights are retained and permitted without the need to obtain specific permission from Elsevier.

Phillips KP, Petrunewich MA, Collins JL, Baltz JM. 2002b. The intracellular pH-regulatory HCO3-/Cl- exchanger in the mouse oocyte is inactivated during first meiotic metaphase and reactivated after egg activation via the MAP kinase pathway. Mol Biol Cell. 13(11):3800-10.

Letter of permission to use data from figures published in this article for this thesis is attached.

MOLECULAR BIOLOGY OF THE CELL

PUBLICATIONS OFFICE · 8120 Woodmont Avenue, Suite 750 · Bethesda, Maryland 20814-2762
TEL: 301-347-9300 · FAX: 301-347-9350 · E-MAIL: mbc@ascb.org · www.molbiolcell.org

August 6, 2004

Mary Ann Petrunewich
RR#2
Almonte, ON
K0A 1A0

To Whom It May Concern:

We are pleased to grant Mary Ann Petrunewich permission to use the material requested from the article titled "The Intracellular pH-regulatory HCO_3^-/Cl^- Exchanger in the Mouse Oocyte Is Inactivated during First Meiotic Metaphase and Reactivated after Egg Activation via the MAP Kinase Pathway", published in *Molecular Biology of the Cell*.

We require acknowledgment as follows for each reproduction: "Reprinted from *Molecular Biology of the Cell* (Mol. Biol. Cell 2002 13: 3800-3810; published online before print as 10.1091/mbc.E02-04-0242) with the permission of The American Society for Cell Biology."

Sincerely yours,

Rachel Altemus
MBC Editorial Office

ABSTRACT

Inactivation of MAPK with the MEK1/2 inhibitor U0126 simultaneously parthenogenetically activates eggs, disrupts spindle-cortex docking and destabilizes spindle organization, yielding parthenogenotes that resemble *mos*$^{-/-}$ oocytes. Inactivation of MPF with the Cdk1 inhibitor roscovitine also parthenogenetically activates eggs, some of which resemble *mos*$^{-/-}$ oocytes, suggesting a reciprocal role for MPF in modulating MAPK activity. MAPK inactivation with U0126 was quick (1 h) and preceded the fall in MPF activity whereas MAPK inactivation after roscovitine treatment was similar to that of fertilization (5-7 h), suggesting the presence of a physiological inactivating mechanisms. A severe phenotype developed after U0126 and roscovitine co-treatment, characterized by incomplete cleavages and ball of actin that follows the drifting spindle. Development of the severe phenotype suggests MPF and MAPK inactivation have a synergistic effect on spindle dynamics and that the timing of inactivation is important for normal egg activation.

TABLE OF CONTENTS

LIST OF FIGURES

LIST OF TABLES

LIST OF ABBREVIATIONS

ADP – adenosine diphosphate

AE – anion exchanger (bicarbonate/chloride exchanger)

APC – anaphase promoting complex

ATP – adenosine triphosphate

Cdk – cyclic dependent kinase

CSF – cytostatic factor

Deme – demecolcine

DMSO – dimethyl sulfoxide

ERK – extracellular-regulated kinase

FSH – follicle-stimulating hormone

GDP – guanosine diphosphate

GFP – green fluorescent protein

GTP – guanosine triphosphate

GV – germinal vesicle

GVBD – germinal vesicle breakdown

hCG – human chorionic gonadotropin

HCO_3^-/Cl^- exchanger – bicarbonate/chloride exchanger

IP – intraperitoneal

IVF – *in vitro* fertilization

KFHM – KSOM-flushing and handling media

KSOM – K^+ supplemented optimized medium

LH – luteinizing hormone

MA – mitotic/meiotic apparatus

MAPK – mitogen activated protein kinase

MBP – myelin basic protein

MEK – MAPK/ERK kinase

MI – metaphase I; meiosis I

MII – metaphase II; meiosis II

MISS –MAPK Interacting and Spindle-Stabilizing Protein

MPF – mitogen-promoting factor

MTOC – microtubule-organizing centre

mRNA – messenger ribonucleic acid

NEBD – nuclear envelope breakdown

NHE – Na^+/H^+exporter; sodium/hydrogen antiporter

OA – okadaic acid

PAGE – polyacrylamide gel electrophoresis

PB (PB-1, PB-2) – polar body (first polar body, second polar body)

PCM – pericentriolar material

pH_i – intracellular pH

PMSG – pregnant mare serum gonadotropin

PN – pronucleus

PP1 – protein phosphatase 1

PP2A – protein phosphatase 2A

R-U – roscovitine-U0126

$t_{½}$ – half life

Veh – vehicle

Zyg – zygote

ACKNOWLEDGEMENTS

Financially, this work was supported through an Ontario Graduate Scholarship (OGS) and an Ontario Graduate Scholarship in Science and Technology (OGSST). It was conducted in the laboratory of Jay Baltz. I would like to thank him for his guidance and insight in keeping the "big picture" in sight as experiments were designed and carried out. I also appreciate his patience in reading through what seemed like an endless number of drafts of this and other manuscripts.

In the lab, I would like to acknowledge the excellent technical support I received from Mary-Anne Hammer. It was from her that I received my initial training in animal and embryo handling. Also, because of her, stocks were always up-to-date and the microscope was available when I needed it, making my tedious timecourses no longer than they needed to be.

Also sharing the Baltzlab experience were my fellow graduate students Candace Steeves and Karen Phillips. To Candy, thanks for commiserating with me about life in and out of the lab. We shared our IVF adventures and the perils of owning moody rust bucket cars. You helped me see the importance of know when to speak up, and when to shut up. Because of you, I have discovered an appreciation for jewelry, country music, pickup trucks and the men who drive them.

To Karen, my lab-mate and co-author, I don't know if I'll ever be able to adequately thank you for all that you've done for me in the last four years. Your gentle guidance in designing experiments, data collection and thesis writing were invaluable. You taught me how to survive life with mouse eggs: from streamlining the prep work (to maximize sleep time) to sleeping tips to helping me develop a taste for loud music at 6:00 AM. You were always ready to celebrate another's successes and to help get back up after the setbacks. As the organizer and host of many dinners and survivor nights, you were the "glue" that helped us all get along.

I started this graduate degree at the same time as Carolyn Wilson, my undergrad roommate and friend. Along the way, we've shared the ups and downs of grad school as we

learned exactly what we had gotten ourselves into. To Carolyn, thanks for being my friend and for our many phone conversations that always seemed to be filled with laughter.

Since high school, Jason Letts has always been by my side. Jason, you are my best friend and my partner in life. Thank you for always being there for me and for talking me out of it the first time I wanted to quit. I appreciate all that you did to try and help me along the way, even if I didn't always appreciate it at the time. Thanks for coming to our lab functions and for listening to me when I needed it. Thanks for packing up our apartment when we moved two weeks before I submitted my thesis. Mostly, thanks for putting up with me for all these years.

From my parents, Mike and Mary Ellen Petrunewich, I will always appreciate the unwavering support you showed me in everything I've ever undertaken. Even though you might not have understood what I was doing, thanks for being interested and asking questions about my project. More importantly, though, thanks for having the insight to know when to change the subject. Thank you for never even considering that I might not finish and for making such a big fuss when I did.

1 INTRODUCTION

1.1 BACKGROUND

1.1.1 The Cell Cycle

The stages through which a cell passes from one cell division to the next are the cell cycle (Fig. 1). In M-phase, duplicated chromosomes are separated into two nuclei (mitosis) and the cytoplasm of the cell is divided to form two daughter cells (cytokinesis). Interphase is divided into G_1, S andG_2. The period of DNA replication is S-phase while G_1 and G_2 occur before and after S-phase, respectively (Karp, 1996). At the transitions primarily between G_1 and S and between G_2 and M-phase, cells possess feedback controls, or "checkpoints," that monitor the status of cell cycle events such as replication and chromosome condensation to control the progress of the cell cycle (O'Farrell, 2001.).

The two main processes by which eukaryotic cells divide are mitosis and meiosis (Fig. 2). In mitosis, the chromosome complement is duplicated (4n) and separated from one another to form two identical diploid (2n) nuclei (Snustad *et al.*, 1997). This is the process by which single cells reproduce and multicellular organisms grow. Meiosis is the process of sex cell formation. In meiosis, duplicated chromosomes undergo two successive nuclear and cytoplasmic divisions without an intervening S-phase, reducing the genetic complement from 4n to 1n (Snustad *et al.*, 1997). The resultant gametes are therefore haploid. The successive divisions are termed meiosis I and II. In meiosis I, homologous chromosomes that have paired during prophase I are separated. Meiosis II separates sister chromosomes, giving rise to four haploid cells (Karp, 1996). During sexual reproduction, fertilization joins the male and female gametes restoring diploidy such that half the genetic complement of the resulting organism is maternal in origin while the other half is paternal (Karp, 1996).

Figure 1: The eukaryotic cell cycle. The cell passes through 4 main stages from one division to the next. M phase includes all the stages of mitosis and cytokinesis. The other 3 stages comprise interphase. In G_1, the cell grows and carries out normal metabolism. The period of DNA synthesis is S-phase while the cell prepares for mitosis in G_2.

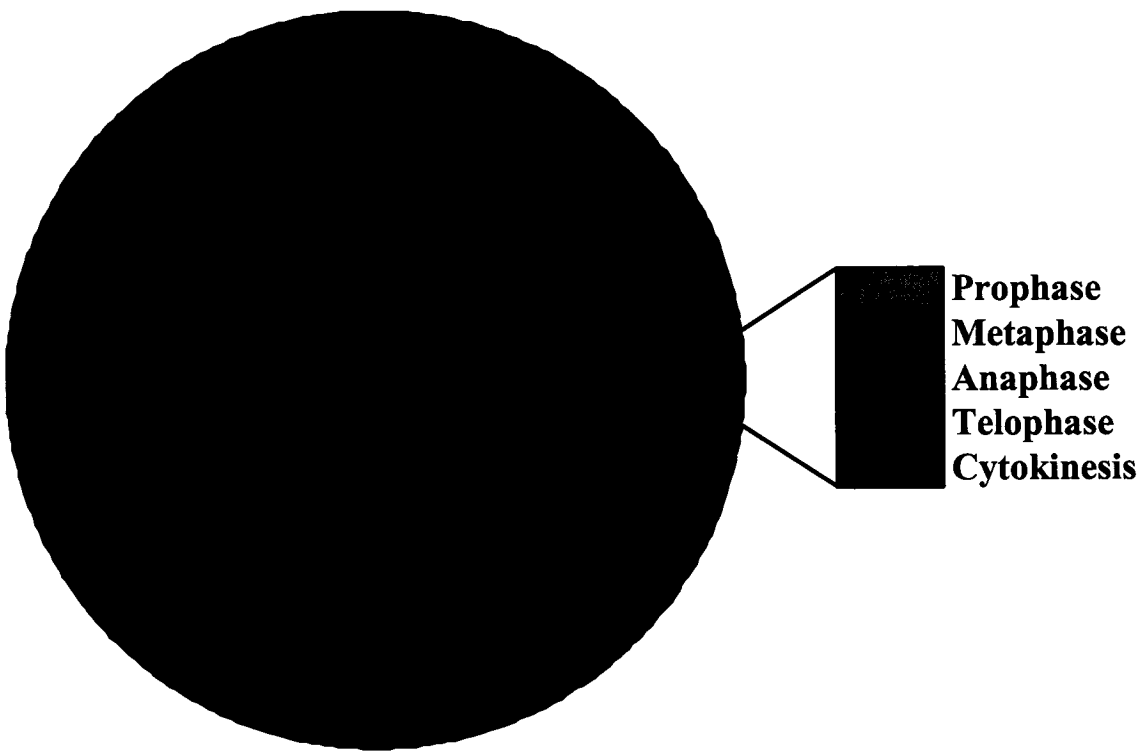
Prophase
Metaphase
Anaphase
Telophase
Cytokinesis

Figure 2: Mitosis versus meiosis. In mitosis, the diploidy is retained (2n) in the sister cells while each gamete from meiosis is haploid (1n).

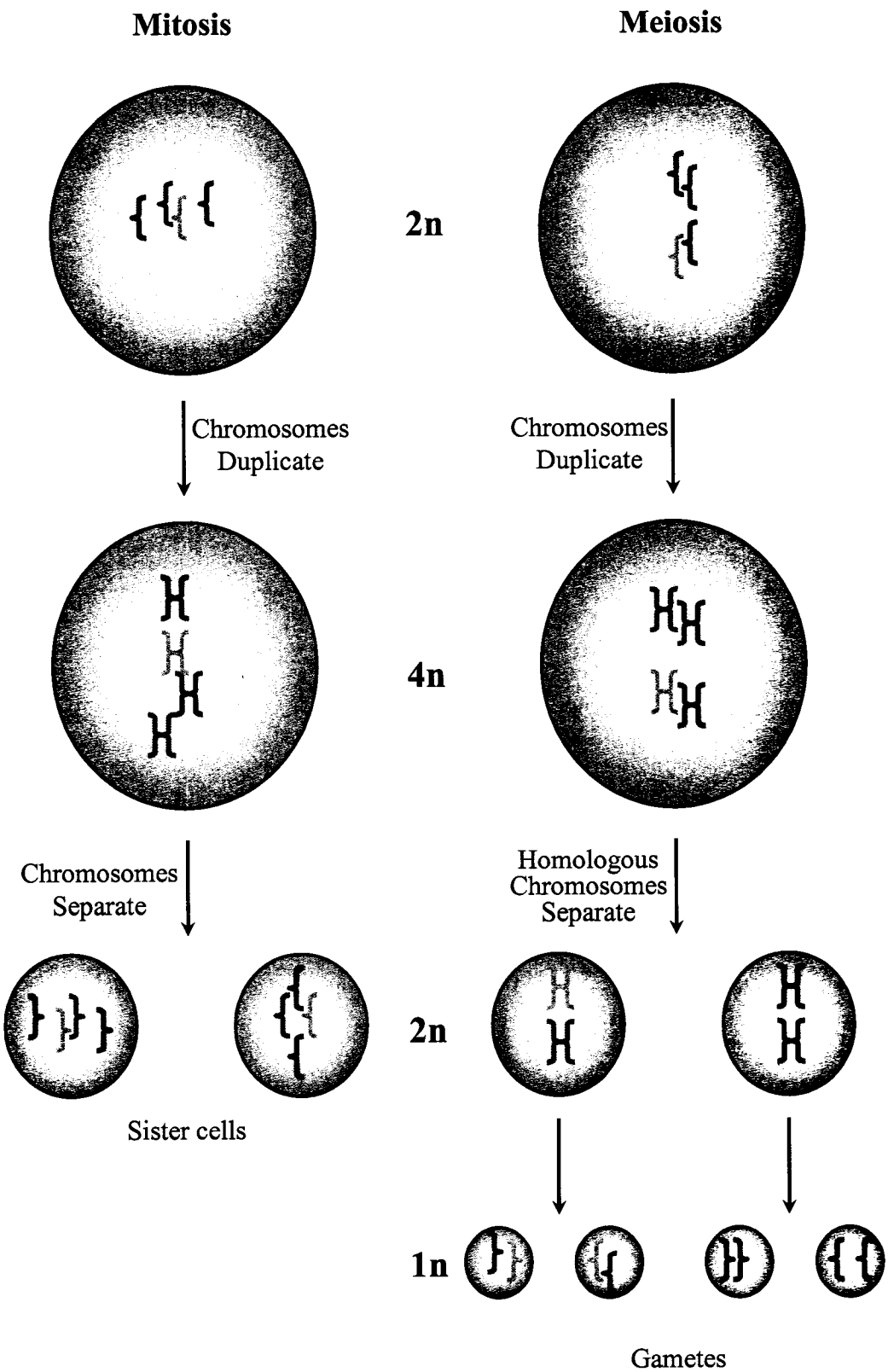
Mitosis
Meiosis
2n
Chromosomes Duplicate
Chromosomes Duplicate
4n
Chromosomes Separate
Homologous Chromosomes Separate
2n
Sister cells
1n
Gametes

1.2 Overview of Ovulation and Preimplantation Embryo Development

1.2.1 Oogenesis

The process of forming female gametes is termed oogenesis. This occurs in the ovary – a solid organ composed of germ cells within follicles, corpus lutea and interstitial cells (Knobil and Neill, 1988). In the early stages of embryo development, germ cells multiply rapidly, undergoing several rounds of mitotic division before differentiating into primary oocytes. These oocytes have begun meiosis but are arrested in G_2 at prophase I. In the mouse, this arrest occurs about five days after birth (Hogan *et al.*, 1986). At this stage the oocyte is small (about 20 μm in diameter in the mouse), is characterized by a prominent nucleus or germinal vesicle, and is referred to as a GV oocyte. The primary oocyte is surrounded by the zona pellucida (an acellular coat) and is maintained by a single layer of granulosa cells (Knobil and Neill, 1988).

At sexual maturity (6 weeks of age in the mouse), cyclic hormonal signals stimulate a few primary oocytes to grow and resume meiosis (Hogan *et al.*, 1986; Knobil and Neill, 1988). Granulosa cells proliferate and the follicle accumulates fluid to form an antral (Graafian) follicle. At the same time, the oocytes grow to 70-80 μm, accumulating proteins, and other molecules important to complete meiosis and support preimplantation metabolism, if fertilization were to occur. The accumulation of inactive pools of cell cycle regulatory molecules is important for the oocyte to develop competence, which occurs when it reaches about 80% of its fully-grown size. Meiotic competence refers to the ability of the oocyte to progress through MI and produce a mature MII egg (Grondahl *et al.*, 2000).

Just before ovulation, the fully-grown GV oocyte resumes meiosis, undergoing germinal vesicle breakdown (GVBD; Fig. 3). The oocyte then proceeds through meiosis I, separating the pairs of homologous chromosomes. Cytokinesis is uneven, distributing virtually all the cytoplasm to one cell, the secondary oocyte, while the polar body receives almost no cytoplasm at

Figure 3: Overview of oocyte maturation and fertilization. The fully-grown (competent) GV oocyte is stimulated to resume meiosis and undergoes germinal vesicle breakdown (GVBD). The egg completes meiosis I and the first polar body is extruded. The egg begins meiosis II, and is arrested at metaphase II. Ovulation occurs and the egg awaits fertilization (or parthenogenetic activation). After fertilization (or parthenogenetic activation, not shown), the oocyte completes MII, emitting the second polar body. The male and female chromosomes decondense and each set becomes surrounded by their own nuclear membrane to form two separate pronuclei (2PN).

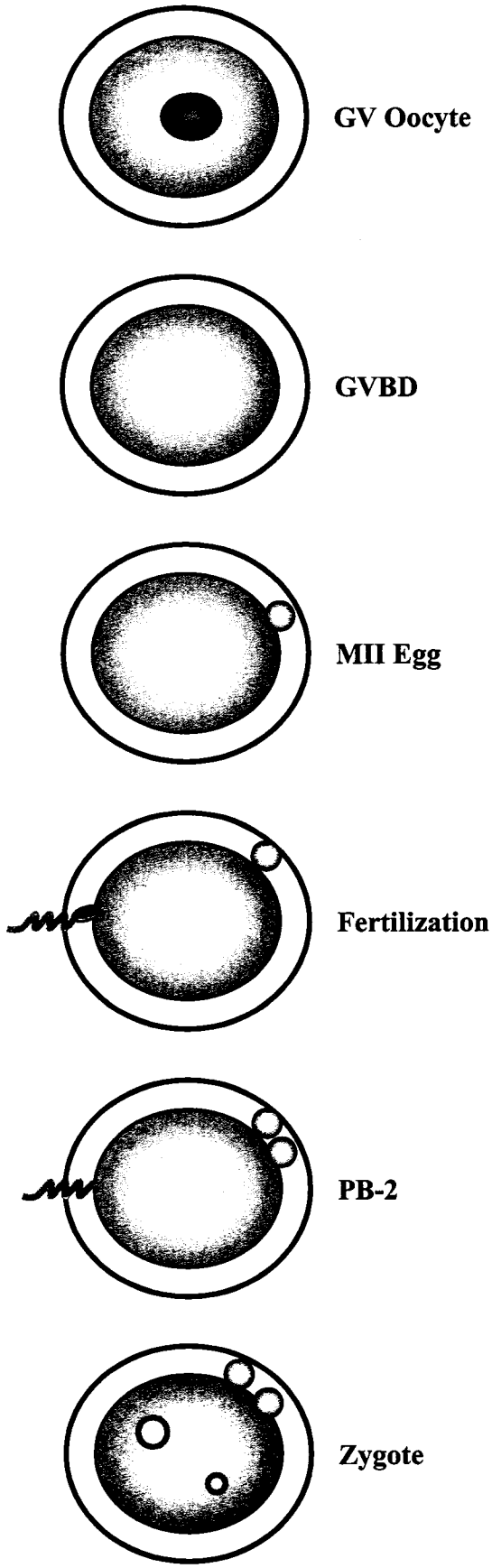
GV Oocyte
GVBD
MII Egg
Fertilization
PB-2
Zygote

all. This type of asymmetrical division allows the egg to keep all reserves accumulated during the growth period to help ensure the success of the early development. The oocyte and polar body each continue meiosis but the polar body eventually degenerates since it contains little or no cytoplasm to support metabolism. The oocyte becomes arrested in second meiotic metaphase (MII). The mature egg is released (ovulated) into the female tract enclosed by cumulus cells where it awaits activation by fertilization or parthenogenetic activation so that it can complete meiosis (Karp, 1996; Snustad *et al.*, 1997).

1.2.2 Preimplantation Development: Fertilization, Cleavage and Development to the Blastocyst

The egg is ovulated arrested at metaphase II into one of a pair of tubes that connect the ovaries to the uterus. In the human, these tubes are referred to as Fallopian tubes but in other animals, they are called the oviducts (Knobil and Neill, 1988). The completion of meiosis, termed egg activation, is triggered by the fusion of sperm and egg (fertilization) or by parthenogenetic activation (see below). During *in vivo* fertilization, sperm move through the female tract to the cumulus cells, binding to the zona pellucida and one sperm fuses to the egg cytoplasm. Despite many years of research, the cellular processes that trigger the egg to re-enter the cell cycle and begin embryonic development are not completely understood (reviewed by Runft *et al.*, 2002). A universal feature of the egg activation process is an increase in cytosolic free Ca^{2+} within the egg. This increase is necessary and sufficient to trigger completion of meiosis (Whittingham and Siracusa, 1978). Changes in the zona pellucida prevent further sperm from binding and fertilizing the egg (polyspermy; Kline and Stewart-Savage, 1994). The oocyte undergoes the second unequal cleavage to emit the second polar body. Following this cytokinesis, the male and female chromosomes decondense and each set becomes surrounded by their own nuclear membrane to form two separate pronuclei. These combine by the end of the

first mitotic cell cycle to form the complete embryonic genome in the zygote, or one-cell embryo (Schatten *et al.*, 1985).

As it moves through the oviduct to the uterus, the zygote undergoes a series of mitotic cleavage divisions (Fig. 4). In contrast to normal mitotic cycles in somatic cells, these mitotic divisions are not accompanied by any increase in total cytoplasmic volume, so the individual cells (or blastomeres) of the embryo become smaller and smaller as the total volume remains approximately the same (Knobil and Neill, 1988). Around the 6- to 8-cell stage, the blastomeres increase expression of cell adhesion molecules and they develop cell-cell communication via gap junctions. This process leads to compaction of the blastomeres, forming a morula (Hogan *et al.*, 1986). Compaction also marks the beginning of blastomere differentiation. The morula develops a fluid-filled cavity to become a blastocyst (Knobil and Neill, 1988). The blastocyst is comprised of two distinct cell types – the trophectoderm surrounds a fluid-filled cavity (the blastocoel) while the remaining cells form an inner cell mass attached to the trophectoderm within the blastocoel (Schultz, 1999).

At this stage, the embryo has moved into the uterus and is still surrounded by the zona pellucida. The blastocyst hatches from the zona pellucida in the uterus and implants in the uterine wall (Hogan *et al.*, 1986).

1.2.3 Parthenogenesis – Activation without Sperm

In vivo, the process of fertilization releases the vertebrate egg from its metaphase arrest. Eggs can also be released from their metaphase arrest without sperm – parthenogenesis. A wide range of stimuli can induce parthenogenetic activation. Eggs left in the oviduct to age will spontaneously activate, and eggs from some strains of mouse will parthenogenetically activate from the stimuli involved in being isolated and released into culture media. Likewise, the use of anesthetics such as ether, chloroform or Nembutal following ovulation can induce parthenogenesis (Kaufman, 1978).

Figure 4: Overview of preimplantation embryo development to the blastocyst stage. The fertilized egg undergoes a series of mitotic divisions without much growth in between so the individual cells (or blastomeres) of the embryo become smaller and smaller as the total volume remains approximately the same. Around the 6- to 8-cell stage, the blastomeres compact, forming a morula. The morula becomes a blastocyst. The blastocyst is comprised of the trophectoderm and the inner cell mass.

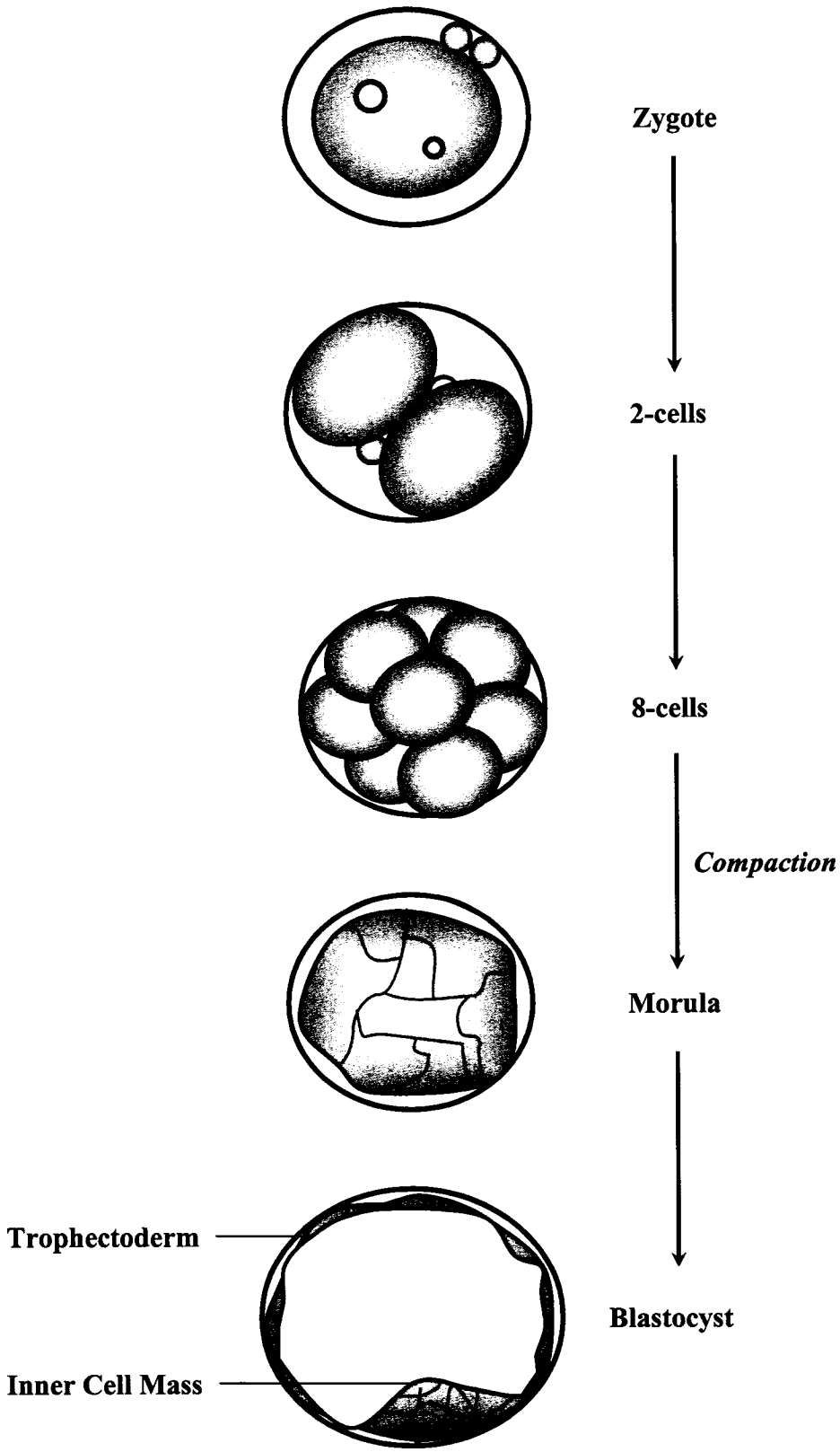
Zygote
2-cells
8-cells
Compaction
Morula
Blastocyst
Trophectoderm
Inner Cell Mass

Other experimental methods of parthenogenetic egg activation mimic the characteristic intracellular increase of intracellular calcium at activation. Addition of a Ca^{2+} ionophore such as A23187 both allows Ca^{2+} entry into the cell from the external medium and releases sequestered Ca^{2+} into the cytoplasm to activate the ovulated egg. In this case, one prolonged Ca^{2+} transient activates the egg instead of shorter repetitive transients that are observed during fertilization. A brief pulse of ethanol will also parthenogenetically activate eggs by eliciting a Ca^{2+} monotransient.

In this study, parthenogenetic activation was accomplished with the Ca^{2+}-releasing agent, strontium (Sr^{2+}). When introduced externally, this divalent cation induces parthenogenetic activation featuring resumption of the cell cycle, polar body emission and pronuclear formation that is essentially indistinguishable from activation by sperm (Whittingham and Siracusa, 1978). Exposure to Sr^{2+} also produces repetitive Ca^{2+} transients that closely resemble those at fertilization, so this form of activation most closely mimics activation with sperm, making it an ideal method to compare novel forms of parthenogenetic activation with fertilization (Phillips *et al.*, 2002b). Sr^{2+} cations seem to displace bound intracellular calcium, thereby increasing the free intracellular calcium concentration and activating the egg (Fraser, 1987). Compared to fertilization, Sr^{2+} activation allows precise timing of activation – eggs are synchronously activated upon exposure to Sr^{2+} in the media. In our hands, eggs exposed to Sr^{2+} for 2 h consistently yields nearly 100% activation of mature mouse eggs (Phillips *et al.*, 2002a). As with other forms of activation where the second polar body is emitted, this parthenogenote is haploid.

1.2.4 Indicators of Activation – Becoming a Zygote

Mammalian fertilization is a precisely coordinated series of cellular interactions in which sperm recognize and contact eggs, activating the egg to resume meiosis. There are a number of indicators to distinguish eggs that have successfully undergone activation from their arrested counterparts.

The changes in intracellular Ca^{2+} that occur universally at fertilization can be followed using several techniques, the most common of which involves the use of Ca^{2+}-sensitive fluorophores loaded into the egg (Baltz and Phillips, 1999). A single rise in intracellular Ca^{2+} in the first minutes after fertilization marks the onset of activation in echinoderms and *Xenopus*. Conversely, ascidian and mammalian eggs undergo a series of intracellular calcium oscillations that last several hours (reviewed by Ciapa and Chiri, 2000). In mammalian systems, the first increase in intracellular Ca^{2+} occurs 20-30 s after sperm attachment and spreads across the egg like a wave (Xu *et al.* 1994). In the hamster, intracellular Ca^{2+} increases threefold following sperm-egg binding in the hamster (Miyazaki, 1991). Frequency, number, duration and amplitude of the calcium transients are species-specific. The calcium transients decrease in amplitude shortly before pronuclear formation and cease when pronuclei are visible, about 4-6 h after fertilization or parthenogenetic activation in the mouse (Kubiak *et al.*, 1993; reviewed by Ciapa and Chiri, 2000; Marangos *et al.*, 2003).

Following the intracellular increase in calcium, cortical granules just below the oolemma undergo exocytosis. The contents of the cortical granules initiate changes in glycoproteins of the zona pellucida to prevent polyspermy (reviewed by Hogan *et al.*, 1986). Cortical granule exocytosis occurs 2.5-5 min post sperm attachment in zona-free hamster eggs and 5-15 min after sperm attachment in zona free mouse eggs (Kline and Stewart-Savage, 1994).

Although the zona reaction following cortical granule exocytosis is the major protective mechanism against polyspermy in mammalian oocytes, membrane changes also play a role in preventing fertilization by supernumerary sperm. Whereas the zona pellucida is biochemically altered, the change in the membrane is electrical in nature. This process is best studied in marine invertebrates where membrane ion channels on the egg membrane open, changing the membrane potential of the egg, to prevent more sperm from fusing to the egg membrane. Whether this shift is in the positive or negative direction is species-specific (Kobayashi *et al.*, 1994; reviewed by Gould and Stephano, 2003). The block occurs almost immediately after sperm-egg fusion but is

only temporary, lasting until a more permanent block can be established (such as the zona block to polyspermy). A recent report suggests that a membrane block to polyspermy in the mouse occurs 40 min – 2 h post-insemination. This block is biochemical rather than electrical, relying on actin and calcium (McAvey *et al.*, 2002). Likewise, the fusion of sperm to egg allows the oolemma of human oocytes to block subsequent sperm penetration within 2 h of fertilization (Sengoku *et al.*, 1999).

Following membrane and zona changes to prevent polyspermy, the egg resumes meiosis, and 1-3 h post-insemination, emission of the second polar body is observed (Hogan *et al.*, 1986). This signals the end of meiosis. Polar bodies typically degenerate before mitotic division but the polar body persists in over half of mouse embryos. They may even cleave, resulting in three polar bodies at the end of meiosis (Howlett and Bolton, 1985). Nuclear membranes form around the maternal and paternal chromosomes to form two pronuclei, 2-4 h after polar body emission (Hogan *et al.*, 1986; Schatten *et al.*, 1985). The pronucleus of male origin forms at the point of sperm entry and is visible 4-8 h post-insemination. The female pronucleus is smaller and forms slightly later, 5-9.5 h post-insemination (Howlett and Bolton, 1985; Hogan *et al.*, 1986). Each pronucleus is haploid, thereby restoring the egg to a diploid state. The male and female pronuclei slowly move together in a microtubule-dependent manner, reaching the centre of the egg 8-10 h post-insemination (Howlett and Bolton, 1985; Maro *et al.*, 1986b). Pronuclei will abut each other but they do not fuse. Instead, each pronucleus duplicates its genome at the onset of S-phase and the chromosomes align on a single spindle at the first mitotic metaphase (Schatten *et al.*, 1985).

Parthenogenetically activated eggs may be haploid, since there is no male contribution. This is the case with strontium or A23187 activation. On the other hand, if the second polar body is not emitted during parthenogenesis, the resultant parthenogenote is diploid. This is often the case for ethanol activation or can be induced when emission of the second polar body is suppressed by disruption of the actin cytoskeleton. Compared to diploid parthenogenotes, haploid parthenogenotes divide more slowly, have an increased incidence of apoptosis during

preimplantation development, and are more likely to arrest before the blastocyst stage in the mouse (Bos-Mikich *et al.*, 1993; Liu *et al.*, 2002).

Another important indicator of activation is the upregulation of membrane ion transporters such as the sodium/hydrogen (Na^+/H^+) antiporter and the bicarbonate/chloride (HCO_3^-/Cl^-) exchanger, important in maintaining intracellular pH (pH_i; Zhao and Baltz, 1996; Phillips and Baltz, 1999 Lane *et al.*, 1999). Intracellular pH is crucial to the survival of the embryo (Zhao *et al.*, 1995) and regulates or creates a permissive environment for many important cellular processes including enzyme activity, cell division, protein synthesis, and differentiation (Boron, 1986). Also known as the anion exchanger (AE), the HCO_3^-/Cl^- exchanger exports HCO_3^- in exchange for Cl^- in response to intracellular alkalosis (Zhao *et al.*, 1995; Zhao and Baltz, 1996; Alper, 1994). In contrast, the Na^+/H^+ antiporter exchanges protons for Na^+ ions in response to intracellular acidosis. AE activity is largely quiescent in unfertilized eggs, first being observed about 4 h post-fertilization or post-activation and reaching maximal activity by 8 h post-fertilization or post-activation, after the appearance of pronuclei (Phillips and Baltz, 1999; Phillips *et al.*, 2002b). NHE activity is likewise activated at fertilization in the hamster (Lane *et al.*, 1999). This may indicate that the upregulation of pH_i-regulatory mechanisms may be a universal feature of fertilization and not limited to certain marine invertebrates like the sea urchin or *Xenopus* (Shen and Buck, 1990; Swann and Whittaker, 1985; Phillips and Baltz, 1999).

1.3 Inside the Mammalian Egg: The Cytoskeleton

The cytoskeleton is an elaborate interactive network composed of microtubules, microfilaments and intermediate filaments. Microtubules are hollow, cylindrical structures whose wall is composed of subunits formed from the protein tubulin (reviewed by Brinkley, 1997). Microfilaments are solid, thinner structures, composed of the protein actin (reviewed by Revenu *et al.*, 2004). Intermediate filaments are strong, rope-like fibres composed of a variety of proteins having similar structure including lamin and keratin (reviewed by van den Ent *et al.*, 2001).

The cytoskeleton of animal cells functions in a variety of capacities. It provides structural support, maintaining cell shape and forming an internal framework responsible for positioning various organelles within cells (Yarm *et al.*, 2001). It also acts as the force-generating element responsible for the movement of cells from one place to another (pseudopodia, cilia and flagellae) or in changing cell shape. The cytoskeleton provides sites for anchoring mRNAs, facilitating their translation into polypeptides and can act as a signal transducer, transmitting information from the cell membrane to the cell interior (Bretscher, 1991). Although the components of the cytoskeleton appear as stationary, immutable structures under the microscope, in reality they are a highly dynamic group of structures capable of rapid and dramatic reorganization (Brinkley, 1997; Revenu *et al.*, 2004). The remainder of this discussion will focus on the role of microtubules and actin with emphasis on the egg and activation.

1.3.1 Tubulin

Microtubules are hollow, cylindrical structures that are components of a diverse array of structures including the cytoskeleton, the core of cilia or flagella, and the mitotic and meiotic spindles. The subunits that make up the polymer are globular proteins, called tubulin. These tubulin monomers are incorporated into the polymer as heterodimeric building blocks made up of one molecule each of α- and β-tubulin (reviewed by Brinkley, 1997). This heterodimer is incorporated in a consistent head-to-tail fashion by addition to the ends of the polymer, creating a strand parallel to the long axis of the tubule, called a protofilament. In turn, 13 protofilaments arranged in a circle comprise the microtubule (reviewed by Westermann and Weber, 2003). Because each protofilament is oriented in the same direction and each protofilament is composed of α- and β- tubulin, the microtubule has polarity. The plus end is comprised of β-tubulin while α-tubulin makes up the minus end of the microtubule (Waters and Salmon, 1997). Microtubules can be assembled/disassembled spontaneously *in vitro* simply by raising and lowering the temperature of the incubation mixture (Gelfand, 1991).

Microtubule polymerization occurs via noncovalent association of the heterodimer building blocks. GTP is bound to the β-tubulin subunit, which allows the heterodimer to be incorporated into the growing protofilament. Shortly after incorporation, GTP is hydrolyzed to GDP where is remains bound to the polymer. In this way, microtubule polymerization expends energy within the cell (Brinkley, 1997). Following disassembly of the microtubule, GDP is exchanged for GTP on the β-tubulin monomer, allowing the heterodimer to be incorporated into another microtubule. Because tubulin heterodimers are constantly being recycled into new microtubules, the function of a microtubule in a cell depends on its location and orientation (Brinkley, 1997). The tubulin pool is in a dynamic equilibrium between free dimers and polymerized microtubules. Microtubules grow and shrink from both ends, however, both these processes occur more rapidly at the plus end of the microtubule *in vivo* (Karp, 1996).

Microtubule nucleation occurs by means of a group of specialized structures, called microtubule organizing centres (MTOCs). The MTOC controls the number of microtubules that form and the time and location of their formation. One form of MTOC found in many animal cells is made of centrosomes, containing γ-tubulin and two centrioles surrounded by pericentriolar material (PCM). Gamma tubulin is presumed to be an essential element in microtubule nucleation, possibly by acting as a template onto which the α/β-heterodimers can assemble. The minus end of the microtubule associates with the PCM but never actually makes contact with the centrioles (Waters and Salmon, 1997).

Rodent eggs arrested at metaphase II contain 2 populations of MTOCs (or PCM foci). Cortical and spindle MTOCs contain PCM but lack centrioles while only MTOCs of the spindle contain γ-tubulin (Combelles and Albertini, 2001; Maro *et al.*, 1985, 1986a). Spindle foci of PCM are arranged in a ring at each spindle pole while cortical MTOCs are scattered throughout the cortex of the oocyte and do not readily nucleate microtubules while the egg is in metaphase (Pickering and Johnson, 1987; Combelles and Albertini, 2001).

1.3.1.1 The Spindle

In this study, the most important function of microtubules is to form and maintain the spindle. The spindle is also referred to as the mitotic or meiotic apparatus (MA) in mitosis or meiosis, respectively. Unique to M-phase of the cell cycle, the spindle organizes and divides sister chromatids in mitosis so that each daughter cell is genetically identical. In meiosis, the spindle is responsible for reducing the chromosome number to a haploid genome by first separating homologous chromosomes and then separating the sister chromatids (Karp, 1996). Abnormal chromosome complement (aneuploidy) is usually a result of defects in spindle form or function (Snustad *et al.*, 1997).

Whereas the mitotic spindle has pointed poles, an attenuated form and microtubule asters radiating from each pole, the meiotic spindle of mammals is barrel-shaped and anastral (Schatten *et al.*, 1985). The spindle is composed of 2-3 types of microtubule fibres. Although they are not present in mammalian oocytes, astral microtubules radiate out from the centrosomes in a sunburst pattern, into the region outside the body of the spindle. Astral microtubules may participate in determining the plane of cytokinesis (reviewed by Oegema and Mitchison, 1997). Polar/interpolar microtubules extend from the centrosomes/MTOC to interdigitate with polar microtubules from the opposite pole. They form a structural basket that maintains the integrity of the spindle. Finally, kinetochore microtubules extend from the centrosome to the kinetochore of the chromosome. These microtubules are necessary for chromosome movement toward the poles during anaphase (McIntosh and Hering, 1991). In animal cells, the mitotic spindle has pointed poles and an attenuated form, with microtubule asters radiating from each pole (Karp, 1996). The barrel shape of the meiotic spindle is most likely due to the organization of multiple PCM organized in a ring at each spindle pole (Combelles and Albertini, 2001; Messinger and Albertini, 1991).

Just as the shape of the metaphase spindle differs in mitosis and meiosis, the manner in which the spindles are formed is also different. In mitosis of a somatic cell, astral microtubules

radiate from each centrosome. As the centrosomes separate to opposite sides of the cell, astral microtubules elongate and increase in number in the space between centrosomes to form the early stages of the spindle. The presence of two centrosomes therefore predefines spindle polarity. As the microtubules of the spindle penetrate into the space previously occupied by the nucleus, the free ends of some of the microtubules are "captured" by a kinetochore on a condensed chromosome (reviewed by Brunet *et al.*, 1999). Microtubules from opposite poles attach to each kinetochore of every chromosome. Each chromosome positions itself at the centre of the spindle in preparation of anaphase. At metaphase, the plane where chromosomes are aligned is referred to as the metaphase plate or chromosome plate. After metaphase, when the chromosomes have migrated to either spindle pole, this structure is referred to as the midbody (Schatten *et al.*, 1985).

The same cannot be said for spindle development in the mouse oocyte. Numerous acentriolar MTOCs aggregate into a ring at the meiotic spindle pole to form the meiotic spindle (Maro *et al.*, 1986a; Messinger and Albertini, 1991). At metaphase I and II, conditions within the oocyte are unfavourable to form astral microtubules whereas the presence of meiotic chromosomes appear to stabilize microtubules (Maro *et al.*, 1986b). The net effect is that any PCM near the condensed chromosomes tends to nucleate stable microtubules only towards the chromosomes, which then forms the anastral spindle (Pickering and Johnson, 1987). The chromosomal influence on microtubules is important because it helps minimize abnormalities of spindle organization that could lead to aneuploidy (Pickering and Johnson, 1987). Indeed, metaphase is a checkpoint of the cell cycle, where a chromosome not properly aligned along the metaphase plate emits a signal to delay further progression of the cell cycle (Karp, 1996). Paradoxically, a bipolar spindle will develop from asters in mouse cytoplasts lacking chromosomes, indicating that the influence of the chromosomes or chromatin is not obligatory (Brunet *et al.*, 1998). In this case, formation of a bipolar spindle may be a random process resulting from microtubule-microtubule interactions of microtubules emanating from MTOCs. Chromosomes may contribute to localizing and stabilizing the spindle in the area near the genetic

material while the formation of the spindle itself may be a result of microtubule interactions (Brunet *et al.*, 1998; Karp, 1996).

1.3.1.2 The Dynamic Nature of Tubulin

Microtubules exist in a highly dynamic state and are continually being assembled and disassembled. This is termed dynamic instability (Gelfand and Bershadsky, 1991). Even within the spindle, where the plus ends of kinetochore microtubule are connected to kinetochores while the minus ends are embedded in the PCM of the MTOC, tubulin subunits are continually lost and added to each end of the microtubule (Karp, 1996). The extent and spatial organization of polymerization depends upon many parameters such as the level of free tubulin dimers, the presence of nucleating and stabilizing molecules, the ambient environment (pH, GTP levels; Gelfand and Bershadsky, 1991; Karp, 1996) and temperature (Pickering and Johnson, 1987). The ease of microtubule assembly and disassembly allows cells to rapidly remodel the structure of the cytoskeleton in response to environmental changes or progression of the cell cycle. In the mouse egg, tubulin dimers are recruited from the cytoskeleton to form the spindle at metaphase (Albertini, 1992). Similarly, the metaphase spindle is dismantled after activation and those same tubulin dimers form an intricate latticework in the pronucleate egg, characteristic of the interphase (Albertini, 1992).

Microtubules are particularly sensitive to temperature change, with a fall in temperature favouring depolymerization (Pickering and Johnson, 1987). This is significant for the culture of ovulated eggs, which are arrested at metaphase II. In many mammals, exposure to room temperature and below leads to progressive spindle disassembly and dispersal of the chromosomes from the metaphase plate to around the cell cortex (mouse, Pickering and Johnson, 1987; pig, Liu *et al.*, 2003; human, cow and sheep, reviewed by Liu *et al.*, 2003). These changes occur even after brief periods of cooling and are more severe with lower temperatures and/or prolonged exposure to nonphysiologic temperatures. The efficiency of spindle recovery after re-warming appears to be species specific, with mouse eggs being the hardiest. In many, but not all

mouse eggs, the return to 37°C will restore the spindle. Nevertheless, some eggs will form multipolar spindles and disorganized microtubule arrays around clusters of chromosomes. Limited spindle recovery has been reported in human, bovine, sheep and pig oocytes (reviewed by Liu *et al.*, 2003). This is important in this study since it underscores the importance of minimizing the time that gametes spend outside the animal or incubator.

1.3.2 Actin

Each strand of actin is made up of actin protein monomers, called G-actin (globular actin). In the presence of ATP, G-actin can polymerize in a head-to-tail manner. The actin monomer binds ATP before being incorporated into the growing polymer. At some point after incorporation, ATP is hydrolyzed to ADP. Microfilaments are comprised of two strands of actin wound around each other in a double helix. In this state, microfilaments are also called actin filaments or F-actin (Karp, 1996). Actin filaments can be organized into highly ordered arrays, loose ill-defined networks or tightly held bundles. Within a cell, there is a dynamic equilibrium between the monomeric and polymeric forms of actin. For clarity, actin refers to F-actin or microfilaments and G-actin will be referred to as actin monomers in this text. While actin monomers can polymerize spontaneously *in vitro*, these filaments are unable to interact with each other or form an organized structure. Actin-binding proteins are necessary for actin filaments to perform useful activities. These proteins can serve diverse functions such as sequestering actin monomers, cross-linking filaments, blocking polymerization and linking microfilaments to the membrane (Bretscher, 1991). The proteins involved in linking microfilaments to the membrane will be discussed here, as this function is involved in spindle positioning and cytokinesis.

In the metaphase II egg, actin filaments are concentrated at the cell cortex with an area particularly rich in actin overlying the spindle. This domain is free of the microvilli and cortical granules that characterize the rest of the egg cortex (Maro *et al.*, 1984; Connors *et al.*, 1998). This domain develops during meiotic maturation, following GVBD. The development of the

actin-rich domain depends on the interaction of chromosomes or chromosome-associated material with the oocyte cortex. When eggs are treated with microtubule-disrupting drugs, the chromosomes become scattered throughout the oocyte. As each chromosome moves towards the cortex, an actin-rich domain develops over it (Maro *et al.*, 1986b; Connors *et al.*, 1998). This domain may also be necessary to maintain the spindle at the cortex in metaphase II (Kim *et al.*, 1996).

Actin filaments are also involved in rotating the meiotic spindle to an orientation perpendicular to the cortex during activation (Zhu *et al.*, 2003). The actin cytoskeleton has also been implicated in spindle migration and anchorage (Longo and Chen, 1985).

1.3.2.1 Formins – Actin Binding Proteins

While there are many actin-binding proteins (reviewed by Revenu *et al.*, 2004), this work will focus on formins, since they have been implicated in spindle positioning. Formins or FH proteins, are members of a family of actin binding proteins that nucleate straight microfilaments. Present in almost all organisms, they organize cytoskeletal changes required for a diverse array of functions, including female germ cell development (Leader *et al.*, 2002). Using a knockout mouse model, the formin protein Fmn2 was shown to be central to the regulation of microtubule-independent chromatin positioning and asymmetrical spindle positioning. Oocytes from $Fmn2^{-/-}$ mice cannot correctly position the metaphase spindle at the oocyte cortex during meiosis I. These eggs are ovulated arrested at metaphase I, containing a central spindle with a uniform cortical F-actin array, a barrel-shaped spindle and chromosomes aligned at the metaphase plate (Leader *et al.*, 2002). Because the oocytes are ovulated in metaphase I, subsequent fertilization results in a high proportion of polyploid embryos, manifested as recurrent pregnancy loss and subfertility. The metaphase I block could be rescued when Fmn2 mRNA was microinjected into the oocyte, suggesting that Fmn2 helps to generate polarity in the mammalian egg (Leader *et al.*, 2002).

It is still unclear if Fmn2 is itself involved in spindle positioning or is required simply for progression through metaphase I such that loss of Fmn2 arrests the oocyte in metaphase I before

asymmetric spindle positioning. Whereas chromosomes will migrate to the cortex when the spindle is disrupted in wildtype oocytes, chromosomes in $Fmn2^{-/-}$ eggs were unable to do so (Leader *et al.*, 2002). This indicates that the machinery for the positioning of the DNA-spindle apparatus is defective in $Fmn2^{-/-}$ oocytes. However, it is still not clear if this deficit is with positioning or docking. In other organisms, evidence suggests that formins are necessary for linking the DNA-spindle apparatus to the cell cortex (reviewed by Evangelista *et al.*, 2003).

1.3.2.2 Cytokinesis – Dividing the Cytoplasm

Cytokinesis refers to the division of cytoplasm following mitosis or meiosis in a cell (Karp, 1996). In mitotic animal cells, an indentation or furrow forms at the surface of the cell along the equator. During telophase, the furrow moves inward, dividing the cell in half. It is believed that a structure called the contractile ring provides the force necessary to cleave the cell. The contractile ring is made up of actin microfilaments recruited from the same G-actin subunits that were previously part of the cytoskeleton. The filaments are aligned parallel to the cleavage furrow and are believed to slide over one another, driven by small force-generating myosin II filaments (Sanger and Sanger, 2000). As the contractile ring tightens, the furrow continues to deepen until the opposing surfaces make contact with each other, dividing the cell.

The mechanism that determines the site of cytokinesis and contractile ring formation is highly debated. Much of the knowledge of cleavage furrow induction has been derived from Rappaport's work in marine invertebrate eggs (reviewed by Oegema and Mitchison, 1997). In normal cytokinesis, the location of the mitotic/meiotic apparatus (MA) determines where the furrow will form (Rappaport, 1981). In other words, the cleavage furrow bisects the spindle in the same plane previously occupied by the chromosomes at metaphase, perpendicular to the long axis of the spindle. This ensures that the two sets of chromosomes are ultimately separated into two cells.

Currently, there are four theories that model the induction of the cleavage furrow. Based primarily on results from mammalian somatic cells, the spindle midzone model hypothesizes that

proteins remaining in the midzone after chromosome segregation emit a signal to stimulate the cortex to form a contractile ring that would converge at the midzone (reviewed by Oegema and Mitchison, 1997). This theory does not take into account the fact that a cleavage furrow will develop between two asters without an intervening spindle – the so-called Rappaport furrow. Furthermore, when one aster is prevented from developing, the cleavage furrow does not form at the midzone but at a position closer to the anastral pole (reviewed by Yoshigaki, 2003). The other models are based on astral microtubules affecting characteristics at the cell cortex. (For a description of astral microtubules, see 1.3.1). The minimum signal molecule hypothesis postulates that there is a general increase in cortical contractility during M-phase and that astral microtubules decrease this cortical contractility. The cleavage furrow develops midway between spindle poles because the aster relaxation signal is minimal there (reviewed by Yoshigaki, 2003; Oegema and Mitchison, 1997). The opposite theory, the maximum signal model, proposes that the asters create a signal to stimulate cortical contractility. This signal would be at a maximum where the asters overlap, midway between spindle poles, leading to cleavage furrow formation (reviewed by Oegema and Mitchison, 1997. Finally, the free molecule model proposes that astral microtubules extending into the cortex cause directional movement of membrane proteins or "free molecules" towards these astral microtubules. The accumulation of these membrane proteins triggers the formation of the contractile ring microfilaments within the cortex (Yoshigaki, 2003).

With the exception of the spindle midzone model, all the models for contractile ring formation rely on an effect from astral microtubules. However, the meiotic spindle in the mouse and other mammalian species is anastral. This suggests that the mechanism for inducing cleavage furrow in the mouse and other species possessing an anastral spindle is different from the above hypotheses.

1.3.3 Cytoskeletal Events at Egg Activation

The act of fertilization or activation is associated with several changes to the actin and

tubulin cytoskeleton. These changes demand tight temporal and spatial control to allow the events of activation to proceed normally. At ovulation, the majority of tubulin is polymerized into the metaphase II spindle. With the exception of the spindle, the rest of the milieu of the egg is not conducive to microtubule polymerization (Albertini, 1992). The fist polar body is in the perivitilline space and may or may not have degenerated. The actin network is localized to the cortex with an area free of microvilli but rich in actin lying over the spindle (Maro *et al.*, 1984; Connors *et al.*, 1998; Kim *et al.*, 1996).

The spindle in the MII egg is docked to the oocyte cortex, tangential to the oolemma (Fig. 5). Classically, the spindle is described as barrel-shaped, acentriolar and anastral in the human, mouse, horse and cow (reviewed by Tremoleda *et al.*, 2001; human Kim *et al.*, 1998). A recent report suggests that the spindles of mouse oocytes ovulated *in vivo* are less barrel-shaped than their *in vitro* matured counterparts, with more pointed or tapered poles and a smaller overall size (Sanfins *et al.*, 2003). The metaphase spindle is imperative for activation – when the spindle is disrupted with drugs that inhibit microtubule polymerization, activation cannot proceed (Kubiak *et al.*, 1993; Winston *et al.*, 1995).

The first indicator of activation is a marked increase in spindle birefringence (Liu *et al.*, 2000), reflecting an increase in order within the spindle. Two cytoplasmic protrusions appear in the plasma membrane, each overlying a spindle pole (Maro *et al.*, 1984; Liu *et al.*, 2000). The spindle then rotates 90° towards one protrusion while the other protrusion regresses so that the long axis of the spindle is perpendicular to the oocyte cortex (Maro *et al.*, 1984; Schatten *et al.*, 1985; Liu *et al.*, 2000).

As the egg enters anaphase, the chromosomes separate along the spindle. A cortical actin ring forms from the actin-rich region above the spindle, along the same plane formerly occupied by the metaphase plate. This creates an indentation of the cell surface at the spindle equator (Maro *et al.*, 1984). This indentation deepens to a furrow as the actin ring contracts, eventually pinching off the second polar body. One set of chromosomes with a minimal amount of

Figure 5: Cytoskeletal events at egg activation. A. At MII, the spindle (red) is docked to the oocyte cortex, tangential to the oolemma with an area rich in actin over the spindle (blue). B. The spindle rotates 90°. C. As the egg enters anaphase, the contractile ring (dotted blue line) develops from the actin-rich region above the spindle, pinching off the second polar body. D. The spindle remnants persist for an extended period of time as a midbody. The chromatin decondenses to form one a pronucleus (green).

A.

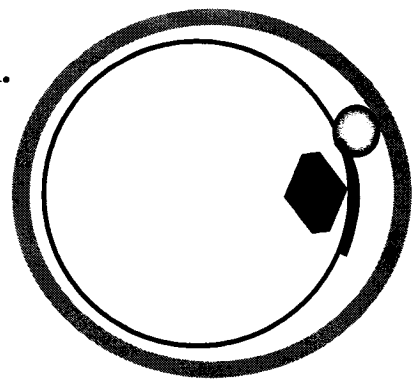

B.

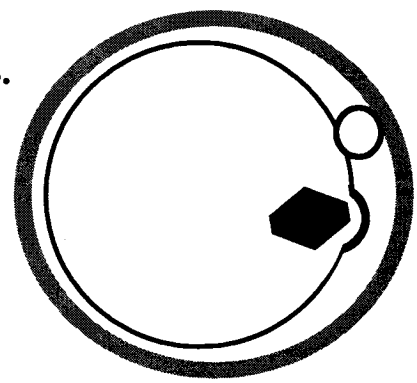

C.

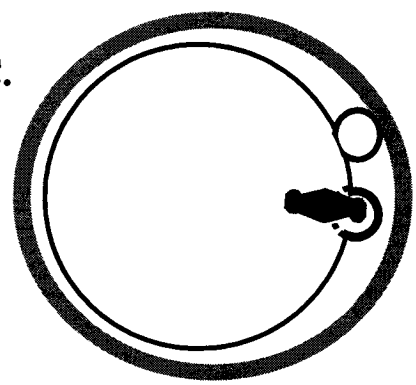

D.

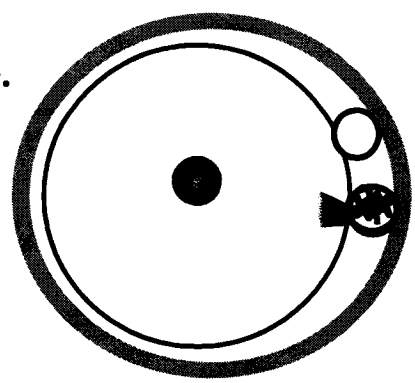

cytoplasm contained within the actin-rich membrane make up the polar body. Evidence suggests that the first polar body of *in vivo*-matured eggs is smaller than those of eggs matured *in vitro* (Sanfins *et al.*, 2003). This may also be the case for *in vitro* conditions leading to second polar body emission, however this has not been investigated implicitly. The remaining spindle and cortical actin ring are disassembled, although the spindle remnants, including microtubules, persist for an extended period of time as a midbody, spanning the junction between the egg and polar body (Maro *et al.*, 1986a).

Following the release from metaphase arrest and as the egg progresses through the cell cycle towards interphase, the cytoplasm becomes more permissive for microtubule polymerization. Maternal and paternal chromatin (in the case of fertilization) decondenses and the nuclear membrane re-forms so that the cells develop one or more pronuclei. In the mouse, multiple microtubule asters nucleated from foci of PCM develop throughout the cytoplasm. Some foci are associated with the pronuclei but in the mouse, the base of the sperm does not nucleate astral microtubules. The pronuclei enlarge and move towards the centre of the egg in a microtubule- and microfilament-dependent manner and the asters expand to fill the entire cytoplasm with a fine latticework of microtubules (Maro *et al.*, 1984; Schatten *et al.*, 1985). Pronuclear fusion is never observed; at the end of interphase, the chromosomes condense separately and assemble on a single, anastral spindle (Schatten *et al.*, 1985; Maro *et al.*, 1984).

1.3.3.1 Spindle Migration: A Putative Role for Formins

Despite more than 20 years of research on polar body formation (Maro 1985), the mechanism leading to asymmetrical division is still under investigation. Migration of the spindle to an eccentric position at metaphase I and maintaining this eccentric position at metaphase II determines the plane of the cleavage furrow and therefore the size of the polar body (Verlhac *et al.*, 2000b). Spindle migration depends on actin (Longo and Chen, 1985; reviewed by Gallicano, 2003). How the spindle migrates to the cortex and the direction of migration is now an area of active research. Maro and Verlhac (2002) have proposed that the nucleation of a network of

straight microfilaments by formin2 at the cortex could interact with an unidentified actin binding protein associated with the chromosomes in metaphase I to move the spindle to its eccentric location. A slight asymmetry in the position of the GV (and therefore also of the spindle) would lead to more chromosome-actin interactions on the side closer to the cortex. This would favour spindle movement along the shortest path to the cortex. The direction of movement would be along the long axis of the spindle, where resistance from the cytoplasm is weakest. They propose that as the spindle moves more eccentrically, actin-chromosome interaction would be increased, favouring movement towards the cortex (Maro and Verlhac, 2002). They further propose that the chromosomes would induce the cortical domain, rich in actin and devoid of microvilli as they move closer to the cortex. Because there appears to be a maximum distance at which the cortical reorganization can be induced, the cortical domain forms gradually as the chromosomes move towards the cortex. They then suggest that stabilization of the actin network could concentrate formin2 to the cortical domain, possibly contributing to the local reorganization of the actin network and recruiting microfilaments from microvilli into the cortical domain (Maro and Verlhac, 2002). In this manner, the putative role for formin2 is not only involved in spindle migration but also in differentiation of the cortical domain (Maro and Verlhac, 2002).

1.4 CSF AND OTHER SIGNALING MOLECULES IN EGG ACTIVATION

1.4.1 What is CSF?

What arrests the oocyte in MII before fertilization and prevents the relatively rapid re-entry into interphase that follows metaphase in somatic cells? Cytostatic factor (CSF) is believed to maintain arrest of ovulated oocytes until after fertilization or parthenogenetic activation (Haccard *et al.*, 1993; Masui and Markert, 1971; Abrieu *et al.*, 2001; Kubiak *et al.*, 1993). Using eggs from the leopard frog *Rana pipiens* as a model, Masui and Markert (1971) demonstrated that injection of cytoplasm from a mature oocyte into one blastomere of a two-cell embryo would arrest its cleavage. Further, the blastomere was arrested at metaphase with a spindle

characteristic of meiotic metaphase II (Masui and Markert, 1971). The hypothetical substance that mediated this activity was named "cytostatic factor" (CSF). It was postulated that it was responsible for the second meiotic metaphase arrest of vertebrate unfertilized eggs (reviewed by Maller *et al.*, 2002). Accordingly, the term CSF-arrested oocyte is synonymous with unfertilized egg while CSF arrest and metaphase II/MII arrest are likewise interchangeable (reviewed by Tunquist and Maller, 2003). By the definition set out by Masui and Markert, the true mediator of CSF should be specific to oocytes arrested at MII and should be inactivated during egg activation. Zygotes arrested by CSF should acquire similar cytological and physiological properties of the unfertilized egg (Masui and Markert, 1971). In other words, they should develop an anastral spindle with condensed chromosomes aligned at the equator and the cell surface should form microvilli that would be absent in blastomeres undergoing mitosis. Finally, inhibition of CSF should be reversible such that CSF-arrested blastomeres would resume the cell cycle when artificially activated, as would unfertilized eggs (Masui and Markert, 1971). CSF activity appears after MI, gradually increases and remains high as oocytes mature, but abruptly decreases shortly after fertilization and does not reappear in cleaving zygotes (Masui and Markert, 1971).

By definition, CSF does not describe a single molecule or protein. Rather, it is an activity found in the egg. Many proteins in the oocyte have CSF activity including Mos, MAPK, and Cdk1 (Yew *et al.*, 1993; Colledge *et al.*, 1994; Hashimoto *et al.*, 1994 Huang *et al.*, 1995). Activation of the Mos-MAPK pathway has been implicated as important for CSF arrest (Yew *et al.*, 1993; Colledge *et al.*, 1994; Hashimoto *et al.*, 1994; Huang *et al.*, 1995). This has been studied most thoroughly in *Xenopus* oocytes, where Mos, MEK, and MAPK have each been shown to be essential for CSF activity. Recently, $p90^{rsk}$ has been identified as a downstream target of the MAPK pathway in CSF activity (Haccard *et al.*, 1993; Bhatt and Ferrell, 1999; Gross *et al.*, 2000). On the other hand, only a requirement for Mos has thus far been firmly established in mammals (Colledge *et al.*, 1994; Hashimoto *et al.*, 1994).

1.4.2 Maturation Promoting Factor (MPF)

Initially described at the same time as CSF, maturation promoting factor (MPF) is a cytoplasmic factor that induces complete maturation when injected into immature (GV) oocytes, without the addition of other exogenous mediators of activation (Masui and Markert, 1971). MPF is labile: following steps to purify and characterize it, extracts would lose MPF activity (reviewed by Masui, 2001). MPF was finally identified as a heterodimer of a serine threonine kinase, $p34^{cdc2}$ protein kinase (Cdk1) and a regulatory cyclin B subunit (Lohka *et al.*, 1988). Together, this and subsequent work has shown that MPF is the common trigger of both meiotic and mitotic metaphases. It is present in dividing cells of almost all eukaryotes and is equally effective at promoting entry into M phase irrespective of the species of recipient or donor cells. Thus, MPF is also referred to as M-phase promoting factor (reviewed by Taieb *et al.*, 1997).

1.4.2.1 MPF Signaling

Modulating the activity of Cdk1 regulates entry into mitosis or meiosis. Association/dissociation of Cdk1 with cyclin, release of inhibitory signals or proteins and activating phosphorylation or reversal of inhibitory phosphorylation all contribute to the control of MPF activity (Fig. 6). This creates molecular circuits that are capable of an all-or-nothing switch-like output to create the decisive transitions that commit the cell to resuming the cell cycle (reviewed by O'Farrell, 2001). For MPF to be active, Cdk1 must be associated with cyclin. The concentration of cyclin rises and falls by a dynamic process of protein synthesis and degradation throughout the cell cycle (Karp, 1996; Ledan *et al.*, 2001). The rate at which cyclins are synthesized and degraded, however, cannot account for the rapid response of MPF activity following activating or inhibitory signals from the cell (reviewed by O'Farrell, 2001). Furthermore, there is a pool of cyclin/Cdk1 held inactive by inhibitory phosphorylation on Thr 14 and Tyr 15 in the quiescent cell. In yeast, this occurs by the nuclear kinase Wee1, whereas a similar function is performed by the cytoplasmic kinase Myt1 in the *Xenopus* oocyte. This allows

Figure 6: MPF signaling cascade. Cdk1 associates with cyclin. Throughout the cell cycle, the concentration of cyclin rises and falls by a dynamic process of protein synthesis and degradation. Inhibitory phosphorylation on Thr 14 and Tyr 15 by Wee1 (yeast) or Myt1 (*Xenopus*) maintains a pool of inactive cyclin/Cdk1, allowing the cell to accumulate a reserve of inactive cyclin/Cdk1 complexes before beginning M-phase. The phosphatase Cdc25 removes the inhibitory kinases from Cdk1. In the mean time, a Cdk-activating kinase (CAK) phosphorylates Cdk1 at Thr161 to activate the catalytic subunit, transforming MPF into an active kinase. Once activated, MPF triggers a rapid entry into M-phase. After a lag period, high MPF activity triggers the anaphase-promoting complex (APC), which marks cyclins for proteolysis, leading to a rapid loss of MPF activity.

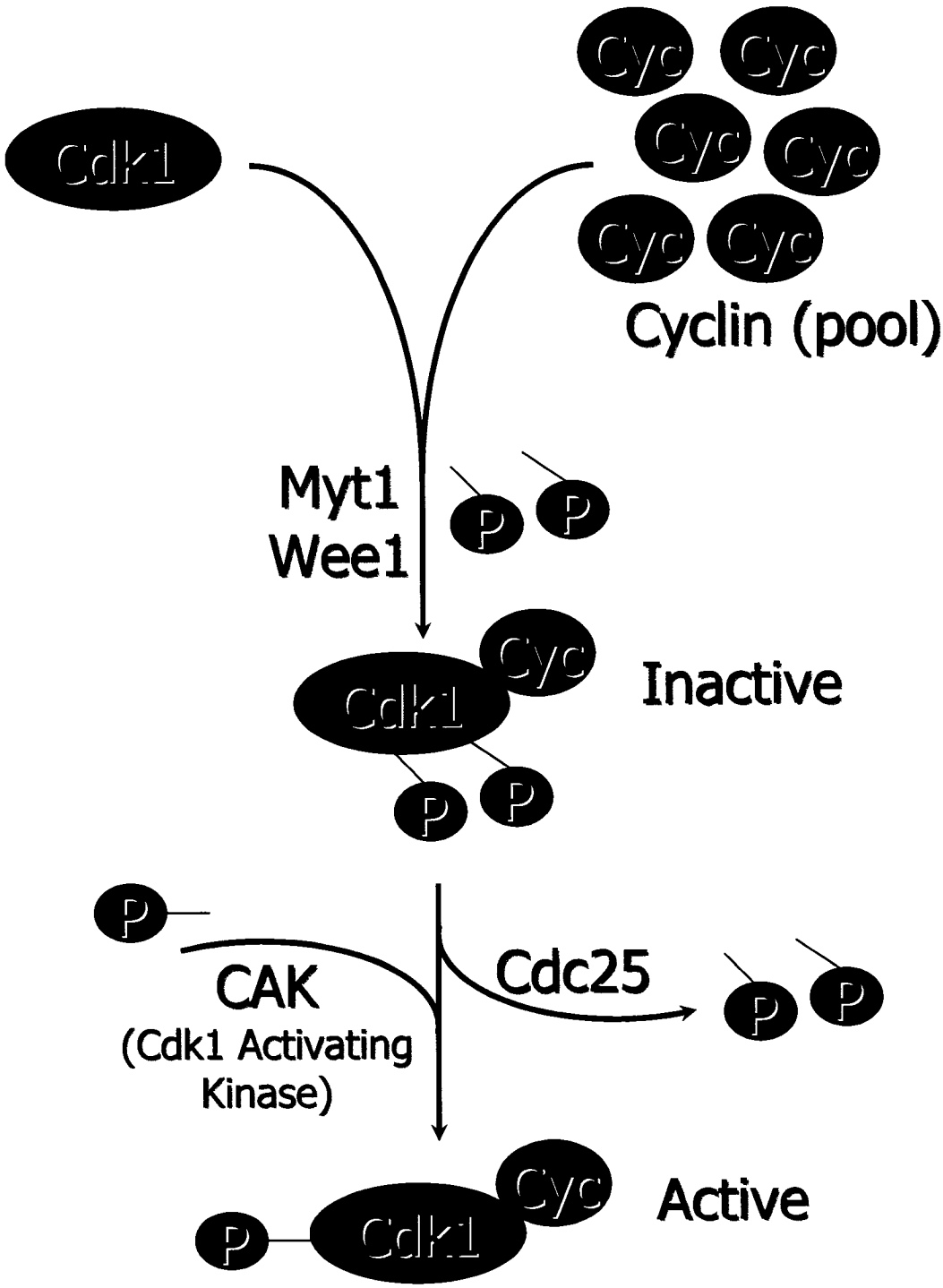
Cdk1
Cyc
Cyc
Cyc
Cyc
Cyc
Cyc
Cyclin (pool)
Myt1
Wee1
P
P
Cyc
Cdk1
Inactive
P
P
P
CAK
(Cdk1 Activating
Kinase)
Cdc25
P
P
Cyc
P
Cdk1
Active

the cell to accumulate a large reserve of inactive cyclin/Cdk1 complexes before making any commitment to M-phase. This accumulation appears to be a hallmark of G_2 in all systems. Inorder to activate MPF, the phosphatase Cdc25 removes the inhibitory kinases from Cdk1 while another kinase adds inhibitory phosphate groups onto Wee1 and Myt1, preventing further inhibition to cyclin/Cdk1. In *Xenopus* egg extracts, Cdc25 is activated by polo-like kinase (Plx; Kumagai and Dunphy, 1996). In the mean time, a Cdk-activating kinase (CAK) phosphorylates Cdk1 at Thr161 to activate the catalytic subunit, transforming MPF into an active kinase (O'Farrell, 2001). Once activated, MPF positively regulates itself, increasing MPF activation, triggering rapid entry into M-phase. After a lag period, high MPF activity triggers the anaphase-promoting complex (APC), an ubiquitin ligase that marks cyclins for proteolysis, leading to a rapid loss of MPF activity. Low MPF activity then shifts the cell from M-phase to interphase (reviewed by O'Farrell, 2001). Activities of each of the aforementioned kinases influence MPF activity. In this manner, activation of MPF is finely modulated.

1.4.2.2 MPF in Meiosis

MPF is pivotal in oocyte maturation. As discussed in 1.2.1 above, the oocyte must acquire competence so that it has the ability to undergo GVBD and progress through MI to produce a mature MII egg (de Vantery *et al.*, 1997; Hegele-Hartung *et al.*, 1999). MPF controls meiotic progression, and the net concentration of Cdk1 increases during the acquisition of competence in the mouse (Mitra and Schultz, 1996). While initial reports suggested that the relative concentration of cyclin B decreases in competent oocytes (Mitra and Schultz, 1996; de Vantery *et al.*, 1997), a recent report measuring the absolute amount of cyclin B in mouse oocytes asserts that the concentration cyclin B does indeed increase. In addition, the molar amount of cyclin is always in excess of Cdk1 (Kanatsu-Shinohara *et al.* 2000). This supports the theory that cyclin synthesis and degradation does not account for MPF activation but that the action of inhibitory and activating phosphorylations on MPF drives its activation (O'Farrell, 2001).

The GV oocyte has low MPF activity and the initiation of oocyte maturation is correlated with an increase in MPF activity, around the time of GVBD (Fig. 7). In *Xenopus*, pig, mouse or rat oocytes, MPF activation precedes GVBD (mouse, Choi *et al.*, 1991; Verlhac *et al.*, 1994; rat, Josefsberg *et al.*, 2003; pig, Kubelka *et al.*, 2002; *Xenopus*, Fisher *et al.*, 1998). Whether or not protein synthesis is required for GVBD is also species dependent: starfish and rodent oocytes do not require protein synthesis (Hashimoto and Kishimoto, 1986) while *Xenopus*, fish, primate, sheep, goat, pig and cow oocytes do require protein synthesis for GVBD (reviewed by Albertini and Carabatsos, 1998; Taieb *et al.*, 1997). Following GVBD, cyclin B is continually degraded and synthesized (Kubiak *et al.*, 1993) but cyclin synthesis is enhanced to maintain high levels of MPF activity (mouse, Winston 1997; *Xenopus*, Fisher *et al.*, 1998). MPF kinase activity gradually increases throughout maturation, reaching a plateau at metaphase I (Choi *et al.*, 1991; Verlhac *et al.*, 1994; Josefsberg and Dekel, 2002). At the MI-MII transition, MPF dips sharply when the homologous chromosomes separate and the first polar body is emitted (Hashimoto and Kishimoto, 1986; Kubiak *et al.*, 1993; Verlhac *et al.*, 1994). Cyclin ubiquitination and degradation is responsible for this fall in MPF activity, not inhibitory phosphorylation of MPF. Although some residual MPF activity persists (Winston, 1997; Iwabuchi *et al.*, 2000), this relatively quick inactivation and reactivation of MPF ensures meiotic progression and prevents entry into interphase between MI and MII (Josefsberg *et al.*, 2003).

MPF activity is high during the MII arrest of mammalian eggs and the spindle persists (Taieb *et al.*, 1997). Cyclin synthesis and degradation exists in equilibrium (Kubiak *et al.* 1993; Ledan *et al.*, 2001). During this sustained metaphase arrest, MPF is stabilized by the action of CSF. Emi1 has also been implicated in maintaining high MPF levels at the MII arrest (Reimann and Jackson, 2002). Emi1 inhibits Cdc20, the enzyme that activates the APC. This prevents APC activation, blocking cyclin destruction to maintain high MPF levels (Reimann *et al.*, 2001).

Figure 7: Relative levels of MPF and MAPK during meiosis. MPF (blue) is low in the GV oocytes and increases around the time of GVBD (whether the increase is before or at GVBD is species-dependent). MPF activity dips sharply at the MI-MII transition, returning to high levels after polar body emission and at the metaphase II arrest. MAPK activity (red), on the other hand, increases after GVBD, stays high during the MI-MII transition and is high in the CSF-arrested egg. MPF activity falls quickly at fertilization/egg activation, at the time of second polar body emission and remains low until the first mitotic division of the zygote. MAPK activity remains high in the fertilized/activated egg, falling to basal levels 4-5 h post-egg activation, at the time of pronuclear development.

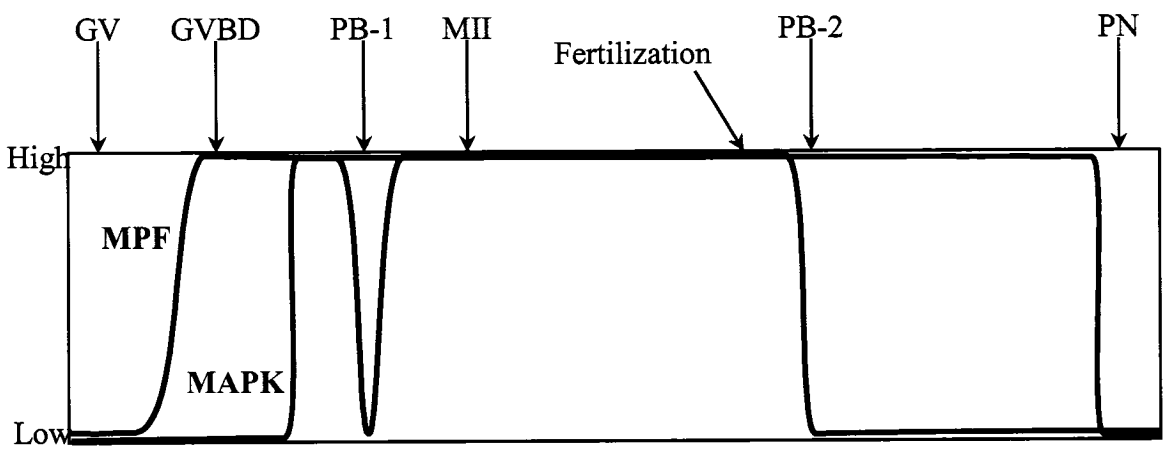
GV
GVBD
PB-1
MII
Fertilization
PB-2
PN
High
MPF
MAPK
Low

Because of its role in maintaining cyclins, there has recently been some interest in the putative role of Emi1 in CSF-mediated meiotic arrest. Further exploration is in the Discussion.

The disappearance of MPF activity after MII induces the transition from metaphase to subsequent processes and is thus a crucial indicator of activation (Hashimoto and Kishimoto, 1986). At fertilization, the increased intracellular Ca^{2+} upregulates the APC, setting the destruction of cyclin into motion (Verlhac *et al.*, 1994; Winston *et al.*, 1995). Combined with inhibitory phosphorylation of Cdk1 by Myt1 or Wee1, MPF is inactivated below a threshold and the egg is released from M-phase. By the time the second polar body is emitted, MPF activity is low (Hashimoto and Kishimoto, 1986). Aged oocytes, that is, eggs left in the oviduct for an extended period, have lower levels of MPF (Tian *et al.*, 2002). They are therefore more easily activated compared to freshly ovulated eggs, since MPF is more readily decreased to a level that permits release from metaphase arrest (Tian *et al.*, 2002). When protein synthesis is inhibited in the ovulated egg, *de novo* cyclin synthesis is likewise inhibited and the pool of cyclin decreases (Fulka *et al.*, 1994). This then decreases the pool of active MPF below a critical level, parthenogenetically activating the egg (Moos *et al.*, 1996a).

1.4.2.3 MPF and the Cytoskeleton

Just as in the mitotic cell, high MPF activity is associated with several changes to the oocyte cytoskeleton. MPF forces nuclear envelope breakdown (NEBD or GVBD in the oocyte) by phosphorylating serine residues of lamin molecules that make up the nuclear envelope (Lohka, 1998). It also promotes chromatin condensation and bipolar spindle formation, although formation of the spindle does not require full MPF activation (Polanski *et al.*, 1998). On the other hand, low MPF activity is associated with G1, S-phase and cytokinesis (Karp, 1996). Low MPF activity is also associated with chromosome decondensation (Josefsberg *et al.*, 2003), although only monovalent chromosomes will respond to the fall in MPF activity in the mouse (Hashimoto and Kishimoto, 1986).

With a rise in MPF activity, microtubules switch from an interphase to an M-phase pattern of distribution. The characteristics of M-phase microtubules are discussed in detail in section 1.3 above. Concomitant with the increase in MPF activity before GVBD, microtubules shorten (Albertini, 1992). The destruction of cyclin B, and thus the loss of MPF activity, requires an intact mitotic spindle. Agents which disrupt microtubules, such as demecolcine or nocadozole, prevent cyclin degradation and cell cycle resumption (Kubiak *et al.*, 1993; Winston *et al.*, 1995). Likewise, drugs that prevent chromatid separation maintain high MPF activity (Fulka Jr *et al.*, 1994).

Within the cell, cyclins and Cdk1 move from cytoplasmic to predominately nuclear locations at the beginning of M-phase (Pines and Hunter, 1991). In interphase (when MPF activity is low), components of MPF are uniformly distributed throughout the cell (Ciemerych *et al.*, 1998). During M-phase, a period of high MPF activity, MPF is localized to the spindle with a strong cyclin B signal on spindle poles (Goto *et al.*, 2002). This localization correlates well with the MPF functions of chromosome condensation and NEBD. While Cdk1 is only weakly detected in the cytoplasm at metaphase II of porcine eggs, enucleation of the spindle does not affect MPF kinase activity of the remaining cytoplast. In other words, MPF activity associated only with the MII spindle is not detectable (Goto *et al.*, 2002). In *Xenopus* oocytes, it is believed that nuclei and microtubule asters can independently stimulate MPF activity and they cooperate to enhance MPF activation locally (Perez-Mongiovi *et al.*, 2000).

1.4.3 Mitogen Activated Protein Kinase (MAPK)

Mitogen activated protein kinases (MAPK) are a family of serine/threonine kinases also referred to as extracellular signal regulated kinases (ERK; Boulton *et al.*, 1991; Payne *et al.*, 1991). In the mouse oocyte, ERK1 (p44) and ERK2 (p42) isoforms have been identified (Verlhac *et al.*, 1993; Verlhac *et al.*, 1994). MAPKs are thought to act at an integration point for multiple biochemical signals because they are activated by a wide variety of extracellular signals

in somatic cells. MAPKs are activated through a cascade of kinase enzymes (Fig. 8). In somatic cells (and possibly during later embryo development), the signal is mediated through the Grb2-Sos, Ras, Raf, MEK, MAPK pathway. Briefly, binding of growth factor to its receptor (a receptor tyrosine kinase or RTK) leads to the autophosphorylation of tyrosine residues on the receptor and the subsequent recruitment of the Grb2-Sos proteins. This activated complex causes the GTP-GDP exchange of Ras, which recruits the protein Raf to the membrane, activating its serine-protein kinase function. Raf then phosphorylates/activates MEK. MEK (MAPK and ERK kinase) is a dual specificity kinase, capable of phosphorylating tyrosine and serine/threonine residues. MEK then activates MAPK (Ferrel, 1999; Sun *et al.*, 1999).

In the oocyte, activation of MAPK is via Mos, a pathway unique to the oocyte (Ferrel Jr., 1999). Mos is found only in meiotic germ cells where it has been identified as an essential regulator of meiosis (Yew *et al.*, 1993; Colledge *et al.*, 1994; Hashimoto *et al.*, 1994). Mos is synthesized from existing *mos* mRNA in the oocyte (Verlhac *et al.* 1996). Active Raf cannot substitute for Mos to activate the MAPK cascade in the mouse (Verlhac *et al.*, 1996). The Mos protein kinase activates MEK by phosphorylating MEK1 at Ser218 and Ser222 (Ferrel Jr., 1999; Huang *et al.*, 1995). In turn, MEK phosphorylates specific threonine and tyrosine residues, activating 2 isoforms of MAPK (ERK1 and ERK2; Ferrel, 1999; Sun *et al.*, 1999). Once activated, MAPK targets various enzymes including 90kDa ribosomal S6 kinase ($p90^{rsk}$), cell cycle regulators and specific transcription factors (Ferrel Jr., 1999; Kalab *et al.*, 1996). The MAPK enzyme is then inactivated by dephosphorylation via protein phosphatases (PP2A; Moos *et al.*, 1996b). This cascade is subject to positive feedback. For example, microinjection of active MEK1 or ERK1 into frog oocytes can induce the accumulation of Mos protein (Ferrel Jr., 1999). Mos also stabilizes MAPK by inhibiting a phosphatase that inactivates MAPK. Without Mos, MEK cannot generate active MAPK in the mouse (Verlhac *et al.*, 2000a). In this manner, the MAPK cascade is a highly integrated signaling pathway.

Figure 8: MAPK cascade in meiosis and somatic cells. In somatic cells (and possibly during later embryo development), the MAPK signal is mediated through the Grb2-Sos, Ras, Raf, MEK, MAPK pathway. Binding of growth factor to its receptor (a receptor tyrosine kinase) leads to the autophosphorylation of tyrosine residues on the receptor and the recruitment of the Grb2-Sos proteins. This activated complex causes the GTP-GDP exchange of Ras, which recruits the protein Raf to the membrane, activating its serine-protein kinase function. Raf phosphorylates and activates MEK, which then activates MAPK. In the oocyte, activation of MAPK is via Mos, a protein unique to the oocyte. Mos is synthesized from existing *mos* mRNA in the oocyte. The Mos protein kinase activates MEK which, in turn, phosphorylates and activates MAPK. MAPK targets various enzymes including 90kDa ribosomal S6 kinase ($p90^{rsk}$), cell cycle regulators and specific transcription factors. The MAPK enzyme is then inactivated by dephosphorylation via protein phosphatases (PP2A). MEK1 can induce the accumulation of Mos protein and stabilizes MAPK by inhibiting its inactivating phosphatase.

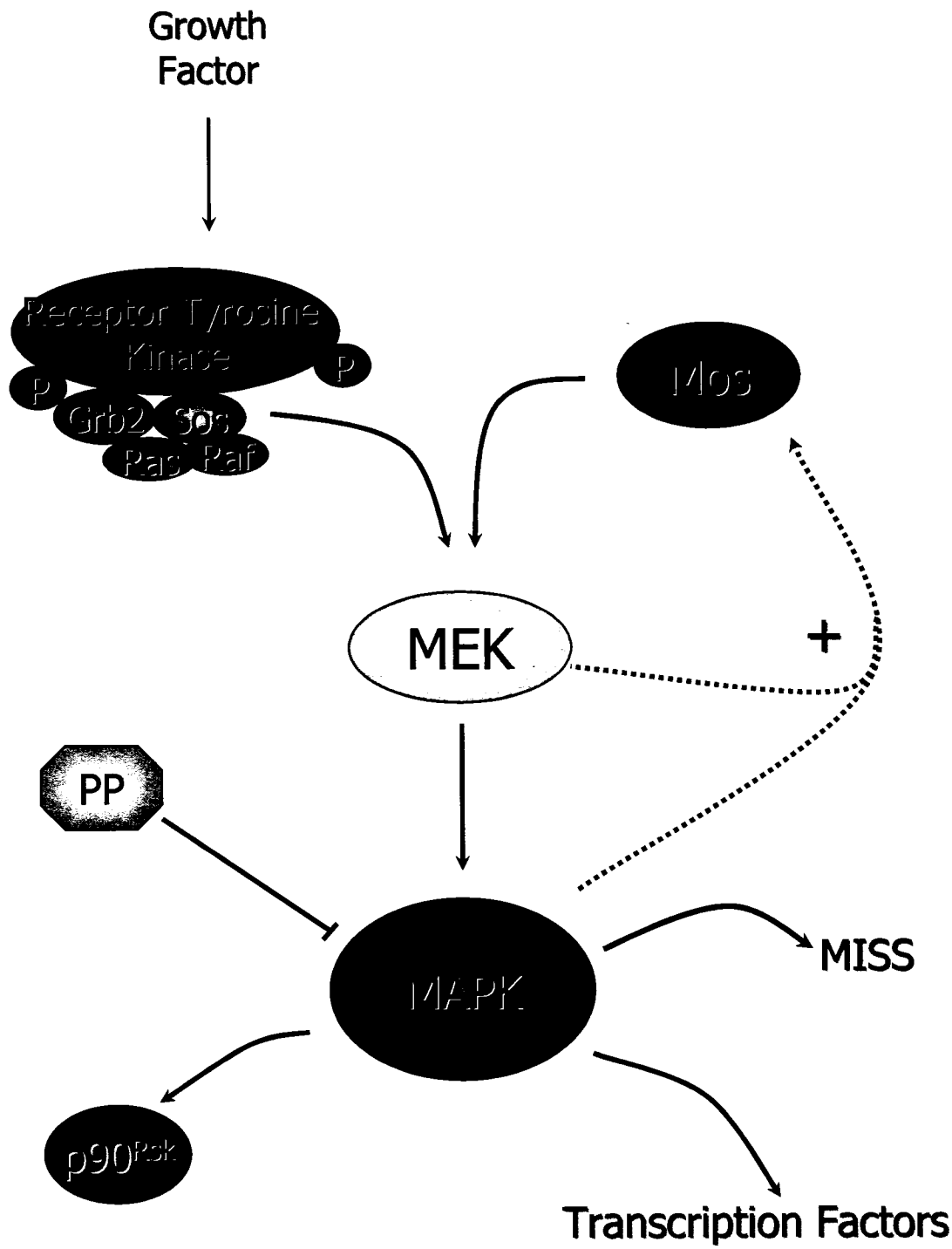
Growth Factor
Receptor Tyrosine Kinase
P
P
Grb2
Sos
Ras
Raf
Mos
MEK
+
PP
MAPK
MISS
p90rsk
Transcription Factors

1.4.3.1 MAPK in Meiosis

The capacity to phosphorylate MAPK by its upstream regulators (Mos and MEK) is required in competent oocytes to resume meiosis (Sun *et al.*, 1999). This ability depends on protein synthesis, probably to synthesize Mos from pre-existing *mos* mRNAs (Sobajima *et al.*, 1993; Verlhac *et al.*, 1993; Sun *et al.*, 1999). Depending on the species, MAPK is activated with different kinetics during maturation. In *Xenopus* and bovine oocytes, MAPK activation occurs coincident with MPF activation, at around the time of GVBD (Ferrel *et al.*, 1991; Gordo *et al.*, 2001). In *Xenopus*, the Mos–MEK–MAPK pathway is sufficient to initiate maturation. Constitutively activated MAPK is both necessary and sufficient to induce GVBD and activate MPF in this species (Haccard *et al.*, 1993). MAPK kinetics are not as clear in the pig. Different reports suggest that MAPK is activated before, after or coincident with MPF activation at GVBD (reviewed by Ye *et al.*, 2000). On the other hand, MAPK is activated about 2-3 h post-GVBD, when MPF is already active in the mouse and other mammalian models investigated (Fig. 7; mouse, Verlhac *et al.*, 1993; rat, Josefsberg *et al.* 2003). The relatively delayed activation of MAPK in mammalian animals suggests that MAPK does not regulate early meiotic events such as GVBD (Josefsberg *et al.*, 2003). Indeed, oocytes without a functional MAPK pathway undergo GVBD normally in a variety of species (mouse, Colledge *et al.*, 1994; Hashimoto *et al.*, 1994; Wianny and Zernicka-Goetz, 2000; cow, Gordo *et al.*, 2001; rat, Josefsberg *et al.*, 2003; pig, Ohashi *et al.*, 2003; Tatemoto and Muto, 2001).

MAPK activity is high through the MI-MII transition when MPF briefly falls and is maintained at elevated levels in metaphase II arrested eggs until after activation (Abrieu *et al.*, 2001; Verlhac *et al.*, 1993; Sobajima *et al.*, 1993; Haccard *et al.*, 1993). It is believed that high MAPK during the MI-MII transition suppresses DNA replication during the intervening S-phase to ultimately produce a haploid gamete (Josefsberg *et al.*, 2003).

Unlike the species-specific role of MAPK on initiation of meiosis, MAPK appears to be the universal regulator of MII arrest in amphibian and mammalian oocytes (reviewed by Gordo *et*

al., 2001). The metaphase II-arrested egg is characterized by high MAPK activity. The Mos–MEK–MAPK pathway in oocytes is thought to be a required component of the cytostatic factor (CSF) activity of eggs (Abrieu *et al.*, 2001; Haccard *et al.*, 1993). To that end, MAPK functions to stabilize MPF during the metaphase II arrest. At fertilization, the egg is released from MII arrest and MAPK activity falls. After MII release, Mos is dephosphorylated and subsequently degraded (reviewed by Tunquist and Maller, 2003). The activity of PP2A (a phosphatase that can inactivate MAPK) is upregulated at fertilization, enhancing MAPK inactivation (Winston and Maro, 1999).

In *Xenopus* and other non-mammalian species, fertilization induces the almost immediate inactivation of MPF followed by that of MAPK, 30-40 min later (reviewed by Bodart *et al.*, 2002). In the mammalian egg, the delay between MPF and MAPK inactivation is longer, about 4-5 h (Fig. 7; Verlhac *et al.*, 1993; Verlhac *et al.*, 1994; Moos *et al.*, 1995). This timecourse of inactivation correlates with pronuclear formation, indicating that MAPK may regulate the formation of pronuclei (Moos *et al.*, 1995; Tian *et al.*, 2002). When MAPK activity is maintained at high levels during activation of mouse oocytes, exit from metaphase II and second polar body emission are not affected but pronuclei do not develop (Moos *et al.*, 1995; Moos *et al.*, 1996a). Similarly, if MAPK activity is re-activated in zygotes or parthenogenetically activated eggs, the pronuclei quickly dissolve (Moos *et al.*, 1995a; Sun *et al.*, 2002). The relationship between pronuclear development and MAPK inactivation is indirect: premature inactivation of MAPK does not accelerate entry into interphase and PN formation (Abrieu *et al.*, 1997; this work).

Based on the current understanding of egg activation largely elucidated in the frog, the molecular nature of CSF activity appears to comprise the Mos/MEK/MAPK pathway. However, of the components of the MAPK cascade, only a requirement for Mos has thus far been firmly established in mammals (Colledge *et al.*, 1994; Hashimoto *et al.*, 1994). Oocytes genetically deficient in *mos* undergo germinal vesicle breakdown (GVBD) and progress through the first meiosis, but fail to arrest in MII. Instead, they undergo spontaneous parthenogenetic activation

(Colledge *et al.*, 1994; Hashimoto *et al.*, 1994), establishing a requirement for Mos activity in the maintenance CSF arrest in the mouse. Inhibition of Mos synthesis in mouse oocytes using RNA interference (RNA_i) also resulted in parthenogenetic activation (Wianny and Zernicka-Goetz, 2000). Similarly, inhibition of the Mos/MEK/MAPK pathway during rat and pig oocyte maturation parthenogenetically activated these eggs (Josefsberg *et al.*, 2003; Ohashi *et al.*, 2003).

1.4.3.2 *mos*$^{-/-}$ Oocytes Lack CSF

The development of a knockout strain of mice genetically lacking the *mos* gene (*mos*$^{-/-}$) has been a valuable tool for studying the effects of the MAPK cascade in meiosis. Oocytes from these mice completely lack MAPK activity (Choi *et al.*, 1996b). While male mice are phenotypically normal and fertile, female animals have low fertility and they frequently develop ovarian teratomas (Colledge *et al.*, 1994; Hashimoto *et al.*, 1994). Either before or just after ovulation, *mos*$^{-/-}$ oocytes parthenogenetically activate (Hashimoto *et al.*, 1994). The small number of normal offspring that arise from *mos*$^{-/-}$ mothers may be derived from eggs that were fertilized shortly after maturation and before parthenogenetic activation. On the other hand, the teratoma may develop due to parthenogenetic activation of the oocyte in the ovary (Colledge *et al.*, 1994; Hashimoto *et al.*, 1994; Hirao and Eppig, 1997).

Compared to wildtype oocytes, *mos*$^{-/-}$ oocytes initiate GVBD with roughly the same timecourse (Choi *et al.*, 1996b; Colledge *et al.*, 1994; Verlhac *et al.*, 1996). However, *mos*$^{-/-}$ oocytes fail to arrest at metaphase II and are ovulated with 2 polar bodies, consistent with parthenogenetic activation (Colledge *et al.*, 1994; Hashimoto *et al.*, 1994). This indicates that in mice, Mos (and the MAPK cascade, by extension) plays a role in MII arrest but has no effect on the initiation of oocyte maturation. After GVBD, however, meiosis proceeds at a slower rate in *mos*$^{-/-}$ oocytes (Hashimoto *et al.*, 1994). Even though MAPK activity is nonexistent in *mos*$^{-/-}$ oocytes, MPF is activated normally and spontaneously decreases at metaphase II (Verlhac *et al.*, 1996; Choi *et al.*, 1996b).

Using an optimal culturing system, only about 5% of activated *mos*$^{-/-}$ oocytes develop to the blastocyst stage while others either stop cleaving or degenerate (Hirao and Eppig, 1997; Colledge *et al.*, 1994). The limited developmental potential of *mos*$^{-/-}$ oocytes is consistent with the limited potential of parthenogenotes in general (Kaufman, 1978).

1.4.3.3 *mos*$^{-/-}$ Parthenogenotes have a Specific Phenotype

Oocytes lacking a functional MAPK cascade not only activate spontaneously, but the parthenogenotes exhibit a distinctive set of phenotypes. In one report, the first polar body of 20-30% of *mos*$^{-/-}$ oocytes was at least twofold larger than normal, resembling a mitotic-like cleavage in half the affected oocytes (Choi *et al.*, 1996b).

Hirao and Eppig (1997) identified three classes of parthenogenetically activated *mos*$^{-/-}$ eggs, which they termed Class I-III. Class I parthenogenotes include oocytes with up to 2 polar bodies. The defining characteristic of this class is that both the oocyte and polar body are comparable to normal unfertilized eggs or fertilized eggs at the one-cell stage. Pronuclei are not necessarily present. Class II and III parthenogenotes appear to have undergone atypical divisions. Class II parthenogenotes encompass a diverse phenotype, including oocytes with an extremely large polar body (Choi *et al.*, 1996b) or oocytes that have undergone fragmentation. Class III parthenogenotes appeared to have undergone mitotic-like division and are normal 2-cell stage embryos, with a nucleus in each blastomere (Hirao and Eppig, 1997). Other methods to ablate Mos (i.e. dsRNAi) yield the same phenotypes, suggesting that the CSF activity and regulation of polar body size are universal features of Mos in meiosis (Wianny and Zernicka-Goetz, 2000). Parthenogenetic activation was also observed when the Mos/MEK/MAPK pathway is prevented during maturation of other species (pig, Ohashi *et al.*, 2003; cow, Gordo *et al.*, 2001).

1.4.3.3.1 Etiology of Phenotype in *mos*$^{-/-}$ Oocytes: MAPK Matters

The precise etiology of three distinctive *mos*$^{-/-}$ phenotypes is unknown. The absence of MEK and MAPK activities during meiosis I are believed to be the cause, since the phenotype can

be rescued by expressing exogenous Mos during maturation in these oocytes (Verlhac *et al.*, 2000b). Even before the development of the *mos*$^{-/-}$ mouse, Mos kinase was suspected to be involved in the reorganization of microtubules and spindle formation (reviewed by Vande Woude, 1994).

The derivation of Class I oocytes is most certain. Following MII, these oocytes probably become activated, producing a second polar body. Those oocytes that do not develop a pronucleus are believed to enter a third metaphase (MIII; Verlhac *et al.*, 1996). MIII is characterized by long, interphase-like microtubules that form a monastral spindle around partially decondensed chromosomes. MIII oocytes remain arrested for at least 10 h, not because they have developed CSF activity but because their spindle is nonfunctional (Verlhac *et al.*, 1996). This provides evidence that the Mos/MAPK cascade controls microtubule and chromatin organization during meiosis and strongly suggests that altered MTOC function impairs proper spindle development (Verlhac *et al.*, 1996).

The lack of the Mos/MEK/MAPK pathway throughout maturation appears to disrupt the mechanisms regulating cytokinesis and normal polar body emission in MI and MII, resulting in the emission of abnormally large polar bodies. At metaphase I, the spindles of *mos*$^{-/-}$ and wildtype oocytes are indistinguishable (Verlhac *et al.*, 2000b). In *mos*$^{-/-}$ oocytes, the spindle fails to migrate to the cortex at the end of metaphase I, as is necessary to allow the emission of a small polar body. Instead, as the chromosomes separate during anaphase I, one spindle pole moves towards the cortex while the other remains stationary. This effectively elongates the MI spindle. Cleavage occurs much nearer the center of the oocyte than in wildtype oocytes, near the centre of this elongated spindle, resulting the emission of an oversized first polar body (Choi *et al.*, 1996b; Verlhac *et al.*, 2000b). Abnormal cytokinesis is therefore a result of abnormalities associated with the spindle.

Normally, high MAPK and low MPF activity (as would exist during anaphase) maintains microtubules in a highly dynamic state and the spindle size would remain constant (Verlhac *et al.*,

1996). In an example of biological irony, the spindle is unable to relocate to the cortex because it lacks MAPK activity but is then able to compensate by stretching towards the cortex because MAPK is inactive.

Class III parthenogenotes could develop during MI in one of two ways. Some *mos*$^{-/-}$ oocytes form a pronucleus immediately after MI (Araki *et al.*, 1996). Those oocytes may then directly undergo a mitotic division to become 2 cells (Hirao and Eppig, 1997). In an extension of the MAPK-mediated failure to migrate case of Class II parthenogenotes, if the MI spindle completely failed to move towards the periphery, a mitotic-like division would replace the emission of the first polar body, producing a Class III parthenogenote. These *mos*$^{-/-}$ parthenogenetic phenotypes identify metaphase spindle migration and regulation as an important role for the Mos/MAPK pathway (Choi *et al.*, 1996b).

1.4.3.4 MAPK and the Cytoskeleton

Within the oocyte, MAPK activity is associated with nuclear envelope breakdown, condensed chromosomes and short, M-phase microtubule dynamics. Similarly, low MAPK activity may also be essential for nuclear envelope formation. Okadaic acid, a specific inhibitor of phosphatase 1 and 2A, maintains high MAPK and leads to premature chromosome condensation and GVBD in the GV oocyte or precocious NEBD in the pronucleate egg (Moos *et al.*, 1995, 1996b; Sun *et al.*, 2002). Similarly, expression of MEKE, a constitutively active form of MEK, maintains high MAPK activity and prevents pronuclear development after activation, even though MPF is inactivated normally (Moos *et al.*, 1995, 1996b). MAPK can phosphorylate nuclear lamins *in vitro*, supporting a role for MAPK in nuclear envelope assembly/disassembly (Peter *et al.*, 1992).

Based on its timecourse of inactivation, MAPK has been implicated in maintaining condensed chromatin and suppressing S-phase between MI and MII (Verlhac *et al.*, 1994). Despite a nonfunctional MAPK pathway, *mos*$^{-/-}$ oocytes can mature normally, albeit at a much lower frequency (Hirao and Eppig, 1997). This suggests that qualitatively, MAPK is not essential

for nuclear dynamics and other factors are likely to be involved in these processes (Choi *et al.*, 1996a; Ohashi *et al.*, 2003). However, most *mos*$^{-/-}$ oocytes display partially decondensed chromosomes and longer interphase-like microtubules, supporting a role for MAPK in nuclear envelope and microtubular dynamics (Verlhac *et al.*, 1996).

The association between active MAPK and microtubules has been well established. Even *in vitro*, active MAPK associates with polymerized microtubules (Lu *et al.*, 2002). During meiotic maturation, MAPK associates with MTOCs (Verlhac *et al.*, 1993). In the GV oocyte (when MAPK is inactive), MAPK is diffusely located throughout the cytoplasm (Choi *et al.*, 1996a). In the pig, some MAPK becomes activated and translocates into the nucleus just before GVBD (Inoue *et al.*, 1998). Following GVBD, when active MAPK can be detected in all species, foci of MAPK develop around the condensing chromosomes, migrating to the spindle poles as the cell enters metaphase I (Verlhac *et al.*, 1993; Sun *et al.*, 2001). During metaphase I and II, MAPK colocalizes with tubulin at spindle poles and plates (mouse, Lu *et al.*, 2002; pig, Sun *et al.*, 2001; Goto *et al.*, 2002). Foci of MAPK are also noted in association with cytoplasmic MTOCs throughout the egg (Verlhac *et al.*, 1993; Goto *et al.*, 2002). This cytoplasmic MAPK accounts for up to 80% of MAPK activity in the MII egg, which is consistent with the role of MAPK activity in the local regulation of tubulin dynamics (Goto *et al.*, 2002).

High MAPK activity is associated with short microtubules throughout the cytoplasm and an anastral, eccentrically located spindle (Verlhac *et al.*, 1996; Albertini, 1992; Lu *et al.*, 2002). As discussed above, the microtubules of *mos*$^{-/-}$ oocytes revert to an interphase-like state between MI and MII, characterized by partial chromosome decondensation and longer microtubules (Verlhac *et al.*, 1996). The spindles appear diffuse, are often monastral (Araki *et al.*, 1996; Verlhac *et al.*, 1993) and they fail to translocate to the cortex of the oocyte (Choi *et al.*, 1996b; Verlhac *et al.*, 2000b). Similar effects have been observed in other species when MAPK is inactivated before maturation (cow, Gordo *et al.*, 2001; mouse Lu *et al.*, 2002; *Xenopus* extract,

Horne and Guadagno, 2003). These findings identify spindle formation and positioning as another important function for the MAPK pathway.

1.4.3.5 Downstream of MAPK in the egg

1.4.3.5.1 MISS – MAPK Interacting and Spindle-Stabilizing Protein

Not only does the MAPK pathway act to stabilize MPF but it also has a role in spindle stability. Recently, a new MAPK substrate, MAPK-interacting and spindle-stabilizing protein (MISS) has been identified (Lefebvre *et al.*, 2002). This protein undergoes post-translational modifications and is phosphorylated by MAPK *in vitro*. Compared to the *mos*$^{-/-}$ oocyte, MISS is more phosphorylated in the wildtype MII oocyte, suggesting that MISS is an *in vivo* substrate of the MAPK cascade. Endogenous MISS protein is localized to the metaphase II spindle in discrete dots while overexpressed MISS-GFP localizes to kinetochore microtubules in the MII oocyte. While MISS mRNA is present from GV oocytes to early embryos, endogenous MISS protein is only stable during meiosis II. It begins to accumulate in late MI, around the time of polar body extrusion and remains high during the metaphase II arrest. At egg activation, it again becomes unstable due to a high turnover of the protein via microtubule-dependent, MAPK independent protein degradation (Lefebvre *et al.*, 2002).

While MISS is not believed to contribute to CSF, it is believed to play a role in microtubule dynamics by interacting with microtubule-associated proteins to maintain a bipolar MII spindle during CSF arrest of mouse oocytes (Lefebvre *et al.*, 2002). Interfering with endogenous MISS mRNA by double-stranded RNA interference (dsRNAi) or antisense RNA interference (asRNAi) in the GV oocyte does not affect GVBD, first polar body emission or the first 2 mitotic divisions. Without MISS, spindle disorganization occurred at metaphase II, characterized by a loss of spindle bipolarity and the presence of cytoplasmic asters without an effect on MPF activity (Lefebvre *et al.*, 2002). The phenotype could be rescued by injection of myc-tagged MISS RNA. The phenotype of MISS null oocytes was similar to those *mos*$^{-/-}$

oocytes that had arrested in metaphase III with a monopolar spindle. The similarities between *mos*$^{-/-}$ and MISS-ablated oocytes could be due to MISS, which is not fully phosphorylated in *mos*$^{-/-}$ oocytes and is probably not active. This suggests that MISS stabilizes the spindle during MII/CSF arrest. This is the first example of a physiological substrate for MAPK that is stabilized only in MII and that specifically regulates MII spindle integrity during CSF arrest (Lefebvre *et al.*, 2002).

1.4.3.5.2 SPIN

Another protein linking the MAPK pathway to microtubule networks is SPIN (Oh *et al.*, 1998). Biosynthesis of this protein occurs from maternal transcripts until about the 2-cell stage of mouse oocytes. SPIN undergoes MAPK-dependent and MAPK-independent post-translational modifications that mark oocyte meiotic maturation. While SPIN itself does not have a MAPK target sequence, the MAPK-dependent phosphorylation is likely from a protein downstream of MAPK (Oh *et al.*, 1998). The MAPK-dependent modification may help SPIN localize to spindle poles of oocytes in metaphase. In *mos*$^{-/-}$ oocytes, which lack MAPK-dependent phosphorylation of SPIN, a variable but weak association with the spindle is apparent, despite equivalent immunoreactivity within these oocytes. This variability may account for the variability of phenotype in *mos*$^{-/-}$ parthenogenotes and the less organized spindle observed in these oocytes (Oh *et al.*, 1998).

1.4.3.5.3 p90^{rsk} – Missing Link Between MAPK and MPF?

Another physiological substrate of MAPK in oocytes is p90^{rsk} (ribosome S6 kinase; Kalab *et al.*, 1996; Fan *et al.*, 2003). This protein kinase has two kinase domains. The N-terminal domain is required to phosphorylate substrates while the C-terminal domain contains a MAPK-docking site and is necessary for full kinase activity (Gavin and Nebreda, 1999; Fan *et al.*, 2003). p90^{rsk} is partially phosphorylated by a MAPK-independent mechanism (probably autophosphorylation) but MAPK-dependent phosphorylation is required for full activation (Fan *et*

al., 2003). MAPK is the major, if not exclusive kinase able to phosphorylate $p90^{rsk}$ for full activation (Kalab *et al.*, 1996). The activity of $p90^{rsk}$ is regulated by MAPK and protein phosphatases (Fan *et al.*, 2003). Following egg activation, phosphatases that inactivate $p90^{rsk}$ are activated, necessitating continuous MAPK activity to maintain maximal $p90^{rsk}$ activity (Kalab *et al.*, 1996). The presence of active $p90^{rsk}$ during meiosis is therefore strictly correlated with active MAPK: full activation of $p90^{rsk}$ occurs after GVBD and lasts until the time of pronuclear formation (Kalab *et al.*, 1996; Fan *et al.*, 2003).

MAPK and $p90^{rsk}$ also share a similar pattern of intracellular distribution. Perhaps this is because inactive $p90^{rsk}$ and MAPK are in a complex that dissociates upon activation of both kinases (Gavin *et al.*, 1999; Bhatt and Ferrel, 2000). In the GV oocyte, $p90^{rsk}$ is evenly distributed throughout the cytoplasm but just before GVBD, it migrates to the nucleus (Kalab *et al.*, 1996; Fan *et al.*, 2003). During MI, $p90^{rsk}$ is localized to the spindle, especially to the spindle midzone during polar body emission (Fan *et al.*, 2003). At metaphase II, $p90^{rsk}$ is present on the spindle except at the equatorial region. As the chromosomes migrate to the spindle poles in anaphase II, $p90^{rsk}$ moves to the midzone of the spindle (Fan *et al.*, 2003). Following egg activation, $p90^{rsk}$ is again distributed throughout nuclear and cytoplasmic compartments of the mammalian egg (Kalab *et al.*, 1996).

In *Xenopus*, $p90^{rsk}$ is the sole mediator responsible for establishing CSF (Gross *et al.*, 2000). Injection of constitutively active $p90^{rsk}$ into oocytes lacking MAPK activity causes CSF arrest. In *Xenopus* extracts, $p90^{rsk}$ may be fundamental for establishing cytostatic arrest, but not in maintaining it (Bhatt and Ferrel, 1999). Extracts depleted of endogenous $p90^{rsk}$ cannot establish CSF arrest in response to Mos but extracts already in CSF arrest are unaffected by $p90^{rsk}$ depletion (Bhatt and Ferrel, 1999; Gross *et al.*, 2000). Expression of the constitutively active form of $p90^{rsk}$ arrests cleaving blastomeres in a meiotic-like metaphase state with an anastral, barrel-shaped spindles (Gross *et al.*, 1999).

In *Xenopus*, $p90^{rsk}$ inactivates Myt1, the kinase responsible for inhibitory phosphorylation of MPF (Palmer *et al.*, 1998; Gavin *et al.*, 1999). This leads to a net positive effect on MPF activity and may account for the fact that a gain-of-function mutant of $p90^{rsk}$ can initiate oocyte maturation without progesterone stimulation (Gross *et al.*, 2001). Thus, $p90^{rsk}$ links the MAPK pathway to MPF activation at the onset of maturation in the *Xenopus* oocyte.

The role of $p90^{rsk}$ in mammalian meiosis is less certain. MAPK and $p90^{rsk}$ activity are necessary for the gonadotropin-induced meiotic resumption of pig oocytes (Fan *et al.*, 2003). The distinct subcellular distribution of $p90^{rsk}$ to microtubules during maturation suggests a functional role in the regulation of nuclear status and microtubule organization (Fan *et al.*, 2003). Since inactivation of MEK, MAPK and $p90^{rsk}$ leads to the interphase transition of the cell cycle, $p90^{rsk}$ activity might be necessary for maintaining the MII arrest in porcine and/or other mammalian oocytes (Fan *et al.*, 2003). As in *Xenopus* oocytes, preliminary evidence from porcine oocytes suggests that high levels of $p90^{rsk}$ may facilitate spindle formation and support cyclin B accumulation (Fan *et al.*, 2003).

1.4.4 Interrelationship between MAPK and MPF in meiosis

MPF and MAPK activity are intricately involved in controlling the events of meiotic maturation. Attempts to decipher the interplay between MAPK and MPF in meiosis in amphibians and mammals have yielded contradictory results (reviewed by Josefsberg *et al.*, 2002). Both MPF and MAPK become activated during meiotic maturation, are active in MII eggs, and are inactivated after egg activation (Fig. 7). In *Xenopus*, MAPK activity is necessary and sufficient to induce GVBD (Gotoh *et al.*, 1995). In the mouse, MPF becomes activated coincident with GVBD whereas MAPK activation is delayed until approximately 2 h after GVBD (Verlhac *et al.*, 1994). MAPK activity is high through the MI-MII transition, when MPF drops briefly (Verlhac *et al.*, 1994). Both MPF and MAPK activity are elevated in metaphase II-arrested eggs. At egg activation (fertilization or parthenogenetic activation), MPF falls to

baseline levels before second polar body emission but inactivation of MAPK does not occur until several hours after egg activation, around the time of pronuclear formation (Moos *et al.*, 1995; Zernicka-Goetz, 1995).

In mammalian oocytes, the gap between inactivation of MPF and MAPK at egg activation indicates that the decrease in MPF activity is not mediated through MAPK (Abrieu *et al.*, 2001; Moos *et al.*, 1995a; Zernicka-Goetz, 1995). Similarly, the delay in MAPK activation after MPF activation during maturation argues against a requirement for MAPK in MPF activity (Verlhac *et al.*, 1994). Although the overall level of MPF activity is reduced in *mos*$^{-/-}$ oocytes, it is activated and inactivated without the benefit of MAPK activity, suggesting that MAPK is not required for MPF activation/inactivation (Verlhac *et al.*, 1996). Diminished or unstable MPF activity is likewise observed when MAPK is absent during oocyte maturation in bovine, porcine and *Xenopus* oocytes (Tatemoto and Muto, 2001; Gordo *et al.*, 2001; Ohashi *et al.*, 2003; Dupre *et al.*, 2002). Thus, while MAPK may not be necessary for MPF activation, it may promote and fine-tune MPF activity. This is consistent with the function of CSF in stabilizing MPF at the metaphase II arrest (Masui and Markert, 1971).

The Mos-MEK-MAPK pathway is a required component of CSF activity in eggs. MAPK activity enhances cyclin B translation in MI and may modulate cyclin degradation by inhibiting the APC at MII (Moos *et al.*, 1996; Abrieu *et al.*, 1996; Gordo *et al.*, 2001), thereby stabilizing high MPF activity and metaphase arrest. MPF may in turn modulate MAPK activity. Except for *Xenopus*, MPF is activated before MAPK at meiotic maturation (reviewed by Fan and Sun, 2004). Inhibition of MPF activation at maturation prevents the activation of the MAPK cascade (Kubelka *et al.*, 2002; Josefsberg *et al.*, 2003), unless ectopic expression of Mos or constitutively active MEK is induced (Choi *et al.*, 1996a). This MPF-dependent modulation of MAPK activation may involve polyadenylation of *mos* mRNA, enhancing expression of Mos and leading to MAPK activation (Lazar *et al.*, 2002; Josefsberg *et al.*, 2003). There is a window of about 1 h at the onset of maturation when MAPK activation is sensitive to modulation by MPF, after which

MAPK activity is refractory to changes in MPF until the time of first polar body extrusion (Josefsberg *et al.*, 2003). To this end, if MPF reactivation is inhibited at the MI-MII transition, MAPK activity is unaffected (Josefsberg *et al.*, 2003). Similarly, the decrease in MAPK activity after activation cannot occur when the decline of MPF activity is prevented with microtubule disrupters (Moos *et al.*, 1995). Taken together, this evidence suggests that MAPK and MPF work in concert to finely modulate the activity of one another, ensuring that the events of meiosis are executed with precision.

1.4.5 Disruption of MAPK and MPF

1.4.5.1 U0126 Parthenogenetically Activates Eggs by Inhibition of MEK

U0126 is a potent and specific noncompetitive inhibitor of MEK1 and -2 (Favata *et al.*, 1998; Gross *et al.*, 2000). I have used this drug to investigate the role of the MAPK pathway in cytostatic arrest. Since MEK has no known targets other than MAPK, inhibition of MEK effectively and specifically inhibits MAPK (DeSilva *et al.*, 1998). We have found that mouse eggs treated with U0126 parthenogenetically activate, supporting a role for MAPK in maintaining metaphase II arrest (Phillips *et al.*, 2002a). Furthermore, the phenotypes of these parthenogenotes are indistinguishable from *mos*$^{-/-}$ parthenogenotes. Whereas the specific phenotypes of *mos*$^{-/-}$ parthenogenotes develop due to spindle alterations in MI (1.4.3.3.1 above), U0126-activated parthenogenotes arise despite completely normal MI. U0126-derived parthenogenotes must therefore result from spindle defects in MII. The similarity between *mos*$^{-/-}$ oocytes and U0126-activated oocytes was the original impetus for this study.

1.4.5.2 Roscovitine Activates Eggs by Inhibition of MPF

Roscovitine is a cdc2 kinase inhibitor that is used to inhibit MPF. It is a purine derivative that acts by preventing ATP from binding but does not affect Cdk1 activation. Compared to olomoucine, another cdk inhibitor, roscovitine has a greater inhibitory potency and it has a low sensitivity towards other kinases, like MAPK (Meijer, 1996). Roscovitine has been used to

prevent meiotic progression in GV oocytes released from the ovaries of domestic animals such as the cow and pig. Roscovitine prevents spontaneous GVBD and can maintain the GV arrest for extended periods without affecting developmental potential to the blastocyst stage (Gordo *et al.*, 2001; Ju *et al.*, 2003; Mermillod *et al.*, 2000).

Roscovitine has also been used later in the meiotic cell cycle. It suppresses fertilization-induced Ca^{2+}oscillations, even in eggs where meiotic resumption had been arrested by spindle disruption, which would normally cause the Ca^{2+} oscillations to persist indefinitely (Deng and Shen, 2000). It has been reported that roscovitine is unable to parthenogenetically activate metaphase-arrested eggs (Deng and Shen, 2000; Josefsberg *et al.*, 2003), but that it can facilitate other methods of parthenogenesis (Gordo *et al.*, 2002; Mitalipov *et al.*, 2001). Roscovitine has also been used to inhibit MPF reactivation at the MI-MII transition (Josefsberg *et al.*, 2003).

I used roscovitine to investigate the role of MPF in cytostatic arrest. In my hands, mouse eggs treated with roscovitine become parthenogenetically activated, and a small proportion of these eggs have a similar phenotype to eggs of the *mos*$^{-/-}$ mouse, supporting a role for MPF in maintaining metaphase II arrest.

2 JUSTIFICATION AND OBJECTIVES

Of all the members of the Mos/MEK/MAPK pathway, only Mos has so far been convincingly demonstrated to be required for CSF arrest in the mouse oocyte, and whether MEK and MAPK are required for meiotic arrest in the frog oocyte has recently been questioned (Reimann and Jackson, 2002). Oocytes lacking a functional *mos* gene become parthenogenetically activated, exhibiting a characteristic set of phenotypes that include the presence of abnormally large polar bodies and mitotic-like divisions in meiosis. These phenotypes arise as a result of defects in the spindle structure and spindle positioning during meiosis I (discussed in 1.4.3.3.1, above).

It was recently shown that when activity of MEK, the upstream activator of MAPK, is inhibited with U0126 in mature MII eggs, they become parthenogenetically activated. In addition, U0126 parthenogenotes had a characteristic phenotype that was indistinguishable from that of *mos*$^{-/-}$ parthenogenotes. However, the *mos*$^{-/-}$ phenotype arises from a disruption of spindle movement during MI, so that it does not move normally to the oocyte cortex before cytokinesis and emission of the first polar body. In contrast, the U0126 phenotype arose in MII eggs where the spindle is already positioned at the cortex and merely needs to rotate prior to cytokinesis to produce the second polar body. Therefore, although a disruption of spindle function may be common to both cases, the mechanism by which a large second polar body arises in U0126 parthenogenotes must be different from that which produces the *mos*$^{-/-}$ phenotype.

Based on the presence of these phenotypes following disruption of MEK-MAPK in MII eggs, I therefore wished to discover whether the perturbation of MEK and hence MAPK activities in mature MII oocytes is sufficient to cause abnormal spindle function and abnormal cytokinesis. I also wished to examine the spindle and cytoskeletal dynamics that give rise to the U0126 parthenogenote phenotype.

That inhibition of MEK-MAPK by U0126 parthenogenetically activates MII eggs led me to look at the other major cell cycle regulator required for egg activation, MPF. In this study, I wished to inhibit MPF at MII, which then led to the use of roscovitine, a Cdk1 inhibitor. Surprisingly, roscovitine parthenogenetically activated eggs and yielded a small proportion of oocytes bearing a similar phenotype to *mos*$^{-/-}$ and U0126-activated oocytes. More strikingly, simultaneous inhibition of both MPF and MEK yielded a severe and unique phenotype, indicating dual control of spindle function by both pathways. I therefore sought to determine how inhibition of MPF, or both MPF and MEK, affected the spindle and how spindle and cytoskeletal dynamics compared to those in either *mos*$^{-/-}$ oocytes or U0126-activated parthenogenotes. This led to the following overall objectives.

2.1 OBJECTIVE

To characterize the phenotypes and activities of the key regulators of MII arrest and egg activation (MPF, MAPK) in parthenogenotes induced by pharmacological disruption of MEK-MAPK or MPF, and compare these to those of normally activated eggs (by *in vivo* fertilization, IVF, and Sr^{2+}-induced parthenogenesis).

2.2 OBJECTIVE

To determine if premature inactivation of MAPK and MPF (alone or in combination) has an effect on spindle, chromatin, and cytoskeletal dynamics that could account for the phenotypes observed.

3 MATERIALS AND METHODS

3.1 CHEMICALS AND SOLUTIONS

3.1.1 Chemicals

All components of KSOM and KFHM media (see below) were embryo culture grade or cell culture grade, and were purchased from Sigma (St. Louis). Hyaluronidase, pregnant mare's serum gonadotropin (PMSG), human chorionic gonadotropin (hCG), demecolcine, okadaic acid (OA), EGTA (ethylene glycolbis[b-aminoethyl ether]-N,N,N',N',-tetraacetic acid), Tris–HCl, leupeptin, PMSF (phenyl methylsulfonyl fluoride), ATP, p-nitrophenylphosphate, β-glycerophosphate, Na orthovanadate, Na fluoride, DTT (dithiothreitol), aprotinin, polyvinyl alcohol (PVA), MOPS (3-[N-morpholino]propane-sulfonic acid), Coomassie Blue, formaldehyde, Triton X-100, histone, Tween 20, and mineral oil were obtained from Sigma. U0126, U0124, Pepstatin, Nonidet P-40 (NP-40), roscovitine, and H-89 (N-[2-((p-bromocinnamyl)amino)ethyl]-5-isoquinolinesulfonamide, HCl) were obtained from Calbiochem (La Jolla, CA). $MgCl_2$ was obtained from VWR Canada (Ville Mont-Royal, PQ). [γ-^{32}P]ATP was obtained from Amersham (Baie d'Urfé, PQ). Myelin basic protein and 2× Laemmli sample buffer were obtained from Invitrogen Canada, Inc. (Burlington, ON).

Alexa-594 goat anti-rat, Alexa 594, phalloidin, and SyTox Green were obtained from Molecular Probes (Eugene, OR). Absolute ethanol was obtained from Corby Distilleries Ltd, (Corbyville, ON) and methanol from AnaLar (BDH). Methanol was used to dilute Alexa-594 phalloidin. All stocks were stored at –20°C.

3.1.2 Drugs

Stocks of okadaic acid (250 μM), H-89 (2.5 mM), U0126 (50 mM), U0124 (50 mM) and roscovitine (50 mM) were made in DMSO while demecolcine (1 mg/mL) was diluted in absolute ethanol. All stocks were stored at –20°C.

3.1.3 Solutions

3.1.3.1 Egg/Embryo Handling Media

Media used for embryo culture were based on KSOM mouse embryo culture medium (Lawitts and Biggers, 1993) which contained (in mM) 104 NaCl, 2.5 KCl, 0.35 KH_2PO_4, 0.2 $MgSO_4$, 1 Na lactate, 0.2 glucose, 0.2 Na pyruvate, 25 $NaHCO_3$, 1.7 $CaCl_2$, 1 glutamine, 0.01 tetrasodium EDTA, 0.03 streptomycin SO_4 and 0.16 K penicillin G. Media were supplemented with 1 mg/mL bovine serum albumin (BSA) and equilibrated with 5% CO_2 before use. For handling embryos, KFHM (KSOM flushing and handling media; pH 7.4; Lawitts and Biggers, 1993) was used wherein 21 mM $NaHCO_3$ was replaced by equimolar Hepes. A low-Hepes KFHM was used for culturing embryos on the PolScope. The Hepes concentration was decreased to 14 mM and no BSA was used (Liu *et al.*, 1999). A modified KSOM was used for sperm capacitation and *in vitro* fertilization (IVF-KSOM) in which glucose was increased to 5.56 mM and 30 mg/mL BSA was added (Summers *et al.*, 1995).

3.1.3.2 Kinase Assays

Two different kinase assays were used to measure MAPK and MPF kinase activities. The MAPK assay measured only MAPK activity of the egg lysates, while the simultaneous kinase assay measured both MAPK and MPF kinase activity concurrently in a single lysate.

The extraction buffer for the MAPK assay (modified from Sobajima *et al.*, 1993) contained (in mM) 50 Tris-HCl (pH 7.5), 15 $MgCl_2$, 5 EGTA and 1% NP-40. The extraction buffer was aliquotted and frozen at –20°C. This buffer was supplemented with leupeptin (10 μg/mL) and PMSF (100 μg/mL) at the time of egg lysis. To differentiate it from other lysis buffers (below), this buffer will be referred to as MAPK extraction buffer.

For the simultaneous kinase assay (Moos *et al.*, 1996a), eggs were lysed in a buffer containing 10 μg/mL leupeptin, 10 μg/mL aprotinin, 10 mM p-nitrophenyl phosphate, 20 mM glycerophosphate, 0.1 mM sodium orthovanadate and 5 mM EGTA. This buffer will be referred

to as kinase lysis buffer. The lysis buffer was aliquotted, stored at –20°C and thawed immediately before egg lysis. Leftover buffer was refrozen at –20°C until the next sample was taken. Any buffer remaining at the end of a timecourse was discarded so that each buffer aliquot never underwent more than eight freeze-thaw cycles.

The 4×H1 kinase buffer used in the simultaneous kinase assay contained (in mM) 48 p-nitrophenylphosphate, 180 B-glycerophosphate, 48 $MgCl_2$, 48 EGTA, 0.4 EDTA, 9.2 sodium orthovanadate, 8 NaF, 3.2 dithiothreitol, 120 aprotinin, 120 leupeptin, 80 MOPS (pH 7.2) and 4 mg/mL PVA.

3.1.3.3 Solutions for Protein Immunodetection

Eggs or zygotes were lysed according to Kanatsu-Shinohara *et al.* (2000). The protein stabilization buffer contained 20 mM Tris–HCl (pH 7.5), 100 mM NaCl, 0.5% Triton X-100, 0.5% NP-40, 1 mM PMSF, and 1 μg/ml each of leupeptin and pepstatin. This solution is referred to as protein stabilization buffer to differentiate it from lysis solutions used for the kinase assays.

Tris buffered saline (TBS) contained 10 mM Tris-HCl (pH 7.5) and 150 mM NaCl. Where noted, TBS was supplemented with 0.5% Triton X-100 (TBS-Triton) or 1% BSA. TBS supplemented with 0.02% Tween is TBST (TBS-Tween). Blotto is 5% milk powder in TBST.

3.1.3.4 Solutions for Fixation and Confocal Microscopy

Dulbecco's phosphate-buffered saline (PBS) pH 7.4, contained (in g/L): 8 NaCl, 0.2 KCl, 0.92 Na_2HPO_4, 0.2 KH_2PO_4, 0.132 $CaCl_2 \cdot 2H_2O$ and 0.1 $MgCl_2 \cdot 6H_2O$.

When actin was to be visualized, eggs were fixed in a solution containing 2% formaldehyde and 0.02% Triton X-100 in PBS. This solution is referred to as actin fixative.

Fixative for tubulin visualization was adapted from Carabatsos *et al.* (2000). It is referred to as microtubule stabilization buffer to differentiate it from the fixative for visualization of actin. It contained 2% formaldehyde, 1 μM paclitaxol, 0.5% Triton and 10 μg/mL aprotinin in TBS.

Blocking solution contained 2% each of BSA and fetal bovine serum, 0.1 M glycine and 0.01% Triton X-100 in TBS.

3.1.4 Animals and Gamete/Embryo Manipulations

3.1.4.1 Animals

All mice were obtained from Charles River, Canada. Female CF1 mice were aged 5-6 weeks. Male BDF mice, aged 8-30 weeks, were used as stud males while male CD-1 mice, aged 12-15 weeks were used for sperm collection for IVF.

3.1.4.2 Superovulation and Natural Matings

PMSG is used to mimic follicle-stimulating hormone (FSH) and human chorionic hCG is used to mimic luteinizing hormone (LH). Animals were maintained on a 12 hour light: dark cycle (7:00 am-7:00 pm). Intraperitoneal (IP) injection of 5 IU PMSG was performed at 4:00 pm, followed by an IP injection of 5 IU hCG injected 47-47.5 h later (3:00-3:30 pm). The hCG injection was timed so that it was administered before the endogenous LH surge, which would occur 15-20 h after the midpoint of the second dark period following injection of PMSG (4:00-9:00 pm). Ovulation was assumed to take place between 10 and 13 h following the hCG injection (1:00-4:30 am; Hogan *et al.*, 1986). This procedure maximizes embryo yield.

For *in vivo* fertilized zygotes, each female was caged overnight with one stud male after the hCG injection. When unfertilized eggs were required, mice were injected as above but were not caged with stud males.

3.1.4.3 Egg and Zygote Collection

Unfertilized eggs were collected 13.5-16 h post-hCG while *in vivo* fertilized zygotes were collected 20-22 h post-hCG. Females were killed by cervical dislocation. Oviducts were carefully removed and placed in 2-3 mL KFHM in a 35-mm tissue culture dish (Fisher, Pittsburgh, PA; Falcon #3001). Cumulus masses were released into 300 μg/mL hyaluronidase in KFHM by piercing the swollen ampulla with a 27 g needle under the microscope. Cumulus

masses were then mechanically and enzymatically dissociated for 6-8 minutes, until the embryos were fully denuded of adherent cumulus cells (Hogan *et al.*, 1986). Eggs/embryos were washed through at least 3 changes of KFHM to rinse away any residue of hyaluronidase prior to microdrop culture (next section).

3.1.4.4 Microdrop Culture

In order to examine development, embryos were cultured using microdrop culture according to standard techniques (Lawitts and Biggers, 1993). Briefly, 3-7 droplets of culture media (approximately 50 μL each) were placed in 35-mm tissue culture dishes and overlaid with 2-3 mL of KSOM-washed mineral oil. The dishes were pre-equilibrated in an incubator with 5% CO_2/air at 37°C and 100% humidity before use. Embryos, washed free of cumulus cells and hyaluronidase, were washed through 2-3 drops of KSOM using a mouth-operated pipet, cultured in a drop of KSOM, and the dishes were returned to the incubator. Using this method, zygotes can be cultured up to the blastocyst stage by 5-6 days post-hCG (Lawitts and Biggers, 1993).

3.1.4.5 Sperm Collection and *In Vitro* Fertilization (IVF)

CD-1 males were killed by cervical dislocation. Sperm removed from vas deferens and cauda epididymides were released into 1.5 mL tubes containing 1 mL modified IVF-KSOM and were allowed to capacitate for 1 h at 37°C, 5%CO_2/air and 100% humidity. Unmated female CF-1 mice were killed by cervical dislocation 14.5 h post-hCG. The oviducts were removed and the cumulus masses were released into KFHM. Each cumulus mass was transferred to a separate 25 μL microdrop of modified IVF-KSOM under oil pre-equilibrated at 37°C, 5% CO_2/air and 100% humidity. Following the 1 h capacitation, 500 μL of sperm suspension from the top of each tube was removed and combined in a new tube. To each microdrop containing cumulus masses, a 75 μL aliquot of motile, capacitated sperm was added for a final concentration of approximately 1 million sperm/mL. Eggs and sperm were co-incubated for 1 h and then eggs were washed free of unbound sperm in microdrops of KSOM under oil (16-16.5 h post-hCG) and cultured for 1-8 h.

A cohort group of 10-15 eggs was cultured in a separate drop and was scored hourly for morphological indicators of activation (emission of second polar body and appearance of pronuclei). The remainder of the post-IVF eggs served as a population from which eggs were selected for kinase assays. Selection was based on morphological indices of activation, as explained in 3.1.4.9 below.

3.1.4.6 Parthenogenetic activation – $SrCl_2$

Unfertilized eggs were collected as described above and denuded of cumulus cells. Eggs were transferred to 10 mM $SrCl_2$ in Ca^{2+}-free KSOM and cultured for 2 h (37°C, 5% CO_2). Eggs were then transferred to pre-equilibrated (37°C, 5%CO_2/air) microdrops of KSOM. A cohort group of eggs was cultured in a separate drop and was scored hourly for parthenogenetic activation. The remainder of the activated eggs served as a population from which eggs were selected for kinase assays. As for IVF timecourses, eggs were selected for kinase assays based on the presence of indicators of activation (3.1.4.9 below).

Strontium (Sr^{2+}) is a divalent cation that produces repetitive Ca^{2+} transients resembling those produced by fertilization (Phillips *et al.*, 2002b). It is the form of parthenogenetic activation that most resembles activation by sperm (Whittingham and Siracusa, 1978). Because the timecourse for polar body and pronuclear formation following Sr^{2+} is similar to that following IVF, this form of activation was used to produce parthenogenotes where activation most closely resembled normal egg activation by sperm. Sr^{2+} activation also has the advantage that time of activation is exactly known, as the process begins immediately after eggs are placed in $SrCl_2$ media, whereas the timing of egg activation during IVF is not precisely known. This allowed more precise comparisons of timecourses.

3.1.4.7 Parthenogenetic activation – U0126

Unfertilized eggs were collected and denuded of cumulus cells, as described above. Eggs were transferred to 50 μM U0126 in KSOM and cultured for 8 h (37°C, 5% CO_2) using standard

microdrop culture. A cohort group of eggs was cultured in a separate drop and was scored hourly for activation. The remainder of the activated eggs served as a population from which eggs were selected for kinase assays. The selection for kinase assays was done blindly.

3.1.4.8 Parthenogenetic activation – Roscovitine

Unfertilized eggs were denuded of cumulus cells (as described above). Because roscovitine appears to be oil soluble and thus is removed from culture droplets if they are maintained under oil (Phillips *et al.*, 2002a), eggs were cultured in 48-well culture plates (Nunc) containing 500 μL of media. Eggs were washed through one well of KSOM supplemented with 50 μM roscovitine and were then incubated in a second well containing the same media. Eggs were cultured for 8 h (37°C, 5% CO_2/air). This method was followed for all experiments involving roscovitine (roscovitine and U0126 were used in combination in some experiments, as specified).

3.1.4.9 Fertilization and Assessment of Egg Activation

Generally, fertilization can be confirmed by various morphological indices such as the appearance of 2 pronuclei and the second polar body, both of which were used to assess successful fertilization or egg activation in this study. Fertilization rates resulting from BDF × CF1 matings were routinely high, with animals maintained according to standard mouse breeding colony practices. Eggs fertilized *in vitro* were selected for kinase assays at various time points following sperm-egg incubation from the pool of eggs fertilized each day. Before pronuclei were visible, I assumed eggs were activated if they had two polar bodies (1-4 h post-IVF). As eggs developed pronuclei, these eggs were selected for kinase activity measurements. Fertilization could be assessed as early as 3-4 h post-sperm egg incubation by the appearance of two pronuclei, although these embryos made up a small percentage of the total pool. Pronuclei were clearly visible from 4.5 h post-sperm egg incubation onwards. This selection process excludes eggs from kinase measurement that were not fertilized during the sperm-egg incubation and would therefore

have continually high kinase activity. This approach also selects the most synchronous population of oocytes from which to construct the timecourse of kinase activity.

Likewise, parthenogenetically activated eggs were selected from a pool for kinase measurements based on the same morphological indices of activation. Before the appearance of pronuclei (either one or two), eggs were considered activated if they had two polar bodies.

3.1.5 Kinase Activity Measurement

To determine timecourses, MAPK and MPF activities were measured hourly after each form of egg activation. In some cases, measurements were also obtained at more closely spaced time points immediately after activation. Cohorts of activated eggs were scored for polar body extrusion and pronuclear appearance in parallel with each set of measurements.

3.1.5.1 MAPK Assay

MAPK activity was measured using a MBP kinase assay modified from Sobajima *et al.* (1993). At each sampling time, five eggs or zygotes were grouped together in a minimal amount of media (<1 μL) and transferred to a 1.5 mL Eppendorf tube. To confirm that the eggs were in the tube and did not adhere to the glass pipet, the media remaining in the pipet was expelled into a KSOM wash drop and examined. The eggs or zygotes in the tube were lysed in 22 μL of MAPK extraction buffer and immediately frozen at –80°C until use. The kinase reaction was initiated by the addition of ATP, MBP, and [γ-^{32}P]ATP to final concentrations of 12 μM, 136 μM/mL and 0.2 mCi/mL, respectively. The kinase reaction was carried out at room temperature for 15 min. To stop the reaction, 25 μL of 2×Laemmli sample buffer was added to each tube of lysate and each tube was boiled for at least 3 min. To ensure that each sample was assayed for an equal amount of time, addition of the master mix was staggered by 20 s intervals, as was the addition of Laemmli sample buffer which stopped the reaction in each tube. The mixtures were loaded (15 μL/lane) onto a 15% SDS-polyacrylamide running gel overlaid with a 5% SDS-polyacrylamide stacking gel. The mixtures were separated by electrophoresis until the dye-front just ran out of

the gel (200 V for 45 min–1 h). The stacking gel was removed and the running gel was stained and fixed in 45% Methanol, 45% H_2O, 10% acetic acid (v/v/v) and 2.5 mg/mL Coomassie brilliant blue for 15-20 min. Excess stain was removed by washing it in a series of washes containing 45% methanol 45% H_2O, 10% acetic acid until the protein bands could be seen. The gel was dried on filter paper (3 h, 70°C).

A sample of zygotes and freshly obtained eggs was assayed with each timecourse to act as a negative and positive control, respectively.

3.1.5.2 Simultaneous Kinase Assay

MPF kinase activity and MAP kinase activity were measured simultaneously using histone H1 and MBP as substrates in an assay modified from Moos *et al.* (1996a). Seven eggs or zygotes were grouped together in a minimal amount of media (<1 µL) and transferred to a 0.5 mL Eppendorf tube. To confirm that the eggs were in the tube and did not remain in the glass pipet, all the media from the pipet was expelled into a KSOM wash drop, as described in 3.1.5.1. The eggs or zygotes were lysed in 3.5 µL kinase lysis buffer and immediately frozen at –80°C until the simultaneous kinase assay was performed. The kinase reaction was initiated by the addition of 5 µL of master mix containing 0.01 mM H89, 0.6 mM ATP, 2.0 mg/mL histone H1, 1.0 mg/mL MBP and 150 Ci/mmol [γ-^{32}P]ATP in 50% 4×H1 kinase buffer. The reaction was carried out at room temperature and was stopped after 30 min by the addition of 10 µL 2×Laemmli sample buffer followed by boiling for at least 5 min. As described in 3.1.5.1 above, the kinase reaction was started and stopped by staggering the addition of the solutions by 20 s intervals. The mixtures were loaded onto a 15% SDS-polyacrylamide running gel overlaid with a 5% SDS-polyacrylamide stacking gel (18 µL/lane) and separated by electrophoresis until the dye-front left the gel (200 V for 45 min – 1 h). The stacking gel was removed and the running gel was stained and dried as described for the MAPK assay (3.1.5.1 above).

A sample of zygotes and freshly obtained eggs was assayed with each timecourse to act as a positive and negative control, respectively. A "blank" sample (containing only lysis buffer) was assayed with each timecourse to determine the background level of phosphorylation for MBP and histone H1.

3.1.5.3 Quantification of kinase activity

Scanning and quantification of the signal were performed by using a Typhoon 8600 variable mode imager (Molecular Dynamics, Sunnyvale, CA) and ImageQuant software (Molecular Dynamics). Signals were corrected for background by subtracting the density in the marker lane (MAPK assay) or by subtracting the density of a blank reaction mix which did not contain eggs or zygotes (simultaneous kinase assay). The values of histone H1 or MBP kinase activity for fresh eggs (MAP kinase and simultaneous kinase assays) or for egg lysates exposed to vehicle during the kinase reaction (when drug was added to kinase assay) were arbitrarily set at 100%. The values obtained in the other groups were expressed relative to this value. In both assays, the timecourse was rejected if the kinase activity of the zygote control was greater than 50% of the activity of the egg control. Using these methods, MBP kinase activity reflects the MAPK activity of the sample while histone H1 kinase activity reflects MPF kinase activity of the eggs (Moos *et al.*, 1996a).

3.1.6 Protein Immunodetection

Thirty or forty eggs/zygotes were lysed in 15 μL of protein stabilization buffer followed by the addition of an equal volume of 2× Laemmli sample buffer and boiling (Kanatsu-Shinohara *et al.*, 2000). Proteins in the lysate were separated by SDS–PAGE and were then semidry transferred onto Protran pure nitrocellulose membrane (Scheicher & Schuel, Keene, NH) using constant current so that voltage was approximately 8 V for 1.5 h. Nonspecific binding was minimized by blocking the membrane in Blotto for at least 30 min before incubating in primary antibody. The membrane was incubated overnight with 0.59 μg/mL primary antibody sheep

polyclonal IgG anti-phospho-MAPK (Upstate Biotechnology, Lake Placid, NY). The membrane was washed in TBST for 20 min at least 3 times to remove nonspecific antibody binding. The blot was then incubated for at least 1 h with secondary antibody, 0.08 μg/mL peroxidase-conjugated AffiniPure donkey anti-sheep IgG (Jackson ImmunoResearch Laboratories, West Grove, PA). The blot was again washed at least 3 times in TBST, as above. Binding was visualized by using ECL Western blotting detection reagents (Amersham Pharmacia Biotech, Buckinghamshire, England) followed by exposure to film.

The blot was washed twice in TBST and stripped to remove primary and secondary antibodies. The membrane was incubated twice in a solution of 5 M NaI and 1 mM Sodium Thiosulphate for 10 min. The membrane was then rinsed twice with TBST (5 min each) and re-blocked with Blotto for at least 1 h. The membrane was then re-probed, as above, with 1 μg/mL anti-rat MAPK RL (ERK1-CT) rabbit polyclonal IgG primary antibody (Upstate Biotechnology) and 1:3000 anti-rabbit IgG (peroxidase-linked species-specific whole antibody from donkey; Amersham Life Science) secondary antibody.

3.1.7 Confocal Imaging

3.1.7.1 Immunofluorescence

Eggs were fixed at various times post-activation by incubating the eggs in pre-warmed (30°C) microtubule stabilization buffer for 30 min. Eggs were rinsed twice in blocking solution (10 min each) at 30°C and stored in blocking buffer at 4°C until use (less than 10 h). Eggs were incubated overnight in 20 μg/mL rat anti tubulin primary antibody (Chemicon, Temecula, CA). Five rinses in blocking buffer (10 min each, 30°C) were used to minimize nonspecific antibody binding. The eggs were then incubated in 10 μg/mL Alexa-594 goat anti rat secondary antibody for 2 – 3 h at 30°C in the dark. The remainder of the procedure was carried out such that the cells were exposed to as little light as possible. Unbound secondary antibody was removed with 4 rinses in blocking solution (10 min each). SyTox Green, the counterstain, was diluted to 1-2 μM

in a buffer containing 0.5 × TBS and 0.25% Triton. Eggs were counterstained for at least 3 h. Eggs were rinsed once with 0.5% triton in TBS and once with H_2O. Eggs were stuck to size 0 coverslips and mounted onto glass slides with 75 mg/mL n-propyl gallate in 1:1 glycerol: water (v/v). To prevent distortion of their shape by the coverslip, electrical tape with a hole in it formed a well on the slide into which the eggs could be mounted. The sides of the coverslip were sealed with nail polish and stored in the dark. The slides were examined within 12 h.

3.1.7.2 Actin Staining

Eggs were fixed at various times post-activation by incubating the eggs in pre-warmed (30°C) actin fixative for 30 min. Three ten-minute washes (30°C) in blocking solution rinsed away the fixative. Eggs were stored in blocking solution at 4°C for up to 8 h before the next step. Eggs were incubated overnight (4°C) in the dark in TBS-Triton with 1% BSA containing 5 U/mL Alexa-594-phalloidin and 0.5-1 μM SyTox Green. Excess stain was rinsed away with two washes: eggs were rinsed once with TBS-triton and once with water. Eggs were stuck to coverslips and mounted to slides in the same manner as described in the previous section (3.1.7.1). The slides were examined within 12 h.

Phallotoxins have become an important tool for investigating the cytoskeleton. Isolated from the *Amanita phalloides* mushroom, phallotoxins are bicyclic peptides that competitively bind to F-actin. A fluorophore is conjugated to the phallotoxin, creating an effective probe for visualizing the pattern of F-actin. According to the manufacturers, phallotoxins stain F-actin at nanomolar concentrations and are extremely water-soluble. Labeled phallotoxins have similar affinity for both large and small filaments and the binding affinity does not change appreciably with actin from different species or sources. Nonspecific staining is negligible, and the contrast between stained and unstained areas is large.

Alexa-594 is a member of a new generation of fluorescent dyes, the Alexa fluorophores. Conjugates prepared with the Alexa Fluor 594 dye emit in the red region of the spectrum. When combined with green-fluorescent probes, Alexa 594 is useful for multilabeling experiments.

Alexa Fluor 594 conjugates are efficiently excited by the 594 nm line of the orange He–Ne laser. They also are more fluorescent than Texas Red conjugates and exhibit higher photostability.

3.1.7.3 Counterstain

SyTox green nucleic acid stain is used as the counterstain in both labeling experiments. It is a high affinity nucleic acid stain that easily penetrates cells with compromised or permeabilized plasma membranes. Thus, the nucleic acids of fixed cells fluoresce bright green when excited between 450-490 nm. When bound to nucleic acids the signal from SyTox Green is enhanced by over 500-fold. This makes SyTox Green an excellent counterstain for chromosome labeling. The manufacture recommends that this dye should be used in a phosphate-free buffer for best results. Solutions containing very high concentrations of monovalent or divalent cations may reduce SyTox Green staining. Residual detergent can also influence results by causing brightly stained material to appear in solutions with or without cells present. For this reason, TBS was used as the buffer when SyTox Green was used added.

3.1.7.4 Confocal Imaging

Confocal images were collected using an Olympus IX70 inverted microscope equipped with a BioRad MRC-1024 confocal laser-scanning unit. For the Alexa 594 conjugates, a helium-neon laser produced the excitation. The excitation was 594 nm with emission at 600 nm EFLP. For SyTox Green staining, the fluorescent excitation was produced by a 488 nm Argon-ion laser and collected through a band pass filter centered at 522 nm. Images were collected using an Olympus UApo 40x (NA 1.15) water immersion lens. Sections were taken every 0.5 μm (Z-series) through the thickness of the egg. From the Z-series, composites were created to represent 9 sections through the thickness of the egg (numbered 1-9) as well as a composite of the entire Z-series. Transmitted light was also collected to create a bright-field image of each egg analyzed.

3.1.8 Actin and Tubulin Co-staining

Unfortunately, actin and tubulin could not be stained together in the same egg. As described above, the fixation procedure for each of these cytoskeletal components is different. Specifically, 0.02% Triton X-100 is used in the actin fixative while the microtubule stabilization buffer contains 0.5% Triton-X 100. The higher concentration of Triton is necessary when staining for tubulin to permeabilize the membrane to allow complete penetration of the antibodies. This concentration does not affect microtubules (Carabatsos *et al.*, 2000) but disrupts the actin microfilament network such that Alexa 594-phalloidin cannot pick up the actin network in these eggs. Conversely, when the lower Triton X-100 concentration is used, the primary and secondary antibodies cannot penetrate the cortex of the egg to evenly detect tubulin throughout the egg. Therefore, actin and tubulin staining patterns were compared in separate eggs or zygotes treated identically except for the staining procedure.

3.1.9 PolScope

The PolScope is a microscope imaging system used to study the birefringent properties of biological samples. Birefringence is an optical property of anisotropic substances. Anisotropic materials contain nonrandom molecular order but have two optical axes, with the index of refraction along one axis different from the other axis. When incident light is at an angle other than along an optical axis, it is refracted into two polarized rays travelling at different velocities and with their vibration directions oriented at right angles to one another. The difference between the two indices of refraction is the birefringence (Hoyt and Oldenbourg, 1999). Biological examples of birefringent material include tubulin, myosin filaments of striated muscle, chloroplasts, and plant cell walls (Karp, 1996).

The PolScope measures birefringence as birefringent retardation (retardance), which is the product of the birefringence and the thickness of the sample. PolScope images display retardance magnitude as a grey value between black and white, where black indicates no

retardance and white indicates the maximum retardance displayed in the image (Hoyt and Oldenbourg, 1999).

The PolScope can be used to visualize spindles during egg activation in real-time. Details of spindle structure and location can be observed without the need to fix, stain or label the oocyte. Single oocytes can therefore be followed throughout egg activation. With the PolScope, all the microtubules in the plane of focus show their birefringence regardless of their orientation. The birefringence measurements therefore give an indication of the degree of coherent organization of the spindle, with increased birefringence and hence a more organized spindle displayed as an increase in intensity (Liu *et al.*, 2000).

I carried out this work at the Marine Biological Laboratory in Woods Hole, MA, in collaboration with Dr. Jim Trimarchi. Spindles were imaged using a Zeiss Axiovert 100 inverted microscope equipped with a Cohu analogue video camera and PolScope hardware consisting of liquid crystals and electro-optical controller (Cambridge Research & Instrumentation, Boston, MA). Through MetaMorph PolScope imaging software (Universal Imaging Corp., Boston, MA), settings of the liquid crystals were changed to create specific polarization states of different principal axis orientations. An image was captured at four predetermined settings. On the basis of polarimetric algorithms, the raw image data were converted to images representing the birefringence retardance of the specimen. This gave polarization orientation-independent, quantitative measurements of living oocytes (Oldenbourg *et al.*, 1998).

Unfertilized eggs were collected and denuded of cumulus cells as described above except that KFHM was replaced with low Hepes KFHM. Eggs were washed in low Hepes-KFHM and transferred to a plastic tissue culture dish with a cover glass bottom (MatTek Corp., Ashland, MA). For experiments involving U0126 alone or Sr^{2+} activation, this dish contained 100 µL low Hepes KFHM overlaid with mineral oil. When roscovitine was used, the dish contained 900 µL low Hepes KFHM and no oil. The dish and microscope were enclosed in a custom-made, insulated, heated box for optimal thermal control. The dish was allowed to sit in the box for at

least 5 min to allow for thermal equilibration. A background image from an area without eggs was taken. This image was updated as necessary during the activation experiment, according to the manufacturer's recommendations. Eggs were imaged prior to activation to establish the baseline spindle appearance. A 6 × concentration of the activator was carefully added to the eggs at the onset of the experiment. For example, 20 µL of 300 µM U0126 was added to eggs in U0126 activation experiments and 180 µL of 300 µM roscovitine was added during roscovitine activation experiments. Images were obtained periodically after activation.

3.1.10 Pharmacological Manipulations

3.1.10.1 Spindle Disruption – Demecolcine

Unfertilized eggs were collected as described above and denuded of cumulus cells. Eggs were pretreated with demecolcine for 1 h to disrupt the spindle, followed by activation by either Sr^{2+} or U0126 in the presence of demecolcine (Deme-Sr and Deme-U0126, respectively). As controls, eggs were pretreated with the vehicle for the drug (ethanol) and either activated by Sr^{2+} (Veh-Sr) or U0126 (Veh-U0126), or cultured with the vehicle, DMSO (Veh-Veh).

3.1.10.2 MAPK activation – Okadaic acid

Unfertilized eggs were collected as described above and denuded of cumulus cells. Eggs were Sr^{2+}-activated in the presence of okadaic acid (OA-Sr). As controls, eggs were activated with Sr^{2+} in the presence of the vehicle for the drug (1% DMSO; Veh-Sr) or cultured without activation (Veh-Veh).

3.1.11 Egg/Embryo images

To obtain brightfield images, activated eggs and embryos were transferred into a coverslip chamber (Harvard Apparatus, Cambridge, MA) containing 10 µl microdrops of KFHM overlaid with oil. Images were obtained by using a Zeiss IM35 microscope equipped with a Spot Junior CCD camera (Carl Zeiss Canada, Toronto, ON) and Spot v3.0 software (Spot Diagnostic Instruments Inc., Sterling Heights, MI).

3.1.12 Statistics

Data are presented as the mean ± the standard error of the mean (SEM). In all cases, $p<0.05$ was considered significant. Throughout, "n" indicates the total number of eggs or embryos and N indicates the number of experimental replicates. All SEM calculations were performed using software from SigmaPlot (Jandel Scientific, San Rafael, CA) and statistical significance calculated using InStat (GraphPad Instat, San Diego, CA). Bartlett's test for homogeneity of variances was used to determine whether parametric or non-parametric tests were appropriate. Statistical comparisons between several groups were then made using parametric or non-parametric ANOVA followed by Tukey-Kramer's Multiple Comparisons Test or Dunn's test respectively. t-tests were used for comparison when there were two groups of data.

4 RESULTS

4.1 IN VITRO FERTILIZATION (IVF)

Following sperm-egg incubation, activated eggs were scored for polar body and appearance of pronuclei and were selected for kinase assay measurement. The timecourses for MAPK, MPF, polar body and pronuclei appearance are summarized in Fig. 9. MPF activity, as measured by histone H1 kinase activity using the simultaneous kinase assay, fell quickly, becoming half-maximal by 1 h post IVF (Fig. 9A). On the other hand, MAPK activity, as measured by MBP kinase activity in IVF eggs fell more slowly, remaining high for up to 5 h in the simultaneous kinase assay (Fig. 9A). Similarly, MBP kinase activity decreased about 6 h post-IVF in the MAPK assay (Fig. 9B). Timecourses for polar body emission and pronuclear formation following IVF are presented in Figure 9C. MPF inactivation is approximately correlated with polar body appearance ($t_{½}$ = 2.5 h for both assays) while MAPK inactivation appears to be correlated with pronuclear formation ($t_{½}$ = 4 h for both assays). Unfertilized eggs cultured for 5 h (simultaneous kinase assay; Fig. 9A) or 8 h (single kinase assay; Fig. 9B) maintained high levels of both histone H1 and MBP kinase activities, whereas *in vivo* fertilized zygotes had low histone H1 and MBP kinase activities, as expected (Moos *et al.*, 1995).

4.2 SR^{2+} PARTHENOGENESIS

4.2.1 Kinase Activity

MPF (Histone H1 kinase) and MAPK activity (MBP kinase) decreased after Sr^{2+} activation with nearly identical timecourses as after IVF (Fig. 10A, B). As in IVF, MBP kinase activity in Sr^{2+} eggs remained high for up to 5 h in the simultaneous kinase assay (Fig. 10A). This is consistent with the results from the measurements of MBP kinase alone, where MBP kinase activity was lost between 5 and 7 h post-activation (Fig. 10B). The time courses of polar body emission and pronuclear development in Sr^{2+} activated eggs and in eggs after IVF were

Figure 9: IVF timecourse. A. MPF (•) and MAPK (•) activity (± SEM) measured using the simultaneous kinase assay. B. MAPK (•) activity (± SEM) following IVF. C. Timecourse of polar body and pronuclei appearance. In A and B, zygotes (Zyg; negative control) and eggs cultured for 8 h (Egg; positive control) were assayed. The value of MBP and histone H1 kinase activity of eggs (*t=0*) was arbitrarily set at 100% with subsequent time points expressed relative to this amount. Each time point was repeated 4-6 times. Adapted with permission from Phillips *et al.*, 2002a.

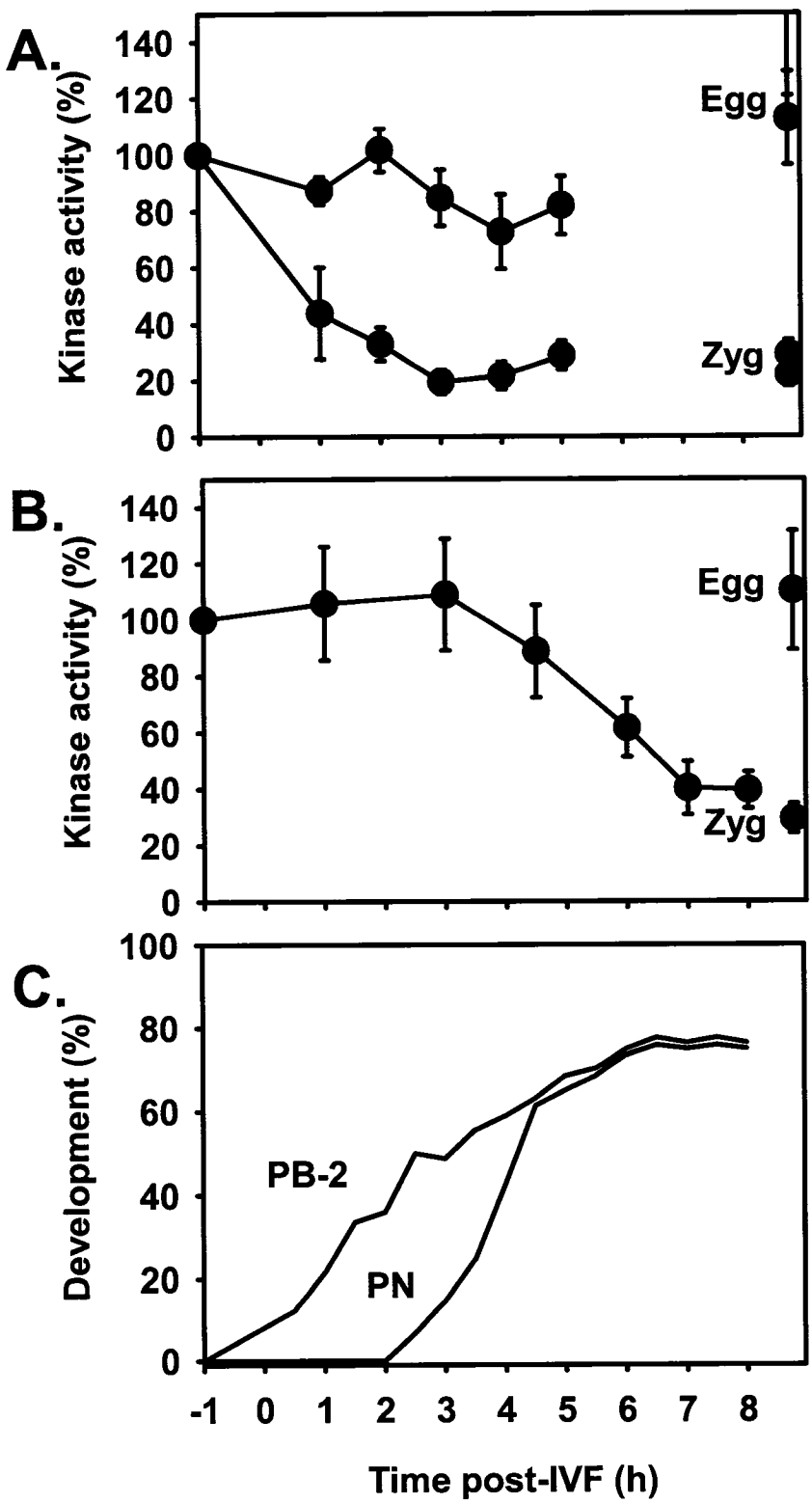
A.
Kinase activity (%)
140
120
100
80
60
40
20
0
Egg
Zyg
B.
Kinase activity (%)
140
120
100
80
60
40
20
0
Egg
Zyg
C.
Development (%)
100
80
60
40
20
0
PB-2
PN
-1
0
1
2
3
4
5
6
7
8
Time post-IVF (h)

Figure 10: Sr^{2+} timecourse. A. MPF (●) and MAPK (●) activity (± SEM) measured using the simultaneous kinase assay. B. MAPK (●) activity (± SEM) following Sr^{2+} parthenogenetic activation using the MAPK assay. Kinase activities in zygotes (zyg; negative control) and eggs cultured for 5 h in the absence of activation (egg; positive control) were also measured for each replicate. C. Time course of polar body and pronuclei appearance. In all graphs, the corresponding IVF timecourse is presented as dashed lines (- - -). The value of MBP or histone H1 kinase activity of eggs (*t=0*) was arbitrarily set at 100% with subsequent time points expressed relative to this amount. Each time point was repeated 4-6 times. Adapted from Phillips *et al.*, 2002b.

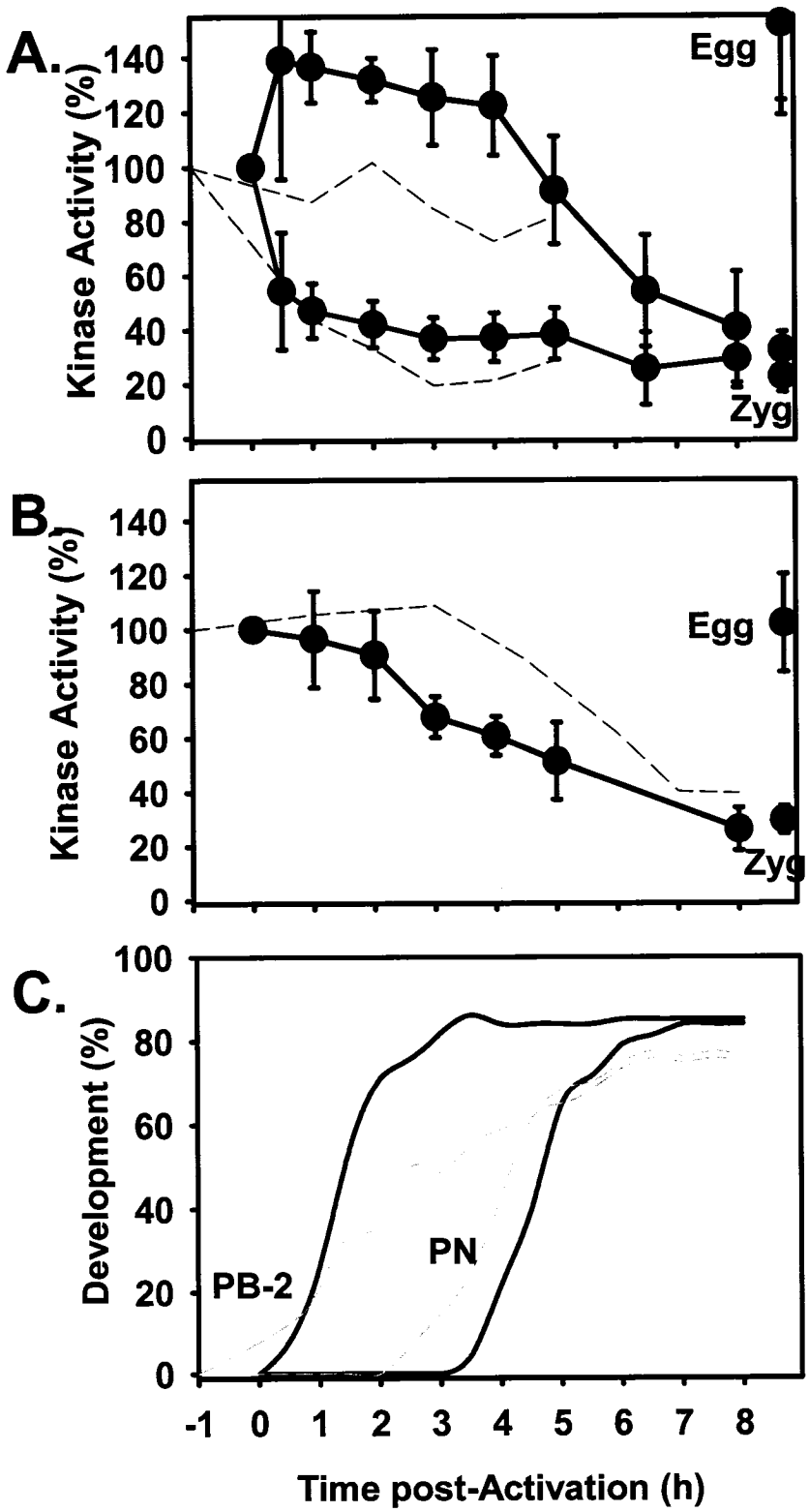
A.
Kinase Activity (%)
140
120
100
80
60
40
20
0
Egg
Zyg
B.
Kinase Activity (%)
140
120
100
80
60
40
20
0
Egg
Zyg
C.
Development (%)
100
80
60
40
20
0
PB-2
PN
-1
0
1
2
3
4
5
6
7
8
Time post-Activation (h)

similar, although Sr^{2+}-activated eggs exhibited more sharply defined sigmoidal curves due to their synchronized activation (Fig. 10C). Unfertilized eggs cultured for 5 h (simultaneous kinase assay; Fig. 10A) or 8 h (single kinase assay; Fig. 10B) maintained high levels of both histone H1 and MBP kinase activities, whereas *in vivo* fertilized zygotes had low histone H1 and MBP kinase activities, as expected (Moos *et al.*, 1995).

Sr^{2+}-activated eggs developed in culture past the two-cell stage (99%) to morulae (52%; n=81, N=6), but development to blastocysts was lower (16%), as is typical for parthenogenotes.

4.2.2 Okadaic Acid Prevents MAPK Inactivation During Sr^{2+}-Induced Egg Activation

Okadaic acid (OA), a specific inhibitor of protein phosphatases PP1 and PP2A, has been used as a tool to maintain high MAPK activity in fertilized eggs (Moos *et al.*, 1995). I confirmed that when eggs are exposed to OA at the time of Sr^{2+} parthenogenesis, high MAPK activity is maintained (Fig. 11). This is consistent with previous reports that the decrease in MAPK activity after fertilization regulates the formation of pronuclei and that OA thus prevents formation of pronuclei (Moos *et al.*, 1995). In contrast, OA had no effect on MPF activity, which was similarly low in OA-treated and control eggs 8 h after Sr^{2+} activation. OA can therefore be used to produce activated eggs with low MPF activity and inappropriately high MAPK activity.

4.2.3 Tubulin Dynamics During Sr^{2+} Activation

Following Sr^{2+} parthenogenesis, microtubule dynamics are similar to those of fertilization, as outlined in section 1.3.3. Before activation, the oocyte is arrested in metaphase II, with an anastral, barrel-shaped spindle (Fig. 12). The spindle is symmetrical but peripherally located near the egg cortex with its long axis parallel to the oolemma. The condensed chromosomes are aligned along the equator of the spindle (metaphase plate) and are visualized as a bright green mass. The rest of the cytoplasm lacks microtubule asters. The first polar body is located within the perivitilline space and contains an amorphous mass of tubulin and chromatin.

Figure 11: Effect of Okadaic acid on Sr^{2+} activation. Mean MBP kinase activity (±SEM; ●) and histone H1 kinase activity (±SEM; ●) following okadaic acid-Sr^{2+} treatment (●) or Veh-Sr^{2+} treatment (- - -). The value of MBP or histone H1 kinase activity of eggs (t=0) was arbitrarily set at 100% with subsequent time points expressed relative to this amount. Each time point was replicated 4-6 times. Adapted from Phillips *et al.*, 2002b.

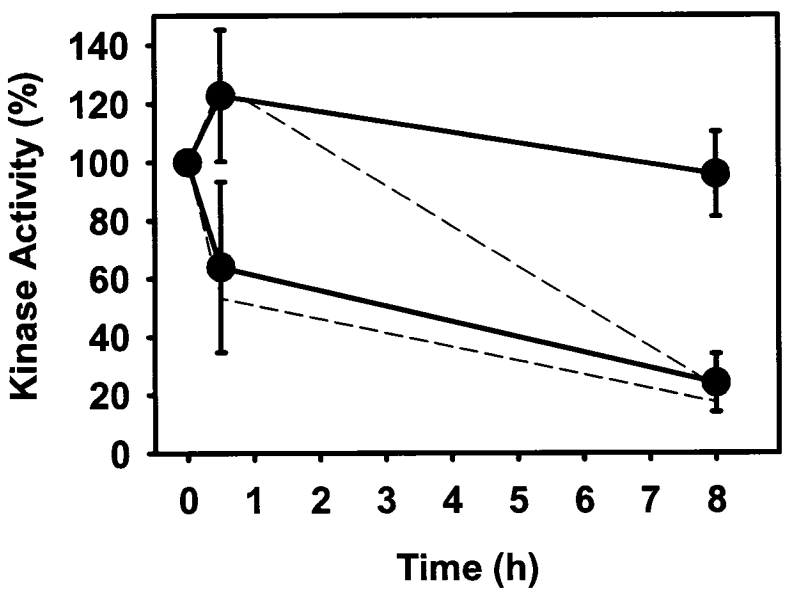
Kinase Activity (%)
140
120
100
80
60
40
20
0
0 1 2 3 4 5 6 7 8
Time (h)

Figure 12: Visualizing the microtubule cytoskeleton in the MII egg. Confocal image of an MII egg fixed and stained to visualize the microtubule cytoskeleton. In this and all other confocal images visualizing the microtubule cytoskeleton, tubulin immunofluorescence is red and chromatin is green. Numbers in the lower left corner indicate which slice, from 1 (top) to 9 (bottom) is shown. A composite of the entire Z-series (C) is followed by a transmitted light image (B).

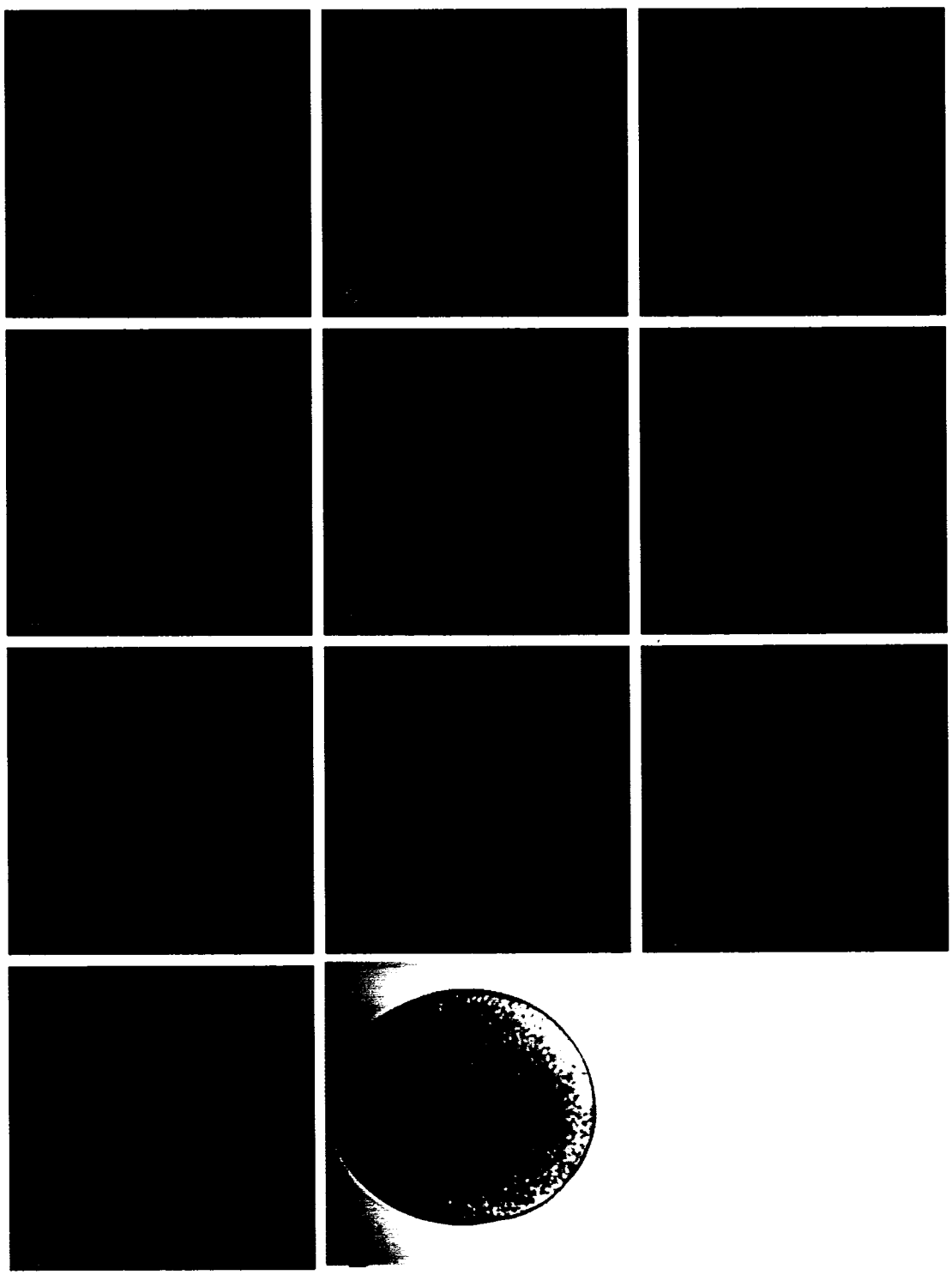

Following activation, the spindle rotates 90° such that the spindle fibres are perpendicular to the cell membrane (Fig. 13). This is shown at 1 h, when the egg is in anaphase. After 2-3 h, the polar body is emitted. The remaining spindle remnants persist as a midbody, spanning the junction between the egg and polar body, shown here up to 8 h post-activation. After 3 h, the chromatin has begun to decondense and the nuclear membrane re-forms around it to form the pronucleus. These results were consistent with other descriptions of Sr^{2+}-activation (Zhu *et al.*, 2003) and are used here as a control experiment.

To assess the specificity of the secondary antibody MII eggs were treated as in incubated in 3.1.7.1, but incubated in a sham primary antibody solution (Fig. 14A; -1°Ab). To confirm that the tubulin antibody was not itself autofluorescent, MII eggs were treated as in 3.1.7.1, but incubated in a sham secondary antibody solution (Fig. 14B; -2°Ab). No autofluorescence or nonspecific secondary antibody staining was apparent, suggesting that the fluorescence observed in each confocal image is specific for tubulin.

4.2.4 Actin Dynamics during Sr^{2+} Activation

Following Sr^{2+} activation, actin dynamics also followed the expected pattern of egg activation, as described in 1.3.3 above. Because actin dynamics during Sr^{2+}-induced activation and fertilization are the same, this is a control experiment here. Before activation, the egg was arrested at metaphase II, with the spindle sitting tangential to the oocyte cortex, as confirmed by the position of the chromosomes, perpendicular to the cortex (Fig. 15). Actin was primarily concentrated in the cortical region, below the membrane of the egg, with an area rich in actin over the spindle and chromosomes. After 1 h of Sr^{2+} parthenogenesis, the chromosome plate had rotated such that it was parallel to the plane of the proximal cell membrane (Fig. 16). The chromosomes were then seen as two masses, one closer to the cortex than the other was, as they presumably move along the spindle in anaphase II. Two hours post-Sr^{2+} activation, a ring of actin had formed along the same plane as the metaphase plate, at the centre of the spindle to form the

Figure 13: Tubulin visualization during Sr^{2+} Activation. Sr^{2+}-activated eggs stained to visualize tubulin (red) and DNA (green). Time post activation is indicated in yellow at the left of each row. Numbers in lower left corner indicate depth of slice from top (of nine slices). The third image in each row is a composite of the entire Z-series for that egg (C).

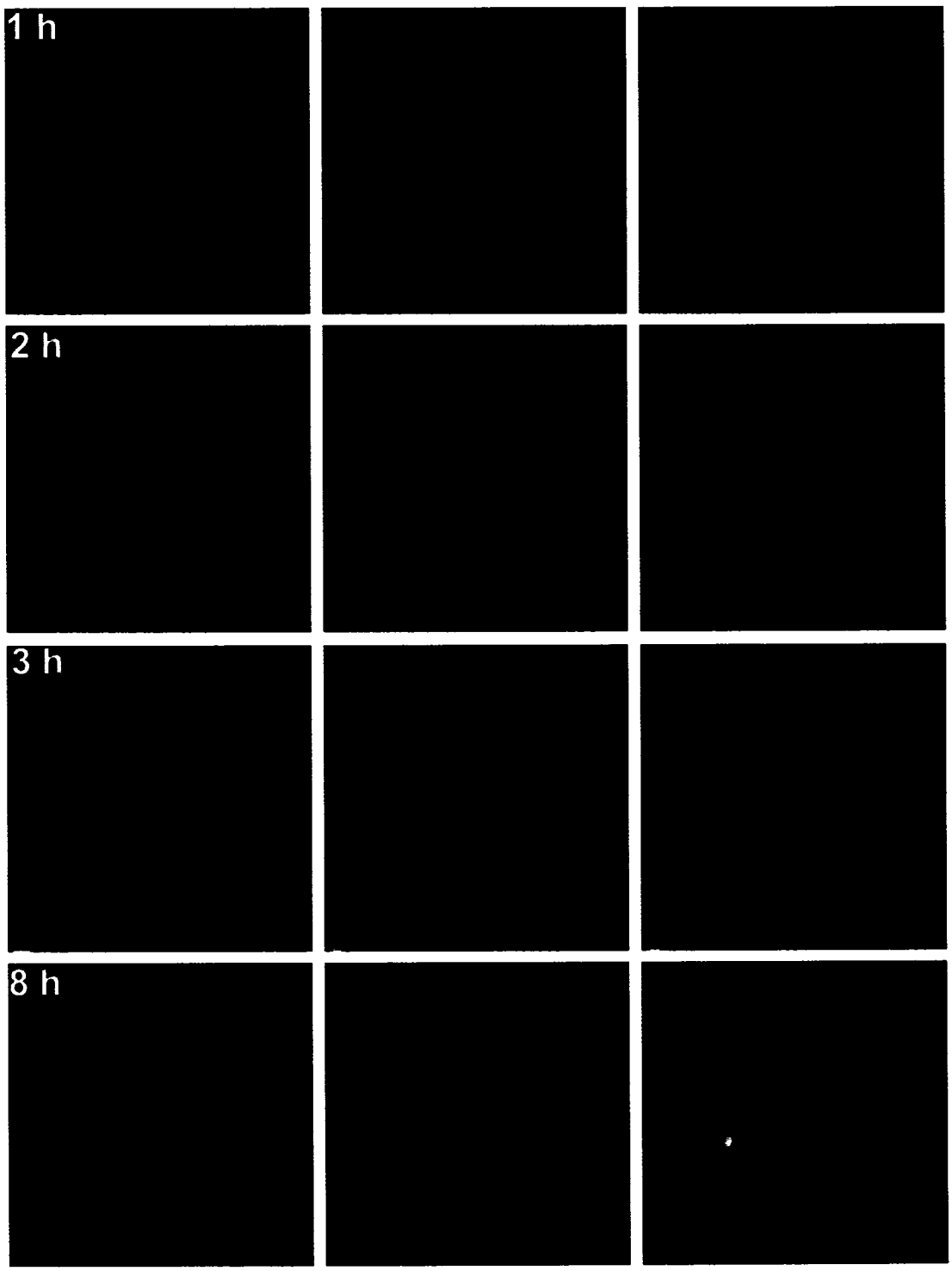
1 h
2 h
3 h
8 h

Figure 14: Confocal Controls. I. Composite image of egg fixed and processed to visualize tubulin but incubated in a sham primary antibody(-1° Ab, C). II. Composite image of egg processed to visualize tubulin when secondary antibody solution was replaced with a sham solution (-2° Ab). To right of each image is a brightfield image (B) of the same egg imaged in the composite.

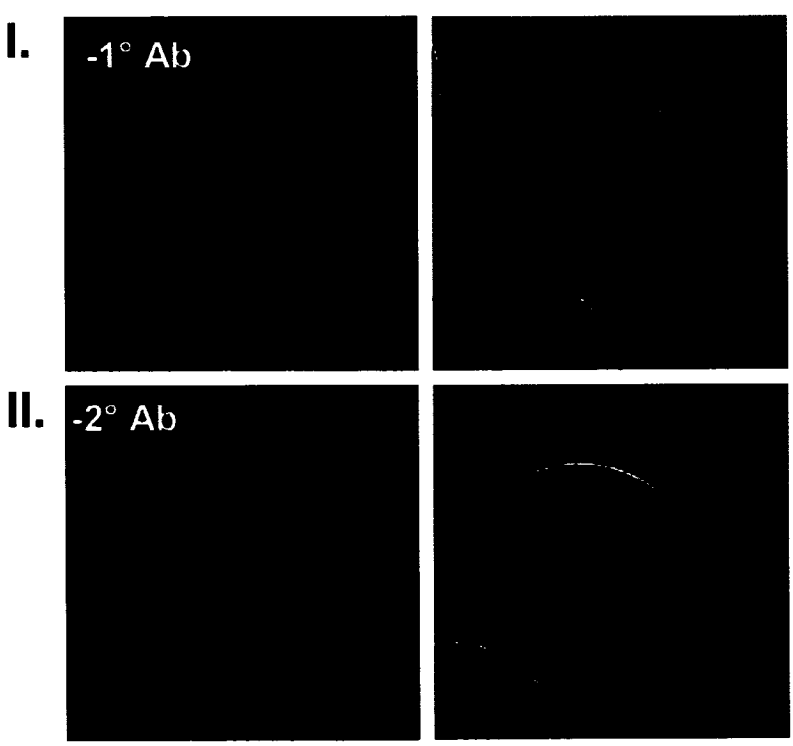
I.
-1° Ab
II.
-2° Ab

Figure 15: Visualizing the actin cytoskeleton of the MII egg. Confocal image of MII egg fixed and stained to visualize the actin cytoskeleton. In this and all other confocal images visualizing the actin cytoskeleton, actin staining is red and chromatin is green. Numbers in the lower left corner indicate which slice, from 1 (top) to 9 (bottom) is shown. A composite of the entire Z-series (C) is followed by a transmitted light image (B).

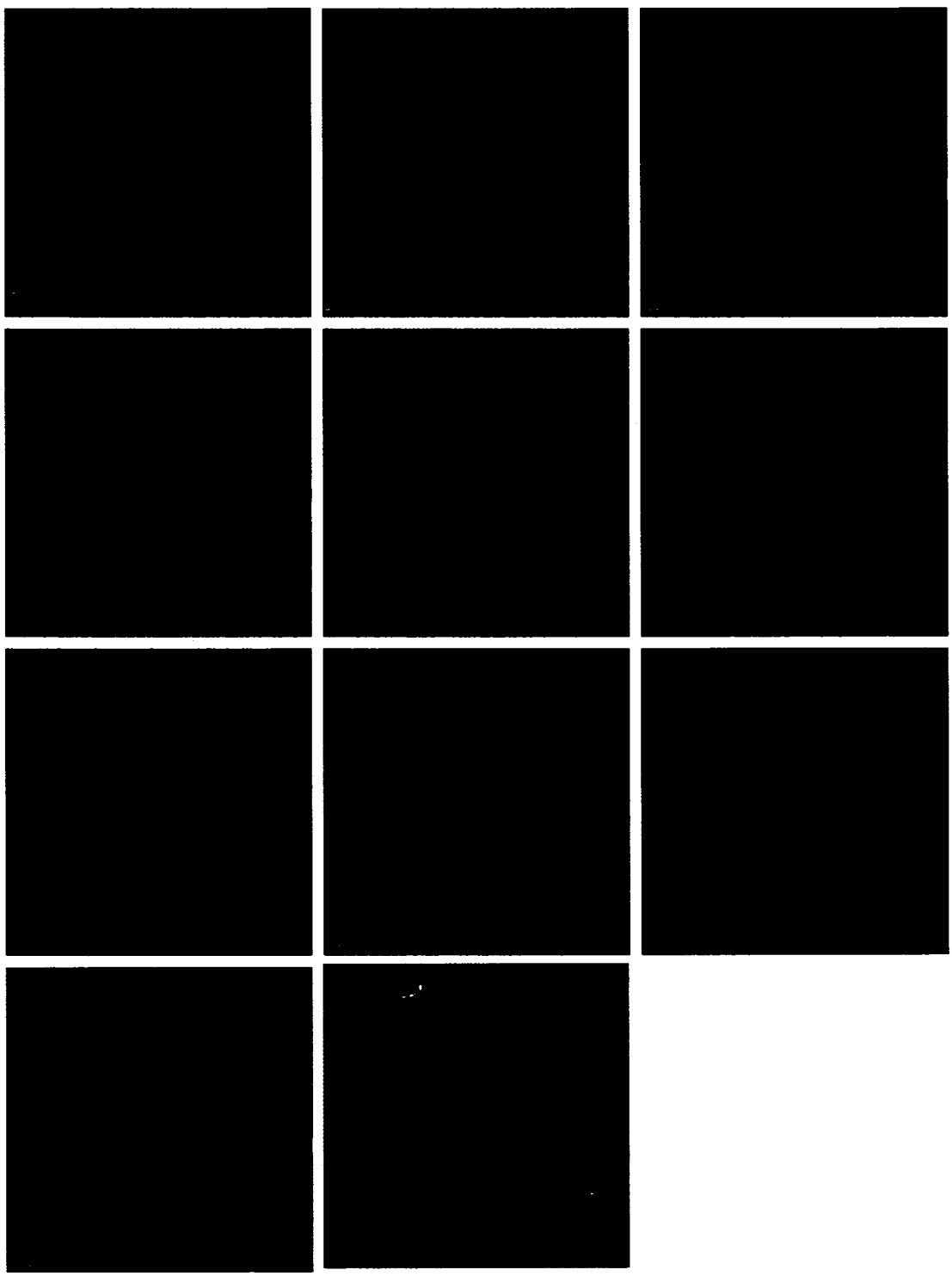

Figure 16: Actin localization throughout Sr^{2+} activation. Sr^{2+}-activated eggs stained to visualize actin (red) and DNA (green). Time post activation is indicated in yellow at the left of each row. Numbers in lower left corner indicate depth of slice from top (of nine slices). Third image in each row is a composite of the entire Z-series for that egg (C).

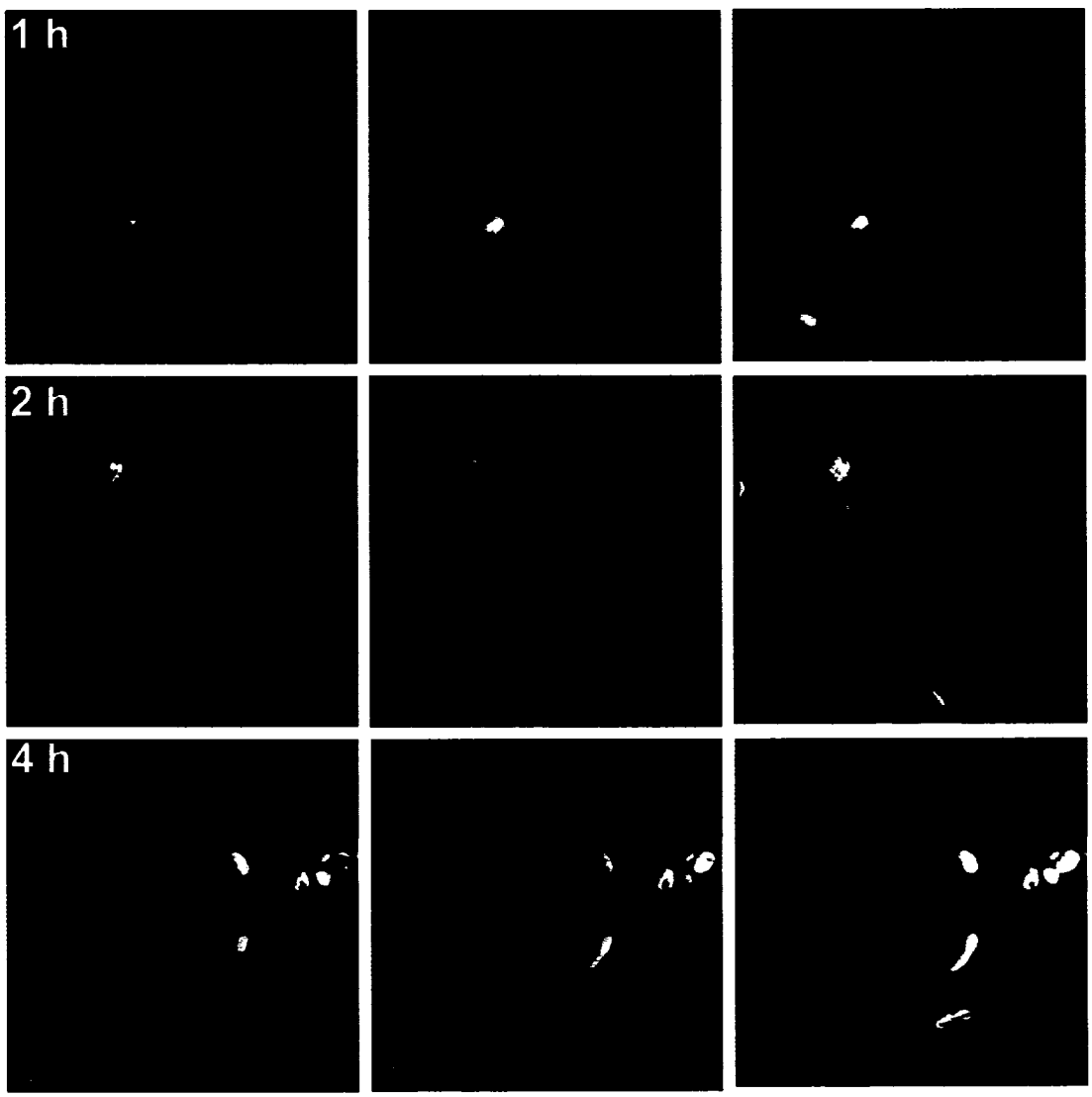
1 h
2 h
4 h

contractile ring. The actin-rich area appeared to protrude slightly from the egg and the actin ring contracted so that the membrane surrounds the set of chromosomes closest to the membrane (2 h). The actin ring contracts further, separating a small amount of cytoplasm and the proximal set of chromosomes from the egg proper to form the second polar body. Since the actin-rich area overlying the spindle formed the second polar body, this structure is likewise rich in actin, as is the membrane of the egg, just below the polar body (where the midbody would be). Four hours after activation, the chromatin had decondensed and the pronucleus could be seen with light microscopy (data not shown). Previous reports suggested that the actin staining of the polar body would decrease as the pronuclei formed, but I did not observe this (Maro *et al.*, 1984).

4.2.5 Birefringence Following Sr^{2+} Activation

Images obtained from the PolScope indicate that after 75 min, the spindle is bright, has rotated, and the second polar body has been extruded (Fig. 17). The midbody is shown as a highly refractive area between the polar body and activated egg. Only one time-point is presented here because the changes in birefringence following Sr^{2+} activation have been described previously (Liu *et al.*, 2000).

4.3 U0126 ACTIVATION

4.3.1 U0126 Parthenogenetically Activates Eggs

Eggs cultured in the presence of the MEK inhibitor U0126 (50 μM) for 8 h were parthenogenetically activated (Fig. 18A). While some eggs activated with a normal phenotype, a proportion of the eggs emitted abnormally large polar bodies while others underwent mitotic-like cleavages. These parthenogenotes were indistinguishable from the parthenogenotes of *mos*$^{-/-}$ oocytes. Unlike *mos*$^{-/-}$ oocytes, however, these eggs had been ovulated arrested in metaphase II, having undergone a completely normal MI. Using the classification system developed for *mos*$^{-/-}$

Figure 17: Birefringence following Sr^{2+} parthenogenesis. The time post-parthenogenesis is indicated in the top left of each image (h:mm). After 1:15 post-Sr^{2+}, the spindle is bright, has rotated and the second polar body has been emitted. Four different eggs from the same cohort are shown at this time point.

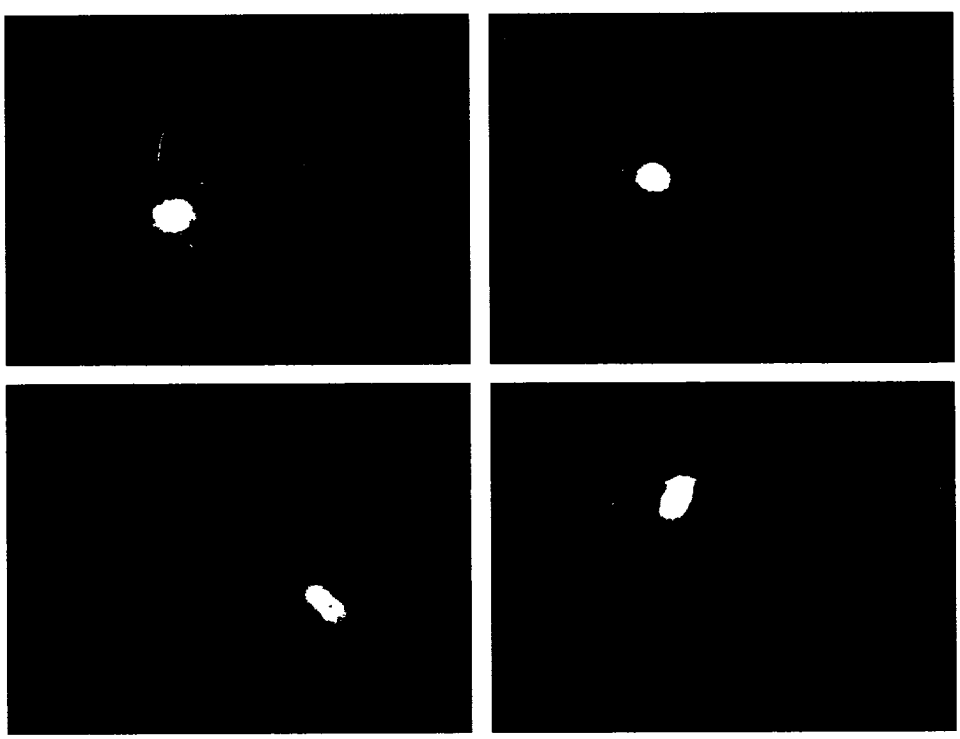

Figure 18: Parthenogenetic activation with the MEK inhibitor U0126. A. Average incidence of parthenogenesis measured 8 h after continuous exposure to 50 μM U0126 or vehicle (0.1% DMSO; control) exposure. B. Phenotype classes of U0126 parthenogenotes. Following 8 h continuous exposure to U0126, parthenogenotes were assigned to one of three parthenogenetic classes (Class I, II, or III) established by Hirao and Eppig (1997) These classes were originally defined to describe the morphology of *mos*$^{-/-}$ parthenogenotes. See text for details. Pictures obtained by K. Phillips. Reproduced with permission from Developmental Biology (247, 210-223, 2002).

A.

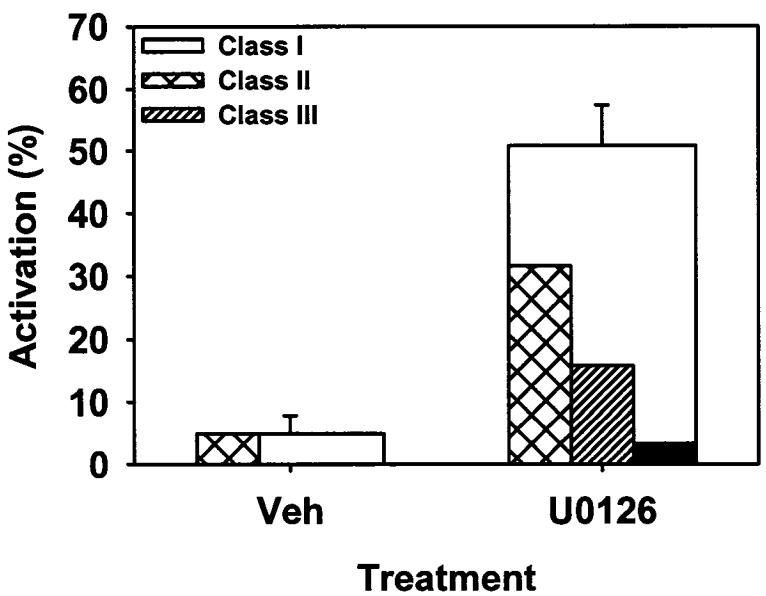
70
60
50
40
30
20
10
0
Activation (%)
Class I
Class II
Class III
Veh
U0126
Treatment

B.

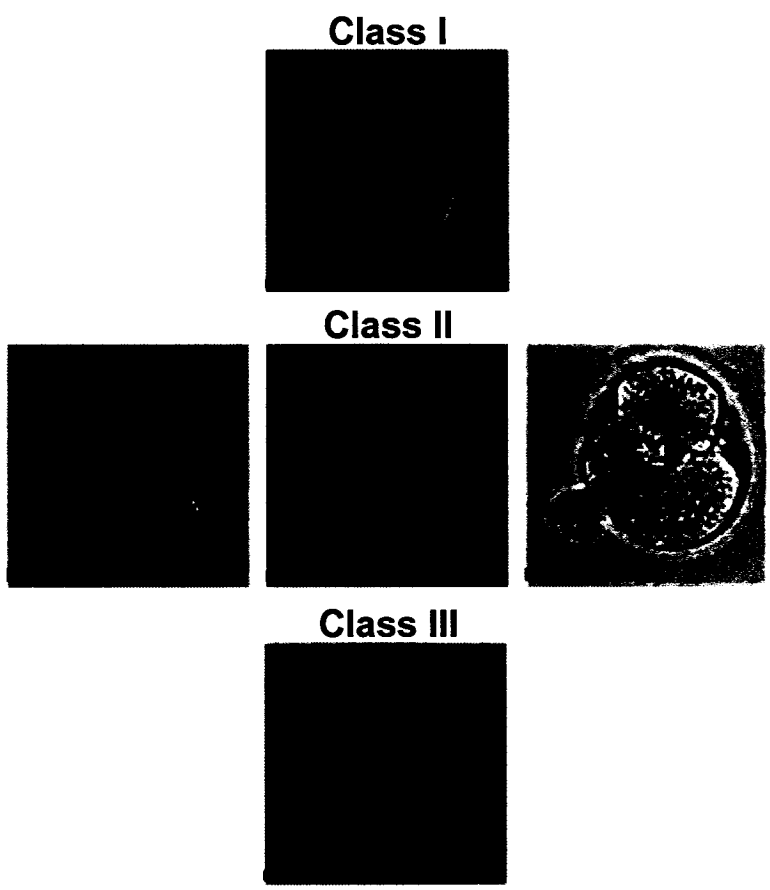
Class I
Class II
Class III

oocytes by Hirao and Eppig (1997), U0126 activation of ovulated eggs produced all three phenotypic classes of parthenogenotes (Fig. 18A, B).

After 8 h of continuous exposure to 50 μM U0126, activated eggs were cultured in standard KSOM microdrop culture. Of the activated eggs, 80 ± 8% cleaved to the two-cell stage by the next day (n = 55; N = 4) but further development was much more limited. Only 11 ± 4% reached morula stage while 5 ± 5 % of the parthenogenotes reached blastocyst stage.

4.3.2 U0126 Rapidly Inactivates MAPK so that it Precedes MPF Inactivation

Representative gels from the simultaneous and MAPK assays of U0126 activation are presented in Fig. 19A and B, respectively. Timecourses of kinase activities, polar body emission and appearance of pronuclei for U0126 egg activation are summarized in Fig. 20. In contrast to the slower timecourse of inactivation following IVF or Sr^{2+}-activation, MAPK activity fell quickly in unfertilized eggs upon exposure to 50 μM U0126, decreasing to half-maximal activity by 30 min (Fig. 20B). By only 1 h post-U0126, MAPK activity had fallen to basal levels, comparable to the activity of *in vivo* fertilized eggs (Zyg), pronucleate eggs 8 h post-IVF (Fig. 9) or 8 h post-Sr^{2+} (Fig. 10).

Using the simultaneous kinase assay, histone H1 kinase inactivation was slower than the decrease in MAPK activity, reaching half-maximal levels after 1 h and basal levels after about 2 h (Fig. 20A). This timecourse of inactivation was similar to that of IVF or Sr^{2+}-activation (Figs. 9 and 10). MBP kinase activity measured by the simultaneous kinase assay was similar to that previously measured by the MAPK assay, reaching basal levels by one hour of culture (Fig. 20A). In both cases, eggs cultured in the drug vehicle (0.1% DMSO) maintained high MBP and histone H1 kinase activity, indicating that MAPK and MPF activity were unaffected by our culture conditions (Egg, Fig. 20A and B). Both emission of the second polar body and pronuclear development were induced by U0126 treatment but with a somewhat slower time course compared with IVF eggs (Fig. 20C; PB-2 = 3-4 h; PN=6-7 h).

Figure 19: MBP and histone H1 kinase activity following U0126 exposure. A. Representative gel showing inactivation of histone H1 kinase and MBP kinase following exposure to U0126 using the simultaneous kinase assay. Upper bands are histone H1 (H1), while lower bands are myelin basic protein (MBP). B. Representative gel of a U0126 timecourse from the MAPK assay The number above each band indicates the time of U0126 exposure (h). Zyg indicates zygotes (negative control) and Egg(5) and Egg(4) indicate eggs culture for 5 and 4 h, respectively, without activation. Adapted from Phillips *et al.*, 2002a.

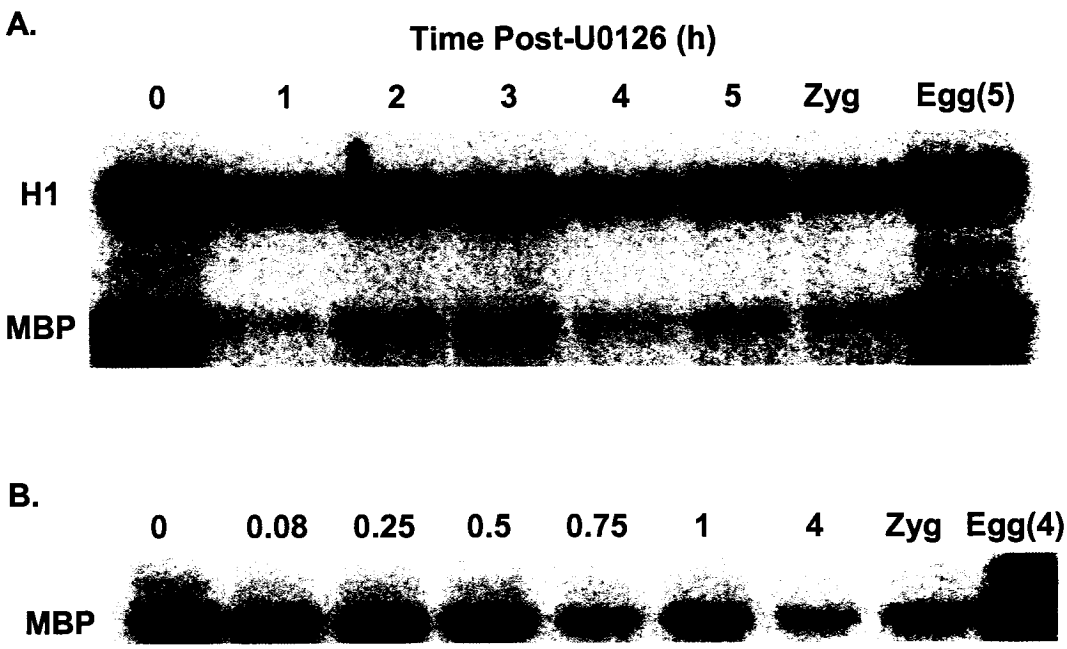
A.
Time Post-U0126 (h)
0
1
2
3
4
5
Zyg
Egg(5)
H1
MBP
B.
0
0.08
0.25
0.5
0.75
1
4
Zyg
Egg(4)
MBP

Figure 20. U0126 parthenogenesis (●) vs. *in vitro* fertilization (- - -). A. MPF (●, - - -) and MAPK (●, - - -) activity following U0126 exposure or IVF using the simultaneous kinase assay. B. MAPK inactivation following U0126 exposure shown using the MAPK assay. The value of MBP or histone H1 kinase activity of eggs (t=0h) was arbitrarily set at 100% with subsequent time points expressed relative to this amount. Kinase activities in zygotes (zyg; negative control) and eggs cultured for 5 h in the absence of activation (egg; positive control) were also measured for each replicate. C. Time course of polar body and pronuclear formation. Each time point was repeated 4-6 times. Adapted from Phillips *et al.*, 2002a.

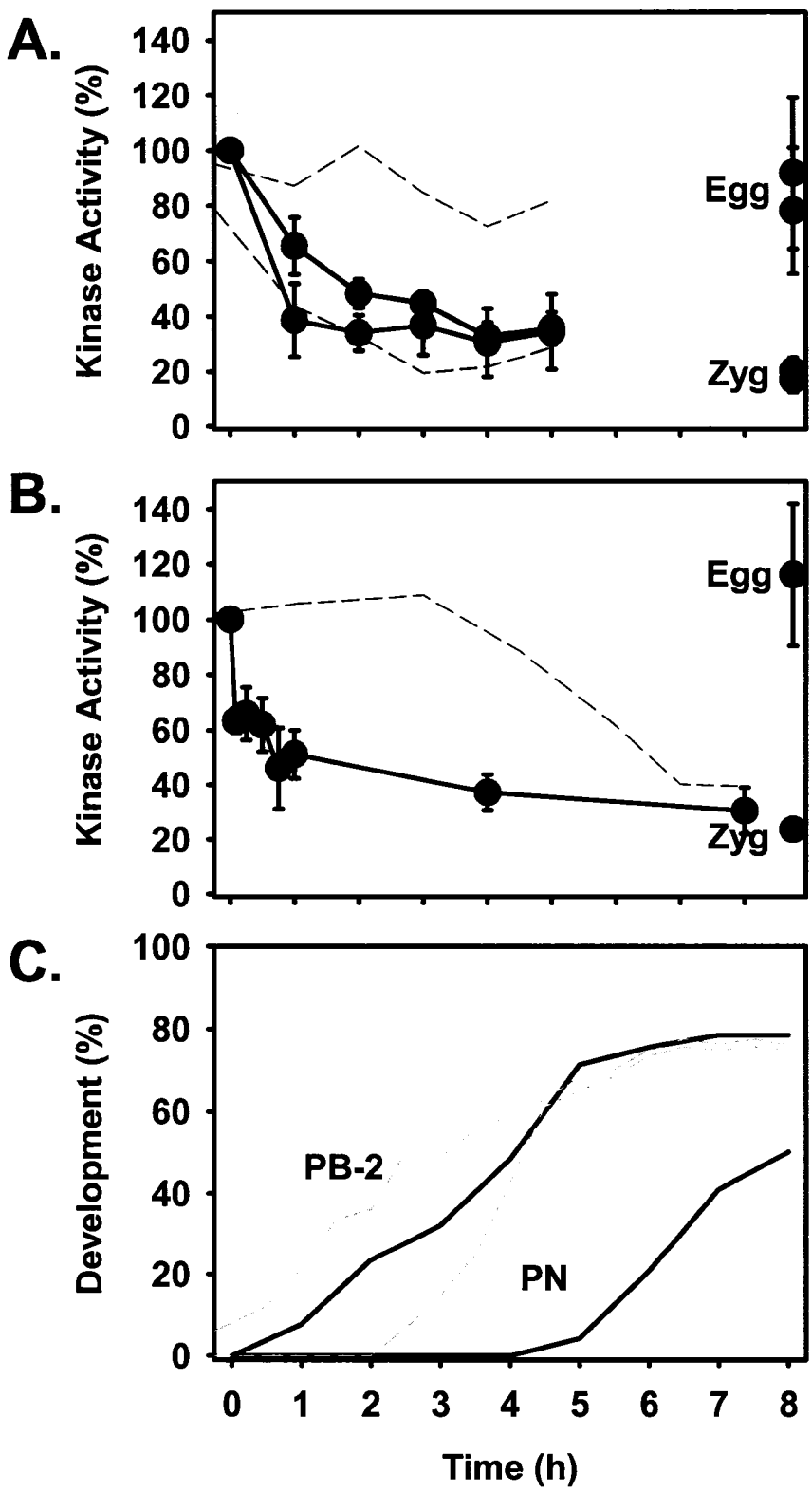
A.
Kinase Activity (%)
140
120
100
80
60
40
20
0
Egg
Zyg
B.
Kinase Activity (%)
140
120
100
80
60
40
20
0
Egg
Zyg
C.
Development (%)
100
80
60
40
20
0
PB-2
PN
0
1
2
3
4
5
6
7
8
Time (h)

4.3.3 Dephosphorylated MAPK is present in eggs treated by U0126

Using an anti-phospho-MAPK antibody, the active, phosphorylated MAPK protein was not detected by Western blot in zygotes or in eggs exposed to U0126 (50 μM) for 1 h (Fig. 21). Active MAPK was, however, present in eggs cultured for 1 h in the vehicle alone. After the blot was stripped and re-probed using anti-ERK1, which detects both phosphorylated and unphosphorylated MAPK proteins, similar amounts of MAPK protein were apparent in zygotes, eggs, and U0126-treated eggs. The bands corresponded to p44ERK1 (upper band) and p42ERK2 (lower band; Fig. 21). Both bands were shifted higher in eggs, indicating a slower electrophoretic mobility of the protein characteristic of active, phosphorylated MAPK. Thus, the fall in MAPK activity following U0126 exposure is a result of results in dephosphorylation and hence inactivation of both ERK1 and ERK2 MAPKs in eggs.

4.3.4 U0126 does not directly inhibit MPF or MAPK

It should be noted that parthenogenetic activation of mouse eggs requires a much higher concentration of U0126 (50 μM; Phillips *et al.*, 2002) than the reported IC_{50} for inhibition of isolated MEK *in vitro* (<100 nM; Favata *et al.*, 1998). This is consistent, however, with results obtained in other cells, in which inhibition of intracellular MAPK phosphorylation in intact cells by U0126 added to the medium requires substantially greater concentrations of U0126 than inhibition of isolated MEK *in vitro* (Favata *et al.*, 1998; Hoffert *et al.*, 2000). This is probably due to a lower intracellular concentration of the drug, possibly due to active export of U0126 from the cell, intracellular degradation, or low permeability.

I therefore wished to determine if such a relatively high concentration of U0126 (compared to its IC_{50}) could directly affect MPF or MAPK activity, rather than acting solely via MEK inhibition. U0126 (50 μM) was added to the kinase assay mixture of untreated egg lysates to confirm that U0126 does not directly inhibit MPF or MAPK. The results are summarized in Table 1. Both histone H1 and MBP kinase activities of egg lysates were high when 50 μM

Figure 21. Effect of U0126 on the phosphorylation state of endogenous MAPK. Western blot is shown following immunodetection of MAPK using antibodies specific for phosphorylated MAPK (pMAPK, top). The blot was subsequently reprobed with anti-ERK1 (MAPK, bottom) which cross-reacts somewhat with ERK2 and does not differentiate between phosphorylated and unphosphorylated MAPK. Lanes are: zygotes (zyg, negative control), eggs (egg, positive control), and eggs treated with 50 μM U0126 for 1 h. Adapted from Phillips *et al.*, 2002a.

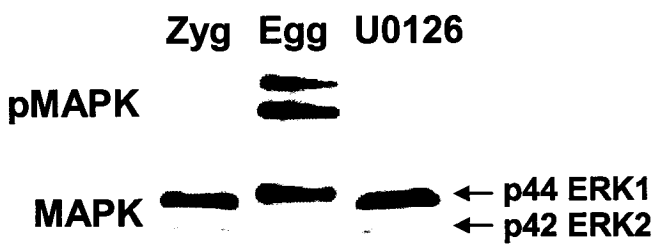
Zyg
Egg
U0126
pMAPK
MAPK
← p44 ERK1
← p42 ERK2

Table 1: Effect of U0126 or roscovitine on the kinase activity of egg lysates. U0126 was added to the kinase assay mixture of untreated egg lysates for a final concentration of 50 μM during the kinase reaction. Kinase activity is expressed relative to the kinase activity measured in unfertilized egg treated with vehicle in the kinase mixture, which was arbitrarily set at 100%. * represents statistical significance, $P < 0.001$; Student's t test; $N = 5$.

Drug in lysates	Histone H1 Kinase (%)	MPB Kinase (%)
U0126 (50 μM)	87±18	98±5
Roscovitine (50 μM)	27±7*	74±7

U0126 was present in the simultaneous kinase assay mixture but was absent before lysis. This indicates that neither MPF nor MAPK activities were directly affected by U0126. MAPK activity should not be affected by MEK inhibition in egg lysates, because the normal intracellular regulation of MAPK by MEK and phosphatases is disrupted upon cell lysis. Thus, any effects on MAPK and MPF activities in U0126-treated eggs are secondary to inhibition of MEK and not due to any unintended direct effect of U0126 on MAPK or MPF activities.

4.3.5 MAPK inactivation by U0126 requires continuous U0126 exposure.

To determine whether U0126 inhibition of MAPK activity was reversible, unfertilized eggs were exposed to 50 μM U0126 for 1 h, and then the eggs were washed free of the drug and placed into standard KSOM microdrop culture. Inactivation of MAPK upon U0126 exposure was reversible, so that MBP kinase (MAPK) activity recovered within 0.5 h following washout of the drug (Fig. 22). This indicates the need for the continuous presence of U0126 to maintain low MAPK activity and hence parthenogenetically activate eggs.

4.3.6 MAPK inactivation by U0126 is dose-dependent.

Eggs were cultured in 1, 5, or 50 μM U0126 and MBP kinase (MAPK) activity was measured at 30 min and 1 h using the MAPK assay (Fig. 23). After 30 min, MBP kinase activity was significantly reduced in eggs treated with 50 μM U0126 compared with 1 and 5 μM U0126 ($P < 0.05$; ANOVA, Tukey–Kramer Multiple Comparisons Test). Eggs cultured in 50 μM U0126 for 1 h had significantly lower MBP kinase activity compared with 1 μM ($P < 0.001$) and 5 μM U0126 ($P < 0.01$; ANOVA, Tukey–Kramer Multiple Comparisons Test). This is consistent with the observation that parthenogenetic activation with U0126 is dose-dependent, with maximal activation at 50 μM, little activation at 5 μM, and even less at 1 μM (Phillips *et al.*, 2002a).

4.3.7 Activation by U0126 or Sr^{2+} Requires an Intact Spindle

Disruption of the metaphase II spindle has been shown to maintain metaphase arrest by preventing cyclin destruction and hence maintaining high MPF activity for an extended time even

Figure 22. MAPK inactivation by U0126 requires continuous U0126 exposure. Eggs were cultured in 50μM U0126 for one hour (●). Following washout of the drug (O), mean MBP kinase activity (±SEM) measured using the MAPK assay rebounded to original levels by 0.5 h. Arrow indicates removal of U0126. Each time point was repeated 4-6 times. The value of MBP kinase activity of eggs (t=0h) was arbitrarily set at 100% with subsequent time points expressed relative to this amount. MBP kinase activity in zygotes (negative control) and eggs cultured for 5 h in the absence of U0126 were also measured for each replicate (data not shown). Adapted from Phillips *et al.*, 2002a.

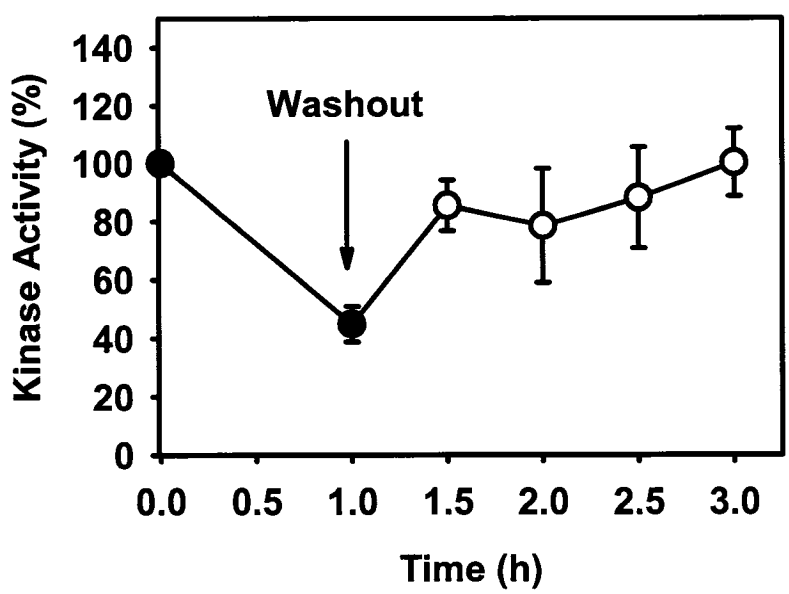
Kinase Activity (%)
140
120
100
80
60
40
20
0
Washout
0.0
0.5
1.0
1.5
2.0
2.5
3.0
Time (h)

Figure 23. Dose-dependent inactivation of MBP kinase following treatment with U0126. Mean MBP kinase activity (±SEM) following 1 (●), 5 (■), or 50 μM U0126 exposure (▲). The value of MBP kinase activity of eggs (t=0h) was arbitrarily set at 100% with subsequent time point expressed relative to this value. MBP kinase activity in zygotes (negative control) and eggs cultured for 5 h in the absence of U0126 were also measured for each replicate (data not shown). Each time point was replicated 4-6 times. * and ** represent statistical significance, $P < 0.05$ and $P < 0.01$, respectively; ANOVA; Tukey-Kramer's Multiple Comparisons Test. Adapted from Phillips *et al.*, 2002a.

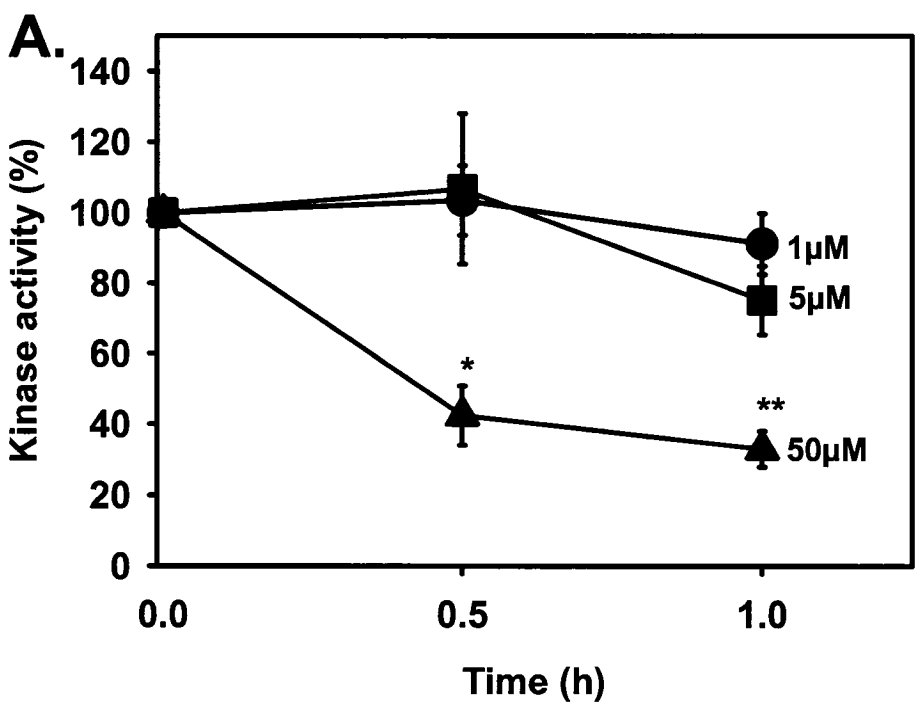
A.
Kinase activity (%)
140
120
100
80
60
40
20
0
0.0
0.5
1.0
Time (h)
1μM
5μM
50μM
*
**

after stimuli (e.g., fertilization), which would otherwise activate eggs (Winston *et al.*, 1995). Spindle disruption with demecolcine essentially eliminated U0126-induced parthenogenetic activation. Only 2% of eggs exposed to U0126 emitted a polar body when the spindle was disrupted with demecolcine and pronuclear development was limited to 1% of the spindle-disrupted eggs (Phillips *et al.*, 2002a). In the presence of demecolcine, histone H1 kinase activity was maintained at a high level for at least 4 h in U0126-activated eggs (Fig. 24A) while in the absence of demecolcine, histone H1 kinase activity fell to basal levels in U0126-treated eggs (Fig. 24C). At 8 h, histone H1 kinase activity in eggs treated with demecolcine and U0126 had begun to decrease, but was still significantly higher than histone H1 kinase activity in eggs treated with U0126 alone (Fig. 24A, C). This suggests that disruption of the spindle cannot maintain high MPF activity indefinitely when MAPK is inhibited, but very significantly slows its inactivation. In contrast, MBP kinase activity was reduced to basal levels by 4 h of exposure to U0126 either in the presence or in absence of demecolcine (Fig. 24A, C). On the other hand, in the presence of demecolcine, both MBP and histone H1 kinase remained high in Sr^{2+}-activated eggs for at least 8 h (Fig. 24A, B), while MBP and histone H1 kinase activity in Sr^{2+}-treated eggs in the absence of demecolcine had fallen to basal levels (Fig. 24C, D).

Only the inactive, unphosphorylated form of MAPK was detectable by Western blot in eggs treated for 4 h with U0126 either in the presence or absence of demecolcine, as determined by the faster electrophoretic mobility in samples containing inactive (unphosphorylated) protein (Fig. 25). This confirmed that demecolcine could not maintain active, phosphorylated MAPK in the presence of U0126, despite inhibition of parthenogenesis.

4.3.8 Tubulin Dynamics during U0126 Activation

Disruption of MEK with U0126 produces *mos*$^{-/-}$-like parthenogenetic phenotypes in MII-arrested eggs. I therefore investigated the effect of premature loss of MAPK at MII on spindle, chromatin, and actin dynamics to determine if they could account for the classes of *mos*$^{-/-}$-like

Figure 24. Disruption of the metaphase II spindle prevents U0126-induced parthenogenetic activation. The simultaneous kinase assay was used to measure mean histone H1 kinase (●; ±SEM) and MBP kinase activities (●; ±SEM). Eggs were treated with 1 μg/mL demecolcine (A, B) or vehicle (C, D) for 1 h, followed by activation with 50 μM U0126 (A, C) or Sr^{2+} (B, D) in the presence of demecolcine (A, B) or vehicle (C, D). MBP or histone H1 kinase activity of eggs (t=0h) was arbitrarily set at 100% with subsequent time points expressed relative to this amount. Each time point was replicated 5-8 times. Adapted from Phillips *et al.*, 2002a.

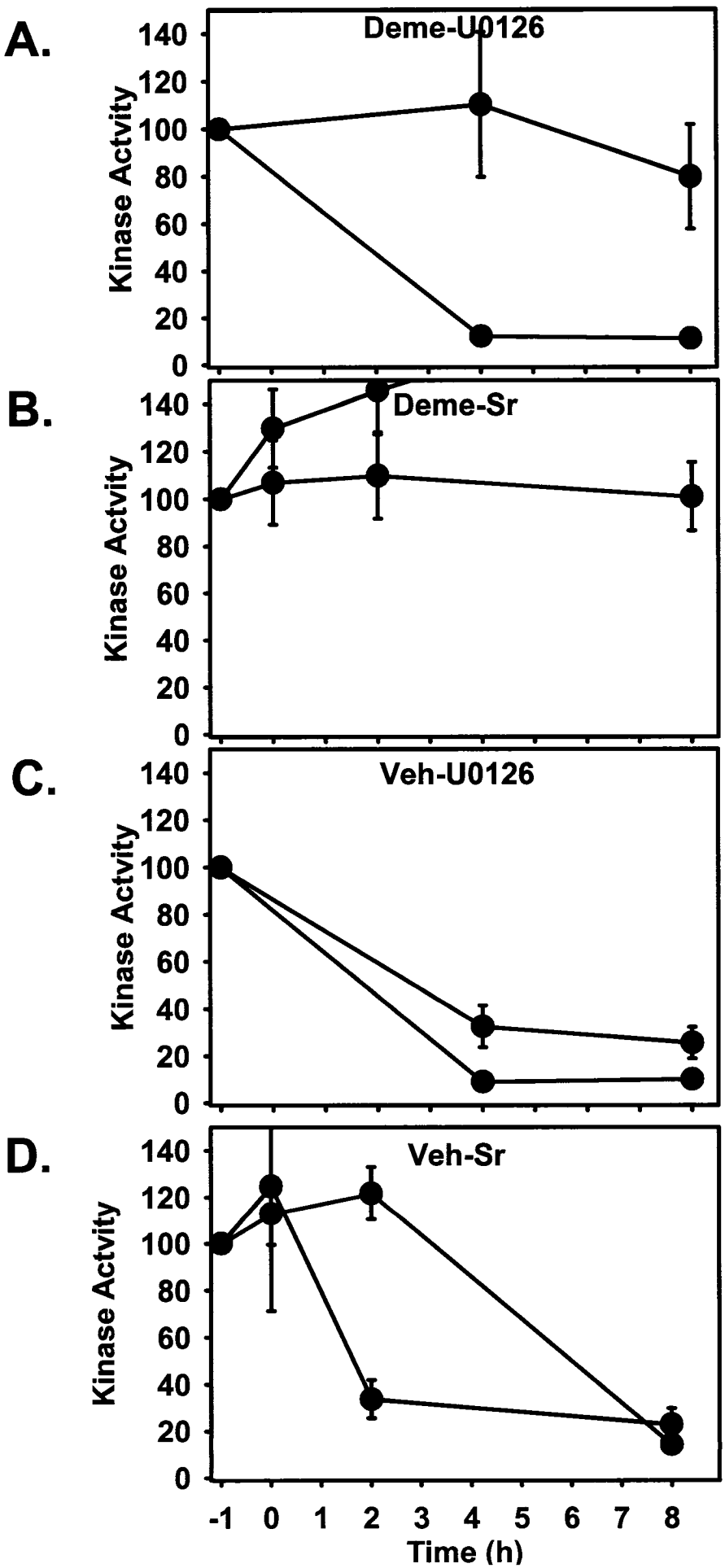
A.
Deme-U0126
Kinase Actvity
140
120
100
80
60
40
20
0
B.
Deme-Sr
Kinase Actvity
C.
Veh-U0126
Kinase Actvity
D.
Veh-Sr
Kinase Actvity
-1 0 1 2 3 4 5 6 7 8
Time (h)

Figure 25. Immunodetection of MAPK. Anti-ERK1 antibodies which cross-react somewhat with ERK2 (lower band) were used to detect MAPK. Lanes are demecolcine-U0126 (Deme-U0126), vehicle-U0126 (U0126), zygote (Zyg; negative control), and vehicle-treated eggs (Veh). Adapted from Phillips *et al.*, 2002a.

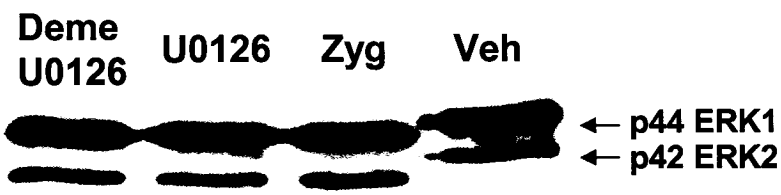
Deme U0126
U0126
Zyg
Veh
p44 ERK1
p42 ERK2

phenotypes observed. Eggs were fixed between 1 and 8 h post-U0126 and stained to visualize tubulin, as described in 3.1.7.1. Images were captured using a confocal microscope, as described above. A total of 253 egg images were examined to determine spindle dynamics during U0126 parthenogenesis. These images were then scored for spindle characteristics including spindle rotation, destabilization, and spindle drift away from the cortex. Eggs could have more than one trait. These characteristics are summarized in Table 2.

Three possible progressions of the spindle leading to the classes are proposed in Figures 26-28. Some eggs activated normally, leading to the class I phenotype (Fig. 26), as described for spindle dynamics following Sr^{2+} activation (4.2.3; Fig. 13). In the proposed example (Fig. 26), after 1 h in U0126, the spindle was still in metaphase but had begun to rotate 90° so that polar body emission could occur normally. By 2 h post-U0126 the rotation had completed and the cell had entered anaphase. After 3 h of exposure to U0126, the chromosomes separated and a small polar body was extruded into the perivitilline space. Between 4-8 h after activation, the chromatin decondensed and the nuclear membrane re-formed around the chromatin to form a pronucleus. In the presented example, the midbody was present after a 4 h exposure to the drug but was not apparent after 8 h.

Following U0126 treatment, spindle destabilization appears to be responsible for the development of Class II and III parthenogenotes. As shown in Fig. 27, after 2 h in U0126, the spindle was slightly more diffuse than during Sr^{2+} activation. The migrating chromosomes can be seen as separate dots instead of a single mass, suggesting that the chromosomes are not migrating at the same rate or that some chromosomes entered anaphase prematurely. The spindle did not appear to stay anchored to the egg cortex and drifted towards the middle of the egg. Two examples of spindle drift are presented after 3 h of exposure to U0126. In the first example, the spindle was near the geometric centre of the egg (Fig. 27, second row). In the second example (Fig. 27, third row) spindle appears much more diffuse and has taken on a curved appearance, suggesting structural destabilization in addition to lost anchorage. An indentation on either side

Table 2: Spindle characteristics during U0126 parthenogenetic activation. Eggs were parthenogenetically activated with 50 μM U0126, fixed and stained to visualize the tubulin cytoskeleton. Each image was assessed for spindle and chromatin characteristics as well as cell stage and genotype. An egg could have more than one characteristic.

Characteristic	Time post-U0126 (h) 1-2 h	3-4 h	5-6 h	7-8 h
Normal Stage for time	16	23	24	32
Spindle rotated	24	16	0	0
Spindle Defects				
Large PB/Fragments	0	6	10	10
Mitotic-like cleavage	0	0	0	7
Spindle Destabilization	24	27	11	7
Spindle drift	9	21	9	11
Spindle "spin"	11	20	13	6
Failure to Rotate	29	22	13	6
Cell Stage				
Metaphase	40	26	17	8
Anaphase/Telophase	26	33	1	1
Interphase	0	18	35	48
Genotype				
1n	11	26	32	35
2n	0	6	3	9
Micronuclei	3	9	5	7
Unknown	52	36	13	6
Total No. Pictures Examined	66	77	53	57

Figure 26. Proposed tubulin dynamics leading to the development of Class I parthenogenotes after treatment with 50 μM U0126. See text for description of cytoskeletal events leading to the development of Class I parthenogenotes. Time post-activation is indicated in yellow in the top left corner of the first image in each row. Numbers in lower left corner indicate depth of slice from top (of nine slices). The third image in each row is a composite of the entire Z-series for that egg (C).

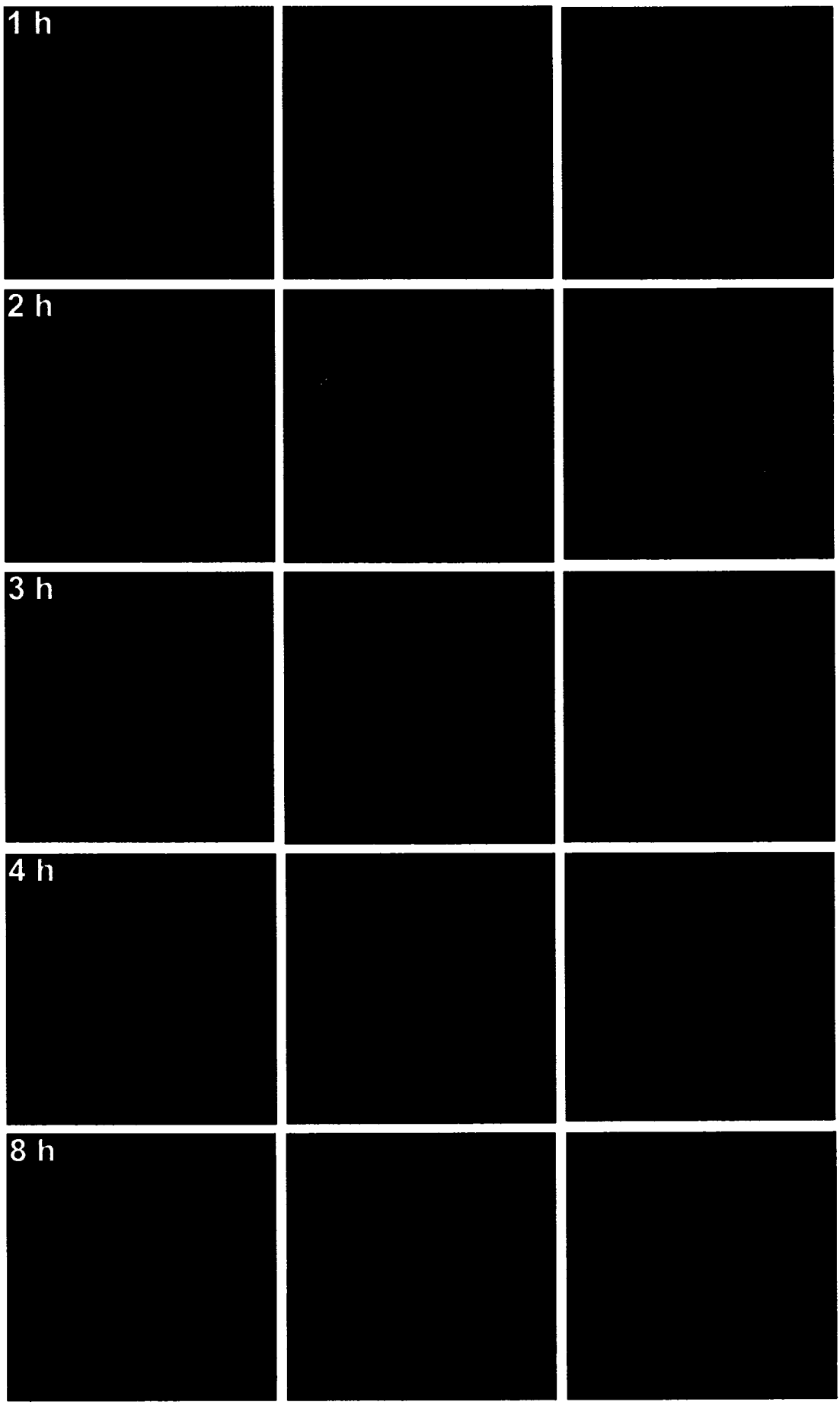
1 h
2 h
3 h
4 h
8 h

Figure 27. Spindle drift is associated with the development of Class II/III parthenogenotes activated by U0126. The spindle appears to drift away from the cortex leading to extrusion of an abnormally large polar body. See text for a detailed description of cytoskeletal events leading to the development of Class II parthenogenotes. Time post-activation is indicated in yellow in the top left corner of the first image in each row. Numbers in lower left corner indicate depth of slice from top (of nine slices). The third image in each row is a composite of the entire Z-series for that egg (C).

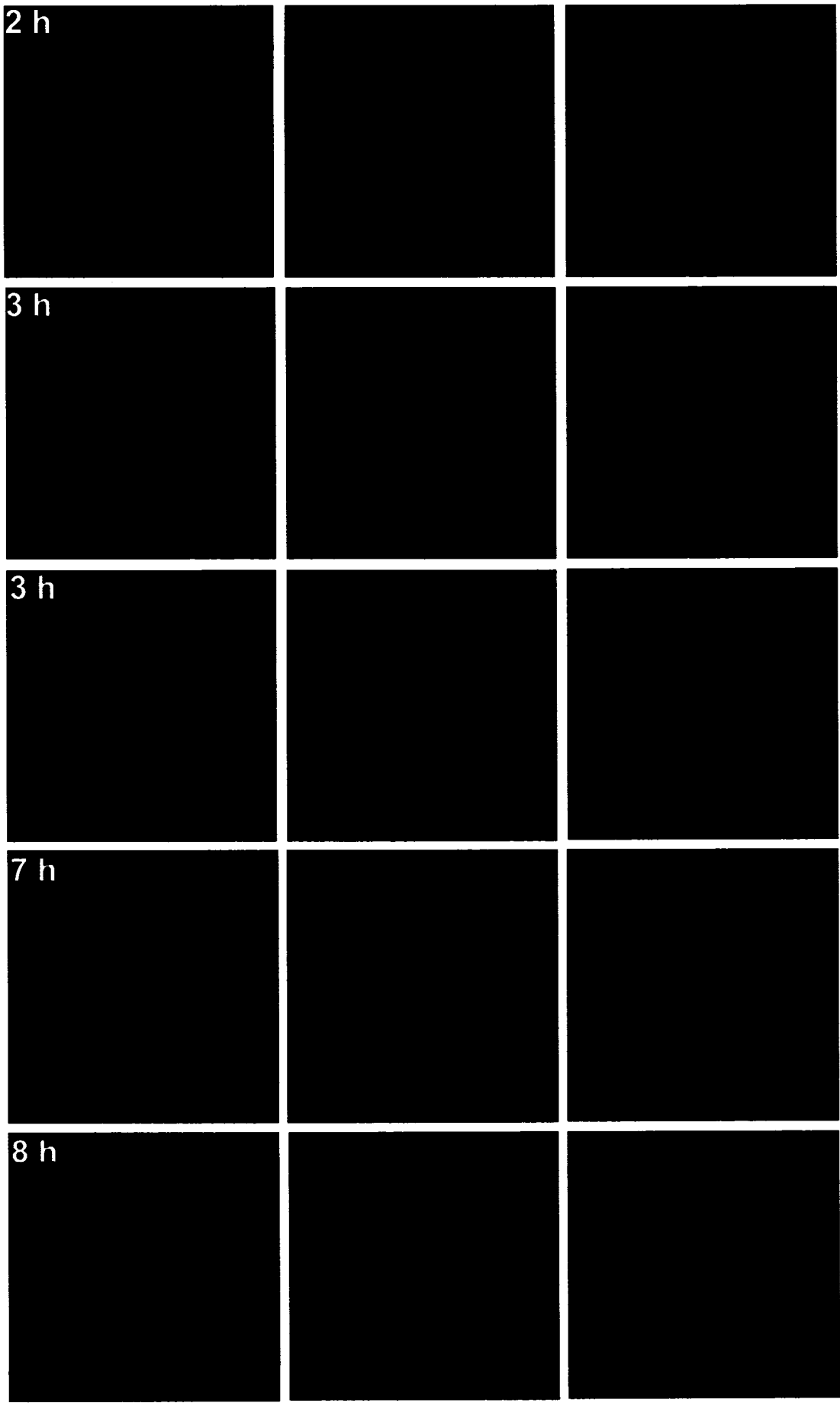
2 h
3 h
3 h
7 h
8 h

of the egg cortex is along the plane that would intersect the middle of the spindle. Because the spindle is much farther from the cortex, the cleavage furrow pinches off a larger volume of cytoplasm to form a larger than normal polar body. Extrusion of the polar body may be accompanied by fragmentation, as is shown at 7 h post-U0126. In the most extreme case, the spindle drifted into the centre of the egg and the polar body and activated egg were the same size, forming Class III parthenogenotes (8 h; Fig. 27).

In a few eggs, the spindle completely failed to rotate and anaphase occurred parallel to the membrane cortex (Fig. 28). This was observed in 8 eggs, between 1-4 h post-U0126. As proposed in Fig. 28, polar body emission could be inhibited in this scenario, leading to a diploid parthenogenote (seen in 18 U0126 parthenogenotes; Fig. 28, 7 h). Alternatively, I also observed a cleavage furrow overlying the non-rotated spindle, in the same plane as the metaphase plate. The cleavage furrow formed a ring deep into the egg, creating a large polar body (Fig 28, 8 h).

4.3.9 Actin Dynamics during U0126 Activation

As described in section 3.1.7.2, eggs were fixed 1-8 h post-U0126 exposure and stained to visualize the actin cytoskeleton. A total of 132 egg images were captured using the confocal microscope and were examined and scored for actin characteristics including presence of contractile ring, development of a "ball" of actin, puckering of the cortex and the presence of incomplete cleavage furrows. Further, certain spindle characteristics were estimated based upon the location and shape of chromatin masses (i.e. spindle drift, spindle destabilization). Eggs could have more than one trait. These characteristics are summarized in Table 3.

Compared to normal (i.e. Sr^{2+}) activation, changes in actin dynamics during activation appeared to be a result of changes in spindle dynamics. Normally, at anaphase-telophase II, the actin ring forms along the same plane as the midbody and a normal-sized polar body is emitted. During U0126 activation, the actin ring still formed along the same plane as the metaphase plate. Thus, in cases where the spindle stayed close to the cortex and rotated normally, an appropriate

Figure 28. Spindle can fail to rotate during U0126 parthenogenesis. In some eggs, the spindle fails to rotate and anaphase II occurs parallel to the oolemma (3h). If polar body emission is inhibited, a diploid parthenogenote would result (7 h). Alternatively, a cleavage furrow overlying the non-rotated spindle could form, in the same plane as the spindle midzone (8 h), creating an abnormally large polar body. Each row of three images represents one egg. Yellow numbers in upper left corner of each row indicate the time post-activation for that series of three images. Numbers in lower left corner of the images in the first two columns indicate depth of slice from top (of nine slices). The third image in each row is a composite of the entire Z-series for that egg (C).

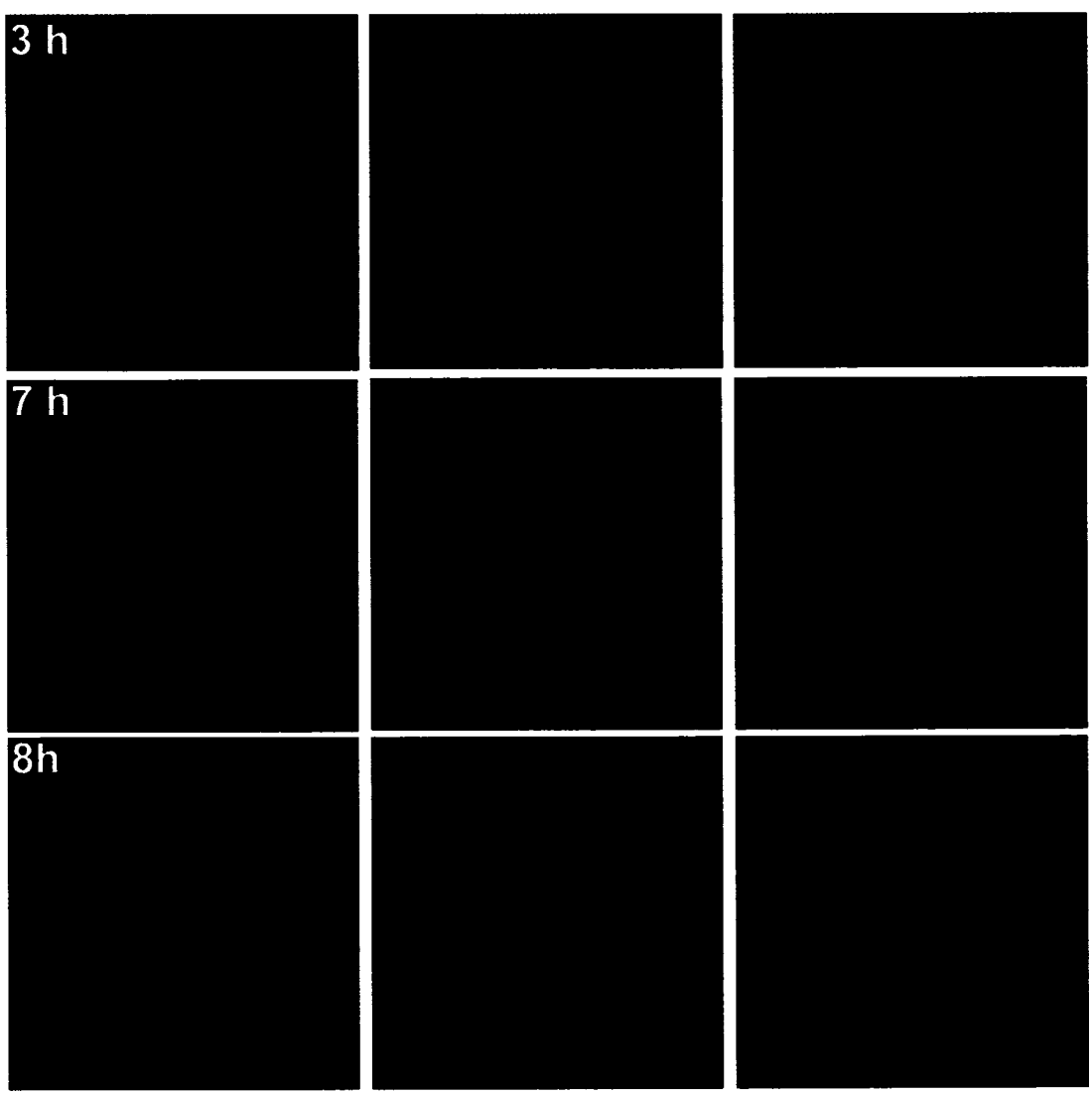
3 h
7 h
8h

Table 3: Actin/microfilament characteristics during U0126 parthenogenetic activation. Eggs were parthenogenetically activated with 50 μM U0126, fixed and stained to visualize the actin Each image was assessed for actin and chromatin characteristics, as well as cell stage and genotype. Spindle characteristics were estimated based on the positioning of the chromatin (spindle was assumed to be between 2 masses of chromatin). Activated eggs could have more than one characteristic.

	Time post-U0126 (h)			
Characteristic	**1-2 h**	**3-4 h**	**5-6 h**	**7-8 h**
Normal Stage for time	10	22	19	20
Spindle rotated	12	5	1	0
Spindle Defects				
Large PB/Fragments	0	2	5	6
Mitotic-like cleavage	0	0	1	3
Spindle Destabilization	13	4	1	1
Spindle drift	5	6	3	4
Spindle "spin"	1	1	1	1
Failure to Rotate	15	2	0	0
Actin Characteristics				
Incomplete Cleavage	0	0	1	0
"Ball" of Actin	0	0	1	0
Cortical Puckering	0	0	0	0
Cell Stage				
Metaphase	8	4	2	5
Anaphase/Telophase	28	18	2	2
Interphase	0	13	25	25
Genotype				
1n	8	24	22	23
2n	0	3	4	5
Micronuclei	3	2	0	1
Unknown	25	6	3	3
Total No. Pictures Examined	36	35	29	32

amount of cytoplasm was pinched off to form the polar body and a Class I parthenogenote developed (Fig. 29).

The actin dynamics leading to Class II parthenogenotes arising from spindle drift and spindle rotation failure are proposed in Figs. 30 and 31, respectively. After 2 h of exposure to U0126 location of the chromatin masses indicated that the cell was in anaphase. Both masses were situated away from the cortex, nearer the middle of the egg (Fig. 30, 2 h), strongly suggesting that the spindle had drifted away from the cortex. Since tubulin and actin could not be visualized simultaneously, the spindle was assumed to be between these two masses, as shown above (Fig. 27). The cleavage furrow formed in a more equatorial position than in Sr^{2+} activation, beginning as a localized band of actin at the cortex that would divide the two masses of chromatin, shown here 5 h post-U0126. Therefore, when the spindle drifts towards the middle of the egg, the actin ring appears to form nearer the equator. After 6 h of exposure to U0126, the cleavage furrow contracted, dividing the cytoplasm along a plane that would pass through the middle of the spindle. This created an abnormally large polar body, capable of developing its own pronucleus by 6-7 h after activation (Fig. 30). Fragmentation was observed in one or both blastomeres, as shown in Fig 30 after 7 h of U0126 activation. As a special case of Class II parthenogenesis, when the actin ring formed at the equator of the egg, the polar body and egg were the same size and a Class III parthenogenote developed (Fig. 30, 7 h).

In those eggs where the spindle did not appear to rotate (Fig. 31), two fates are proposed. In some eggs, second polar body emission did not occur, leading to a diploid Class I parthenogenote by 8 h of U0126 treatment (Fig. 31, 8 h). In other eggs, a cleavage furrow formed through the non-rotated spindle, in the same plane as the metaphase plate. The cleavage furrow thus formed a ring deep into the egg and a large polar body developed, creating a Class II parthenogenote (Fig. 31, 3 h).

Figure 29. Proposed actin dynamics leading to Class I parthenogenotes after treatment with 50 μM U0126. See text for a description. Each row of three images represents one egg. Yellow numbers in upper left corner of each row indicate the time post-activation for that series of three images. Numbers in lower left corner of the images in the first two columns indicate depth of slice from top (of nine slices). The third image in each row is a composite of the entire Z-series for that egg (C).

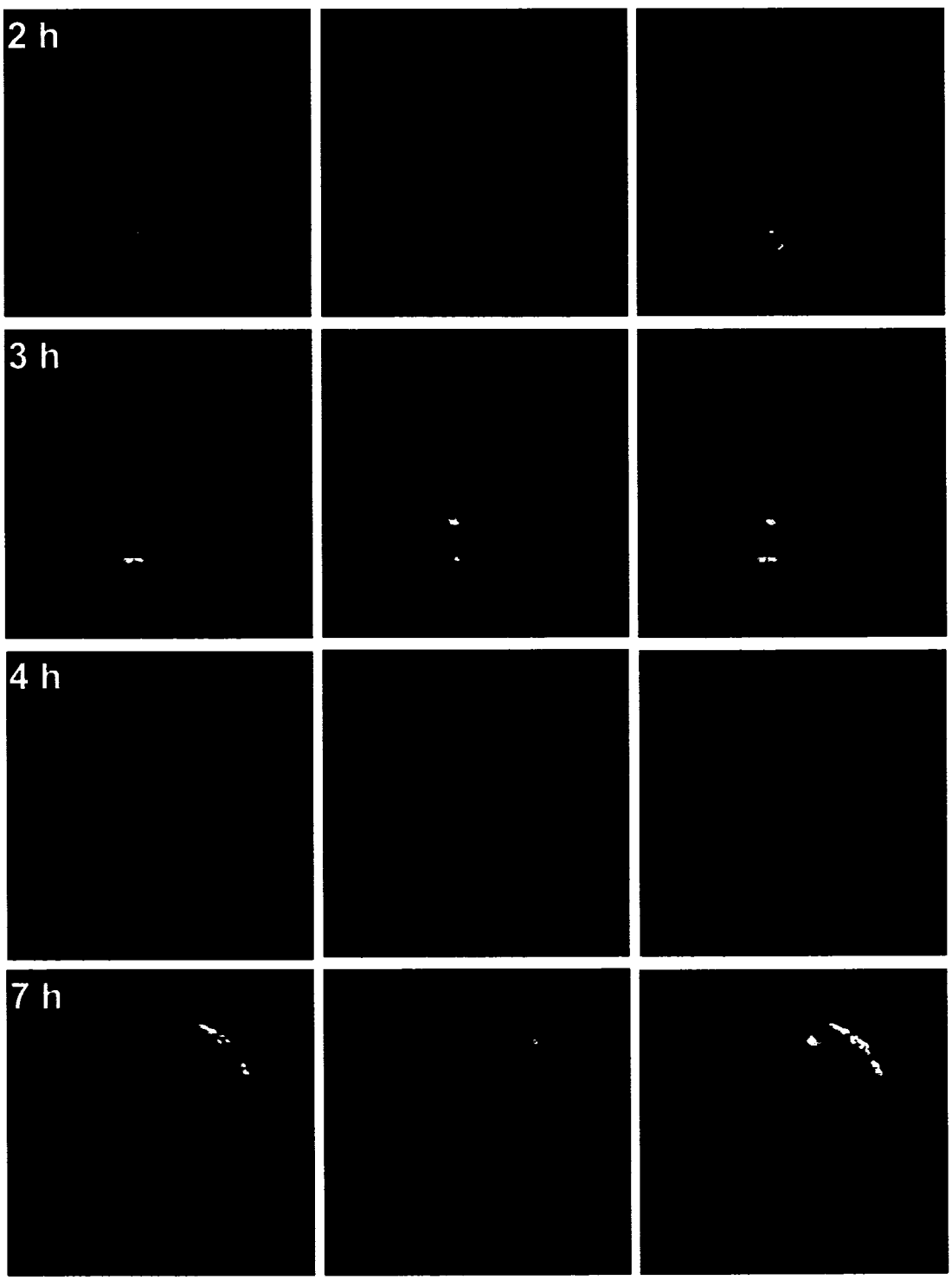
2 h
3 h
4 h
7 h

Figure 30. Proposed actin dynamics leading to Class II parthenogenotes after treatment with 50 μM U0126. The spindle appears to drift away from the cortex leading to extrusion of an abnormally large polar body. See text for a detailed description. Each row of three images represents one egg. Yellow numbers in upper left corner of each row indicate the time post-activation for that series of three images. Numbers in lower left corner of the images in the first two columns indicate depth of slice from top (of nine slices). The third image in each row is a composite of the entire Z-series for that egg (C).

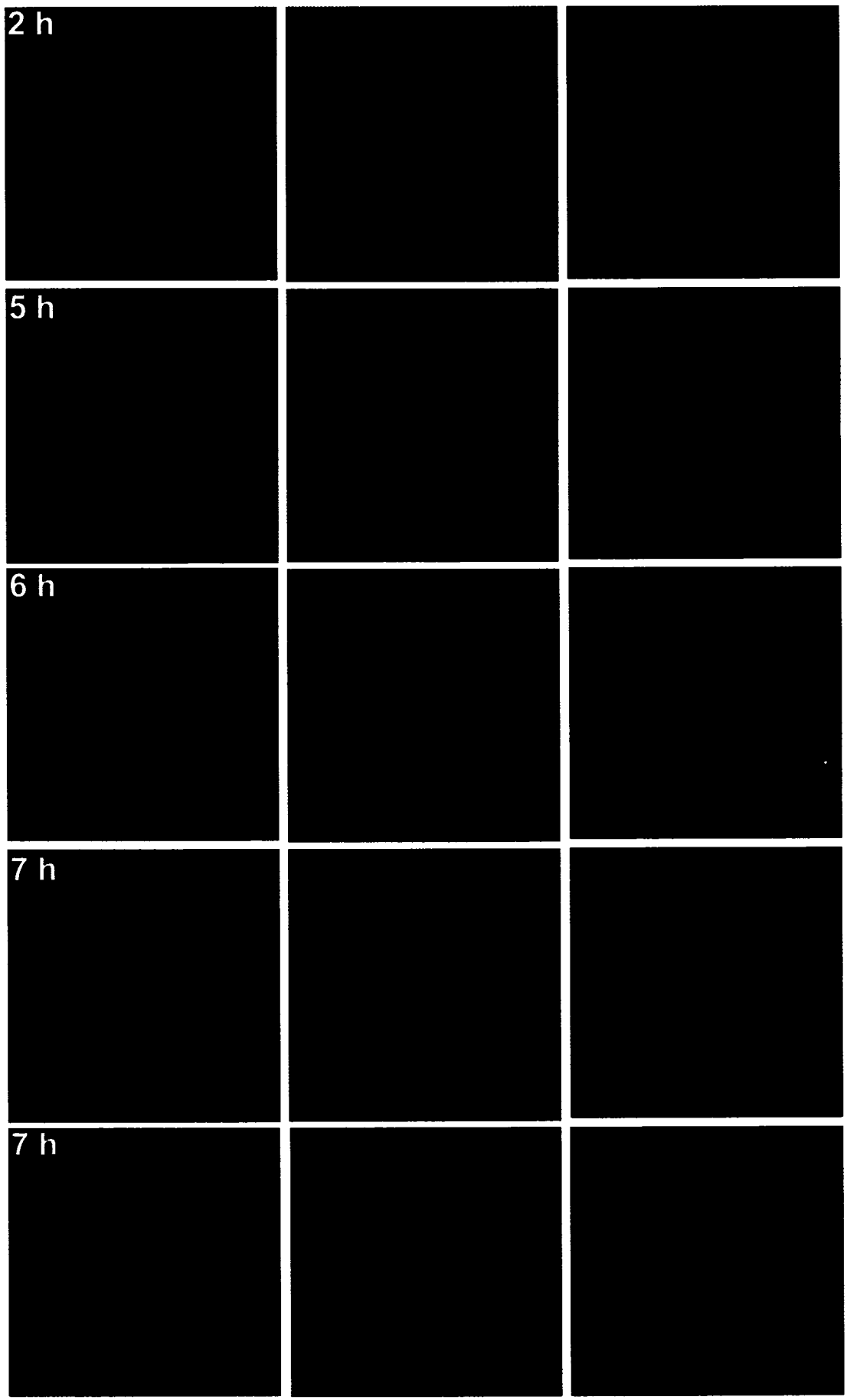
2 h
5 h
6 h
7 h
7 h

Figure 31. The spindle may fail to rotate following U0126 parthenogenesis – actin visualization. In some eggs, the spindle failed to rotate and anaphase II occurred parallel to the oolemma (2h). At 3 h post-U0126, an oversized polar body has formed and has begun to fragment. See text for a detailed description. Yellow numbers in upper left corner of each row indicate the time post-activation for that series of three images. Numbers in lower left corner of the images in the first two columns indicate depth of slice from top (of nine slices). The third image in each row is a composite of the entire Z-series for that egg (C).

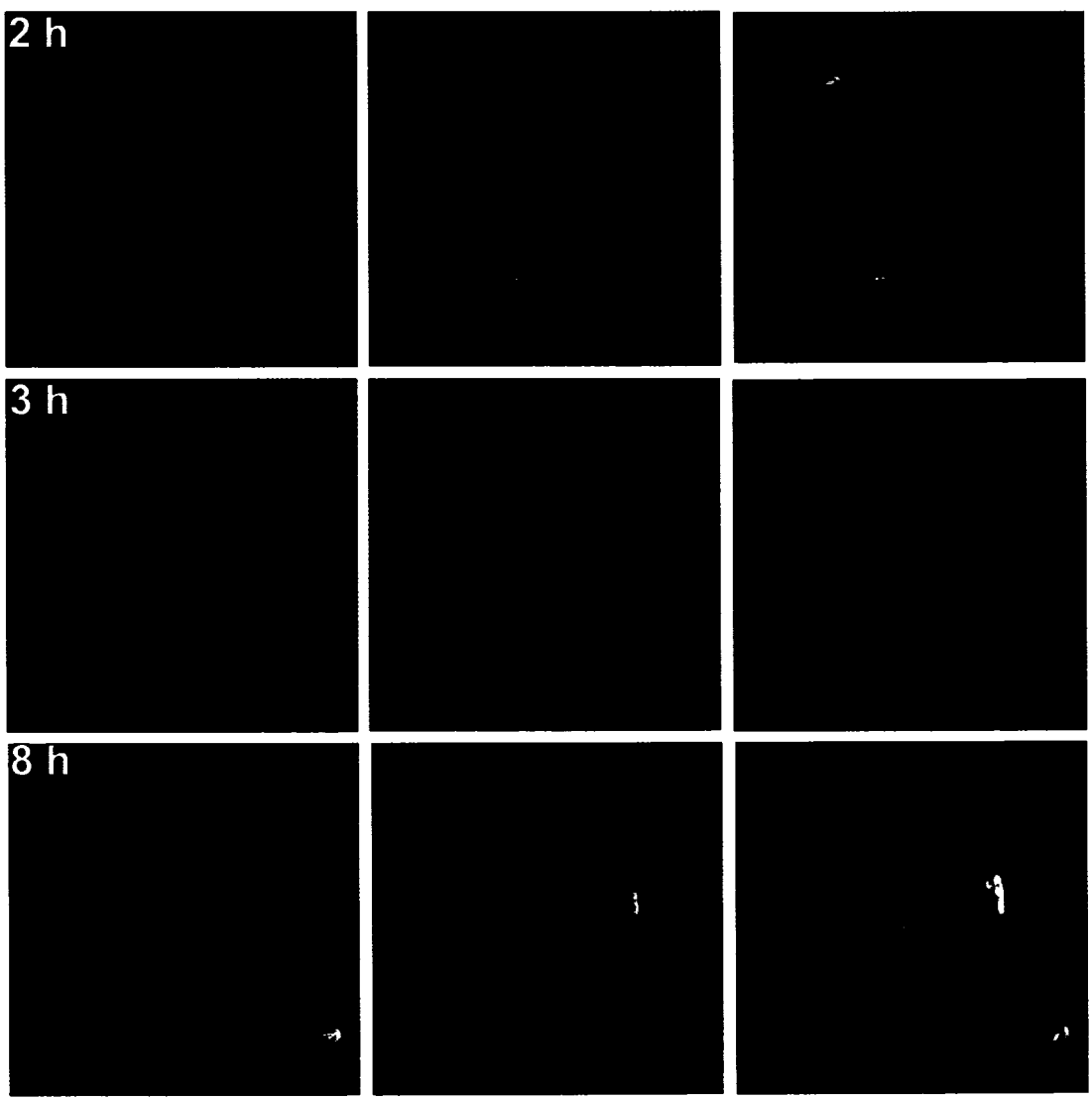
2 h
3 h
8 h

4.3.10 Spindle Dynamics Determined by Birefringence following U0126 Activation

Eggs were activated with U0126, and spindle dynamics/birefringence were followed through activation using the Polscope. Following U0126 treatment, the spindle appeared to thicken slightly and then the birefringence markedly decreased (Fig. 32). Two minutes after treatment (0:02), the spindle is visible. By 18 min post-U0126, the birefringence of the spindle had fallen below detection limits and was not apparent after 18, 45 or 59 min of exposure to U0126. No spindle-associated birefringence was apparent, even when the focus was adjusted through the thickness of the egg (data not shown), suggesting that the loss of birefringence is genuine and not a result of the spindle drifting out of the plane of focus. Because the Polscope measures birefringence, a property of organized spindles, the disappearance suggests destabilization or disorganization of the spindle in these parthenogenotes. Cooling would affect tubulin polymerization and spindle organization (Pickering and Johnson, 1987), possibly altering birefringence. However, oocytes were imaged in a chamber specifically designed to maintain constant physiological temperature so it is unlikely that the loss of birefringence was an artifact of oocyte handling. Furthermore, the spindle is present before activation and then lost (and is not similarly lost in Sr^{2+}-activated eggs under identical conditions), suggesting that the lost birefringence is a specific effect of U0126 activation.

Using the PolScope, I have also observed that the spindle of a subset of eggs treated with U0126 appears to "spin" parallel to the plasma membrane. In the example presented in Fig. 33, the MII spindle was oriented so that the barrel shape is horizontal (0:19). With respect to the viewer, the spindle poles are side by side. After 45 min of activation with U0126, the spindle had rotated parallel to the membrane so that one spindle pole was higher than the other. After one hour of activation (1:04), the spindle had turned such that the spindle was still parallel to the membrane but the spindle poles were one atop the other, giving the impression of "looking down" on the spindle. At this perspective, the chromosomes of the metaphase plate could be seen as

Figure 32. Changes in birefringence following U0126 parthenogenesis. The spindle seems to "disappear" following exposure to U0126. Numbers in top left corner of each picture indicate time post-U0126 (h:mm).

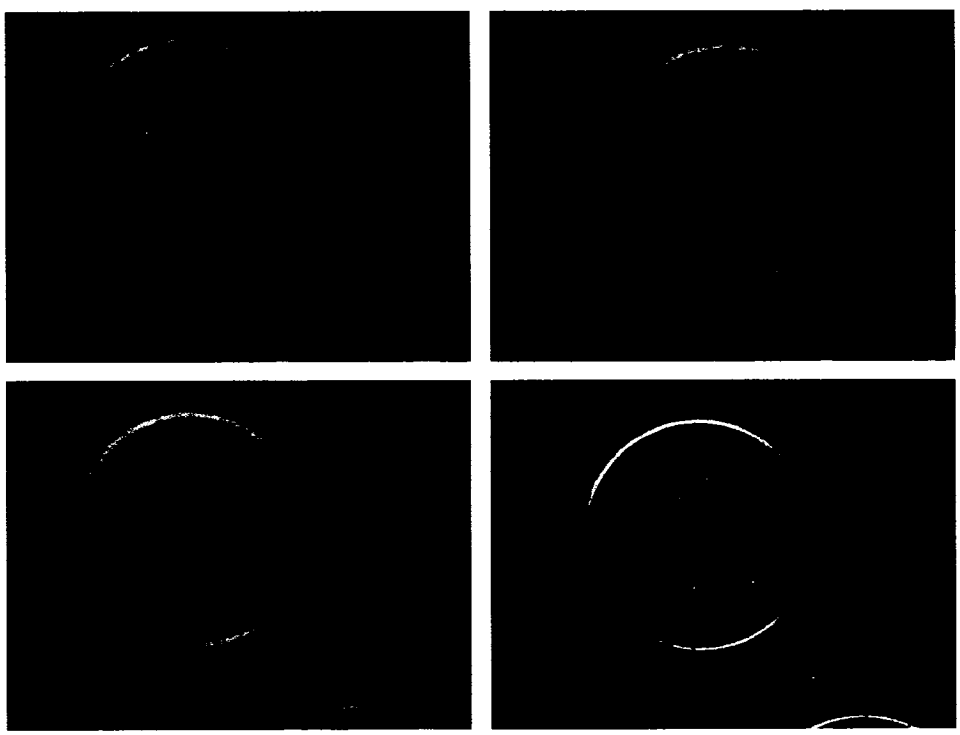

Figure 33. Changes in birefringence following U0126 parthenogenesis – "spinning spindle". Eggs were parthenogenetically activated with U0126 and the spindle in a single egg was followed over a period of 2 h. Numbers in the top left corner of each image indicate the time post-U0126 (h:mm).

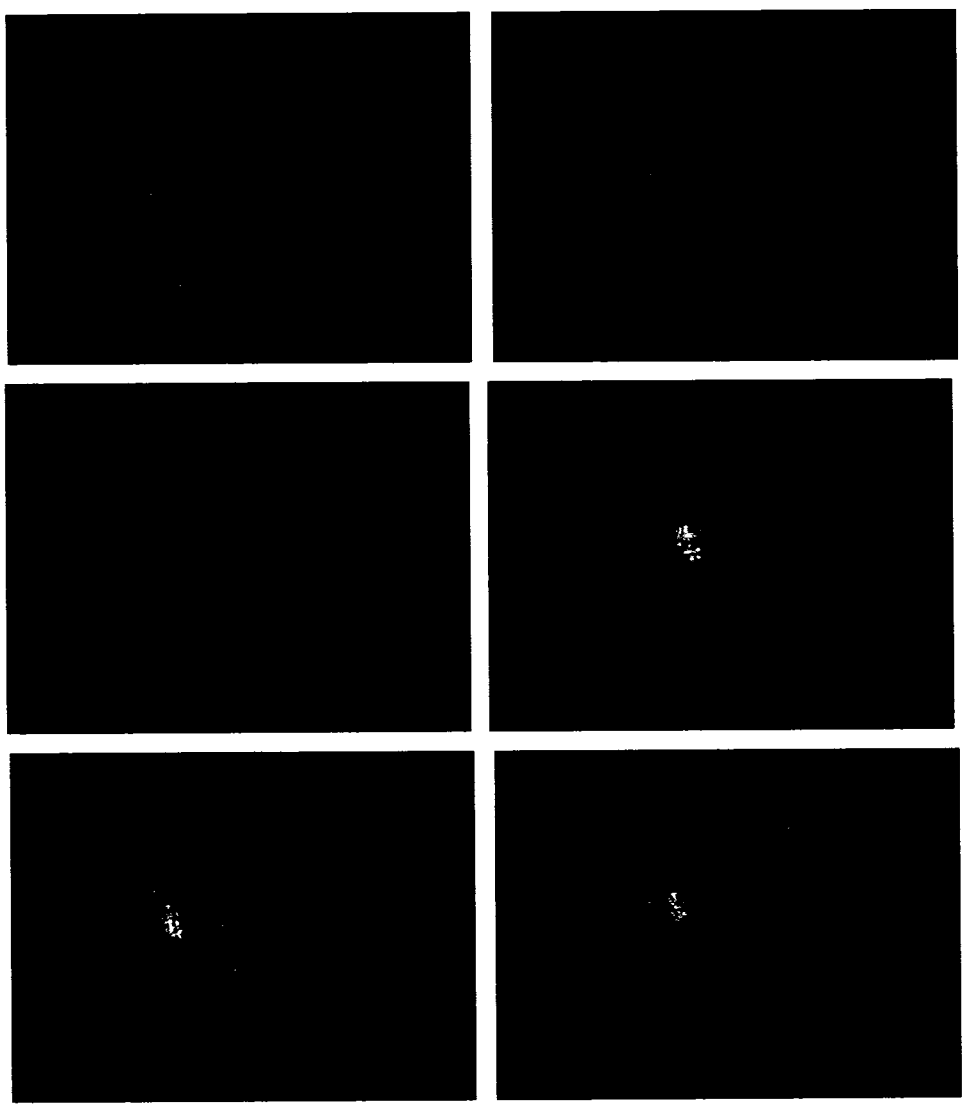

discrete dots in a circle, in one plane of focus. Forty minutes later (1:44), the spindle had continued rotating parallel to the membrane and was now horizontal to the plane of focus, with the barrel shape clearly visible. By 1:59 and 2:11 post-U0126, the spindle continued its rotation parallel to the plasma membrane and one spindle pole had rotated out of the plane of focus. At each observation point, the polar body is situated at the 6:30 position. This served as a control to confirm that the spindle is moving independently of the egg as a whole. Eggs displaying this spinning spindle event do not develop a parthenogenetic phenotype, even 8 h post-U0126. This phenomenon appears to be more common in slightly aged eggs (collected 16-18 h post-hCG). The spinning spindle could only be observed by following a living egg (using the PolScope) throughout the course of U0126 activation, since immunofluorescent methodologies with fixed eggs can provide only a single point in time observations of oocytes at various times after activation, and thus can't reveal spinning of the spindle parallel to the plasma membrane.

4.4 ROSCOVITINE ACTIVATION

4.4.1 Roscovitine Parthenogenetically Activates Eggs

Eggs treated with the cdc2 kinase inhibitor, roscovitine (50 μM) became parthenogenetically activated (Fig. 34A). Histone H1 kinase activity, assessed using the simultaneous kinase assay, had decreased by roughly 50% after 1 h of exposure to roscovitine, and was completely gone before 4 h (Fig. 34B). MBP kinase activity, measured with the simultaneous kinase assay, also declined following roscovitine exposure, though at a much slower rate, falling to basal levels between 4 and 8 h (Fig. 34B). The time courses for both MPF and MAPK deactivation by roscovitine were similar to that which follows IVF (Fig. 9).

The phenotypes produced after parthenogenetic activation with roscovitine were assessed. Unexpectedly, a subset of phenotypes similar to that produced by U0126 arose, including the large polar bodies and precocious cleavages typical of *mos*$^{-/-}$ oocytes (Fig. 34C). In contrast, eggs activated by IVF or by Sr^{2+} under conditions identical to those used with

Figure 34. Roscovitine parthenogenetically activates eggs. A. Average incidence of parthenogenesis measured after 8 h of exposure to 50 μM roscovitine or vehicle (0.1% DMSO). Numbers above bars are N(n), where n is the total number of eggs and N is the number of replicates. B. Mean MBP kinase (±SEM; •) and histone H1 kinase activities (±SEM; •) following 50 μM roscovitine exposure. The value of MBP and histone H1 kinase activities of eggs (t=0h) were arbitrarily set at 100% with subsequent time points expressed relative to this amount. Each time point was replicated 6-8 times. C. Some roscovitine parthenogenotes resembled *mos*$^{-/-}$ parthenogenotes after 8 h of exposure to the drug. I: Class I phenotype with pronucleus (PN) and second polar body (PB2). II: Class II phenotype with very large polar body (PB2). III: Class III phenotype with 2 blastomeres, each containing a nucleus (N). Scale bar represents 50 μm. Adapted from Phillips *et al.*, 2002.

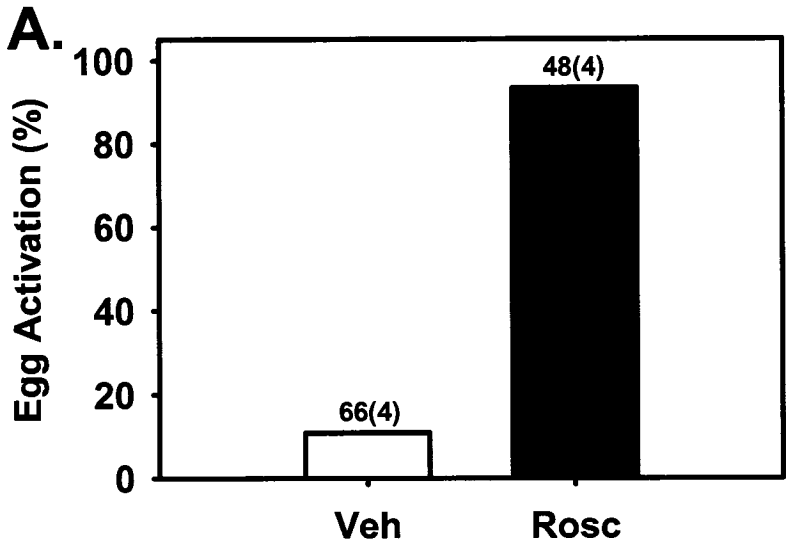
A.
Egg Activation (%)
100
80
60
40
20
0
48(4)
66(4)
Veh
Rosc

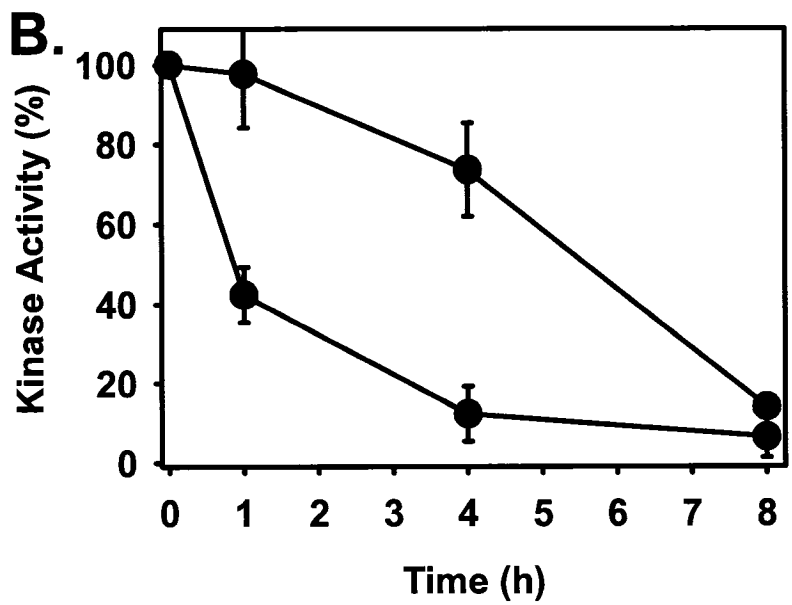
B.
Kinase Activity (%)
100
80
60
40
20
0
0 1 2 3 4 5 6 7 8
Time (h)

C.

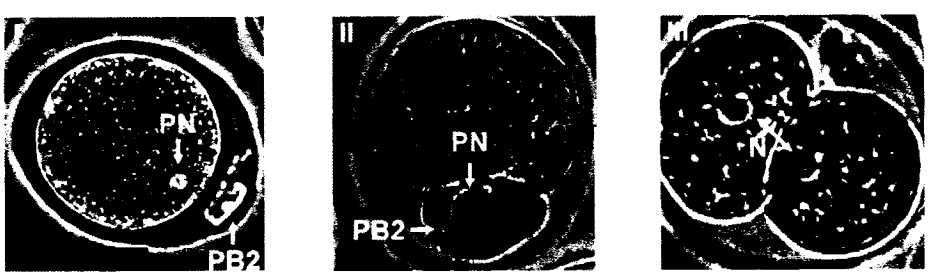
PN
PB2
II
PN
PB2
III
N

roscovitine or U0126 never produced Class II or III parthenogenotes (not shown). This implied that normal spindle dynamics and the cytokinesis that produces the polar body might require both CSF and MPF activities.

4.4.2 Roscovitine Does Not Directly Inhibit MAPK

It is unlikely that the inactivation of MAPK upon roscovitine exposure is due to direct inhibition of MAPK activity, since both ERK1 and ERK2 are reported to be relatively insensitive to roscovitine, and MAPK activity declined only slowly in roscovitine treated eggs. However, since roscovitine produced some parthenogenotes with phenotypes like those that arose upon MEK/MAPK inactivation, I tested whether roscovitine might be directly affecting MAPK at the concentration used. When 50 μM roscovitine was included in the simultaneous kinase assay mixture with egg lysates, MBP kinase activity was only slightly affected (Table 1). As expected, the presence of roscovitine in the assay mixture inhibited H1 kinase activity to a level comparable to the basal H1 kinase activity in zygotes, and was significantly different from the 100% activity in egg lysates in the absence of roscovitine ($P < 0.001$; Student's t test; $N = 5$). Thus, roscovitine appears to be specifically inhibiting MPF activity under these conditions.

4.4.3 Tubulin Dynamics During Roscovitine Activation

Following exposure to roscovitine, eggs were fixed, stained for tubulin visualization, imaged and spindle characteristics were classified, as described in 4.3.8 for tubulin/spindle dynamics during U0126 parthenogenesis. Spindle characteristics for roscovitine parthenogenesis are summarized in Table 4. In total, 46 eggs were characterized.

The majority of parthenogenotes formed following disruption of cdc2 kinase by roscovitine share the same phenotype as Sr^{2+} parthenogenotes and fertilized eggs. Tubulin localization in fixed samples indicated that such Class I parthenogenotes develop as in IVF or Sr^{2+} parthenogenesis (Fig. 35). Briefly, the spindle rotated 90° to become perpendicular to the plasma membrane, and the chromosomes had separated (Fig. 35, 2 h). After 3 h of roscovitine

Table 4: Spindle characteristics during roscovitine parthenogenetic activation. Eggs were parthenogenetically activated with 50 μM roscovitine, fixed and stained to visualize the tubulin cytoskeleton. Each image was assessed for spindle and chromatin characteristics as well as cell stage and genotype. An egg could have more than one characteristic.

Characteristic	Time post-Roscovitine (h) 1-2 h	3-4 h	5-6 h	7-8 h
Normal Stage for time	1	7	7	4
Spindle rotated	9	3	1	0
Spindle Defects				
Large PB/Fragments	2	3	0	4
Mitotic-like cleavage	0	0	1	0
Spindle Destabilization	4	1	0	0
Spindle drift	8	2	0	2
Spindle "spin"	0	0	0	0
Failure to Rotate	1	0	0	0
Cell Stage				
Metaphase	8	1	0	0
Anaphase/Telophase	9	2	1	0
Interphase	0	9	7	9
Genotype				
1n	4	10	8	7
2n	0	1	0	2
Micronuclei	0	0	0	0
Unknown	13	1	0	0
Total No. Pictures Examined	17	12	8	9

Figure 35. Proposed tubulin dynamics leading to Class I parthenogenotes after treatment with 50 μM roscovitine. See text for description of cytoskeletal events leading to the development of Class I parthenogenotes. Yellow numbers in the upper left corner of each row indicate the time post-activation for that series of three images. Numbers in the lower left corner of the images in the first two columns indicate depth of slice from the top (of nine slices). The third image in each row is a composite of the entire Z-series for that egg (C).

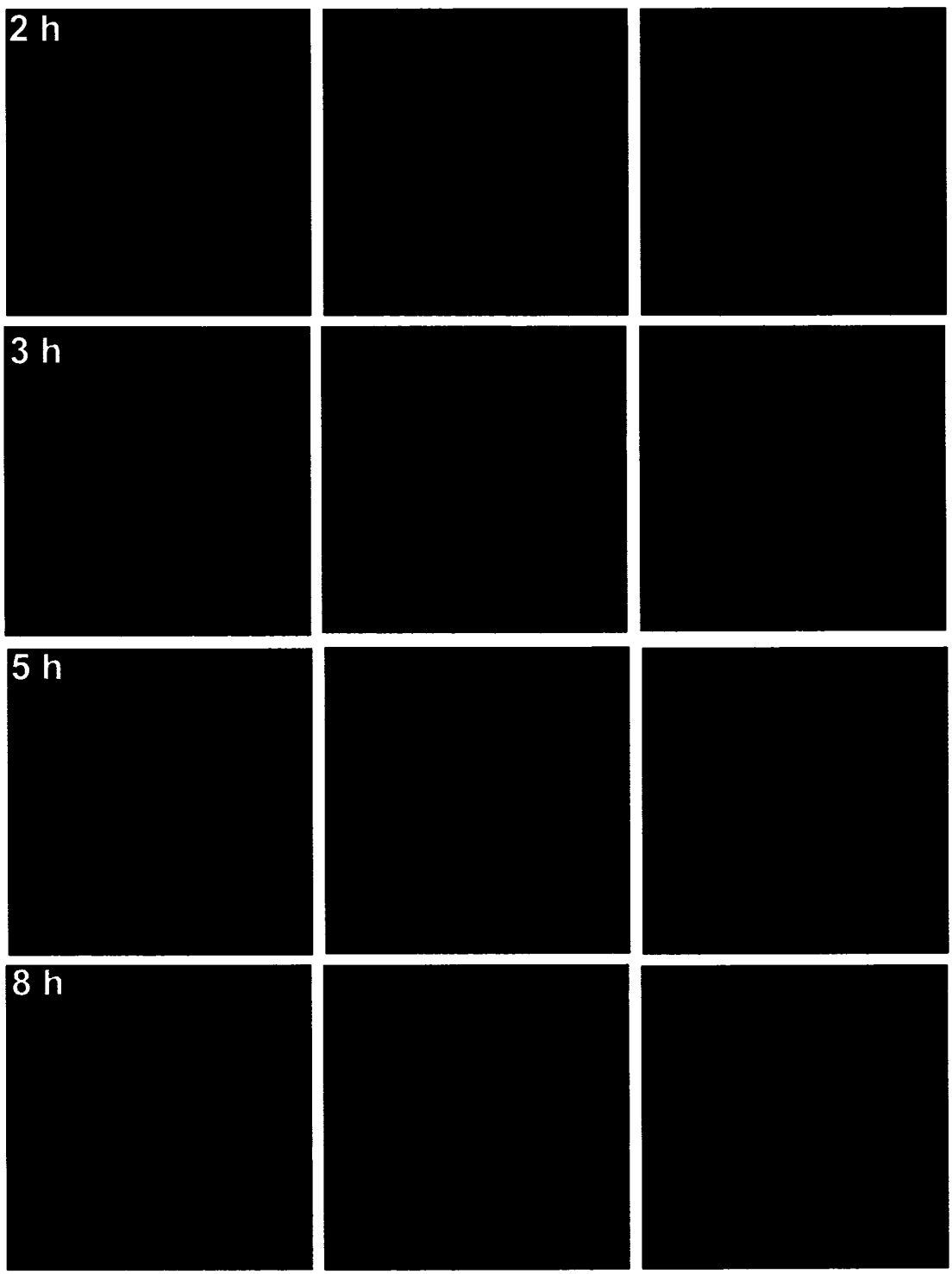
2 h
3 h
5 h
8 h

treatment, the polar body had been emitted and the midbody was present between the polar body and the egg proper. The chromatin decondensed between 4-8 h post-activation and the nuclear membrane developed to form a pronucleus. By 8 h post-roscovitine, only a minute amount of the midbody remained associated with the polar body.

In the small proportion of Class II and III parthenogenotes arising from roscovitine treatment, microtubule dynamics appeared to resemble those in U0126 treatment where the spindle undocks from the cortex (Fig. 36). After a 2 h exposure to roscovitine, the spindle had moved away from the cortex and the chromosomes had separated (Fig. 36, 2 h). Because of the central location of the spindle, a larger than normal volume of cytoplasm was pinched off into the polar body by the cleavage plane that passes through the middle of the spindle. The midbody was observed between the polar body and the egg after 4 h. By 4 h post-roscovitine, the chromatin had begun to decondense and the nuclear membrane had formed the pronucleus. When the spindle drifted into the very middle of the egg, the cleavage was mitotic-like in that the polar body and activated egg were the same size, forming Class III parthenogenotes (shown in Fig. 36 at 6 h).

4.4.4 Actin Dynamics During Roscovitine Activation

As described in section 4.3.8 above, eggs were fixed between 1-8 h post-roscovitine and stained to visualize the actin cytoskeleton. A total of 102 egg images were captured using the confocal microscope and were examined to determine actin dynamics leading to the observed phenotypes. Each image was then scored for actin characteristics including contractile ring, development of a "ball" of actin, puckering of the cortex and the presence of incomplete cleavage furrows. Further, certain spindle characteristics were estimated based upon the location and shape of chromatin masses (i.e. spindle drift, spindle destabilization). Eggs could have more than one trait. These characteristics are summarized in Table 5.

Figure 36. Proposed tubulin dynamics leading to Class II parthenogenotes after treatment with 50 μM roscovitine. The spindle appears to drift away from the cortex leading to extrusion of an abnormally large polar body. See text for a detailed description of cytoskeletal events leading to the development of Class II parthenogenotes. Yellow numbers in upper left corner of each row indicate the time post-activation for that series of three images. Numbers in the lower left corner of the images in the first two columns indicate depth of slice from the top (of nine slices). The third image in each row is a composite of the entire Z-series for that egg (C).

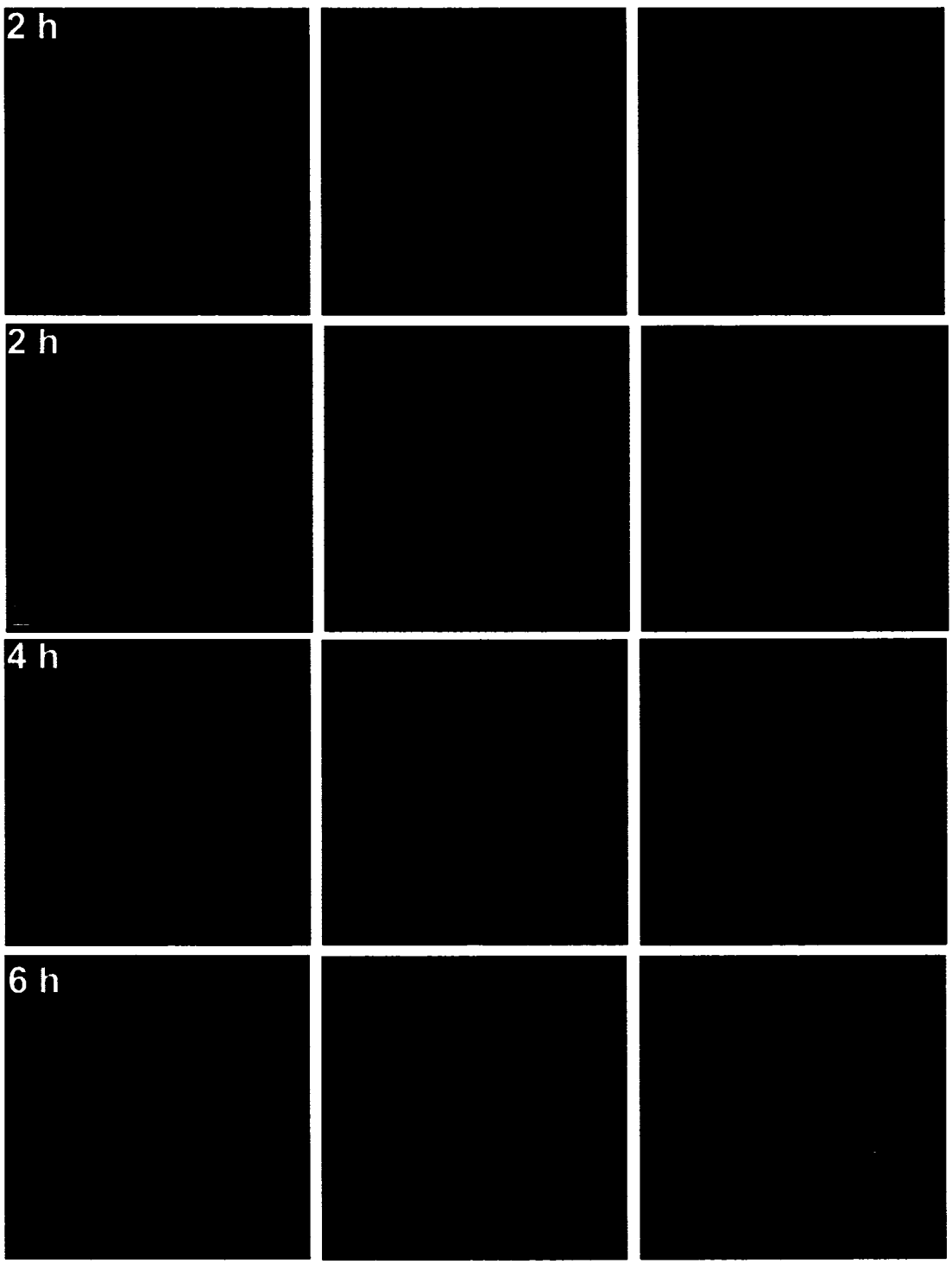
2 h
2 h
4 h
6 h

Table 5: Actin/microfilament characteristics during roscovitine parthenogenetic activation. Eggs were parthenogenetically activated with 50 μM roscovitine, fixed and stained to visualize the actin cytoskeleton. Each image was assessed for actin and chromatin characteristics, as well as its stage and genotype. Spindle characteristics were estimated based on the positioning of the chromatin (spindle was assumed to be between 2 masses of chromatin). Activated eggs could have more than one characteristic.

Characteristic	Time post-Roscovitine (h) 1-2 h	3-4 h	5-6 h	7-8 h
Normal Stage for time	12	24	13	14
Spindle rotated	25	15	0	0
Spindle Defects				
Large PB/Fragments	2	3	1	2
Mitotic-like cleavage	0	0	2	0
Spindle Destabilization	5	2	0	0
Spindle drift	7	3	0	0
Spindle "spin"	0	0	0	0
Failure to Rotate	9	0	0	0
Actin Characteristics				
Incomplete Cleavage	0	0	0	0
"Ball" of Actin	1	0	0	0
Cortical Puckering	0	0	0	0
Cell Stage				
Metaphase	24	2	0	0
Anaphase/Telophase	16	14	0	0
Interphase	0	14	16	16
Genotype				
1n	10	27	15	15
2n	0	0	0	0
Micronuclei	1	0	1	1
Unknown	29	3	0	0
Total No. Pictures Examined	40	30	16	16

Actin staining of fixed samples indicates that Class I parthenogenotes develop in the same manner as in IVF activation or Sr^{2+} parthenogenesis (Fig. 37). The spindle rotated at the cortex (1 h, 2 h; Fig 37). By 3 h post-roscovitine, the contractile ring had pinched off a small polar body and the chromatin decondensed so that the pronuclei were visible 5-8 h post-roscovitine.

The actin dynamics leading to the small proportion of Class II parthenogenotes are proposed in Fig. 38. After 1-2 h of exposure to roscovitine, the cell was in anaphase, and two distinct chromatin masses could be seen away from the cortex, nearer the middle of the egg. Since tubulin and actin could not be visualized simultaneously, the spindle was assumed to be between these two masses, as shown above, in Fig. 36. The cleavage furrow formed in a more equatorial, beginning as a localized band of actin between the two masses of chromatin. Between 5-6 h after roscovitine parthenogenesis, the cleavage furrow contracted, dividing the cytoplasm in a plane passing through the middle of the spindle. This created an abnormally large polar body, capable of developing its own pronucleus shown here 5 h after activation (Fig. 38). Fragmentation was observed in one or both blastomeres, as shown after 8 h of egg activation with roscovitine (Fig. 38). When the actin ring formed at the equator of the egg, the polar body and egg were the same size (5 h; Fig. 38).

4.4.5 Spindle Dynamics Determined by Birefringence Following Parthenogenetic Activation with Roscovitine

Because eggs are fixed for actin and tubulin visualization, the developmental fate of each egg cannot be determined. Imaging single activated eggs on the Polscope can overcome this deficiency, as described above.

Parthenogenesis by roscovitine leading to Class I parthenogenotes is presented in Fig. 39. The birefringence of the spindle initially increased (0:08). As the spindle rotated 90° and the chromosomes separated (anaphase), the spindle fibres appeared as highly birefringent bundles

Figure 37. Proposed actin dynamics leading to Class I parthenogenotes after treatment with 50 μM roscovitine. See text for description of cytoskeletal events leading to the development of Class I parthenogenotes. Yellow numbers in upper left corner of each row indicate the time post-activation for that series of three images. Numbers in lower left corner of the images in the first two columns indicate depth of slice from top (of nine slices). The third image in each row is a composite of the entire Z-series for that egg (C).

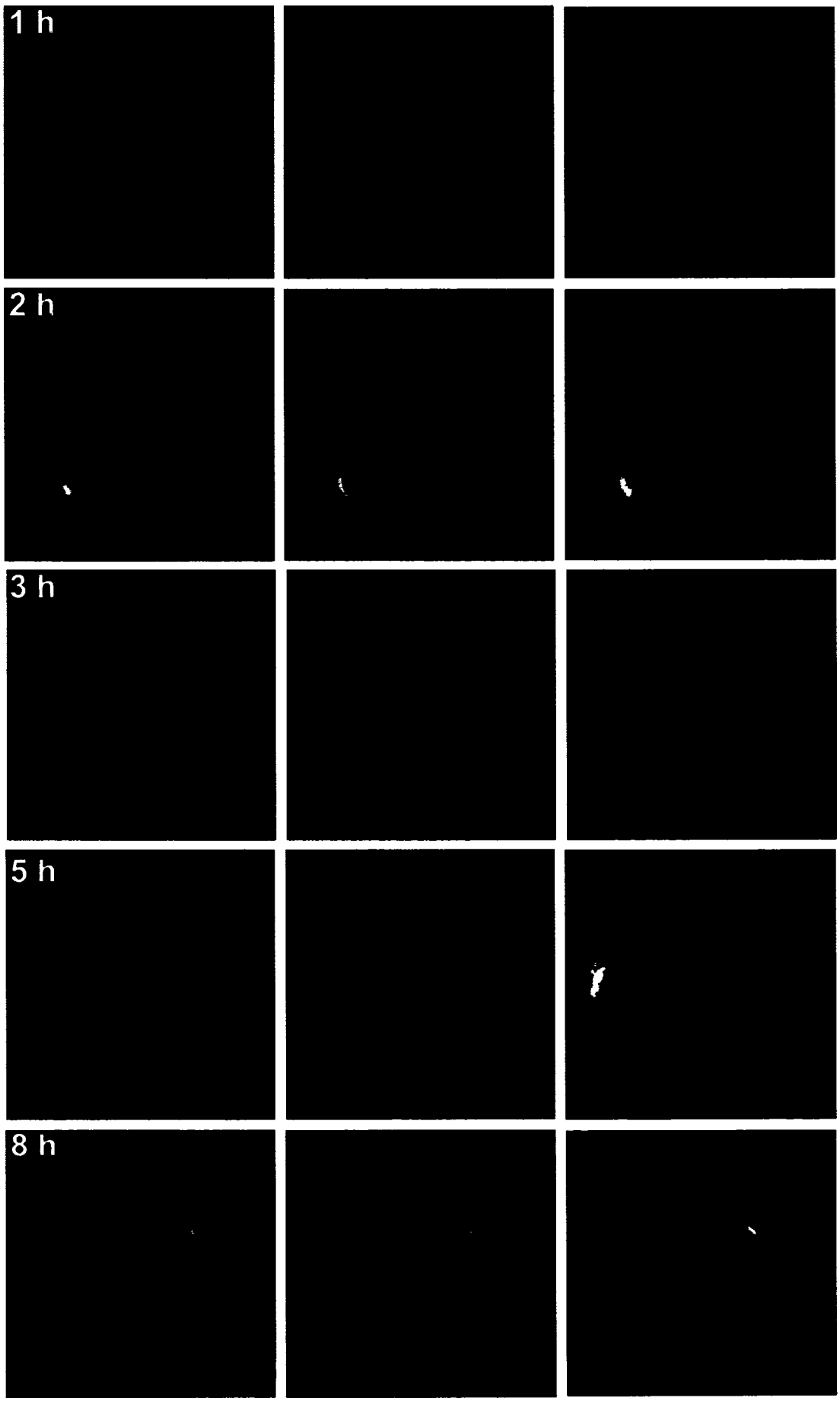
1 h
2 h
3 h
5 h
8 h

Figure 38. Proposed actin dynamics leading to Class II parthenogenotes after treatment with 50 μM roscovitine. The spindle appears to drift away from the cortex leading to extrusion of an abnormally large polar body. See text for a detailed description. Yellow numbers in upper left corner of each row indicate the time post-activation for that series of three images. Numbers in lower left corner of the images in the first two columns indicate depth of slice from top (of nine slices). The third image in each row is a composite of the entire Z-series for that egg (C).

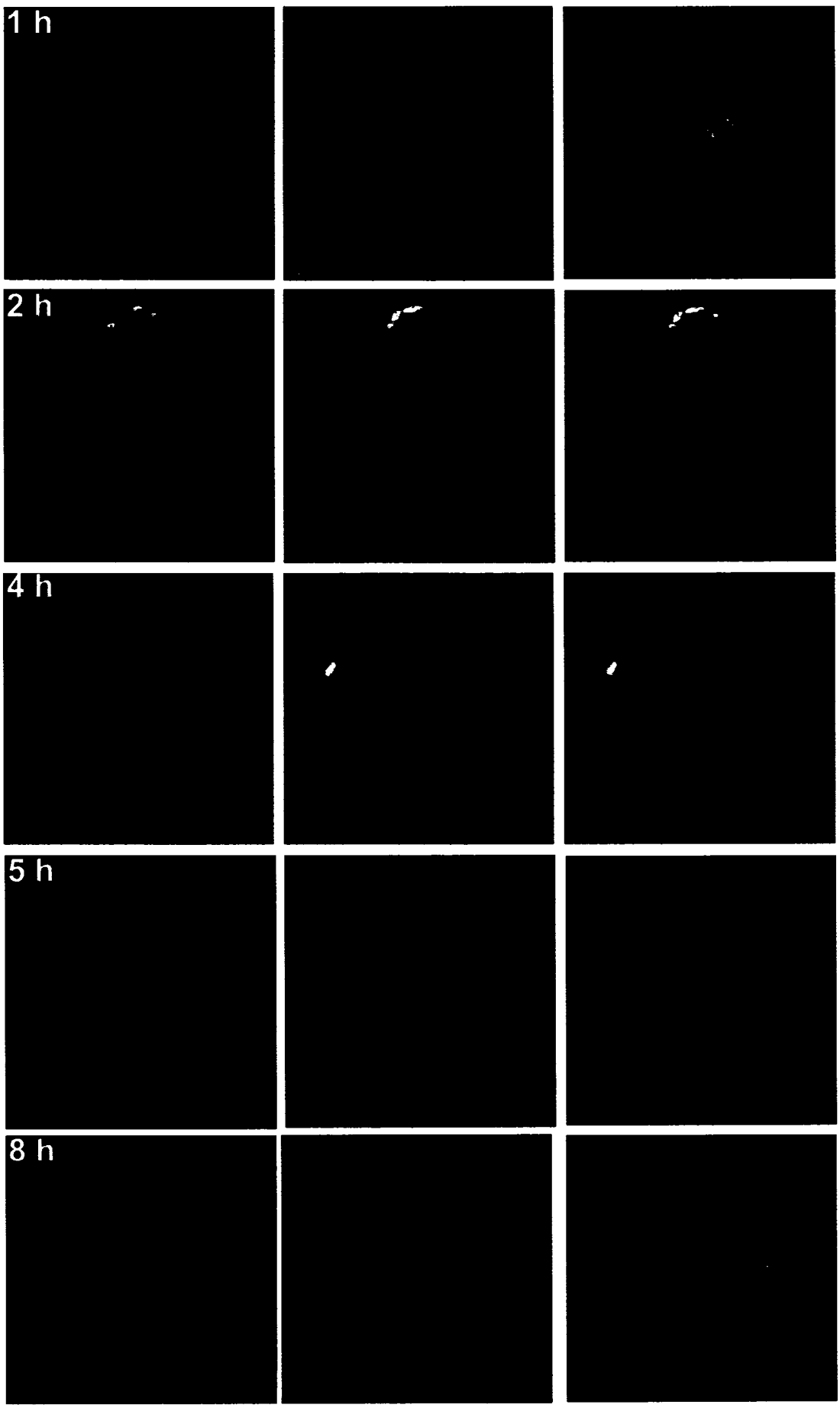
1 h
2 h
4 h
5 h
8 h

Figure 39. Changes in spindle birefringence following roscovitine egg activation. Numbers indicate time post-roscovitine exposure (h:mm). Birefringence increases shortly after the drug was added (0:08). The spindle rotates 90°, perpendicular to the plasma membrane (0:26-1:25) and a polar body is emitted (1:39). The midbody remains as an area of birefringence just after polar body emission (2:03).

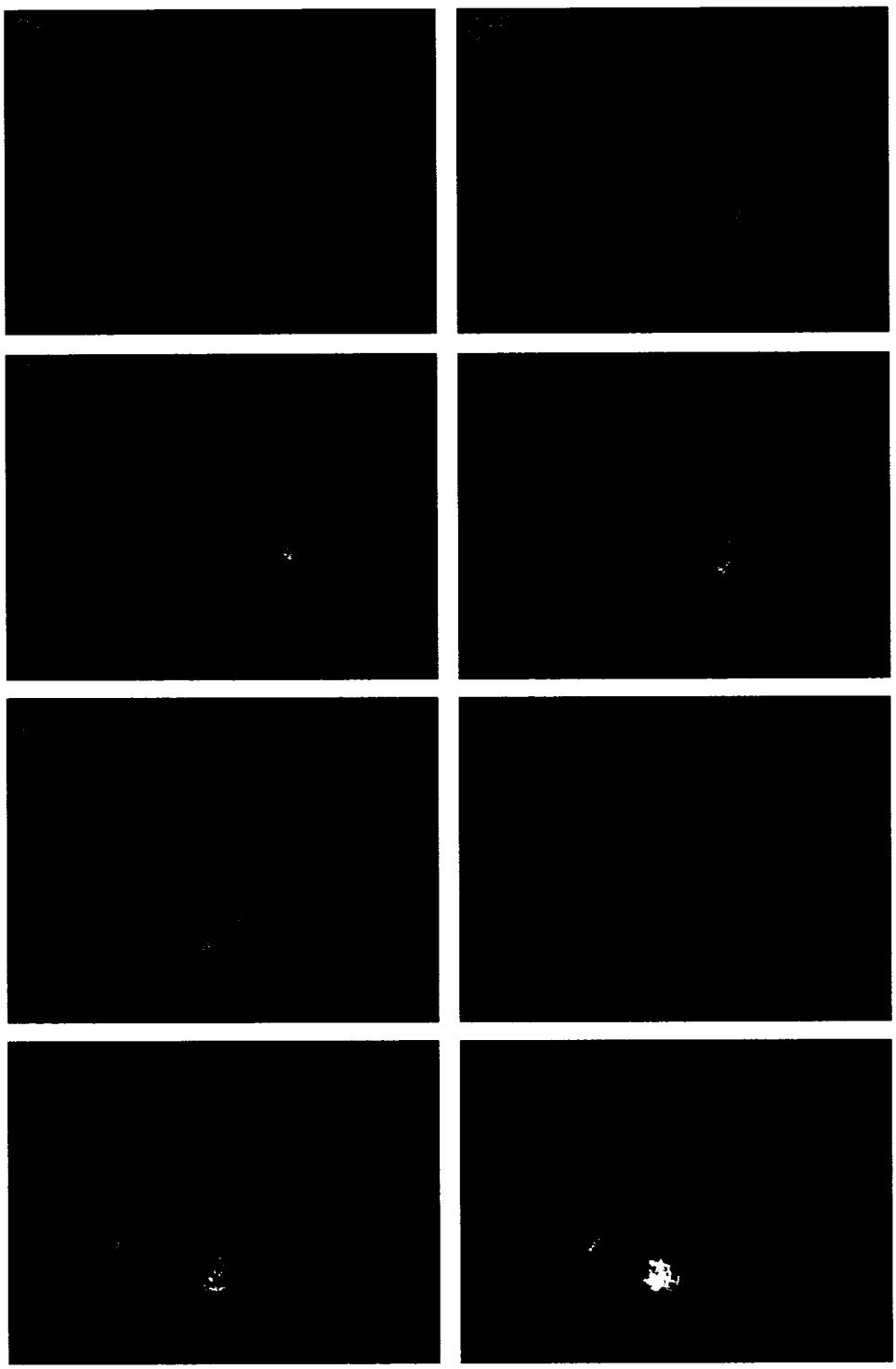

(1:25). Birefringence remained elevated throughout spindle rotation and immediately after polar body extrusion, as the midbody (2:03).

Unfortunately, no class II or III parthenogenotes developed from roscovitine-treated eggs followed with the PolScope, preventing any conclusions to be drawn regarding changes in birefringence or spindle migration in this population of parthenogenotes.

4.5 ROSCOVITINE-U0126 CO-TREATMENT

4.5.1 Simultaneous Treatment with Roscovitine and U0126 Produces a Unique Severe Parthenogenetic Phenotype

I assessed the effect of inhibiting cdc2 kinase and MAPK activities simultaneously by using roscovitine and U0126 in combination. Co-treatment of eggs with roscovitine and U0126 produced a majority of phenotypes that most closely resembled Class II-like parthenogenotes in that they appeared to initiate unequal cleavage, however, they differed markedly from other Class II parthenogenotes. To distinguish them from parthenogenotes that arose from treating eggs with U0126 or roscovitine alone, they are referred to here as roscovitine-U0126 parthenogenotes (R-U parthenogenotes). Most of these eggs exhibited a pronounced irregular shape. The feature characteristic of Class II parthenogenotes, these activated eggs had what appeared to be incomplete cleavages and cleavage furrows (Fig. 40). The cleavage furrow appeared to be at the equator of the egg but only went part of the way around the circumference of the egg. As the cleavage furrow contracted, it pulled the two hemispheres of the egg to the side, creating a kidney bean-shaped parthenogenote. Complete emission of a second polar body was much less frequent in eggs treated with both roscovitine and U0126 (21%; n = 62, N = 4) than in eggs treated with roscovitine (92%; n = 61, N = 4) or U0126 (84%; n= 58, N = 4) alone. Under the light microscope, the plasma membrane appeared irregular or lumpy. Because of the uneven surface of these parthenogenotes, I could not tell if they contained pronuclei under the light microscope as had been determined for the other types of activation (Sr^{2+}, IVF, U0126 or roscovitine).

Figure 40. Roscovitine-U0126 parthenogenotes have a severe phenotype. Examples of parthenogenotes arising from unfertilized eggs exposed to roscovitine in combination with U0126 for 8 h. Scale bar represents 50 μm. Adapted from Phillips *et al.*, 2002a.

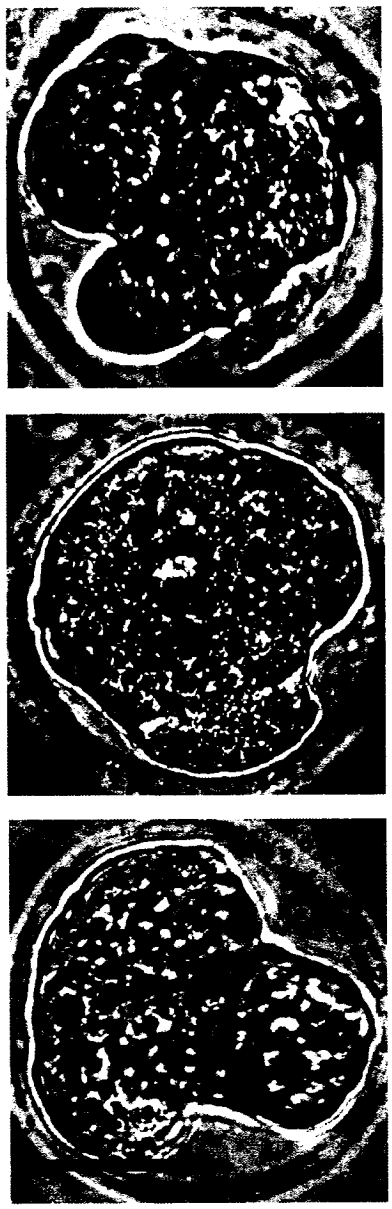

To determine the developmental potential of these partially cleaved eggs, eggs were treated with U0126 and roscovitine co-treatment (50 μM each) for 8 h, washed free of the drugs, and then parthenogenotes were cultured in standard KSOM microdrop culture. These parthenogenotes cleaved at least to the two-cell stage by the next day (72 ± 17%; n = 90, N = 6), producing normal-looking 2-cell embryos. As is common for parthenogenotes, further development was limited. Of the activated eggs, 15 ± 9% of parthenogenotes reached morula stage and 3 ± 2% of parthenogenotes reached blastocyst stage after four and five days of culture, respectively. This suggests that eggs treated with both U0126 and roscovitine were parthenogenetically activated and capable of at least some further development despite the severe phenotype induced by inhibition of both MEK/MAPK and cdc2 kinase.

4.5.2 Tubulin Dynamics During Roscovitine-U0126 Co-Treatment

To determine tubulin/spindle dynamics in roscovitine-U0126 parthenogenotes, 91 images were obtained of fixed eggs that had been stained to visualize tubulin. These pictures ranged from one to eight hours after exposure to the drug. Each image was then scored for spindle characteristics as described in 4.3.8 and 4.4.3. This information is summarized in Table 6.

As discussed above, co-treatment of eggs with roscovitine and U0126 produced a unique phenotype with a pronounced irregular shape and what appeared to be incomplete cleavages and cleavage furrows. Complete emission of a second polar body was much less frequent than in eggs treated with roscovitine or U0126 alone. The roscovitine-U0126 parthenogenotes therefore had 2 pronuclei which, while they could not be visualized by light microscopy (above), were evident in the transmitted light image during confocal microscopy and in the eggs fixed and stained for actin visualization. As with either U0126 or (to some extent) roscovitine, the spindle appears to lose its anchorage to the egg cortex, drifting into the middle of the egg (Fig.41). After 1 h of U0126 and roscovitine co-treatment, the cell was still in metaphase but the spindle had rotated to be perpendicular to the cortex. An hour later, the spindle was in the middle of the egg

Figure 41. Proposed tubulin dynamics leading to roscovitine-U0126 parthenogenotes after co-treatment with 50 μM roscovitine and 50 μM U0126. Spindle drift and incomplete cleavage furrows characterize this parthenogenetic phenotype. Because cleavage is never completed, the midbody persists. See text for a detailed description of the cytoskeletal events. Yellow numbers in the upper left corner of each row indicate the time post-activation for that series of three images. Numbers in the lower left corner of the images in the first two columns indicate depth of slice from the top (of nine slices). The third image in each row is a composite of the entire Z-series for that egg (C).

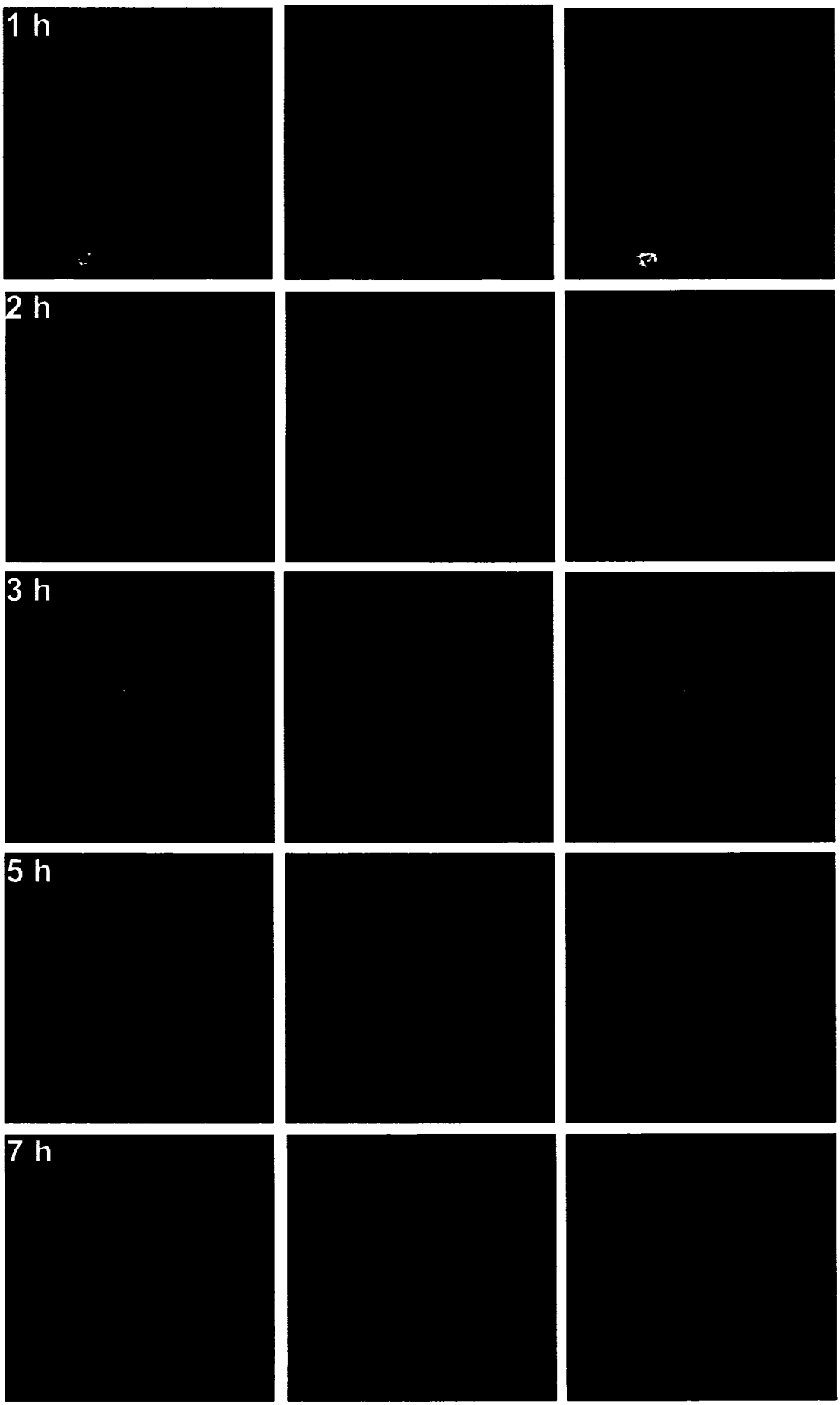
1 h
2 h
3 h
5 h
7 h

Table 6: Spindle characteristics during roscovitine-U0126 parthenogenetic activation. Eggs were parthenogenetically activated with 50 μM U0126 and 50 μM roscovitine, fixed and stained to visualize the tubulin cytoskeleton. Each image was assessed for spindle and chromatin characteristics as well as cell stage and genotype. An egg could have more than one characteristic.

	Time post-Roscovitine-U0126 (h)			
Characteristic	1-2 h	3-4 h	5-6 h	7-8 h
Normal Stage for time	1	1	2	1
Large PB/Fragments	0	0	0	0
Mitotic-like cleavage	0	0	0	0
Spindle Destabilization	7	1	2	0
Spindle drift	6	11	7	16
Spindle "spin"	0	0	0	0
Failure to Rotate	11	0	1	0
Spindle rotated	14	16	2	2
Cell Stage				
Metaphase	14	0	0	0
Anaphase/Telophase	17	9	0	0
Interphase	1	18	13	19
Genotype			0	0
1n	1	1	2	1
2n	4	8	10	14
Micronuclei	3	10	1	4
Unknown	24	8	0	0
Total No. Pictures Examined	32	27	13	19

and the chromosomes had separated to be at either spindle pole (2 h; Fig. 41). After 3 h of U0126 and roscovitine co-treatment, the egg was still in anaphase with the spindle in a central location within the egg. After 5-7 h, the chromatin had decondensed and had drifted away from the remains of the spindle forming two pronuclei, and sometimes additional micronuclei. The membrane had formed indentations such that the furrow or indentation was in the plane of the spindle remnant and that the deepest part of the furrow abutted the spindle midregion. By 7 h post-roscovitine-U0126 treatment, the chromatin had decondensed into pronuclei and indentations towards the spindle remnant were more pronounced. Microtubules remained organized in a pronounced midbody/spindle remnant up to 8 h after activation, possibly because the cleavage furrows never fully complete cytokinesis (shown only at 7 h, Fig. 41).

4.5.3 Actin Dynamics During Roscovitine-U0126 Co-Treatment

As described in section 4.3.8 above, eggs were fixed between 1-8 h post-roscovitine-U0126 exposure and stained to visualize the actin cytoskeleton. In total, 240 eggs co-treated with roscovitine and U0126 were studied to characterize actin dynamics leading to the development of R-U parthenogenotes. Each image was then scored for actin characteristics including contractile ring, development of a "ball" of actin, puckering of the cortex and the presence of incomplete cleavage furrows. Further, certain spindle characteristics were estimated based upon the location and shape of chromatin masses (i.e. spindle drift, spindle destabilization). Eggs could have more than one trait. These characteristics are summarized in Table 7.

When eggs were treated simultaneously with U0126 and roscovitine (50 μM each), actin appeared to become disorganized. At 1 h post-roscovitine-U0126 treatment, the spindle had moved away from the cortex and the chromosomes were visible as a single mass, presumably at the chromosome plate, indicating that the egg was still in metaphase but that the spindle was no longer docked at the cortex (Fig. 42). There was a localized area rich in actin at the cortex but the area was smaller than the cortical domain of an MII egg. An hour later (2 h post-roscovitine-

Table 7: Actin/microfilament characteristics during roscovitine-U0126 parthenogenetic activation. Eggs were parthenogenetically activated with 50 μM U0126, fixed and stained to visualize the actin cytoskeleton. Each image was assessed for actin and chromatin characteristics, as well as cell stage and genotype. Spindle characteristics were estimated based on the positioning of the chromatin (spindle was assumed to be between 2 masses of chromatin). Activated eggs could have more than one characteristic.

	Time post-Roscovitine-U0126 (h)			
Characteristic	1-2 h	3-4 h	5-6 h	7-8 h
Normal Stage for time	3	6	3	1
Spindle rotated	19	6	0	0
Spindle Defects				
Large PB/Fragments	1	1	1	0
Mitotic-like cleavage	0	0	0	0
Spindle Destabilization	9	5	0	0
Spindle drift	28	24	8	0
Spindle "spin"	0	0	0	0
Failure to Rotate	17	2	0	0
Actin Characteristics				
Incomplete Cleavage	0	14	19	42
"Ball" of Actin	20	48	42	41
Cortical Puckering	1	5	21	9
Cell Stage				
Metaphase	20	0	0	0
Anaphase/Telophase	45	19	2	0
Interphase	1	46	53	54
Genotype				
1n	3	5	2	0
2n	1	30	36	37
Micronuclei	0	21	17	16
Unknown	62	9	0	1
Total No. Pictures Examined	66	65	55	54

Figure 42. Proposed actin dynamics leading to R-U parthenogenotes after co-treatment with 50 μM roscovitine and 50 μM U0126. The spindle drifts away from the cortex, as determined by the position of the chromatin masses. Instead of forming a contractile ring, actin appears to become disorganized, forming a ball of actin that follows the drifting spindle, creating a one-sided cleavage furrow in its wake. See text for a detailed description of cytoskeletal events. Yellow numbers in the upper left corner of each row indicate the time post-activation for that series of three images. Numbers in the lower left corner of the images in the first two columns indicate depth of slice from the top (of nine slices). The third image in each row is a composite of the entire Z-series for that egg (C).

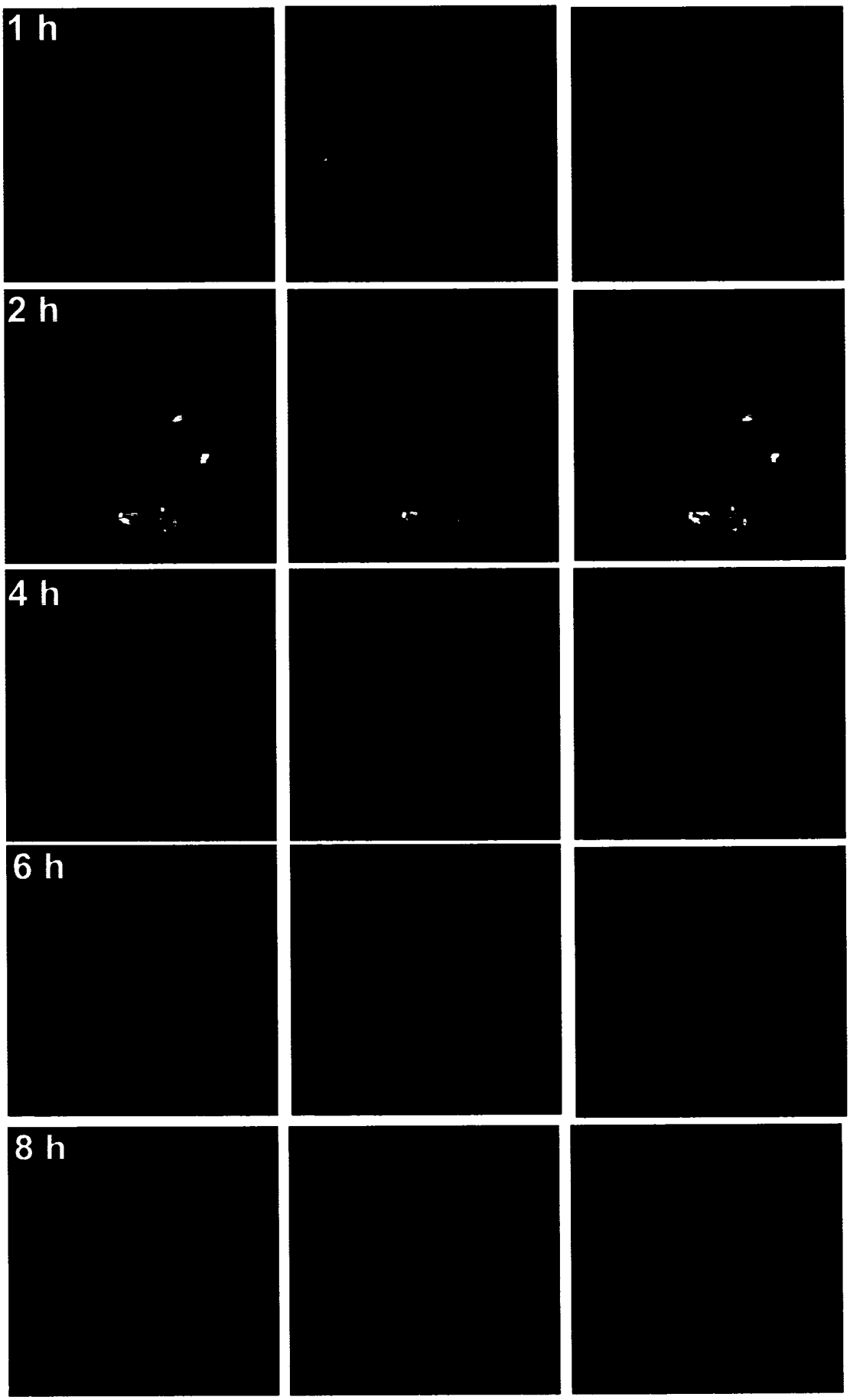
1 h
2 h
4 h
6 h
8 h

U0126), the spindle remained near the middle of the egg and had entered anaphase. At the cortex, the localized area of actin had not developed any form of organized contractile ring and remained as an amorphous mass. After 6 h of roscotivie-U0126 treatment, both masses of chromatin had decondensed to form pronuclei. Actin had formed a ball at the cortex and had moved between the pronuclei, creating a furrow along one side of the egg. Based on observations of tubulin during this time, the ball of actin was moving toward the midregion of the spindle remnant. Actin formed a ball instead of a ring, creating a one-sided "cleavage furrow" along one side of the egg. Cytokinesis was therefore not completed, even after 8 h of exposure to U0126 and roscovitine (6-8 h Fig. 42).

4.5.4 Birefringence Following Roscovitine-U0126 Activation

When assessed using the Polscope, eggs treated with U0126 and roscovitine behaved as eggs treated with U0126 alone. That is, the spindle lost birefringence relatively quickly and therefore could not be seen. An example of this phenomenon is presented in Fig. 43. Before activation, the birefringent spindle is present at the cortex, aligned parallel to the plasma membrane. Eight minutes after administration of the drugs, the birefringence of the spindle was less than the previous time point. The birefringence of the spindle had decreased even further at 9 minutes and could no longer be detected 16 min after drug exposure. No birefringence could be detected 27 min and 2 h (2:06) after roscovitine-U0126 treatment.

4.6 Comparison of Parthenogenetic Activation with Roscovitine, U0126, or Both

To compare all four forms of activation and the proportion of each class of parthenogenote, eggs were parthenogenetically activated in parallel with either U0126 (50 μM), roscovitine (50 μM) or roscovitine-U0126 co-treatment (50 μM each). The results are summarized in Fig. 44.

Figure 43. Changes in birefringence following roscovitine-U0126 parthenogenesis. The spindle loses birefringence following co-treatment with U0126 and roscovitine. Numbers indicate time post-U0126 (h:mm). The loss of birefringence occurs quickly: by 0:08, birefringence has significantly decreased and is no longer detectable by 0:16. Birefringence cannot be detected, even at 0:27 and 2:06 after activation.

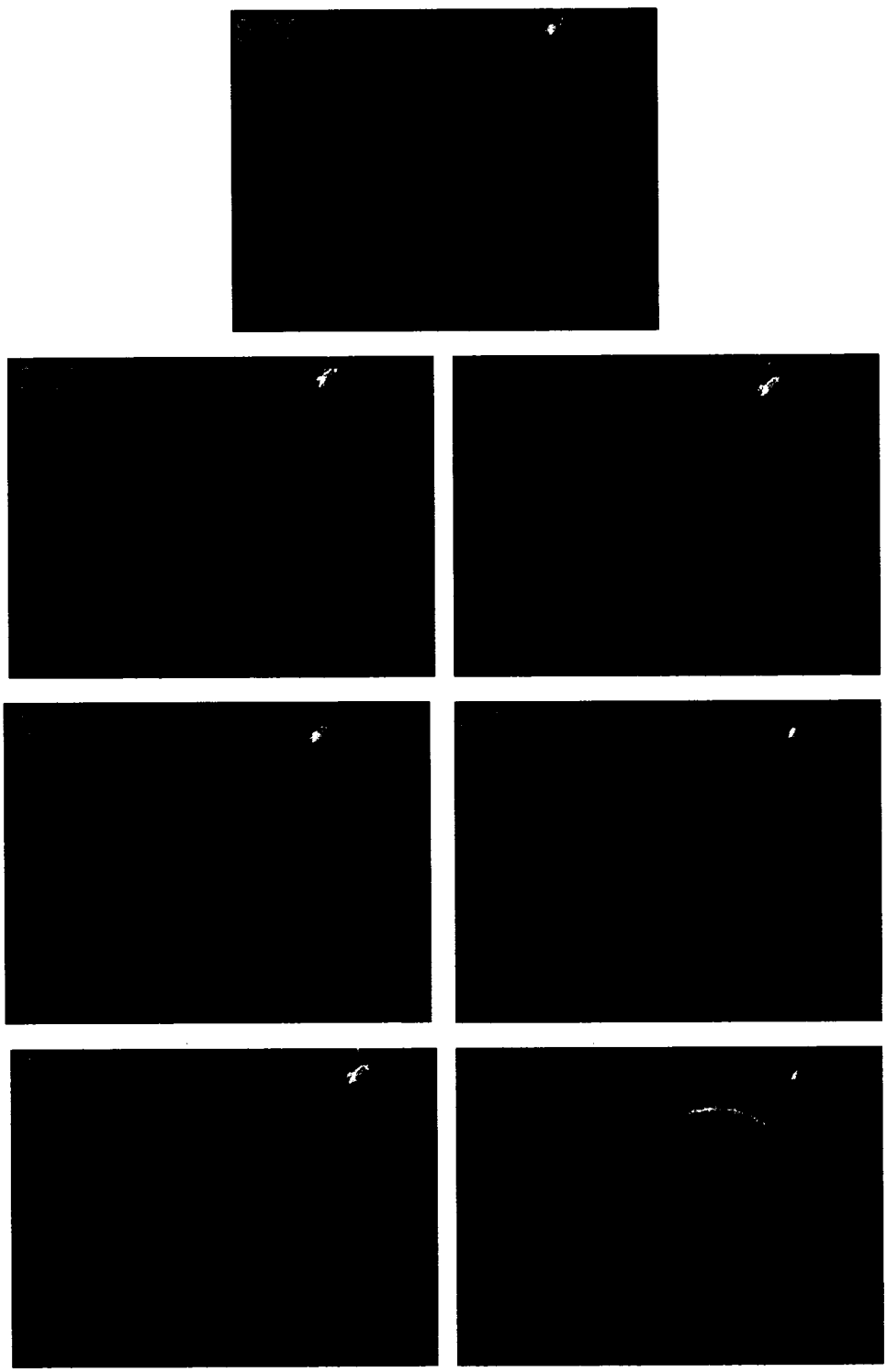

Figure 44. Phenotypic classes following parthenogenetic activation with U0126, roscovitine, or both. Eggs were parthenogenetically activated in parallel with either U0126 (U0126; 50 μM), roscovitine (Roscovitine; 50 μM), roscovitine-U0126 co-treatment (R-U; 50 μM each), or vehicle alone (Veh; 0.2% DMSO). After 8 h, eggs were scored for parthenogenetic activation and assigned to one of the three phenotypic classes of parthenogenote (inset of each bar). Numbers above bar are n(N), where n is the total number of eggs and N is the number of replicates.

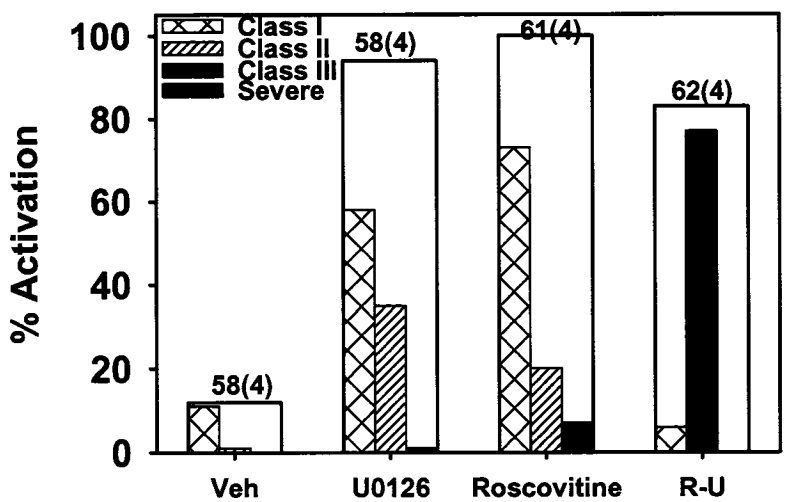
Class I
Class II
Class III
Severe
% Activation
100
80
60
40
20
0
58(4)
58(4)
61(4)
62(4)
Veh
U0126
Roscovitine
R-U

5 DISCUSSION

5.1 MOUSE EGGS ARE PARTHENOGENETICALLY ACTIVATED WITH A SPECIFIC PHENOTYPE BY INHIBITING MEK/MAPK OR CDC2 KINASE

I have presented data demonstrating that mouse eggs were parthenogenetically activated when treated with drugs to inhibit either MEK1/2 (U0126) or cdc2 kinase (roscovitine). Eggs activated by MEK inhibition or, to a lesser extent, cdc2 kinase inhibition, develop characteristic phenotypes that are similar to *mos*$^{-/-}$ oocytes. The *mos*$^{-/-}$ phenotypes have previously been divided into three classes by Hirao and Eppig (1997), as described in section 1.4.3.3, above. Parthenogenotes from oocytes treated with U0126 to inhibit MEK1/2 (upstream of MAPK) corresponded primarily to Hirao and Eppig's Classes I and II, with the Class III parthenogenotes that resemble precocious two-cell embryos usually being less common, as previously found for *mos*$^{-/-}$ oocytes (Hirao and Eppig, 1997). Whereas the unique Class II and III phenotypes develop in *mos*$^{-/-}$ oocytes because of effects on the spindle during MI (Verlhac *et al.*, 2000b), the similar phenotypes I have observed arose following normal development of oocytes through MI and were instead induced during MII. While the phenotypes of parthenogenotes are superficially similar, this is therefore not simply another method of recreating the *mos*$^{-/-}$ phenotype, but is a novel finding.

5.2 DISRUPTION OF MEK/MAPK CAUSES PARTHENOGENETIC ACTIVATION

That U0126 parthenogenetically activates mouse eggs directly demonstrates a requirement for MEK in CSF activity in the mammalian egg, confirming its similarity to nonmammalian species such as *Xenopus* and starfish (Tachibana *et al.*, 1997; Ferrell, 1999; Abrieu *et al.*, 2001). This is the first report of complete parthenogenetic activation by inhibition of MEK in a mammalian egg. Partial parthenogenetic activation had been reported in a fraction of porcine oocytes exposed to U0126 for 20 h during maturation, forming a pronucleus but not

cleaving nor emitting a second polar body (Tatemoto and Muto, 2001). U0126 has since been reported to release *in vitro*-matured porcine eggs from MII arrest (Fan *et al.*, 2003) and to enhance pronuclear development when combined with a Ca^{2+} ionophore in porcine oocytes (Ito *et al.*, 2004). Rat GV oocytes allowed to mature in the presence of U0126, hence without functional MAPK, also fail to arrest at metaphase II and enter an interphase state (Josefsberg *et al.*, 2003). Likewise, bovine GV oocytes overexpressing a MAPK phosphatase (therefore ablating MAPK activity) undergo GVBD and then parthenogenetically activate (Gordo *et al.*, 2001b).

5.2.1 MAPK Activity Rapidly Declines Following Exposure to U0126

Egg activation by IVF (Fig. 9; Moos *et al.*, 1995) or Sr^{2+} (Fig. 10) is characterized by a rapid inactivation of MPF followed by a more gradual inactivation of MAPK. In Sr^{2+} or IVF egg activation, MAPK activity stays high until about 5-h post-IVF or post-Sr^{2+} activation. A similar timecourse of inactivation has been reported for parthenogenetic activation by cycloheximide (Moos *et al.*, 1996a) or ethanol (Verlhac *et al.*, 1994). In contrast, MAPK was completely inactivated within 1 h in eggs treated with U0126 and therefore preceded the fall in MPF activity. Inactivation of MAPK occurred well before morphological indicators of parthenogenetic activation such as emission of the second polar body or pronuclear formation were apparent.

The minimum effective U0126 concentration for inactivation of MAPK is between 5 and 50 μM (Fig. 23), as is the minimum effective concentration for parthenogenetic activation (Phillips *et al.*, 2002). This supports the hypothesis that both parthenogenesis and MAPK inactivation by U0126 occur via a common mechanism of action, in which the decrease in MAPK activity results in the loss of CSF activity and subsequent MPF inactivation.

I have also found that the effect of U0126 was reversible, explaining the need for the continuous presence of U0126 to parthenogenetically activate eggs. When U0126 was washed out after 1 h, MAPK rebounded to its original (high) levels within an hour (Fig. 22). Similarly, parthenogenetic activation was significantly lower when U0126 exposure was 2 h or less (Phillips

et al., 2002a). This implies that other downstream signaling events that require inactive MAPK must occur for loss of CSF and complete parthenogenetic activation. These events may include APC activation and complete cyclin degradation.

5.2.1.1 MAPK and Activation

Previous studies have shown that high MAPK activity is incompatible with the formation of pronuclei (Moos *et al.*, 1995, 1996b) and it has been proposed that pronuclear formation is regulated by MAPK inactivation. Okadaic acid, a phosphatase inhibitor, maintains high MAPK activity by preventing MAPK dephosphorylation/inactivation. Parthenogenesis was inhibited when eggs were treated with okadaic acid during Sr^{2+} parthenogenetic activation (Fig. 11), as expected (Moos *et al.*, 1995). In addition, expression of an exogenous constitutively activated MEK in eggs prevented pronuclear formation (Moos *et al.*, 1996b). The decrease in MAPK activity that occurs after fertilization is therefore necessary to allow pronuclei to form. If, however, a decrease in MAPK activity by itself could cause pronuclear formation, precocious pronuclear development would be expected to accompany the rapid inactivation of MAPK following U0126 treatment. Instead, pronuclear development was somewhat delayed compared with IVF eggs (4 h vs. 6 h; Fig. 20) rather than being accelerated. This suggests that, while MAPK inactivation may play a permissive role in nuclear envelope assembly, there are other prerequisites for pronuclear formation that must occur before the inactivation of MAPK can result in nuclear envelope assembly. This may include decondensation of the metaphase chromosomes, which is under the control of MPF.

In support of a role for other checkpoints involved in pronuclear formation, I have found that disruption of the metaphase II spindle with demecolcine and subsequent maintenance of high MPF activity prevented parthenogenetic activation by U0126 (Fig. 24). No pronuclei ever formed, despite continuously low MAPK activity (data not shown). These eggs appeared similar to eggs treated with Sr^{2+} following spindle disruption with demecolcine, where both MPF and MAPK remained high for at least 8 h and both polar body emission and pronuclear development

were inhibited (data not shown). Thus, it is probable that some events controlled by MPF deactivation or another spindle-dependent mechanism must occur before MAPK inactivation in order to create a state permissive for nuclear envelope assembly and pronuclear formation.

5.2.2 Long Term Development of U0126 parthenogenotes

Development of U0126 parthenogenotes was mostly limited to one or two cleavages in culture. Only 11% of parthenogenotes developed into morula and 5% into blastocysts in my hands following activation by U0126 and washout of the drug before subsequent culture. Class I and II parthenogenotes arising from *mos*$^{-/-}$ oocytes are also reported to develop poorly, with only about 5% blastocyst development, while Class III parthenogenotes fared only slightly better, with 15% development to the blastocyst stage (Hirao and Eppig, 1997). Thus, the limited development of U0126 parthenogenotes seen here is consistent with the poor long-term development of *mos*$^{-/-}$ parthenogenotes in general (Hirao and Eppig, 1997), and may reflect the longer-term developmental consequences of inappropriately early MAPK inactivation.

5.3 DISRUPTION OF MPF CAUSES PARTHENOGENETIC ACTIVATION

5.3.1 Roscovitine Parthenogenetically Activates Mouse Eggs

As with U0126, eggs exposed to the cdc2 kinase inhibitor, roscovitine, were parthenogenetically activated. This was the first demonstration that direct inhibition of cdc2 kinase parthenogenetically activates mouse eggs. Previously, bovine eggs had been parthenogenetically activated by bohemine, a related cdk inhibitor (Alberio *et al.*, 2000). Another related cdk inhibitor, olomoucine has been shown to accelerate pronuclear formation in mouse eggs that had been activated by other means (Abraham *et al.*, 1995). Others have found that roscovitine treatment facilitates other means of egg activation in rhesus and mouse eggs, but that roscovitine by itself was unable to activate eggs (Deng and Shen, 2000; Mitalipov *et al.*, 2001). That roscovitine is oil-soluble and is subsequently lost from media culture droplets under oil may

account for this discrepancy, since our laboratory has shown that parthenogenetic activation of oocytes using roscovitine only occurred when oocytes were cultured without oil (Phillips *et al.*, 2002a).

5.3.2 MAPK is Inactivated Normally During Egg Activation by Roscovitine

Inhibition of MPF with roscovitine caused MAPK activity to fall with a time course essentially indistinguishable from its inactivation after fertilization. This supports a role for MPF in maintaining CSF activity in the mouse, complementing the well-known converse role of CSF in maintaining MPF. It is also consistent with a report that activated cyclin B/cdc2 kinase stabilizes Mos in *Xenopus* oocytes (Castro *et al.*, 2001) so that its inactivation leads to loss of activity of the Mos-MEK-MAPK cascade in that species. Studies in the rat have also demonstrated that during oocyte maturation, initial MAPK activation is subject to MPF regulation, even though MAPK activation occurs at least 6 h after MPF activation (Josefsberg *et al.*, 2003). I hypothesize that the gradual decrease in MAPK activity after inhibition of MPF by roscovitine is the same physiological mechanism that governs MAPK deactivation after fertilization in the mouse, specifically, withdrawal of Mos stabilization by MPF. This may operate in concert with a Ca^{2+}-induced increase in MAPK phosphatase activity, as in the sea urchin and mouse (Kumano *et al.*, 2001; Winston and Maro, 1999).

5.3.3 Some Roscovitine Parthenogenotes Resemble $mos^{-/-}$ *Parthenogenotes*

The majority of roscovitine-induced parthenogenotes were Class I, but a small proportion were Class II and III. It is unlikely that the subset of $mos^{-/-}$-like parthenogenotes resulting from roscovitine treatment arose by an indirect or direct effect of roscovitine on CSF activity, since MAPK was only slowly deactivated after roscovitine was introduced. The timecourse of inactivation was also similar to that following IVF rather than the sharp decrease in activity that occurred with U0126. Furthermore, direct inclusion of even 50-μM roscovitine in the lysate of the simultaneous kinase assay, which likely far exceeds the intracellular concentration in oocytes,

only slightly reduced measured MAPK activity. It is also not likely to be a nonspecific effect of the egg handling or culture conditions. Phenotypes resembling those arising from *mos*$^{-/-}$ oocytes were never observed with any other means of egg activation, such as IVF or Sr^{2+} treatment, even when activated in parallel to U0126 or roscovitine activation with the vehicle (DMSO) present at the same concentration. Therefore, it appears that inhibition of MPF itself in MII eggs independently produces some parthenogenotes with the same phenotypes that arise from disruptions of the CSF pathway. This is the first report of the development of *mos*$^{-/-}$-like phenotypes in parthenogenotes produced without direct disruption of the Mos-MEK-MAPK pathway.

The original impetus for using roscovitine was the hypothesis that normal egg activation could be mimicked by using roscovitine to first inactivate MPF, then adding U0126 a few hours later to inactivate MAPK, replicating the timecourses found during normal fertilization. The thinking was that this might eliminate the Class II and III phenotypes that resulted from using U0126 alone. Thus, the appearance of *mos*$^{-/-}$-like parthenogenotes following exposure of MII eggs to the cdc2 kinase inhibitor roscovitine alone was unexpected. Furthermore, it has been assumed that the Mos-MEK-MAPK pathway is the main regulator of spindle function and second polar body cytokinesis (Verlhac *et al.,* 1994). Here, some *mos*$^{-/-}$-like parthenogenotes arose when MPF was inhibited in the initial step of parthenogenesis, even though MAPK deactivation followed its normal post-fertilization timecourse. This finding supports the possibility that both CSF and MPF activity are required during MII for normal spindle function and second polar body cytokinesis, at least until cyclin degradation commences. Because only a small proportion of roscovitine parthenogenotes displayed the *mos*$^{-/-}$-like phenotype, the Mos-MEK-MAPK pathway may very well be the main regulator of spindle dynamics, with MPF modulating this effect.

5.4 SIMULTANEOUS INHIBITION OF MPF AND MAPK LEADS TO A SEVERE PHENOTYPE

I originally hypothesized that co-treatment of eggs with U0126 and roscovitine would accelerate parthenogenesis since both MAPK and MPF were simultaneously inactivated. Instead, co-treatment of eggs with U0126 and roscovitine produced a majority of parthenogenotes characterized by incomplete cleavages and cleavage furrows. These cleavage furrows were one-sided, apparently originating in the egg cortex near to the spindle, and pulling that side of the egg towards the other side. The resulting parthenogenote appeared "bent" or folded over on itself, often with multiple lobes. The surface of the egg was no longer smooth, originally making it difficult to determine the presence of pronuclei using a light microscope, although pronuclear-like structures were revealed by confocal microscopy of fixed and stained parthenogenotes. The development of this severe phenotype is novel and indicates that MPF and MAPK inactivation have a synergistic effect on spindle dynamics and localization, which would not be expected if only CSF activity was required for normal spindle dynamics. In addition, development of this phenotype reinforces the importance of temporal fidelity in MAPK and MPF inactivation during parthenogenetic activation. I propose that normal spindle function and second polar body emission require that both MPF and CSF be active until the end of second meiotic metaphase (i.e., just before second polar body emission), and that MPF deactivation must precede that of MAPK. The regulation of spindle and cytoskeletal dynamics by CSF and MPF are discussed in more detail below.

5.5 CYTOSTATIC FACTOR (CSF)

5.5.1 The Role of MAPK as CSF

By definition, CSF does not describe a single molecule or protein but rather an activity found in the egg (reviewed by Tunquist and Maller, 2003). According to the definition by Masui and Markert (1971), CSF must accumulate during maturation, must be capable of functioning in

meiosis II to produce a metaphase arrest, and must be inactivated on fertilization or parthenogenetic activation. Increasing evidence has accumulated in support of MAPK and the MAPK pathway as the principle mediator of CSF activity. In *Xenopus*, each member of the Mos-MEK-MAPK-p90^{rsk} pathway has CSF activity (Sagata *et al.*, 1988; Haccard *et al.*, 1993; Gross *et al.*, 1999). While work remains to be done in the mammalian model, a similar picture is emerging where each member of this pathway is necessary to interact with each other to establish and maintain CSF arrest. However, to date, only Mos has been shown definitively to be required for CSF activity in the mouse (Colledge *et al.*, 1994; Hashimoto *et al.*, 1994). The present work now includes MEK as necessary for CSF activity in the mouse.

MAPK is important in the pathway leading to CSF because it represents the enzyme onto which signaling pathways for CSF converge. Activation of MAPK depends both on activation of MEK and Mos-dependent inactivation of antagonizing phosphatases (Fig. 8; Verlhac *et al.*, 1996). Once activated, MAPK is responsible for activating p90^{rsk} and exerting its effect on CSF. Disruption of one aspect of the pathway leads to disruption of CSF. Ablation of Mos in oocytes leads to parthenogenetic activation (Colledge *et al.*, 1996; Hashimoto *et al.*, 1996). Likewise, I have shown that eggs treated with U0126 to inactivate MEK1/2 lose CSF and parthenogenetically activate.

5.5.2 CSF and the Spindle Assembly Checkpoint

Maintaining the metaphase II arrest in the unfertilized egg is regulated by the MAPK pathway. In *Xenopus*, as in mammals, translation and activation of the gamete-specific protein, Mos, activates MEK, whose primary function is to activate MAPK (reviewed by Enslen and Davis, 2001). The activity of Mos also acts to inactivate the phosphatases that maintain MAPK in an inactive form (Verlhac *et al.*, 2000a). MAPK maintains p90^{rsk} in its active, phosphorylated state (Kalab *et al.*, 1996). In *Xenopus* and starfish oocytes, active p90^{rsk} then phosphorylates and inactivates Myt1, facilitating cdc25 activation of MPF (Palmer *et al.*, 1998). Concomitantly,

$p90^{rsk}$ activates Bub1, a kinetochore-associated protein of the spindle assembly checkpoint. Bub1 targets another kinetochore-associated protein, Mad2 to Cdc20, the activator of the APC. While bound to Mad2, Cdc20 cannot activate the APC. This links MAPK-dependent APC inhibition and the spindle assembly checkpoint in CSF arrest in *Xenopus* (Schwab *et al.*, 2001). It has not yet been determined if the link between $p90^{rsk}$ and the spindle assembly checkpoint also exists in mammalian species.

Normally, the spindle assembly checkpoint is activated when there are kinetochore-chromosome attachment errors, but at metaphase II this checkpoint is activated despite an assembled, error-free spindle. It has been proposed that the presence of Mos ensures that every molecule of MAPK and $p90^{rsk}$ are activated, thereby activating the spindle assembly checkpoint responsible for metaphase arrest, even in the presence of a normally assembled spindle (Schwab *et al.*, 2001). If this is the case, CSF arrest would be caused by the spindle assembly checkpoint pathway due to Mos-dependent activation of the MAPK pathway that leads to activation of Bub1 and the inhibition of the APC.

5.5.3 Emi1 and its putative role as CSF

It is clear that the Mos-MEK-MAPK pathway is at least partly responsible for CSF activity in the oocyte. Emi1, an inhibitor of the anaphase-promoting complex (APC), may be another signaling pathway with CSF activity (Reimann and Jackson, 2002). By binding to and inhibiting the APC activator, Cdc20, Emi1 prevents the ubiquitination and destruction of cyclins that accompanies exit from metaphase (Reimann *et al.*, 2001). Emi1 meets the criteria set out by Masui and Markert (1971) in that injection of Emi1 into mitotic blastomeres arrests their division (Reimann *et al.*, 2001). Although the cytology of these arrested blastomeres has not yet been investigated, they should be in meiotic-like metaphase to meet the definition of CSF. By itself, Emi1 is not sufficient to establish CSF arrest since it does not arrest $mos^{-/-}$ oocytes at metaphase II (Duesbery and Vande Woude, 2002). Initially investigated using *Xenopus* egg lysates, the

results have not yet been replicated in other species. Furthermore, Emi1 is synthesized and degraded during each cell cycle in the early embryo, and its activity reaches much higher levels than are present during meiosis, yet these higher levels of Emi1 do not cause CSF-like arrest, arguing against Emi1 as CSF (Masui and Markert, 1971; Reimann *et al.*, 2001). While Emi1 may not be the sole mediator of CSF activity, it may be involved in maintaining CSF arrest while Mos-MEK-MAPK pathway is more important in establishing and stabilizing CSF, thus reconciling findings from CSF extracts and *mos*$^{-/-}$ oocytes.

5.6 How Does MAPK and/or MPF Inactivation Affect the Spindle and Cytoskeleton?

Disruption of MEK or cdc2 kinase produces *mos*$^{-/-}$-like parthenogenetic phenotypes while co-treatment produces a unique, more severe phenotype characterized by incomplete cleavages and a multilobed appearance. I therefore investigated the effect of premature loss of MAPK and MPF (alone or in combination) on spindle, chromatin, and actin dynamics to determine if they could account for the classes of *mos*$^{-/-}$-like phenotypes observed.

5.6.1 Proposed Spindle Dynamics Leading to the mos$^{-/-}$ *Phenotype*

5.6.1.1 Spindle Drift Leads to Class II and III Parthenogenotes

Parthenogenetic egg activation with U0126 appears to destabilize spindle positioning and anchorage to the cortex. This is evidenced by several findings. First, in eggs activated normally by fertilization (IVF) or with Sr^{2+}, the spindle was never observed to move away from the cortex, but always rotated *in situ* to become perpendicular to the egg surface. In contrast, anchorage to the egg cortex was often lost in U0126 activated eggs so that the spindle drifted into the middle of the egg, which was sometimes seen with roscovitine activated eggs as well. Second, in living eggs activated with U0126 in which the spindle was imaged using the PolScope, the spindle was seen to rotate parallel to the egg's surface. This phenomenon was never seen after IVF or activation with Sr^{2+}, and may also reflect a loss of anchorage of the spindle at the egg cortex.

Since some eggs appear to activate with an essentially normal phenotype, spindle drift after loss of anchorage may be a random event. This movement may be a result of disorganized spindle rotation or may simply be a consequence of passive movement in response to cytoplasmic motility. Thus, Class I phenotypes could occur in activated eggs where the spindle, although it is not anchored to the cortex, does not drift very far and thus rotates into its nearly normal position perpendicular to the surface prior to cleavage. Alternatively, Class I parthenogenotes could result if anchorage to the cortex is retained or only incompletely disrupted in a proportion of the eggs.

In this model, presented in Fig. 45, Class II and III parthenogenotes would result in eggs where the spindle, after losing its anchorage to the cortex, drifts a significant distance into the cytoplasm. Formation of the actin ring that precedes cytokinesis normally occurs along the plane of the spindle midzone, where chromosomes were aligned at metaphase. Therefore, in eggs where the spindle has drifted into the cytoplasm, the cleavage plane would bisect a large portion of the egg, producing a large polar body. In the most extreme case, where the spindle has moved close to the centre of the egg, two nearly equal cells would result from cleavage though the spindle, producing Class III parthenogenotes. Class II or III parthenogenotes could also arise if the spindle completely failed to rotate and anaphase occurred parallel or nearly parallel to the membrane cortex.

5.6.1.2 Inhibition of CSF Destabilizes the Spindle

While imaging spindle birefringence during U0126 activation with the PolScope, I found that the spindle appears to thicken slightly, followed by a decrease in birefringence. No birefringent spindle was apparent after 1 h, even when the focus was adjusted through the thickness of the egg. This suggests that the loss of birefringence is genuine and not just a consequence of the spindle drifting out of the plane of focus. However, the spindle was persistently detected by confocal microscopy of parthenogenotes stained for tubulin, where it was present for many hours and formed the midbody after cleavage. This evidence indicates that the spindle continues to exist as a discrete structure during the entire period of these observations, but

Figure 45. Proposed molecules contributing to Class II and III parthenogenetic phenotypes following egg activation by U0126.

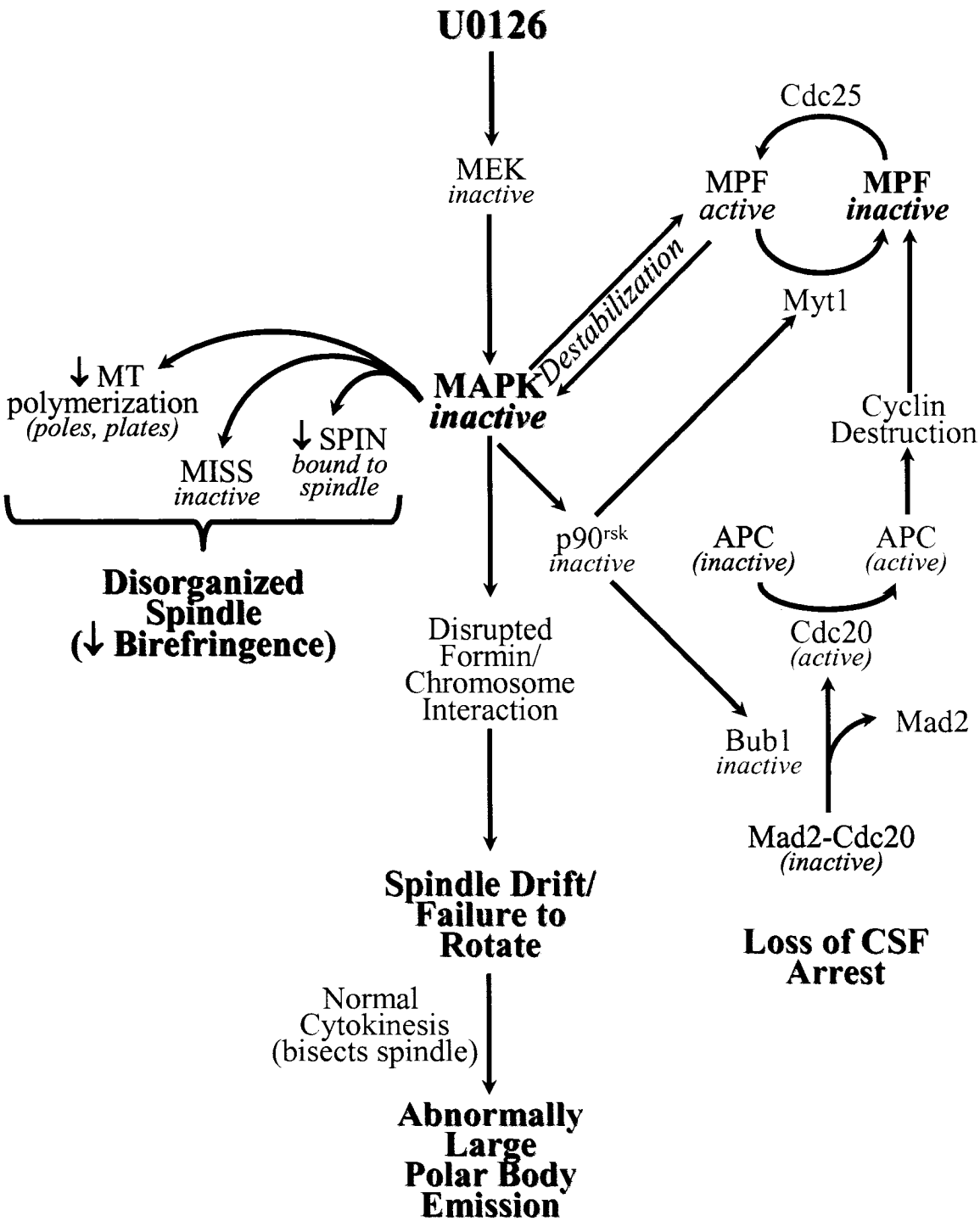
U0126
MEK
inactive
Cdc25
MPF
active
MPF
inactive
Myt1
Destabilization
↓ MT
polymerization
(poles, plates)
MISS
inactive
↓ SPIN
bound to
spindle
MAPK
inactive
Cyclin
Destruction
p90rsk
inactive
APC
(inactive)
APC
(active)
Disorganized
Spindle
(↓ Birefringence)
Disrupted
Formin/
Chromosome
Interaction
Cdc20
(active)
Bub1
inactive
Mad2
Mad2-Cdc20
(inactive)
Spindle Drift/
Failure to
Rotate
Loss of CSF
Arrest
Normal
Cytokinesis
(bisects spindle)
Abnormally
Large
Polar Body
Emission

that it quickly loses detectable birefringence following activation by U0126. Interestingly, this effect is opposite to what is normally observed during egg activation, where markedly increased spindle birefringence is one of the first features of egg activation (Liu *et al.*, 2000).

Because the PolScope measures birefringence, a property of structures that are highly ordered and organized over distances on the order of the wavelength of light, the disappearance of spindle birefringence may be due to destabilization or disorganization of the spindle. There is a precedent for this hypothesis. When *in vitro* matured MII oocytes that did not appear to have a birefringent spindle using the PolScope were stained immunofluorescently, these oocytes either did not have a spindle, or had irregular or multipolar spindles (Wang and Keefe, 2002). This suggests that the spindle structure can still be present, although insufficiently ordered to be birefringent.

MAPK can phosphorylate tubulin *in vitro,* although the physiological significance or even if it does occur *in vivo* is not known at this time. Since immunofluorescent results exhibit all tubulin, organized or not, a disturbance in the ordering of microtubule bundles within the spindle would not be readily apparent with immunofluorescence but would greatly diminish birefringence.

Before activation, the eggs were allowed to equilibrate in the PolScope chamber for at least five minutes. That the spindles were present and then disappeared suggests that the lost birefringence was not due to spindle destabilization from temperature perturbations during handling. To my knowledge, this is the first form of activation where birefringence was lost during activation. Because the birefringence fell below detectable levels, it was not possible to confirm spindle drift leading to Class II and III parthenogenotes in individual eggs using the PolScope.

5.6.1.2.1 How Inhibition of MAPK Could Lead to Loss of Birefringence

MAPK associates with MTOCs during mouse oocyte meiotic maturation. Once MAPK is activated, MAPK colocalizes with microtubules, at the poles and plates of meiotic spindles (Lu

et al., 2002). Active MAPK is therefore in the right place at the right time to exert an effect on the spindle (spatial and temporal regulation of meiotic spindle organization). Microtubule-associated proteins (MAP), such as MAP-1, MAP-2 and tau, are phosphorylated by MAPK-dependent microtubule dynamics. MAPK may influence meiotic spindle formation and spindle integrity by phosphorylating these microtubule-associated proteins that, in turn, regulate microtubule polymerization and/or depolymerization (reviewed by Gundersen and Cook, 1999). MAPK may also influence the spindle organization by activating other spindle-associated proteins, such as MISS or SPIN (discussed below).

When MAPK is inhibited during oocyte maturation, after GVBD but before metaphase II, no spindles and very short microtubules surrounding loosely condensed chromosomes are observed (Lu *et al.*, 2002). When the maintenance of metaphase II is considered as a dynamic process, inhibition of MAPK via U0126 at metaphase II could disrupt the integrity of the already-formed spindle. I propose that disruption of microtubule organization at the spindle poles or plates (where MAPK is localized at MII) would cause the microtubules to drift out of parallel alignment with one another. This subtle disruption would not be readily apparent in confocal images of parthenogenotes stained for tubulin but would be sufficient to ablate the molecular order necessary for birefringence, accounting for the loss of birefringence that I observed. At the same time, U0126 could disrupt the spindle anchorage to the cortex, leading to the observed abnormally large polar bodies. These proposed mechanisms leading to loss of birefringence when U0126 is used are summarized in Fig. 45 and 47 (egg activation with U0126 or roscovitine-U0126 co-treatment, respectively).

5.6.1.3 MAPK and the Spindle

As described in the Introduction, the development of Class II and III phenotypes in *mos*$^{-/-}$ oocytes has been proposed to result from dysregulation of meiotic spindle dynamics, believed to be a result of the lack of the Mos-MEK-MAPK pathway during first meiotic metaphase (MI) of maturation (Verlhac *et al.* 2000). In the *mos*$^{-/-}$ oocyte, the spindle fails to migrate to the cortex in

MI, instead elongating from its position at the centre of the egg so that one pole remains at the centre of the egg while the other pole moves alone to the cortex, stretching the spindle (Verlhac *et al.*, 2000b). The metaphase plate then is situated deeper into the egg than in normal polar body emission, so the cleavage furrow forms nearer the centre of the egg, resulting in emission of abnormally large polar bodies (Class II; Verlhac *et al.*, 2000b). Class III parthenogenotes may represent an extreme situation in which the cleavage furrow develops in the elongated spindle near the equator of the egg, thereby producing a parthenogenote resembling a precocious 2-cell embryo (Verlhac *et al.*, 2000b).

The ability of U0126 to produce each of the *mos*$^{-/-}$ phenotypes suggests that loss of Mos activity likely causes parthenogenesis by the same mechanism as U0126, namely inhibition of MEK and MAPK, although here the phenotype is produced in MII eggs rather than the MI *mos*$^{-/-}$ phenotype. Since the only known physiological function of MEK is to activate MAPK, the observed effects are most likely due to inactivation of MAPK and its downstream targets. The most important difference between U0126 activation and *mos*$^{-/-}$ oocytes is that the Mos-MEK-MAPK pathway is never functional in *mos*$^{-/-}$ oocytes (Colledge *et al.*, 1994; Hashimoto *et al.*, 1994) and the phenotype arises during MI, not MII.

In the experiments presented herein, oocytes developed through meiotic maturation and become arrested in MII normally; MAPK and MPF were activated normally during MI and throughout MII. The spindle migrated to the periphery of the egg during MI and the first polar body was emitted normally. Only once the egg had been arrested in MII was MAPK or MPF inactivated by the application of specific inhibitors. In *mos*$^{-/-}$ oocytes, it was not possible to determine whether an active Mos-MEK-MAPK pathway is required for normal MII spindle function and second polar body formation in the mouse due to the disruption of the MI/MII transition in that model. The present work, however, isolates the effects at metaphase II from those occurring during meiotic maturation. It indicates that MAPK activity is also required specifically during MII for normal spindle dynamics and formation of a second polar body, since

the Mos-MEK-MAPK pathway was functional throughout meiotic maturation and was only disrupted here by U0126 treatment in normal, fully mature MII oocytes. It also supports the hypothesis that the mechanisms maintaining the spindle in the correct subcortical position during metaphase II arrest are dynamic and can be disrupted, and implicates MAPK in anchoring the spindle at the cortex and permitting its normal positioning and rotation during cytokinesis to produce the second polar body.

Abnormal polar body emission also results from direct inhibition of MEK during egg activation in several invertebrate species, including *Urechis caupo* and oyster (Gould and Stephano, 1999; Stephano and Gould, 2000). Thus, regulation of the cytokinesis, which produces the polar body, may be a universal role of MAPK.

5.6.1.4 Inhibition of MAPK Spins the Spindle

Using the PolScope, I have also observed that the spindle of a subset of eggs treated with U0126 appears to "spin" along the axis of the plasma membrane. Because the spindle is always parallel to the cell cortex in this case, these eggs would appear no differently than vehicle-treated eggs when fixed and stained for tubulin to visualize the spindle. This phenomenon could only be observed by following the same living egg over time, i.e., with the PolScope. These eggs do not develop a parthenogenetic phenotype, even when followed for up to 8-h post-U0126. This phenomenon appears to be more common in slightly aged eggs (collected 16-18 h post-hCG).

I propose that this spindle "spinning" could be a variation of the spindle undocking from the cortex. Instead of losing complete anchorage to the cortex, the spindle remains inappropriately or incorrectly docked at the egg cortex and spindle movement is a result of a failed attempt to rotate perpendicularly to the cortex for polar body emission. Actin or an actin-associated protein (like formins, discussed later) may be implicated in this phenomenon.

5.6.1.5 Etiology of *mos*$^{-/-}$-like Phenotypes in Egg Activation by Roscovitine

Since only a fraction of roscovitine-treated parthenogenotes displayed the *mos*$^{-/-}$-like phenotype, they may represent a population of oocytes that are more sensitive to the effects of roscovitine or that have a more sensitive meiotic apparatus. The effect of roscovitine on intracellular structural components may not be strong enough to yield a phenotype in all but a small proportion of mouse eggs.

The mechanisms in play leading to the development of Class II and III parthenogenotes following egg activation by roscovitine are summarized in Fig. 46. In support of MPF modulating the effects of the Mos-MEK-MAPK pathway, Tong *et al.* (2003) recently showed that the MI spindle is affected by U0126 at concentrations below that which are able to dephosphorylate (hence inactivate) MAPK during oocyte maturation in the mouse. Spindles were unable to maintain their structure, sometimes elongating extraordinarily leading to the formation of abnormally large polar bodies or precocious two-cell formation, as has been described during the development of Class II and III phenotypes of *mos*$^{-/-}$ oocytes (Verlhac *et al.*, 2000b). With a reciprocal relationship between MPF and MAPK, a fall in MPF activity from roscovitine administration could exert an effect on MAPK-dependent spindle dynamics at a level undetectable by the kinase assays but sufficient to destabilize anchorage to the spindle in susceptible oocytes. This could lead to the observed spindle drift and the development of Class II and III parthenogenotes with roscovitine activation. This argument suggests that the initial fall in MPF activity slightly affects MAPK activity at the spindle but that the total fall in MAPK activity occurs by physiological methods, following cyclin degradation.

Alternatively, the development of Class II and III parthenogenotes may be partially a result of temperature changes during handling coupled with effects of roscovitine on spindle stabilization. Changes in temperature are known to affect spindle dynamics (Pickering and Johnson, 1987). Since Cdk1 is localized to the spindle, the site of action for roscovitine in metaphase II eggs is the spindle. Administration of this drug could therefore exacerbate

Figure 46. Proposed molecules implicated in the development of Class II and III parthenogenetic phenotypes following egg activation by roscovitine.

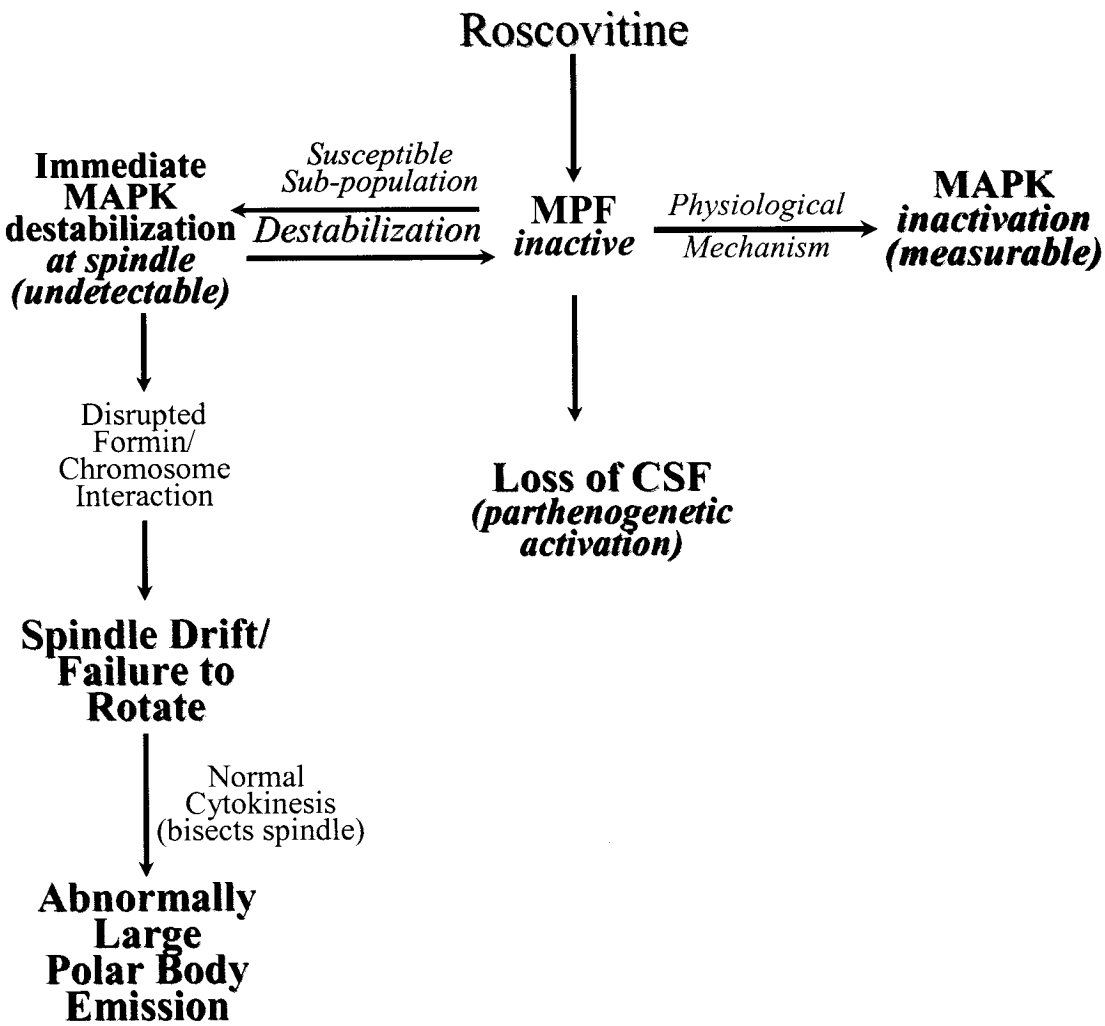
Roscovitine
Immediate MAPK destabilization at spindle (undetectable)
Susceptible Sub-population
Destabilization
MPF inactive
Physiological
Mechanism
MAPK inactivation (measurable)
Disrupted Formin/ Chromosome Interaction
Loss of CSF (parthenogenetic activation)
Spindle Drift/ Failure to Rotate
Normal Cytokinesis (bisects spindle)
Abnormally Large Polar Body Emission

perturbations of the spindle, leading to loss of anchorage and the resultant large polar body or precocious 2-cell formation. Activation by either IVF or Sr^{2+} acts first via intracellular Ca^{2+} and does not immediately target components of the spindle, so mild perturbations of this organelle during handling would not lead to the *mos*$^{-/-}$-like phenotypes.

The effect of roscovitine on the spindle becomes even more apparent when eggs are treated with U0126 and roscovitine. In this case, the effect of U0126 enhances the effect of roscovitine, leading to the severe phenotype I have observed (discussed below). That both Cdk1 and MAPK act at the spindle supports the hypothesis that *mos*$^{-/-}$-like phenotypes arising from roscovitine or U0126 are due to the action of these drugs on spindle components at the time of egg activation.

5.6.1.6 Roscovitine Activation and the Cytoskeleton

The majority of parthenogenotes formed from disruption of cdc2 kinase activity by roscovitine share the same phenotype as Sr^{2+} parthenogenotes. Actin and tubulin localization of fixed samples indicated that the Class I parthenogenotes develop in a manner similar to Sr^{2+} parthenogenesis. This was confirmed by imaging single living activated eggs over time on the PolScope. Since MAPK activity fell slowly after MPF inactivation upon activation by either Sr^{2+} or roscovitine, and both resemble normal activation following fertilization, the similarity between roscovitine and Sr^{2+} parthenogenotes was expected. In the small proportion of Class II and III roscovitine parthenogenotes, microtubule and actin dynamics appears as in U0126 treatment where the spindle drifts towards the middle of the egg. This supports the proposed reciprocity in spindle stabilization between CSF and MPF. Unfortunately, no class II or III parthenogenotes developed from eggs followed with the PolScope, preventing any conclusions to be drawn regarding changes in birefringence or spindle migration in Class II or III parthenogenotes.

5.6.1.7 Roscovitine-U0126 Parthenogenotes Have a Severe Phenotype

As discussed above, simultaneous co-treatment of eggs with roscovitine and U0126 produced a majority of eggs with a unique, severe phenotype with a pronounced irregular shape and what appear to be incomplete cleavages and cleavage furrows. Emission of the second polar body did not occur. Consequently, roscovitine-U0126 parthenogenotes have two pronuclei (visible in eggs that had been fixed and stained). As with either U0126 or (to a smaller extent) roscovitine, the spindle appears to lose its anchorage to the egg cortex, sometimes drifting all the way into the middle of the egg. Unlike U0126 parthenogenotes, the cleavage furrow never fully completes cytokinesis when eggs are exposed to both drugs. This may account for why the microtubules remain organized in a structure resembling a midbody at the arrested cleavage furrow up to 8 h after activation – long after it would have been expected to disappear following polar body extrusion.

Using the PolScope, eggs co-treated with U0126 and roscovitine lost their birefringent spindle, as did eggs treated with U0126 alone. Since this phenomenon appears to occur only when U0126 is used, I believe this event is an effect of premature MAPK inactivation and relates to the MAPK-microtubule interaction discussed above. This hypothesis is limited because no Class II or III parthenogenotes were observed with the PolScope following activation with roscovitine alone. Thus, I cannot compare the development of Class II or Class III between roscovitine activation and the other methods of activation. That the spindle birefringence increased when Class I parthenogenotes developed in egg activation by roscovitine but not in Class I parthenogenotes activated by U0126 would argue against the possibility that destabilization of the spindle is a universal feature of Class II or III parthenogenesis. If the spindles of eggs developing into Class II and III parthenogenotes following roscovitine parthenogenetic activation remained birefringent during egg activation, the effect of MPF inhibition on MAPK/spindle dynamics may be sufficient to disrupt spindle anchorage to the cortex but insufficient to affect spindle order and therefore birefringence. At this time, however,

this hypothesis is purely speculative. I propose that the premature loss of either CSF or MPF activity alone in eggs physiologically arrested in MII partially disrupts spindle function and cytokinesis, and that inhibition of either activity is sufficient to permit the formation of some relatively normal Class I parthenogenotes. Loss of both activities, however, appears to cause a much more acute disruption, so that almost all the parthenogenotes produced have a severe phenotype and exhibit incomplete cleavages.

5.6.2 Proposed Actin Dynamics Leading to mos$^{-/-}$*-like Phenotypes*

5.6.2.1 Actin Dynamics Follow the Meiotic Apparatus (MA)

I believe that the data presented above support the hypothesis that the formation of abnormally large polar bodies in Class II and III parthenogenotes is not a result of actin dysfunction per se, but is a function of abnormal spindle localization at telophase II. Normally, the plane of the cleavage furrow is perpendicular to the long axis of the spindle, midway between spindle poles at the midzone/metaphase plate (reviewed by Glotzer, 2004). When either MAPK or MPF are inactivated, actin dynamics are normal in that the cleavage furrow forms with its usual relationship to the midzone of the spindle. That is, the contractile ring centres on the midpoint of the spindle, halfway between the two sets of anaphase chromosomes. Since the spindle is normally positioned at the cortex of the egg, with its long axis perpendicular to the surface, this cleavage results in a small polar body being cleaved off the large egg (Maro, 1986b).

However, the spindle itself often was seen to dislodge from the egg cortex during U0126 or roscovitine activation, becoming displaced deeper into the cytoplasm in these parthenogenotes. Therefore, abnormal spindle microtubule dynamics or positioning apparently determined the size of the polar body. This hypothesis is supported by studies in the *mos*$^{-/-}$ parthenogenote where the spindle fails to migrate to the cortex during first meiotic metaphase, and instead becomes elongated (Verlhac *et al.*, 2000b). The cleavage furrow develops at the spindle midzone, which is

deeper in the egg, causing a larger volume of cytoplasm to be pinched off in an abnormally large polar body (Verlhac *et al.*, 2000b).

5.6.3 Simultaneous Inhibition of cdc2 and MEK/MAPK Disorganizes Actin

In contrast to inhibition of either MEK/MAPK or cdc2 alone, where the spindle becomes disorganized but the actin ring forms normally, when both MAPK and MPF are inactivated simultaneously with U0126 and roscovitine, actin also becomes disorganized. The proposed mechanism leading to development of R-U parthenogenotes is outlined in Fig. 47. Instead of forming a ring at the plane of the chromosome plate in anaphase, actin appears to form a concentrated ball at the cortex nearest to the spindle. When the actin ring would normally contract to pinch off the polar body, this ball of actin contracts towards the spindle, creating a "cleavage furrow" on only one side of the egg. For the most part, polar body emission is inhibited. This leads to the more severe phenotype characterized by incomplete cleavage and irregular, multilobed membrane.

Given the current understanding of cleavage furrow formation, it is unclear why actin would form a ball instead of a ring around the metaphase plate. Perhaps low MAPK and MPF activities signal that anaphase is over. In this situation, the ball of actin could actually represent a contracted contractile ring. Rather than drift away following normal cytokinesis, the midbody remains at the junction between the activated egg and polar body. This might suggest the presence of signals emanating from the midzone that would connect the remains of the spindle to the contractile ring. In this theory, the contracted contractile ring that formed following parthenogenetic activation with roscovitine and U0126 would still be connected or attracted to the spindle remnant, even though polar body emission did not occur. Because the spindle remnant was no longer docked to the cortex, the ball of actin would follow the spindle remnant as it drifted deeper into the cytoplasm, creating a one-sided furrow and multilobed appearance. Clearly, this is an area in need of future study.

Figure 47. The proposed molecules implicated in the development of the severe phenotype caused by co-treatment of eggs with U0126 and roscovitine.

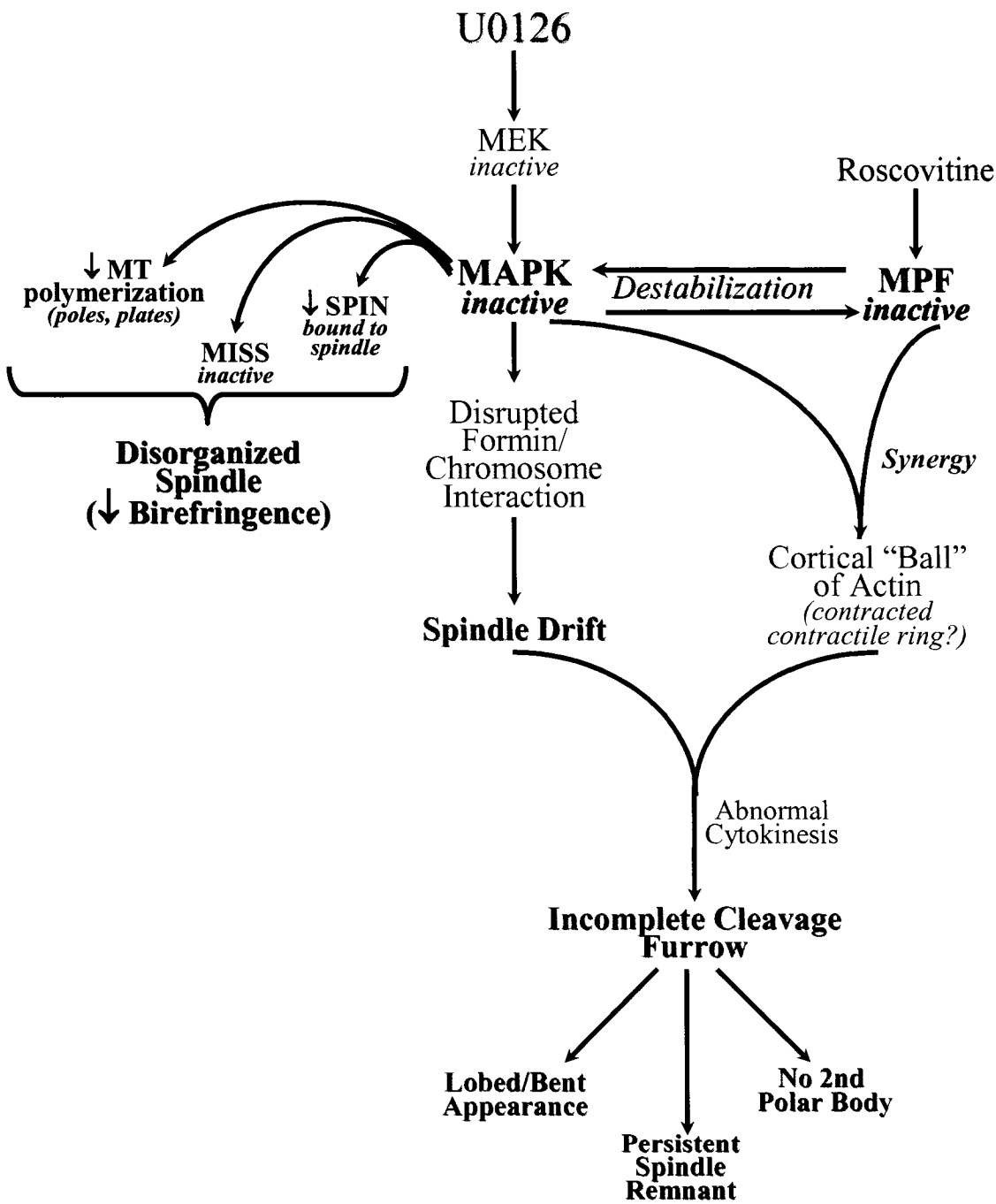
U0126
MEK
inactive
Roscovitine
↓ MT
polymerization
(poles, plates)
↓ SPIN
bound to
spindle
MISS
inactive
MAPK
inactive
Destabilization
MPF
inactive
Disorganized
Spindle
(↓ Birefringence)
Disrupted
Formin/
Chromosome
Interaction
Synergy
Cortical "Ball"
of Actin
(contracted
contractile ring?)
Spindle Drift
Abnormal
Cytokinesis
Incomplete Cleavage
Furrow
Lobed/Bent
Appearance
Persistent
Spindle
Remnant
No 2nd
Polar Body

5.6.4 What Mediates the Changes Leading to Class II and III Parthenogenotes? A Few Candidate Molecules

5.6.4.1 Could Formins Dock the Spindle at the Cortex?

There is currently no evidence connecting formins, responsible for asymmetrical spindle positioning (Leader *et al.*, 2002) to the MEK-MAPK pathway. Yet, the similarities between the *mos*$^{-/-}$-like phenotype I observed following parthenogenetic activation by U0126 or roscovitine, Fmn2$^{-/-}$, *mos*$^{-/-}$ oocytes, are compelling. Based on observations of *mos*$^{-/-}$ oocytes, Maro and Verlhac (2002) have proposed that the Mos/MEK/MAPK pathway acts as an amplifier of the migration signal emanating from chromosomes. A MAPK-dependent chromosome-binding protein would somehow initiate formin-mediated spindle migration towards the cortex. Recall that in meiosis I of *mos*$^{-/-}$ oocytes, the spindle elongates instead of migrates at the metaphase-anaphase transition, leading to an abnormally large polar body (Verlhac *et al.*, 2000b). According to the proposed formin-MAPK model, without MAPK to amplify the migration signal, the chromosomes cannot initiate spindle migration until they are closer to the cortex. This does not occur in *mos*$^{-/-}$ oocytes until near the end of anaphase, when one set of chromosomes is closer to the cortex and results in an asymmetrical and elongated spindle (Verlhac *et al.*, 2000b; Maro and Verlhac, 2002). In these oocytes, the cortex is still able to respond to the signal coming from the chromosomes to establish the cortical domain, but at a shorter distance.

This cannot be the mechanism operating in MII eggs, however. In the case of U0126 parthenogenetic activation, the metaphase II spindle is normally positioned, with the actin-rich cortical domain intact. If the role of the MAPK pathway in spindle migration was solely signal amplification, parthenogenetic activation with U0126 would be expected to yield parthenogenotes of a normal phenotype. The chromosomes would be close enough to the cortex to maintain the cortical domain and would remain docked at the cortex despite the lower signal magnitude.

On the contrary, I have found that the spindles of eggs activated with U0126 (or to a lesser extent, roscovitine) appear to lose their attachment to the cortex and drift towards the centre of the egg. I propose that the same mechanism responsible for moving the spindle to the cortex during MI put forward by Maro and Verlhac (2002) is responsible for tethering the spindle to the cortex in MII: the MAPK-mediated formin-chromosome interaction (model, Fig. 48). Following the rapid drop in MAPK activity after U0126 treatment, the putative MAPK-dependent chromosome binding protein would destabilize the formin-actin-chromosome interactions responsible for maintaining the spindle at the cortex. Once this interaction was destabilized, the spindle would drift towards the equator of the egg during U0126 parthenogenetic activation (or to a lesser extent during roscovitine parthenogenetic activation). Since the MAPK-mediated formin-chromosome interaction could not to maintain the eccentric spindle position, it would likewise be unable to generate sufficient force to move the chromosomes back to their cortical location. That the same drift is observed in a proportion of eggs parthenogenetically activated with roscovitine supports a reciprocal role in spindle stabilization between MAPK and MPF.

In my hypothesis, the capacity to sustain the cortical spindle location in MII and the capacity to generate sufficient force necessary to initiate movement towards the cortex in MI would both be diminished when MAPK activity was disrupted. For the moment, the association between spindle drift and formins remains purely speculative but is an interesting and provocative area for future study.

5.6.4.2 MISS – A Target for MAPK that Affects the Spindle

As described in 1.4.3.5.1 of the Introduction, MISS (MAPK-interacting and spindle stabilizing protein) is a target for MAPK and stabilizes the metaphase spindle specifically in MII (Lefebvre *et al.*, 2002). Oocytes lacking MISS protein possessed MII spindle defects, characterized by a loss of spindle bipolarity and the presence of cytoplasmic asters (Lefebvre *et al.*, 2002), and were similar to those $mos^{-/-}$ oocytes arrested in metaphase III with a monopolar spindle.

Figure 48. Proposed pathway linking formins to the observed spindle drift observed in Class II and III parthenogenotes activated by roscovitine or U0126.

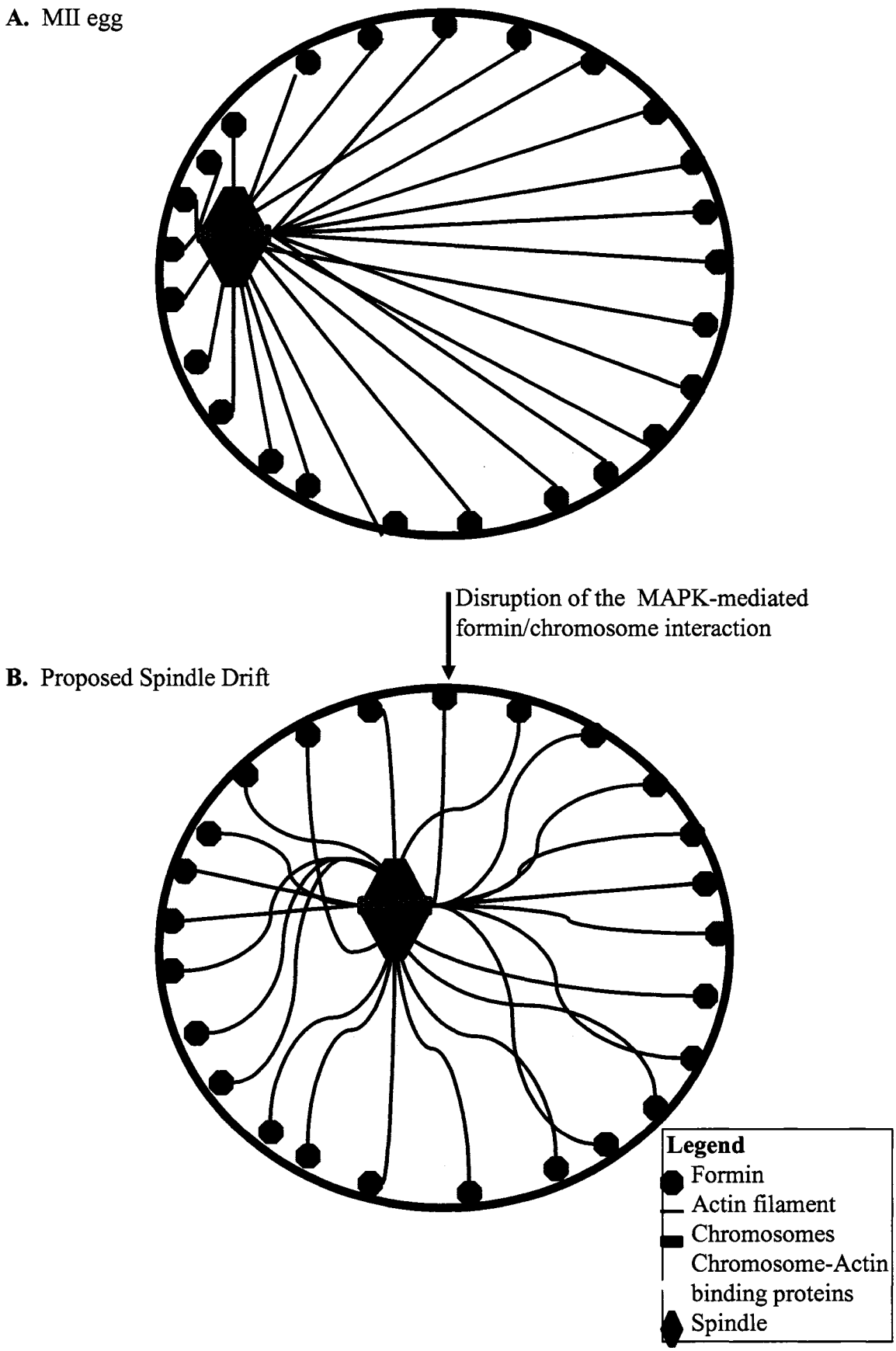
A. MII egg
Disruption of the MAPK-mediated formin/chromosome interaction
B. Proposed Spindle Drift
Legend
Formin
Actin filament
Chromosomes
Chromosome-Actin binding proteins
Spindle

This protein may be related to the observed spindle destabilization during U0126 parthenogenetic activation and my hypothesis of disrupted spindle dynamics following premature loss of MAPK activity. Because of the relatively recent identification of MISS, much remains unknown about its regulation and mode of action. Full activation of MISS is via the MAPK cascade. The timing of MISS inactivation is intriguing: following parthenogenetic activation, some MISS protein is present after 1 h but cannot be detected 6 h after activation. It is not clear whether MISS is active after 1 h or how long it is present after activation. If MISS functionality follows MAPK activity, the premature fall of MAPK activity following U0126 activation could account for the loss of spindle birefringence and inferred loss of spindle organization and integrity when this drug is used alone or in combination with roscovitine. Clearly, this is another area where more research is needed before any conclusions can be made correlating MAPK inactivation with MISS function during parthenogenetic activation.

5.6.4.3 SPIN – Another Molecule that Affects the Spindle

SPIN, another spindle-associated protein present in oocytes, has also been implicated in MAPK-dependent stabilization of the spindle. As described above, in 1.4.3.5.2, SPIN is probably not itself a target of MAPK but may be downstream of MAPK since it undergoes MAPK-dependent post-translational modifications (Oh *et al.*, 1998). The decreased and variable association of SPIN to the spindle in *mos*$^{-/-}$ oocytes makes it a potential candidate molecule involved in the dynamics of microtubule organization. It has been suggested that the variability in SPIN-spindle binding accounts for the variability of parthenogenote phenotypes in *mos*$^{-/-}$ oocytes (Oh *et al.*, 1998). Because SPIN is affected by a protein downstream of MAPK, the loss of MAPK activity following U0126 exposure (alone or in combination with roscovitine) would also result in the loss of SPIN function. A lack of SPIN could disrupt the spindle sufficiently to lead to lost birefringence that is observed. Likewise, the variable proportion of each parthenogenote class in U0126 activation could be due to the variability of SPIN localization to the spindle (Fig. 46, 47).

6 SUMMARY

I have presented data showing that pharmacological inactivation of MAPK with the MEK1/2 inhibitor U0126 leads to a loss of CSF and parthenogenetic activation of MII eggs. This is the first report of complete parthenogenetic activation by inhibition of MEK in a mammalian egg and directly demonstrates a requirement for MEK in CSF activity of the mammalian egg. Until now, only a requirement for Mos has been firmly established in mammals (Colledge *et al.*, 1994; Hashimoto *et al.*, 1994). This contributes even more evidence in support of MAPK and the MAPK pathway as the principal mediator of CSF activity. I have also demonstrated, for the first time, that direct inhibition of cdc2 kinase with the Cdk1 inhibitor, roscovitine, leads to parthenogenetic activation of MII eggs.

Whereas MAPK inactivation following egg activation by IVF or Sr^{2+} does not occur until 5-7 h post-IVF or post-Sr^{2+} activation, MAPK is inactivated within 1 h of exposure to U0126. MPF inactivation followed a similar timecourse in all 3 forms of egg activation, becoming inactivated by 2 h post-egg activation. The fall in MAPK activity in eggs treated with U0126 therefore preceded the fall in MPF activity.

Inactivation of MPF by roscovitine resulted in the subsequent inactivation of MAPK, with a time course similar to that following fertilization. This supports a role for MPF in maintaining CSF activity in the mouse, complementing the well-known converse role of CSF in maintaining MPF. I hypothesize that the gradual decrease in MAPK activity after inhibition of MPF by roscovitine is the same physiological mechanism that governs MAPK deactivation after fertilization in the mouse, specifically, withdrawal of Mos stabilization by MPF. That the spindles in all egg exposed to roscovitine and subsequently followed on the PolScope displayed an increase in spindle birefringence (a feature of egg activation; Liu *et al.*, 2002) also supports the presence of a physiological mechanism responsible for this method of parthenogenesis.

Oocytes lacking a functional *mos* gene become parthenogenetically activated. In

addition to parthenogenetic activation, metaphase-arrested eggs treated with U0126 have a similar phenotype to *mos*$^{-/-}$ oocytes, forming three phenotypic classes (Hirao and Eppig, 1997). Some parthenogenotes develop normally and emit appropriately sized polar bodies (Class I) while others emit abnormally large polar bodies or resemble precocious 2-cell embryos. The ability of U0126 to produce each of the *mos*$^{-/-}$ phenotypes (albeit in MII instead of MI) suggests that parthenogenesis by U0126 occurs by the same mechanism as the loss of Mos activity: inhibition of MEK and MAPK. Since the only known physiological function of MEK is to activate MAPK, the observed effects are most likely due to inactivation of MAPK and its downstream targets.

The phenotypes of *mos*$^{-/-}$ oocytes arise from a disruption of spindle movement during MI, so abnormally large polar bodies develop because the metaphase plate is deeper into the egg and the cleavage furrow therefore forms nearer the centre of the egg (Verlhac *et al.*, 2000b). Whereas the defects leading to these three classes of parthenogenotes arise from a general lack of the Mos/MEK/MAPK pathway throughout oogenesis and maturation in *mos*$^{-/-}$ oocytes, I was able to obtain the identical phenotypes in oocytes that had matured normally, with normal activation of the Mos/MEK/MAPK pathway. The U0126 or roscovitine *mos*$^{-/-}$-like phenotype arose in MII eggs, where the spindle was already positioned at the cortex. Although a disruption of spindle function may be common to both cases, the mechanism by which a large second polar body arises in U0126 parthenogenotes must be different from that which produces the *mos*$^{-/-}$ phenotype. While the phenotypes of parthenogenotes are superficially similar, this is therefore not simply another method of recreating the *mos*$^{-/-}$ phenotype, but is a novel finding.

During parthenogenesis with U0126 or roscovitine (to a lesser extent), the spindle appeared to lose its anchorage to the cortex, drifting into the middle of the egg. This spindle drift appears to be responsible for development of large polar bodies as cytokinesis appeared to be normal, with the cleavage furrow bisecting the spindle. It indicates that MAPK activity is required specifically during MII for normal spindle dynamics, and implicates MAPK in anchoring the spindle at the cortex. It also suggests that spindle anchorage in MII is a dynamic

process that can be disrupted. Tethering the spindle to the cortex may be mediated through formins, a family of actin nucleators recently implicated in asymmetrical spindle positioning. For the moment, this association is purely speculative.

Spindle drift after loss of anchorage may be a random event, leading to the appearance of some relatively normal Class I parthenogenotes. Class I phenotypes could also arise when the spindle anchorage is only incompletely disrupted or when it does not drift very far and thus rotates into its nearly normal position perpendicular to the surface prior to cleavage. My observation that some eggs activated with U0126 appear to rotate parallel to the surface of the egg may be a variation on this loss of anchorage.

In contrast to the expected increase in spindle birefringence at the onset of egg activation (Liu *et al.*, 2000), live cell studies with the PolScope indicate that birefringence is lost quickly after egg are exposed to U0126 either alone or in combination with roscovitine. Nevertheless, the spindle and midbody were persistently detected by confocal microscopy of parthenogenotes stained for tubulin in this treatment group. This indicates that the spindle continues to exist as a discrete structure during the entire period of these observations, but that it is insufficiently ordered to be birefringent following activation with U0126. This is the first form of activation where birefringence was lost during activation and indicates that MAPK activity is necessary to stabilize the organization of the spindle. This may occur by altering the microtubule dynamics at the poles and plates (where MAPK is localized) or by activating other spindle-associated proteins, such as MISS or SPIN.

Despite the apparent physiological mechanism of MAPK inactivation following egg activation with roscovitine, a subset of parthenogenetically activated eggs had a similar phenotype to *mos*$^{-/-}$ and U0126-activated oocytes. Inhibition of MPF itself in MII eggs appears to independently produce some parthenogenotes with the same phenotypes that arise from disruptions of the CSF pathway. This is the first report of the development of *mos*$^{-/-}$-like phenotypes in parthenogenotes produced without direct disruption of the Mos-MEK-MAPK

pathway. It also supports the possibility that both CSF and MPF activity are required during MII for normal spindle function and second polar body cytokinesis, at least until cyclin degradation commences. Because only a small proportion of roscovitine parthenogenotes displayed *mos*$^{-/-}$-like phenotypes, the Mos-MEK-MAPK pathway may very well be the main regulator of spindle dynamics, with MPF modulating this effect. The effect of roscovitine on intracellular structural components may be limited to the spindle, where MAPK and MPF are localized in MII. Alternatively, the effect may not be strong enough to yield a phenotype in all but a small proportion of mouse eggs.

I propose that the initial fall in MPF activity slightly affects MAPK activity at the spindle but that the total fall in MAPK activity occurs by physiological means, following cyclin degradation. The initial modulation in MAPK activity would be at a magnitude undetectable by the kinase assays but sufficient to cause the spindle to drift away from the cortex, ultimately leading to the emission of an abnormally large polar body.

Co-treatment of eggs with U0126 and roscovitine produced a majority of parthenogenotes characterized by one-sided cleavage furrows, originating in the egg cortex near to the spindle, and pulling that side of the egg towards the other side, giving the parthenogenote a bent and multilobed appearance. The development of this severe phenotype is novel and indicates that MPF and MAPK inactivation have a synergistic effect on spindle dynamics and localization, which would not be expected if only CSF activity was required for normal spindle dynamics. It also suggests that spindle function and second polar body emission require that both MPF and CSF be active until the end of second meiotic metaphase (i.e., just before second polar body emission), and that MPF deactivation must precede that of MAPK.

When roscovitine and U0126 were used in combination, the spindle not only lost its capacity to remain docked at the cortex, but actin also appeared to become disorganized, forming a ball in the cortical region nearest to the spindle. When the actin ring would normally contract to pinch off the polar body, this ball of actin contracted towards the spindle, creating a "cleavage

furrow" on only one side of the egg. The microtubules remain organized in a structure resembling a midbody at the arrested cleavage furrow up to 8 h after activation. Why actin would form a ball instead of a ring around the metaphase plate is unclear it may be a contracted contractile ring: a result of low MAPK and MPF activity incorrectly signaling that anaphase is over. I propose that simultaneous loss of both MAPK and MPF activities causes a much more acute disruption in spindle and actin dynamics, so that almost all the parthenogenotes produced have a severe phenotype and exhibit incomplete cleavages.

7 REFERENCES

Abrieu A, Fisher D, Simon MN, Dorée M, Picard A. 1997. MAPK inactivation is required for the G2 to M-phase transition of the first mitotic cell cycle. EMBO J. 16(21):6407-6413.

Abrieu, A., Dorée, M., and Fisher, D. 2001. The interplay between cyclin-B–Cdc2 kinase (MPF) and MAP kinase during maturation of oocytes. J. Cell Sci. 114:257–267.

Alberio R, Kubelka M, Zakhartchenko V, Hajduch M, Wolf E, Motlik J. 2000. Activation of bovine oocytes by specific inhibition of cyclin-dependent kinases. Mol Reprod Dev. 55(4):422-32.

Albertini DF. 1992. Regulation of Meiotic Maturation in the Mammalian Oocyte: Interplay between exogenous cues and the cytoskeleton. Bioessays. 14(2):97-103

Albertini DF, Carabatsos MJ. 1998. Comparative aspects of meiotic cell cycle control in mammals. J Mol Med. 76(12):795-9.

Abraham RT, Acquarone M, Andersen A, Asensi A, Belle R, Berger F, Bergounioux C, Brunn G, Buquet-Fagot C, Fagot D, et al. 1995. Cellular effects of olomoucine, an inhibitor of cyclin-dependent kinases. Biol Cell. 83(2-3):105-20.

Alper SL. 1994. The Band 3-related anion exchanger (AE) gene family. Cell Physiol. Biochem. 4:265-281.

Araki K, Naito K, Haraguchi S, Suzuki R, Yokoyama M, Inoue M, Aizawa S, Toyoda Y, Sato E. 1996. Meiotic abnormalities of c-mos knockout mouse oocytes: activation after first meiosis or entrance into third meiotic metaphase. Biol Reprod. 55(6):1315-24.

Baltz JM, and Phillips KP. 1999. Intracellular ion measurements in single eggs and embryos using ion-sensitive fluorophores. In: A Comparative Methods Approach to the Study of Oocytes and Embryos, Ed. JD Richter, New York and Oxford: Oxford University Press, 39-82.

Bhatt RR, and Ferrell Jr. JE. 1999. The protein kinase p90Rsk as an essential mediator of cytostatic factor activity. Science 286:1362–1365.

Bhatt RR and Ferrell Jr JE. 2000. Cloning and Characterization of *Xenopus* Rsk2, the Predominant $p90^{rsk}$ Isozyme in Oocytes and Eggs. J. Biol. Chem. 275(42):32983–32990.

Bodart JF, Flament S, Vilain JP. 2002. Minireview: Metaphase Arrest In Amphibian Oocytes: Interaction Between CSF And MPF Sets The Equilibrium. Molec. Reprod. Dev. 61:570-574.

Boron WF. 1986. Intracellular pH regulation in epithelial cells. Annu Rev Physiol. 48:377-388

Bos-Mikich A, Whittingham DG, Jones KT. Dev Biol. 1997 Feb 1;182(1):172-9. Meiotic and mitotic Ca2+ oscillations affect cell composition in resulting blastocysts.

Boulton TG, Nye SH, Robbins DJ, Ip NY, Radziejewska E, Morgenbesser SD, DePinho RA, Panayotatos N, Cobb MH, Yancopoulos GD. 1991. ERKs: a family of protein-serine/threonine

kinases that are activated and tyrosine phosphorylated in response to insulin and NGF. Cell. 65(4):663-75.

Bretscher A. 1991. Microfilament Structure and Function in the Cytoskeleton. Annu. Rev. Cell Biol. 7:337-374.

Briggs D, Miller D, Gosden R. 1999. Molecular biology of female gametogenesis *in* Molecular Biology in Reproductive Medicine. CJM Fause, ed. Parthenon Publishing. New York.

Brinkley WBR. 1997. Microtubules: A Brief Historical Perspective. J. Str. Biol. 118: 84-88.

Brunet S, Polanski Z, Verlhac MH, Kubiak JZ. 1998. Bipolar spindle formation without chromatin. Curr. Biol. 8:1231-1234.

Brunet S, Santa Maria A, Guillaud P, Dujardin D, Kubiak J. 1999. Kinetochore Fibers are Not Involved in the Formation of the First Meiotic Spindle in Mouse Oocytes, but Control the Exit from the First Meiotic M Phase. J. Cell Biol. 146(1):1-11.

Carabatsos MJ, Combelles CMH, Messinger SM, Albertini DF. 2000. Sorting and Reorganization of Centrosomes During Oocyte Maturation in the Mouse. Microscopy Research and Technique 49:435-444.

Choi T, Aoki F, Mori M, Yamashita M, Nagahama Y, Kohmoto K. 1991. Activation of p34cdc2 protein kinase activity in meiotic and mitotic cell cycles in mouse oocytes and embryos. Development. 113(3):789-95.

Choi T, Fukasawa K, Zhou R, Tessarollo L, Borror K, Resau J, Vande Woude GF. 1996a. The Mos/mitogen-activated protein kinase (MAPK) pathway regulates the size and degradation of the first polar body in maturing mouse oocytes. Proc Natl Acad Sci USA. 93(14):7032-5.

Choi T, Rulong S, Resau J, Fukasawa K, Matten W, Kuriyama R, Mansour S, Ahn N, Vande Woude GF. 1996. Mos/mitogen-activated protein kinase can induce early meiotic phenotypes in the absence of maturation-promoting factor: a novel system for analyzing spindle formation during meiosis I. Proc Natl Acad Sci USA. 93(10):4730-5.

Ciapa B and Chiri S. 2000. Egg Activation: Upstream of the fertilization calcium signal. Biol. Cell. 92:215-233.

Ciemerych MA, Tarkowski AK, Kubiak JZ. 1998. Autonomous activation of histone H1 kinase, cortical activity and microtubule organization in one- and two-cell mouse embryos. Biol Cell. 90(8):557-64.

Colledge WH, Carlton MB, Udy GB, Evans MJ. 1994. Disruption of c-mos causes parthenogenetic development of unfertilized mouse eggs. Nature. 370(6484):65-68.

Combelles MH, Albertini DF. 2001. Microtubule Patterning during Meiotic Maturation in Mouse Oocytes is Determined by Cell Cycle-Specific Sorting and Redistribution of γ-Tubulin. Dev. Biol. 239:281-294.

Connors SA, Kanatsu-Shinohara M, Schultz RM, Kopf GS. 1998. Involvement of the cytoskeleton in the movement of cortical granules during oocyte maturation, and cortical granule anchoring in mouse eggs. Dev Biol. 200(1):103-15.

Deng MQ, Shen SS. 2000. A specific inhibitor of p34cdc2/cyclin B suppresses fertilization-induced calcium oscillations in mouse eggs. Biol. Reprod. 62, 873–878.

DeSilva DR, Jones EA, Favata MF, Jaffee BD, Magolda RL, Trzaskos JM, Scherle PA. 1998. Inhibition of mitogen-activated protein kinase kinase blocks T cell proliferation but does not induce or prevent anergy. J Immunol. 160(9):4175-81

deVantery C, Stutz A, Vassalli JD, Schorderet-Slatkine S. 1997. Acquisition of meiotic competence in growing mouse oocytes is controlled at both translational and posttranslational levels. Dev Biol. 187(1):43-54.

Duesbery NS, Vande Woude GF. 2002. Developmental biology: an arresting activity. Nature. 416(6883):804-5.

Dupre A, Jessus C, Ozon R, Haccard O. 2002. Mos is not required for the initiation of meiotic maturation in *Xenopus* oocytes. EMBO. 21(15):4026-4036.

Enslen H, Davis RJ. 2001. Regulation of MAP kinases by docking domains. Biol. Cell. 93:5-14.

Evangelista M, Zigmond S, Boone C. 2003. Formins: signaling effectors for assembly and polarization of actin filaments. J Cell Sci. 116:2603-2611.

Fan H-Y, Ton C, Lian L, Li S-W, Gao W-X, Cheng Y, Chen D-Y, Schatten H, Sun Q-Y. 2003. Characterization of Ribosomal S6 Protein Kinase $p90^{rsk}$ During Meiotic Maturation and Fertilization in Pig Oocytes: Mitogen-Activated Protein Kinase-Associated Activation and Localization. Biol. Reprod. 68:968-977.

Fan H-Y, Sun Q-Y. 2004. Involvement of Mitogen-Activated Protein kinase Cascade During Oocyte Maturation and Fertilization in Mammals. Biol. Reprod. 70:535-547.

Favata MF, Horiuchi KY, Manos EJ, Daulerio AJ, Stradley DA, Feeser WS, Van Dyk DE, Pitts WJ, Earl RA, Hobbs F, Copeland RA, Magolda RL, Scherle PA, Trzaskos JM. 1998. Identification of a novel inhibitor of mitogen-activated protein kinase kinase. J Biol Chem. 273(29):18623-32.

Ferrel JE Jr, Wu M, Gerhart JC, Martin GS. 1991. Cell cycle tyrosine phosphorylation of $p34^{cdc2}$ and a microtubule-associated protein kinase homolog in *Xenopus* oocytes and eggs. Mol Cell. Biol. 11(4):1965-71.

Ferrell JE Jr. 1999. Xenopus oocyte maturation: new lessons from a good egg. Bioessays. 21(10):833-842.

Fisher D, Coux O, Bompard-Marechal G, Doree M. 1998. Germinal vesicle material is dispensable for oscillations in cdc2 and MAP kinase activities, cyclin B degradation and synthesis during meiosis in Xenopus oocytes. Biol Cell. 90(6-7):497-508.

Fraser LR. 1987. Strontium support capacitation and the acrosome reaction in mouse sperm and rapidly activates mouse eggs. Gamete Res. 18: 363-374.

Fulka J Jr, Bradshaw J, Moor R. 1994. Meiotic cycle checkpoints in mammalian oocytes. Zygote. 2(4):351-4.

Gallicano GI. 2001. Composition, Regulation and Function of the Cytoskeleton in Mammalian Eggs and Embryos. Front. Biosci. 6:1089-1108.

Gavin AC, Ainle AN, Chierci E, Jones M, Nebreda AR. 1999. A $p90^{rsk}$ Mutant Constitutively Interacting with MAP Kinase Uncouples MAP kinase from p34cdc2/cyclin B Activation in *Xenopus* Oocytes. Molec Biol. Cell. 10:2971-2986.

Gelfand VI. Bershadsky AD. 1991. Microtubule Dynamics: Mechanism, Regulation and Function. Annu. Rev. Cell Biol. 7:93-116.

Glotzer M. 2004. Cleavage furrow positioning. J Cell Biol. 164(3):347-351.

Gordo AC, He CL, Smith S, Fissore RA. 2001b. Mitogen Activated Protein Kinase Plays a Significant Role in Metaphase II Arrest, Spindle Morphology, and Maintenance of Maturation Promoting Factor Activity in Bovine Oocytes. Molec. Reprod. Dev. 59:106-114.

Gordo AC, Kurokawa M, Wu H, Fissore RA. 2002. Modifications of the Ca2+ release mechanisms of mouse oocytes by fertilization and by sperm factor. Mol Hum Reprod. 8(7):619-29.

Gotoh Y, Nishida E. 1995. The MAP kinase cascade: its role in Xenopus oocytes, eggs and embryos. Prog Cell Cycle Res. 1:287-97.

Goto S, Naito K, Ohashi S, Sugiura, Naruoka H, Iwamori N, Tojo H. 2002. Effects of Spindle removal on MPF and MAP Kinase Activities in Porcine Matured Oocytes. Molec. Reprod. Dev. 63:388-393.

Gould, MC., and Stephano, JL. 1999. MAP kinase, meiosis, and sperm centrosome suppression in Urechis caupo. Dev. Biol. 216:348–358.

Gould MC, and Stephano JL. 2003. Polyspermy in Marine Invertebrates. Microsc. Res. Tech. 61:379-388.

Gross SD, Schwab MS, Taieb FE, Lewellyn AL, Qian YW, Maller JL. 2000. The critical role of the MAP kinase pathway in meiosis II in Xenopus oocytes is mediated by p90(Rsk). Curr Biol. 10(8):430-8.

Grondahl C, Lessl M, Faerge I, Hegele-Hartung C, Wassermann K, Ottesen JL. Meiosis-activating sterol-mediated resumption of meiosis in mouse oocytes in vitro is influenced by protein synthesis inhibition and cholera toxin. Biol Reprod. 2000 Mar;62(3):775-80.

Gross SD, Lewellyn AL, Maller JL. 2001. A constitutively active form of the protein kinase p90Rsk1 is sufficient to trigger the G2/M transition in Xenopus oocytes. J Biol Chem. 276(49):46099-103.

Guertin DA, Trautmann S, McCollum D. 2002. Cytokinesis in Eukaryotes. Micro. Molec. Bio. Rev. 66:155-178.

Gundersen GG, Cook TA. 1999. Microtubules and signal transduction. Curr Opin Cell Biol. 11:81-94.

Haccard O., Sarcevic B., Lewellyn A., Hartley R., Roy L., Izumi T., Erickson E., and Maller JL. 1993. Induction of metaphase arrest in cleaving Xenopus embryos by MAP kinase. Science 262:1262–1265.

Hashimoto N, Kishimoto T. 1986. Cell Cycle Dynamics of Maturation-Promoting Factor during Mouse Oocyte Maturation. Tokai J Exp Clin Med. 11(6):471-477.

Hashimoto N, Watanabe N, Furuta Y, Tamemoto H, Sagata N, Yokoyama M, Okazaki K, Nagayoshi M, Takeda N, Ikawa Y, et al. 1994. Parthenogenetic activation of oocytes in c-mos-deficient mice. Nature. 370(6484):68-71.

Hegele-Hartung C, Kuhnke J, Lessl M, Grondahl C, Ottesen J, Beier HM, Eisner S, Eichenlaub-Ritter U. 1999. Nuclear and cytoplasmic maturation of mouse oocytes after treatment with synthetic meiosis-activating sterol in vitro. Biol Reprod. 61(5):1362-72.

Hirao, Y., and Eppig, J. J. 1997. Parthenogenetic development of Mos-deficient mouse oocytes. Mol. Reprod. Dev. 48:391–396.

Hoffert JD, Leitch V, Agre P, King LS. 2000. Hypertonic induction of aquaporin-5 expression through an ERK-dependent pathway. J Biol Chem. 275(12):9070-7.

Hogan, B., Costantini, F., and Lacy, E. 1986. "Manipulating the Mouse Embryo." Cold Spring Harbor Laboratory Press, Cold Spring Harbor, NY.

Horne MM, Guadagno TM. 2003. A requirement for MAP kinase in the assembly and maintenance of the mitotic spindle. J Cell Biol. 161(6):1021-8.

Howlett SK, Bolton VN. 1985. Sequence and regulation of morphological and molecular events during the first cell cycle of mouse embryogenesis. J Embryol Exp Morphol. 87:175-206.

Hoyt CC, Oldenbourg. 1999. Structural analysis with quantitative birefringence imaging. American Laboratory. 34-42.

Huang W, Kessler DS, Erikson RL. 1995. Biochemical and biological analysis of Mek1 phosphorylation site mutants. Mol Biol Cell. 6(3):237-45.

Inoue M, Naito K, Nakayama T, Sato E. 1998. Mitogen-activated protein kinase translocates into the germinal vesicle and induces germinal vesicle breakdown in porcine oocytes. Biol Reprod. 58(1):130-6.

Ito J, Shimada M, Terada T. 2004. Mitogen-Activated Protein Kinases Kinase Inhibitor Suppresses Cyclin B1 Synthesis and Reactivation of $p34^{cdc2}$ Kinase, Which Improves Pronuclear Formation Rate in Matured Porcine Oocytes Activated by Ca^{2+} Ionophore. Biol Reprod. 70: 797-804.

Iwabuchi M, Ohsumi K, Yamamoto TM, Sawada W, Kishimoto T. 2000. Residual Cdc2 activity remaining at meiosis I exit is essential for meiotic M-M transition in *Xenopus* oocyte extract. EMBO J. 19(17):4513-4523.

Josefsberg LB, Galiani D, Lazar S, Kaufman O, Seger R, Dekel N. 2003. Maturation-promoting factor governs mitogen-activated protein kinase activation and interphase suppression during meiosis of rat oocytes. Biol Reprod. 68(4):1282-1290.

Josefsberg LB, Dekel N. 2002. Translational and post-translational modifications in meiosis of the mammalian oocyte. Mol Cell Endocrinol. 22;187(1-2):161-71.

Ju JC, Tsay C, Ruan CW. 2003. Alterations and Reversibility in the Chrmatin, Cytoskeleton and Development of Pig Oocytes Treated with Roscovitine. Molec Reprod. Dev. 64:482-491.

Kalab F, Kubiak JK, Verlhac MH, Colledge WH, Maro B. 1996. Activation of $p90^{rsk}$ during meiotic maturation and first mitosis in mouse oocytes and eggs: MAP kinase-independent and –dependent activation. Development. 122:1957-1964.

Kanatsu-Shinohara M, Schultz RM, Kopf GS. 2000. Acquisition of meiotic competence in mouse oocytes: absolute amounts of p34(cdc2), cyclin B1, cdc25C, and wee1 in meiotically incompetent and competent oocytes. Biol Reprod. 63(6):1610-6.

Karp G, ed. 1996. Cell and Molecular Biology: Concepts and Experiments. John Wiley & Sons Inc. New York.

Kim NH, Funahashi H, Prather RS, Schatten G, Day BN. 1996. Microtubule and microfilament dynamics in porcine oocytes during meiotic maturation. Mol Reprod Dev. 43:248-255.

Kim NH, Chung HM, Cha KY, Chung KS. 1998. Microtubule and microfilament organization in maturing human oocytes. Hum. Reprod. 13(8):2217-2222.

Kline, D., and Stewart-Savage, J. 1994. The timing of cortical granule fusion, content dispersal, and endocytosis during fertilization of the hamster egg: an electrophysiological and histochemical study. Dev Biol. 162(1):277-87.

Knobil E, Neill JD, eds. 1988. The Physiology of Reproduction. Raven Press. New York.

Kobayashi W, Baba Y, Shimozawa T, Yamamoto TS. 1994. The Fertilization Potential Provides a Fast Block to Polyspermy in Lamprey Egg. Dev. Biol. 161:552-562.

Kubiak JZ, Weber M, de Pennart H, Winston NJ, Maro B. 1993. The metaphase II arrest in mouse oocytes is controlled through microtubule-dependent destruction of cyclin B in the presence of CSF. EMBO J. 12(10):3773-8.

Kubelka M, Anger M, Kalous J, Schultz RM, Motlik J. 2002. Chromosome condensation in pig oocytes: lack of a requirement for either cdc2 kinase or MAP kinase activity. Mol Reprod Dev. 63(1):110-8.

Kumagai A, Dunphy WG. 1996. Purification and molecular cloning of Plx1, a Cdc25-regulatory kinase from Xenopus egg extracts. Science. 273(5280):1377-80.

Kumano M, Carroll DJ, Denu JM, Foltz KR. 2001. Calcium-mediated inactivation of the MAP kinase pathway in sea urchin eggs at fertilization. Dev Biol. 236(1):244-57.

Lane M, Baltz JM, Bavister BD. 1999. Na^+/H^+ antiporter activity in hamster embryos is activated during fertilization. Dev Biol. 208:244-252.

Lazar S, Galiani D, Dekel N. 2002. cAMP-Dependent PKA negatively regulates polyadenylation of c-mos mRNA in rat oocytes. Mol Endocrinol. 16(2): 331-341.

Lawitts JA, Biggers JD. 1993. Culture of preimplantation embryos. Methods Enzymol. 225:153-164.

Leader B, Lim H, Carabatsos MJ, Harrington A, Ecsedy J, Pellman D, Maas R, Leder P. 2002. Formin-2, polyplody, hypofertility and positioning of the meiotic spindle in mouse oocytes. Nat. Cell Biol. 4(12):921-928.

Ledan E, Polanski Z, Terret M-E, Maro B. 2001. Meiotic Maturation of the Mouse Oocyte Requires and Equilibrium between Cyclin B Synthesis and Degradation. Dev. Biol. 232:400-413.

Lefebvre C, Terret ME, Djiane A, Rassinier P, Maro B, Verlhac MH. 2002. Meiotic spindle stability depends on MAPK-interacting and spindle-stabilizing protein (MISS), a new MAPK substrate. J Cell Biol. 157(4):603-613.

Liu L., Trimarchi JR, Keefe DL. 1999. Thiol Ocidation-Induced Embryonic Cell Death in Mice is Prevented by the Antioxidant Dithiothreitol. Biol. Reprod. 61:1162-1169.

Liu L, Trimarchi JR, Oldenbourg R, Keefe DL. 2000. Increased Birefringence in the Meiotic Spindle Provides a New Marker for the Onset of Activation in Living . Biol Reprod. 63:251-258.

Liu L, Trimarchi JR, Keefe, DL. 2002. Haploidy But Not Parthenogenetic Activation Leads To Increase Incidence Of Apoptosis In Mouse Embryos. Biol. Reprod. 66:204-210.

Liu R-H, Sun Q-Y, Li Y-H, Jiao L-H, Wang W-H. 2003. Effects of Cooling on Meiotic Spindle Structure and Chromosome Alignment Within *In vitro* Matured Porcine Oocytes. Mol. Reprod. Dev. 65:212-218.

Lohka MJ, Hayes MK, Maller JL. 1988. Purfication of maturation-promoting factor, an intracelllular regulator of early mitotic events. Proc. Natl. Acad. Sci. USA 85:3009-3013.

Lohka MJ. 1998. Nuclear responses to MPF activation and inactivation in Xenopus oocytes and early embryos. Biol Cell. 90(8):591-9.

Longo FJ, Chen DY. 1985. Development of cortical polarity in mouse eggs: involvement of the meiotic apparatus. Dev Biol. 107:382-394.

Lu Q, Dunn RL, Angeles R, Smith GD. 2002. Regulation of Spindle Formation by Active Mitogen-Activated Protein Kinase and Protein Phosphatase 2A During Mouse Ooctye Meiosis. Biol. Reprod. 66:29-37.

Maller JL, Schwab MS, Gross SD, Taieb FE, Roberts BT, Tunquist BJ. 2002. The mechanism of CSF arrest in vertebrate oocytes. Mol Cell Endocrinol. 187(1-2):173-8.

Marangos P, FitzHarris G, Carroll J. 2003. Ca^{2+} oscillations at fertilization in mammals are regulated by the formation of pronuclei. Development. 130(7):1461-1472.

Maro B, Johnson MH, Pickering SJ, Flack G. 1984. Changes in actin distribution during fertilization of the mouse egg. J. Embryol. Exp. Morph. 81:211-237.

Maro B, Howlett SK, Webb M. 1985. Non-spindle microtubule organizing centers in metaphase II-arrested mouse oocytes. J Cell Biol. 101(5 Pt 1):1665-72.

Maro B, Johnson MH, Webb M, Flach G. 1986b. Mechanism of polar body formation in the mouse oocyte: an interaction between the chromosomes, the cytoskeleton and the plasma membrane. J Embryol Exp Morphol. 92:11-32.

Maro B, Howlett SK, Houliston E. 1986a. Cytoskeletal dynamics in the mouse egg. J Cell Sci Suppl. 5:343-59.

Maro B, Verlhac MH. 2002. Polar body formation: new rules for asymmetric divisions. Nat Cell Biol. 4(12):E281-3.

Masui Y, Markert CL. 1971. Cytoplasmic control of nuclear behavior during meiotic maturation of frog oocytes. J Exp Zool. 177(2):129-45.

Masui Y. 2001. From oocyte maturation to the in vitro cell cycle: the history of discoveries of Maturation-Promoting Factor (MPF) and Cytostatic Factor (CSF). Differentiation. 69(1):1-17.

McAvey BA, Wortzman GB, Williams CJ, Evans JP. 2002. Involvement of Calcium Signaling and the Actin Cytoskeleton in the Membrane Block to Polyspermy in Mouse Eggs. Biol. Reprod. 67:1342-1352.

McIntosh JR, Hering GE. 1991. Spindle Fiber Action and Chromosome Movement. Ann. Rev. Cell Biol. 7:403-426.

Meijer, L., Borgne, A., Mulner, O., Chong, J. P. J., Blow, J., Inagaki, N., Inagaki, M., Delcros, J-G., and Moulinoux, J-P. 1997. Biochemical and cellular effects of roscovitine, a potent and selective inhibitor of cyclin-dependent kinases, cdc2, cdk2, and cdk5. Eur. J. Biochem. 243:527–536.

Mermillod P, Tomanek M, Marchal R, Meijer L. 2000. High developmental competence of cattle oocytes maintained at the germinal vesicle stage for 24 hours in culture by specific inhibition of MPF kinase activity. Mol Reprod Dev. 55(1):89-95.

Messinger SM and Albertini DF. 1991. Centrosome and microtubule dynamics during meiotic progression in the mouse oocyte. J. Cell Sci. 100:289-298.

Mitalipov SM, Nusser, KD, Wolf DP. 2001. Parthenogenetic Activation of Rhesus Monkey Oocytes and Reconstructed Embryos. Biol. Reprod. 65:253-259.

Mitra J, Schultz RM. 1996. Regulation of the acquisition of meiotic competence in the mouse: changes in the subcellular localization of cdc2, cyclin B1, cdc25C and wee1, and in the concentration of these proteins and their transcripts. J Cell Sci. 109:2407-15.

Miyazaki S. 1991. Repetitive calcium transients in hamster oocytes. Cell Calcium. 12(2-3):205-16.

Moos J, Visconti PE, Moore GD, Schultz RM, Kopf GS. 1995. Potential role of mitogen-activated protein kinase in pronuclear envelope assembly and disassembly following fertilization of mouse eggs. Biol Reprod. 53(3):692-9.

Moos J, Kopf GS, Schultz RM. 1996a Cycloheximide-induced activation of mouse eggs: effects on cdc2/cyclin B and MAP kinase activities. J Cell Sci. 109 (Pt 4):739-48.

Moos J, Xu Z, Schultz RM, Kopf GS. 1996b. Regulation of nuclear envelope assembly/disassembly by MAP kinase. Dev Biol. 175(2):358-61.

O'Farrell PH, 2001. Triggering the all-or-nothing switch into mitosis. Trends Cell Biol. 2001 Dec;11(12):512-9.

Oegema K, Mitchison TJ. 1997. Rappaport Rules: Cleavage furrow induction in animal cells. Proc. Natl. Acad. Sci. 94:4817-4820.

Oh B, Hamp A, Eppig JJ, Solter D, Knowles BB. 1998. SPIN, a substrate in the MAP Kinase Pathway in Mouse Oocytes. Molec. Reprod. Devel. 50:240-249.

Ohashi S, Naito K, Sugiura K, Iwamori N, Goto S, Naruoka H, Tojo H. 2003. Analyses of Mitogen-Activated Protein Kinase Function in the Maturation of Porcine Oocytes. 68:604-609.

Oldenbourg R, Salmon ED, Tran PT. 1998. Birefringence of Single and Bundled Microtubules. Biophys J. 74:645-654.

Palmer A, Gavin AC, Nebreda AR. 1998. A link between MAP kinase and p34(cdc2)/cyclin B during oocyte maturation: p90(rsk) phosphorylates and inactivates the p34(cdc2) inhibitory kinase Myt1. EMBO J. 17(17):5037-47.

Payne DM, Rossomando AJ, Martino P, Erickson AK, Her JH, Shabanowitz J, Hunt DF, Weber MJ, Sturgill TW. 1991. Identification of the regulatory phosphorylation sites in pp42/mitogen-activated protein kinase (MAP kinase). EMBO J. 10(4):885-92

Perez-Mongiovi D, Beckhelling C, Chang P, Ford CC, Houliston E. 2000. Nuclei and microtubule asters stimulate maturation/M phase promoting factor (MPF) activation in Xenopus eggs and egg cytoplasmic extracts. J Cell Biol. 150(5):963-74.

Peter M, Sanghera JS, Pelech SL, Nigg EA. 1992. Mitogen-activated protein kinases phosphorylate nuclear lamins and display sequence specificity overlapping that of mitotic protein kinase p34cdc2. Eur J Biochem. 205(1):287-94.

Phillips KP, Baltz JM. 1999. Intracellular pH regulation by HCO3-/Cl- exchange is activated during early mouse zygote development. Dev Biol. 208:392-405.

Phillips KP, Petrunewich MAF, Collins JL, Booth RA, Liu XJ and Baltz JM. 2002a. Inhibition of MEK or cdc2 Kinase Parthenogenetically Activates Mouse Eggs and Yields the Same Phenotype as Mos-/- Parthenogenotes. Dev. Biol. 247: 210-223.

Phillips KP, Petrunewich MAF, Collins JL, Baltz, JM. 2002b. The intracellular pH-regulatory HCO3- /Cl- exchanger in the mouse oocyte is inactivated during first meiotic metaphase and reactivated after egg activation via the MAP kinase pathway. Mol. Biol. Cell. 13: 3800-3810.

Pickering SJ, Johnson MH. 1987. The influence of cooling on the organization of the meiotic spindle of the mouse oocyte. Hum. Reprod. 2(3):207-216.

Pines J, Hunter T. 1991. Human cyclins A and B1 are differentially located in the cell and undergo cell cycle dependent nuclear transport. J Cell Biol. 115:1-17.

Polanski Z, Ledan E, Brunet S, Louvet S, Verlhac MH, Kubiak JZ, Maro B. 1998. Cyclin synthesis controls the progression of meiotic maturation in mouse oocytes. Development. 125(24):4989-97.

Rappaport R. 1981. Cytokinesis: Cleavage Furrow Establishment in Cylindrical Sand Dollar Eggs. J. Exp. Zool. 217:365-375.

Reimann JDR, Freed E, Hsu JY, Kramer ER, Peters JM, Jackson PK. 2001. Emi1 is a Mitotic Regulator that Interacts with Cdc20 and Inhibits the Anaphase Promoting Complex. Cell. 105:645-655.

Reimann JDR, Jackson PK. 2002. Emi1 is required for cytostatic factor arrest in vertebrate eggs. Nature. 416:850-854.

Revenu C, Athman R, Robine S, Louvard D. 2004. The Co-Workers of Actin Filaments: From Cell Structures to Signals. Nat. Rev. Molec. Cell Biol. 5:1-12.

Runft LL, Jaffe LA, Mehlmann LM. 2002. Egg activation at fertilization: where it all begins. Dev Biol. 245(2):237-54.

Sagata N, Oskarsson M, Copeland T, Brumbaugh J, Vande Woude GF. 1988. Function of c-mos proto-oncogene product in meiotic maturation in Xenopus oocytes. Nature. 335(6190):519-25.

Sanfins A, Lee GY, Plancha CE, Overstrom EW, Albertini DF. 2003. Distinctions in Meiotic Spindle Structure and Assembly During *In vitro* and *In vivo* Maturation of Mouse oocytes. Biol Reprod. In press.

Sanger JM, Sanger JW. 2000. Assembly of Cytoskeletal Protein into Cleavage Furrows of Tissue Culture Cells. Micro. Res. Tech. 49:190-201.

Schatten G, Simerly C, Schatten H. 1985. Microtubule configurations during fertilization, mitosis and early development in the mouse and the requirement for egg microtubule-mediated motility during mammalian fertilization. Proc. Natl. Acad. Sci. USA. 82:4152-4156.

Schultz RM, 1999. Preimplantation Embryo Development. In Molecular Biology in Reproductive Medicine. Fauser, BCJM ed. Parthenon Publishing.

Schwab MS, Roberts BT, Gross SD, Tunquist BJ, Taieb FE, Lewellyn AL, Maller JL. 2001. Bub1 is activated by the protein kinase p90(Rsk) during Xenopus oocyte maturation. Curr Biol. 11(3):141-50.

Schwartz, D.A., and Schultz, R.M. 1991. Stimulatory effect of okadaic acid, an inhibitor of protein phosphatases, on nuclear envelope breakdown and protein phosphorylation in mouse oocytes and one-cell embryos. Dev. Biol. 145:119–127.

Shen SS, Buck WR. 1990. A synthetic peptide of the pseudosubstrate domain of protein kinase C blocks cytoplasmic alkalinization during activation of the sea urchin egg. Dev Biol. 140(2):272-80.

Sengoku K, Tamate K, Takaoka Y, Horikawa M, Goishi K, Okada K, Ishikawa M. 1999. Requirement of Sperm-Oocyte Plasma Membrane Fusion for Establishment of the Plasma Membrane Block to Polyspermy in Human Pronuclear Oocytes. Mol. Reprod. Dev. 52:183-188.

Snustad DP, Simmons MJ, Jenkins JB, eds. 1997. Principles of Genetics. John Wiley & Sons. New York.

Sobajima T, Aoki F, Kohmoto K. 1993. Activation of mitogen-activated protein kinase during meiotic maturation in mouse oocytes. J Reprod Fertil. 97(2):389-94.

Stephano, J. L., and Gould, M. C. 2000. MAP kinase, a universal suppressor of sperm centrosomes during meiosis? Dev. Biol. 222:420–428.

Summers MC, Bhatnagar PR, Lawitts JA, Biggers JD. 1995. Fertilization in vitro of mouse ova from inbred and outbred strains: complete preimplantation embryo development in glucose-supplemented KSOM. Biol Reprod. 53(2):431-7.

Sun QY, Breitbart H, Schatten H. 1999. Role of the MAPK cascade in mammalian germ cells. Reprod Fertil Dev. 1999. 11(7-8):443-50.

Sun QY, Lai L, Park K-W, Kühlolzer B, Prather RS, Schatten H. 2001. Dynamic Events are Differently Meidated by Microfilaments, Microtubules, and Mitogen Activated Protein Kinase During Porcine Oocyte Maturation and Fertilization *In vitro*. Biol. Reprod. 64:879-889.

Sun QY, Wu GM, Lai L, Bonk A, Cabot R, Park KW, Day BN, Prather RS, Schatten H. 2002. Regulation of mitogen-activated protein kinase phosphorylation, microtubule organization, chromatin behavior, and cell cycle progression by protein phosphatases during pig oocyte maturation and fertilization in vitro. Biol Reprod. 66(3):580-8.

Swann K, Whitaker M. 1985. Stimulation of the Na/H exchanger of sea urchin eggs by phorbol ester. Nature. 314(6008):274-7.

Tachibana K, Machida T, Nomura Y, Kishimoto T. 1997. MAP kinase links the fertilization signal transduction pathway to the G1/S-phase transition in starfish eggs. EMBO J. 16(14):4333-9.

Taieb F, Thibier C, Jessus C. 1997b. On cyclins, Oocytes, and Eggs. Molec. Reprod. Dev. 48:397-411.

Tatemoto, H., and Muto, N. 2001. Mitogen-activated protein kinase regulates normal transition from metaphase to interphase following parthenogenetic activation in porcine oocytes. Zygote 9:15–23.

Tian XC, Lonergan P, Jeong BS, Evans ACO, Yang X. 2002. Association of MPF, MAPK, and Nuclear Progression Dynamics during Activation of Young and Aged Bovine Oocytes. Molec. Reprod. Dev. 62:132-138.

Tong C, Fan HY, Chen DY, Song XF, Schatten H, Sun QY. 2003. Effects of MEK inhibitor U0126 on meiotic progression in mouse oocytes: microtuuble organization, asymmetric division and metaphase II arrest. Cell Research. 13(5): 375-383.

Tremoleda JL, Schoevers EJ, Stout TA, Colenbrander B, Bevers MM. 2001. Organisation of the cytoskeleton during in vitro maturation of horse oocytes. Mol Reprod Dev. 60(2):260-269.

Tunquist BJ, Maller JL. 2003. Under arrest: cytostatic factor (CSF)-mediated metaphase arrest in vertebrate eggs. Genes Dev. 17(6):683-710.

van den Ent F. Amos L, Lowe J. 2001. Bacterial ancestry of actin and tubulin. Curr. Opin Microbiol. 4:634-638.

Verlhac MH, de Pennart H, Maro B, Cobb MH, Clarke HJ. 1993. MAP kinase becomes stably activated at metaphase and is associated with microtubule-organizing centers during meiotic maturation of mouse oocytes. Dev Biol. 1993 Aug;158(2):330-40.

Verlhac MH, Kubiak JZ, Clarke HJ, Maro B. 1994. Microtubule and chromatin behavior follow MAP kinase activity but not MPF activity during meiosis in mouse oocytes. Development. 120(4):1017-25.

Verlhac, M.H., Kubiak, JZ, Weber, M., Geraud, G., Colledge, W.H., Evans, M.J., and Maro, B. 1996. Mos is required for MAP kinase activation and is involved in microtubule organization during meiotic maturation in the mouse. Development 122:815–822.

Verlhac MH, Lefebvre C, Kubiak, JZ, Umbhauer M, Rassinier P, Colledge W, Maro B. 2000a. Mos activates MAP kinase in mouse oocytes through two opposite pathways. EMBO J. 19(22):6065-6074.

Verlhac MH, Lefebvre C, Guillaud P, Rassinier P, Maro B. 2000b. Asymmetric division in mouse oocytes: with or without Mos. Curr Biol. 10(20):1303-6

Wang WH, Keefe DL. 2002. Prediction of chromosome misalignment among *in vitro* matured oocytes by spindle imaging with the PolScope. Fertil. Steril. 78(5):1077-81.

Waters JC, Salmon ED. 1997. Pathways of Spindle Assembly. Curr. Opin. Cell. Biol. 9:37-43.

Westermann S, Weber K. 2003. Post-Translational Modifications Regulate Microtubule Function. Nat. Rev. 4:938-947.

Whittingham DG, Siracusa G. 1978. The involvement of calcium in the activation of mammalian oocytes. Exp Cell Res. 113(2):311-317.

Wianny F., and Zernicka-Goetz M. 2000. Specific interference with gene function by double-stranded RNA in early mouse development. Nat. Cell Biol. 2:70–75.

Winston NJ, Maro B. 1999. Changes in the activity of type 2A protein phosphatases during meiotic maturation and the first mitotic cell cycle in mouse oocytes. Biol. Cell. 91:175-183.

Winston NJ, McGuinness O, Johnson MH, Maro B. 1995. The exit of mouse oocytes from meiotic M-phase requires an intact spindle during intracellular calcium release. J. Cell Sci. 108:143–151.

Winston NJ. 1997. Stability of cyclin B protein during meiotic maturation and the first mitotic cell division in mouse oocytes. Biol Cell. 89:211-219.

Xu Z, Kopf GS, Schultz RM. 1994. Involvement of inositol 1,4,5-trisphosphate-mediated Ca2+ release in early and late events of mouse egg activation. Development. 120(7):1851-9.

Yarm F, Sagot I, Pellman D. 2001. The Social Life of Actin and Microtubules: Interaction versus Cooperation. Curr. Opin. Microbiol. 4:696-702.

Ye J, Flint APF, Luck MR, Campbell KHS. 2003. Independent activation of MAP kinase and MPF during the initiation of meiotic maturation in pig oocytes. Reproduction. 125:645-656.

Yew N, Strobel M, Vande Woude GF. 1993. Mos and the cell cycle: the molecular basis of the transformed phenotype. Curr Opin Genet Dev. 3(1):19-25.

Yoshigaki T. 2003. Why Does a Cleavage Plane Develop Parallel to the Spindle Axis in Conical Sand Dollar Eggs? A Key Question for Clarifying the Mechanism of Contractile Ring Positioning. J. Theor. Biol. 221:229-244.

Zernicka-Goetz, M., Ciemerych, M.A., Kubiak, J.Z., Tarkowski, A.K., and Maro, B. 1995. Cytostatic factor inactivation is induced by a calcium-dependent mechanism present until the second cell cycle in fertilized but not in parthenogenetically activated mouse eggs. J. Cell Sci. 108(Pt 2):469–474.

Zhao Y, Baltz JM. 1996. Bicarbonate/chloride exchange and intracellular pH throughout preimplantation mouse embryo development. Am J Physiol. 271:C1512-C1520.

Zhao, Y., Chauvet, P.J., Alper, S.L. and Baltz, J.M. 1995. Expression and function of bicarbonate/chloride exchangers in the preimplantation mouse embryo. J Biol Chem 270:24428-24434.

Zhu ZY, Chen DY, Li JS, Lian L, Lei L, Han ZM, Sun QY. 2003. Rotation of Meiotic Spindle is Controlled by Microfilaments in Mouse Oocytes. Biol. Reprod. 68:943-946.